ON-LINE COMPUTER TECHNIQUE FOR TRANSIENT CURRENT ANALYSIS IN DIELECTRICS AT VERY LOW FREQUENCIES.

By

S.S. AL-RAWI.

Thesis presented for the degree of Doctor of Philosophy.

The City University.

Electrical Engineering Department.

1978.

ABSTRACT

Two methods are described for the direct measurement by on-line computer technique of the responses of the lumped circuits and solid polymer dielectrics at low frequencies. The first method involves the direct application of the step-voltage to the dielectric sample and the measurement of subsequent transient currents. The second method, a unique computer-aided measurement technique, involves the application of the ideal low-pass filter step-response, generated by the computer, to the dielectric sample and the measurement of its response. Both methods required a very sensitive electrometer amplifier to be constructed in order to detect the response. These responses are then sampled and stored by an on-line computer which then proceeds to evaluate their Fourier transforms.

Discrete Fourier transformation within the computer allows the data to be presented immediately, in various ways which are of direct use to the experimenter. The disadvantages of any previous assumptions about the nature of the dielectric response and the necessity for relatively crude approximations, which characterise the methods previously employed, are eliminated.

Apart from being new and original, especially in its use of non-causal response functions, the second method provides an excellent example of the power of the laboratory on-line computer technique and paves the way for special digital instrument to perform dielectric measurements. The sort of microprocessor which are now becoming available would allow such an instrument to be produced fairly cheaply and simply.

The results obtained are compared against those of previous workers, and an attempt is made to justify them on the basis of molecular theory.

ACKNOWLEGMENTS

The author wishes to thank in very special way his Supervisor, Dr.J.E.Brignell, not only for his guidance and help, but also for his enthusiasm, encouragement, patience and understanding at difficult times.

The author wishes to thank all those who have contributed to this work, but who are too numerous to mention individually by names. Special mention, however, must be made for [redacted] - the Head of Electrical Engineering Department for giving his attention and interest in this work, [redacted] for the help they kindly offered in preparation of the computer programs, [redacted] - Aberystwyth, University of Wales, [redacted] - National Physical Laboratory, [redacted] - Liverpool University, [redacted] - Imperial Chemical Industries Ltd., [redacted] - University College of North Wales and [redacted] - University College, London, for much advice and constructive discussions.

The author would also like to express his gratitude to the members of the Electrical Engineering Department for their continous help during the whole period.

TABLE OF SYMBOLS

A	Area
C	Constant
C_x	Dielectric sample's capacitance
C_a	Dielectric sample's capacitance at high frequency
D	Electric flux density (displacement).
d	Distance
E	External electric field
E_{in}	Internal electric field
e	Electronic charge
F	Force
f	Frequency
G	Conductance
H	Energy
ΔH	Activation energy
h	Plank's constant
I	Current
I_c	Charging current
I_L	Loss current
J	Current density
j	Square root of - 1
K	Boltzman's constant
L	Inductance
l	Length
M	Molecular weight
N	Number of particles (dipoles) per unit volume
N_o	Avogadro's number

$\grave{n}$	Cole-Cole parameter of relaxation-time distribution
P	Polarization
Q	Electric charge
R	Resistance
S	Surface area
T	Absloute temperature
U	Potential energy
u	Energy density
V	Volume
	Voltage
W	Work
Y	Admittance
Z	Intrinsic impedence
Z*	Complex impedence
α	Distribution function
	Polarizability
α_a	Atomic polarizability
α_d	Dipole (orientation) polarizability
α_e	Electronic polarizability
β	Fuoss-Kirkwood parameter of relaxation time distribution
Ω	Solid angle
	Distribution function
δ	Loss angle
tan δ	Loss tangent
$\delta(t)$	Impulse function
ϵ	Dielectric constant (absolute)
ϵ_r	Dielectric constant (relative)
ϵ_o	Dielectric constant of free space (vacuum)

ε^*	Complex permitivity
ε'	Real component complex permitivity
ε''	Imaginary component complex permitivity
ε_s	Low-frequency limit of relative permitivity
ε_∞	High-frequency limit of relative permitivity
θ	Angle
μ	Electric dipole moment
σ	Conductivity
τ	Relaxation time
τ_o	Average relaxation time
ϕ	Relaxation function
ρ	Density
ω	Angular frequency.

CONTENTS

CHAPTER ONE.

GENERAL INTRODUCTION

1.1 DIELECTRIC MATERIALS

Dielectric is a term applied to an insulating material whenever the material is used in such a way that its characteristics enter as parameters in the description of an electrical system. Dielectric materials in the sense of this thesis are not a narrow class of insulator, but will be mainly treated from the standpoint of their interaction with an electric field, and both terms are often used interchangeably to describe materials which are poor electrical conductors. From the practical standpoint, materials in general may be classified according to their electrical conductivities into three categories:

(i) Conductors - Conductivity 10^{6} to 10^{8} $Ohm^{-1}m^{-1}$

(ii) Semiconductors - Conductivity 10^{5} to 10^{-7} $Ohm^{-1}m^{-1}$

(iii) Insulators - Conductivity 10^{-3} to 10^{-20} $Ohm^{-1}m^{-1}$

A further important distinction between conductors, semiconductors and insulators is that whilst the conductivity of the first decreases linearly with increasing temperature, the conductivity of the latter two increases exponentially. These differences in the electric conductivities between the three different types of materials can well be explained by the "band theory" of solids. That is, the properties of any solid material depend upon the nature of the constituent atoms and upon the way in which the atoms are grouped together. Experiments have shown that an atom consists of positively charged nucleus surrounded by electrons located in discrete orbits. Actually, electrons can exist in stable orbits

near the nucleus only for certain discrete values of energy called energy levels of the atom. The allowed energies of electrons in an atom are depicted by horizontal lines on any energy level diagram, Fig. (1-1). The curved lines represent the potential energy of electrons near the nucleus as given by Coulomb's Law. As a consequence of the Pauli exclusion principle, only a certain maximum number of electrons can occupy a given energy level. The result is that in any atom, electrons fill up the lowest possible levels first. Electrons in occupied levels are indicated by a solid dot in the energy level diagram.

However, when a large number of such atoms are brought together to form a solid, it becomes impossible to assign individual electrons to individual atoms, but one must consider the electrons to be more or less collectively shared by individual atomic nuclei. A direct consequence of this "sharing" is that a large number of electrons would occupy the same energy state. This is not possible according to the above principle and, as a result, each original discrete energy level E, of the isolated atom is broadened into a band consisting of as many levels as there are atoms in the crystal. These new levels are very closely spaced and have energy values in the neighbourhood of E; the larger the number of atoms forming the solid, the smaller the distance between the levels within the band. In a similar way, the higher unoccupied levels split and consequently, three energy levels are available. Fig. (1-2).

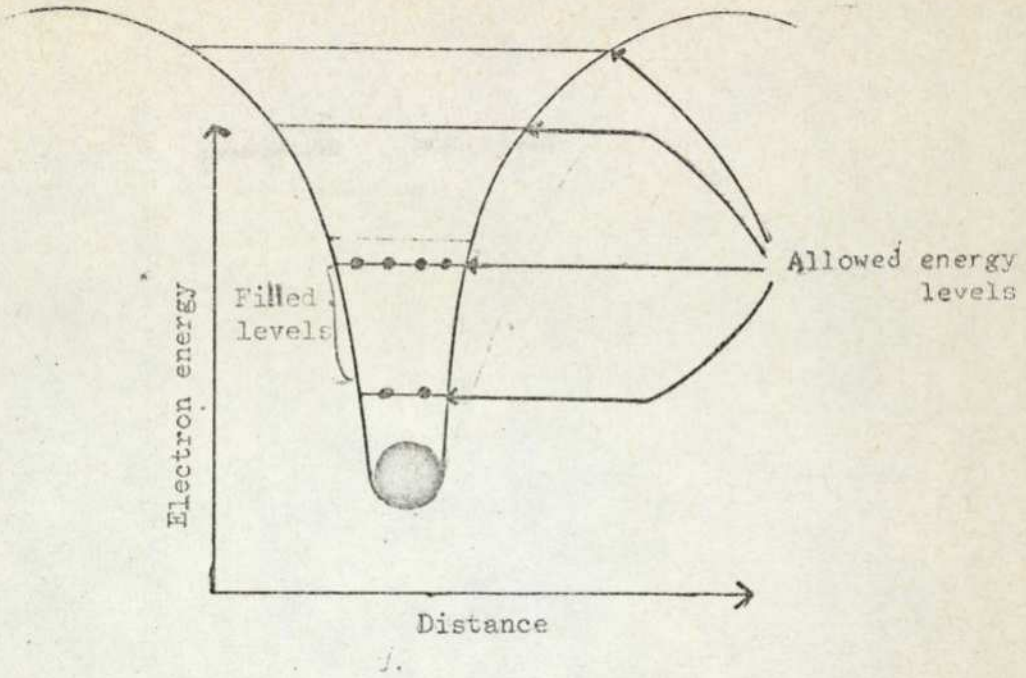

Fig. (1.1): Energy-level diagram for an atom.

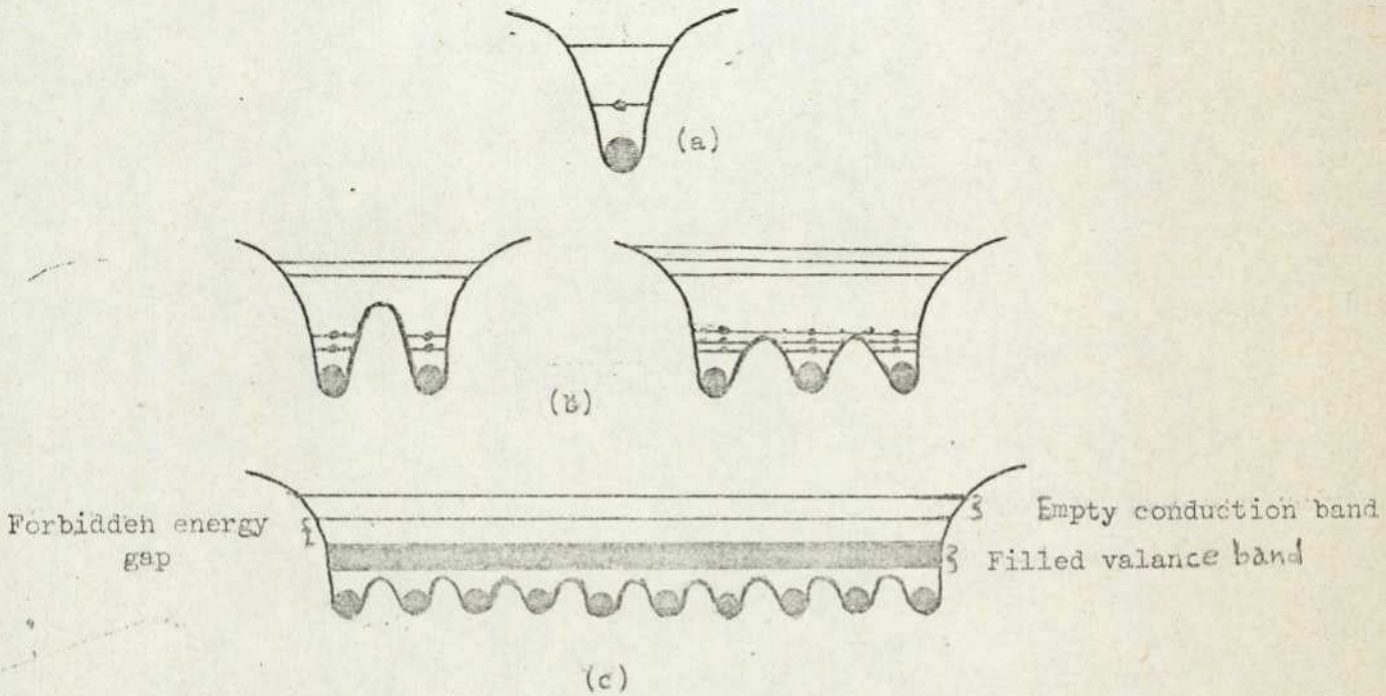

Fig. (1.2): Energy-level diagram for
(a) isolated atom
(b) two and three atoms close together, and
(c) solid crystal.
In the crystal, energy are broadened into bands.

(i) The lowest energy band, called the valence band, is completely filled with electrons, there is one electron for each of the available energy levels.

(ii) The upper energy band, normally called the conduction band, is corresponding to the unoccupied higher levels in the isolated atom.

(iii) The energy region between the valance band and conduction band is called the forbidden energy gap, since there are no electrons with such energies in the crystal.

This picture of the electronic energy levels in the crystal, denoted as the energy-band model of a crystal, is very useful in determining the electrical properties of any solid, since it shows how electrons can move in the crystal. In metals the valence and conduction bands overlap, Fig. (1-3a), and since there is no forbidden energy gap, any of the many valence electrons are free to roam throughout the solid, and to move in response to an electric field. Therefore, metals are excellent electric conductors.

An insulating crystal has a wide forbidden gap Fig. (1-3c). The valence band is completely filled with electrons and the conduction band is completely empty. Obviously, the upper band cannot contribute to electric conductivity since no electrons are present to act as carriers. Conversely, energy levels in the valence band are filled, so it is impossible for any electron to be accelerated by the electric field and, therefore, the crystal is an insulator.

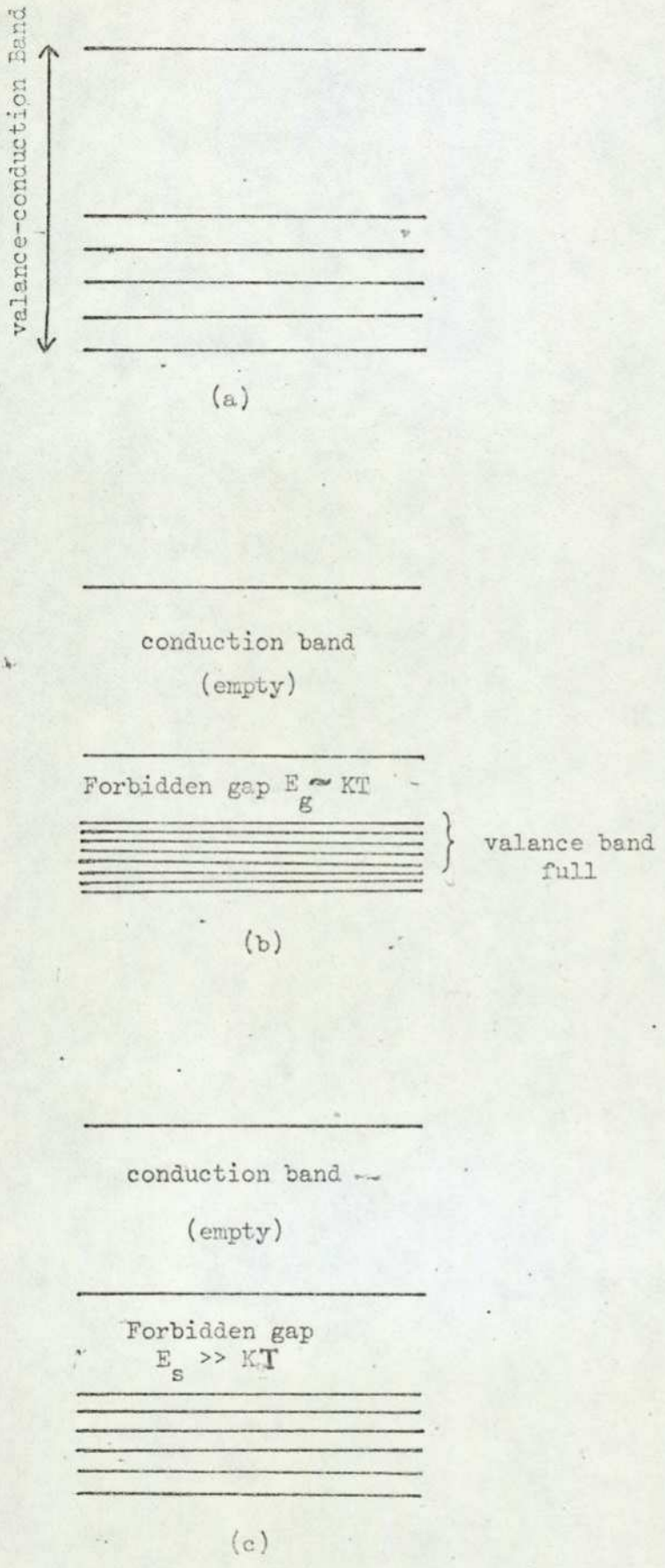

Fig. (1.3): Schematic band model
(a) metal.
(b) semiconductor.
(c) insulator.

The energy-band model of a semiconductor, Fig. (1-3b), is similar to that of an insulator except that the forbidden energy gap is comparatively narrow. In fact, the primary distinction between insulators and intrinsic semiconductors is the width of the forbidden gap; a gradual transition from good insulators to semiconductors occurs as the gap decreases from 5 electron-volts or more, to less that 1 electron-volt. The electron-volt, abbreviated eV, is equal to the kinetic energy gained by an electron in traversing a potential difference of 1 volt.

However, it should be remembered that the energy band concept is strictly relevant only to a single crystal of material. This is because it assumes that every atom and its bonding system is the same as every other so that an electron requires precisely the same energy to be liberated from a bond anywhere in the solid. Many dielectrics used as insulators are highly disordered, so that the environment of each atom tends to be a little different from its neighbours. It is possible, however, to consider the energy band picture to apply, but with band edges smeared out somewhat. This allows for the fact that slightly different energies may be needed to energize an electron from a band at different places in the material.

Having given the main essential differences between the three types of materials, and before turning in the following chapter to study the most important electric characteristics of solid insulators associated with their use as dielectrics, it is desirable to throw some light on:
(a) Chemical structure of the insulator which will be used in this work i.e. solid polymers, and:

(b) The importance of the dielectric measurements and the significance of the present work.

1.2 POLYMERS

A class of substances in which there has been an increasing interest in relatively recent times is the Polymers. These are substances composed of long "chains" of atoms - where atoms form self-contained small groups or units in contrast to these structures in which each atom (ion) is bonded to several near neighbours - usually with the implication that the chains are hundreds or thousands of units long. The individual representative units of the chain are called "monomer units" and the substance consisting of separate monomer units, if it exists, is called the monomer (Sillars, 1973). Many monomers contain one or more double bonds linking its two carbon atoms i.e. monomer ethylene.

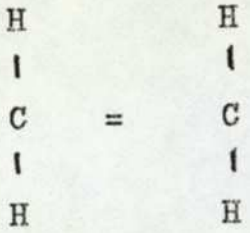

One type of polymerisation "addition polymerisation" however, can be regarded as the "opening" of one of these double bonds and linking up the "loose ends" with other monomers to form the polymer:

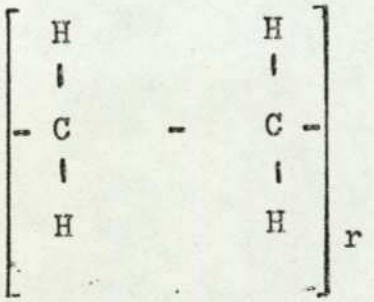

The number of monomer units in the chain, r, is called the degree of polymerization. If the polymer molecules consist of simple chains, the polymer is said to be linear, but branched polymers may, and generally do occur. That is to say, if carbon atoms of one of these chains have one hydrogen and another carbon atom instead of two hydrogen atoms, it will form a branch. This branch may be a single carbon atom with remaining bonds satisfied by three hydrogens, or, it may be another chain similar to the main one. Such branches will clearly get involved with neighbouring molecules and if they are frequent they will tend to restrict the relative movements and make the solid rigid. Those unbranched and slightly chain polymers may be amorphous, partly crystalline or rarely wholly crystalline. In some polymers, the branches may in fact be, or connect to other major chains, so that all chains are linked to other chains, this is known as a cross-linked structure.

Polymers, however, are not necessarily simple carbon carbon atoms, but the backbone may involve oxygen atoms, nitrogen atoms, benzene rings and other features. Many of them are formed not by double-bond splitting, addition Fig. (1-4), but by a reaction such as esterification (reaction of an organic acid or anhydride with an alcohol) with the elimination of water (condensation). An unbranched chain is formed when an alcohol with two (OH) groups (i.e. dihydric), such as glycol reacts with an acid having two COOH groups (i.e. dibasic), such as phthalic acid, Fig. (1-5). Polymers formed by esterification are generally called polyesters.

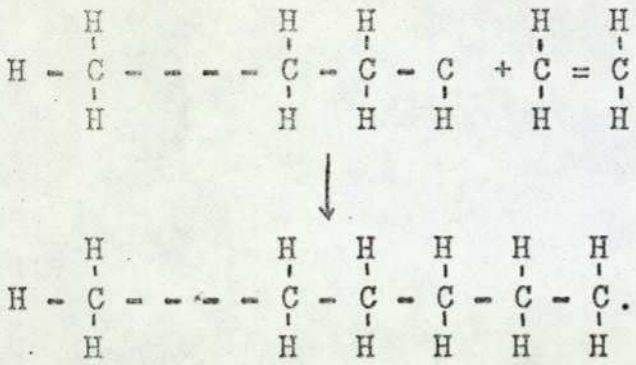

and so on until the chain terminates

Fig. (1-4) Progress of addition polymerisation of Polyethylene

---

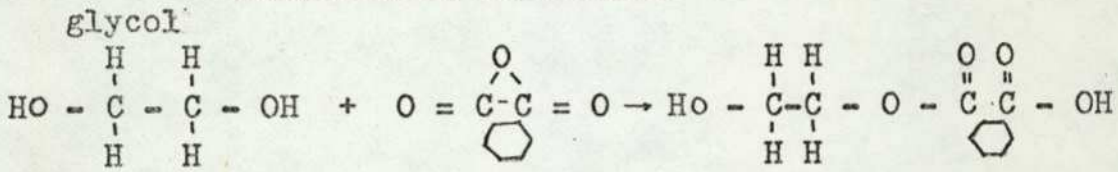

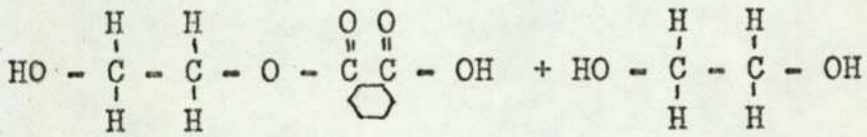

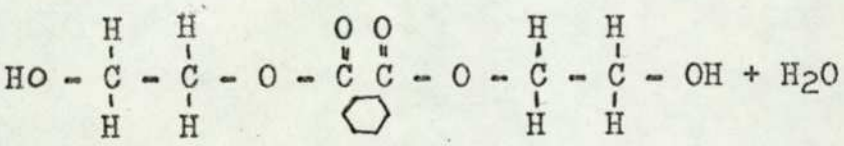

and so on indefinitely

Fig. (1-5) Progress of one type of condensation polymerisation estification forming poly(glycol phthalate).

1.3 IMPORTANCE OF DIELECTRIC MATERIAL MEASUREMENTS AND THE SIGNIFICANCE OF THE PRESENT WORK

Dielectric materials have not in recent years undergone such rapid development as have the related semiconductors. Nevertheless, there is a steady and increasing interest in dielectric properties and behaviour. The majority of dielectric work has been confined to high frequency range (10^2-10^8Hz). It is, however, essential that as large a frequency range as possible should be covered. This rises from:

1-3- 1. Dielectric materials are mostly used as ordinary insulators, but their other unique properties are increasingly employed in electronic devices. Practically, it is hard to think of any dielectric material as not being used in electronic equipments ranging from gases, through liquids to solids. In addition, these materials are required to operate from direct current to the highest frequency range, from very low temperature to the high temperature and from zero relative humidity to the direct moisture condensation. It is not surprising, therefore, the great need for continued research into dielectrics, and the theories governing their behaviour. This search in terms of experimental results will provide the base on which a theoretical model of practical dielectric can be built up. Once this theorectical model, based on the atomic and molecular structure of the material is successful, it will provide the knowledge on which the search for new materials may be founded, and may also be used to deduce the probable behaviour of the dielectric in different electrical environments.

1-3-2. Dielectric relaxation curves for some materials, e.g. polymers, are broad and very sensitive to temperature variations. The study of dielectric relaxation has proved to be a valuable tool for gaining some insight into kinetics of molecular interaction in polar liquids and solids, and their structures. The nature of these interactions between molecules and their arrangements within the materials mainly depends on:

- The behaviour of relaxation time (τ) with temperature variations at a given frequency.
- The magnitude of energy loss factor (ε'') as a function of frequency at a given temperature.
- The width of the energy loss peak Parameter (α).

Now, if $\alpha = 0$, then the material could be classified into one of two types depending on:

(1) If ε'' is very small as well as τ and they do not change with temperature, then the material is called non-polar one and obeys Clausius'-Mosotti formulae (see Chapter 2), which implies:

(i) Polarizations of the molecules are due to elastic displacement only.

(ii) Absence of short-range (non-dipolar) interactions.

(iii) Isotropy of the polarizability of the molecules.

(iv) Isotropy of the arrangements of the molecules.

(2) If ε'' is relatively large and changes with temperature as well as τ, then the material is called polar material and obeys Debye's equation (See Chapter 2) which implies:

(i) Polarizations of the molecules are partly due to the distortion of the molecules by the field and partly due to the orientation of the molecular dipoles in the field.

(ii) The neighbouring molecules do not interfere with one another's motion or cause orientation in the absence of an externally applied field. In other words, when the field is applied, the molecules are free to orientate in it except in so far as their orientation is opposed by their thermal motion.

(iii) The short-range interaction is negligible.

(iv) The molecules are assumed to have two equilibrium positions and they are supposed to change their orientations by a series of small steps during the process of rotation towards the new position.

On the other hand, if $\alpha \neq 0$ then the material has more than one relaxation time and the molecules are supposed to adopt a number of equilibrium positions separated by a range of barrier heights. Many theories stand to explain this behaviour but this is not the place for such details and some of them will be discussed later (see Chapter 2).

1-3-3. Molecular volume could be calculated from measuring the relaxation time. These calculations largely depend on the distribution of relaxation times. Perrin (1934) stated that if the molecule is not spherical the processes of orientation by rotation about different axis should require different relaxation times. Furthermore, he showed that the variation in the environment of the molecules should give rise to variation in the relaxation times.

1-3-4. Measurements of the temperature dependence of ε_s (the static dielectric constant) of dielectric gases, for instance, should make possible a reliable determination of the dipole moment of free molecules. The magnitude

of the dielectric moment gives valuable information about the distribution of electrons (Hill, 1969). Thus, the large dipole moment of HCL ($\mu \sim 1$ Debeye unit) compared with that of CO ($\mu \sim 0.1$ Debye) gives some justification for considering the Hcl molecule (but not the CO molecule as composed of a positive and negative ion $H^+ + CL^-$.

In view of the above discussion and in order to fill as many gaps as possible in dielectric phenomenology, it was thought that it would be of value to make an independent investigation of the dielectric properties and their behaviour at very low frequency range (10^{-5}-10^{-1} Hz) at different, fixed temperatures using the step function technique. The present work deals with descriptions and the results of such an experiment. The significance of this is as follows:

1. Due to rapid growth in number of modern insulating materials and the great need for quick and frequent measurements of their dielectric parameters, complex permittivity and loss tangent as function of frequency, it is desirable to devise a fast, accurate and inexpensive method.

(a) Fast - This can be achieved by using an on-line computer technique with the step-voltage method to evaluate and display the real, and imaginary parts of the complex permittivity using fast Fourier transform.

(b) Accurate - Using fast Fourier transform instead of Hamon's approximation (see Chapter 3) gives the exact value of the real and imaginary parts of complex dielectric constant.

(c) Inexpensive - It could be said that most of the workers in this field did not use fast Fourier transform because the need for the computer which usually entails

high capital and running costs. However, in the present case, the micro-processor computer was intended to be used. This machine has the advantage of being small (portable), powerful and consuming little electrical power.

2. It is desirable that as wide a range of frequency as possible should be covered in a single sweep. A step-function represents a wide Fourier spectrum containing components of very low frequency (depending on the duration of the recording) up to a very high frequency (depending on the rise time of the step function). This means that the recorded response of the dielectric sample to step-voltage contains all the information needed for constructing the dielectric spectrum in a wide frequency range, say from 10^{-5}Hz up to 10^{10}Hz. Thus, measurements could be sensibly extended over a much wider frequency range than allowed by the Hamon's approximation.

3. The value of the measurement of these transient currents is not limited to obtaining loss-factor values at low frequencies. This type of measurement gives a clear way of separating the loss due to relaxation from the loss due to d.c.conductivity (see Chapter 3). The charging currents are superposed relaxation conductivity and d.c. conductivity, while the discharging currents are due to relaxation conductivity only. Thus a clear separation is achieved and the loss factor due to relaxation is obtained by transforming the discharging current. The steady state current gives the loss due to d.c. conductivity. Bridge and other a.c. methods yield the total loss without separation of the components.

4. The real and imaginary parts of complex dielectric

permittivity are not independent. If either part is determined over a substantial range of frequency (ideally $\omega=0$ to ∞), the other may be calculated. From a practical point of view it may not be possible to cover a sufficient range, and the measurement of both real and imaginary parts is desirable. Measurement of both provide a check of the data. The method is also independent of any prior assumption about the nature of the dielectric response function to the applied voltage.

1-4 Scope Of The Present Work:

The experiment described in this thesis was carried out at City University, dielectrics laboratory.

The design and method of construction of the apparatuse used in present experiment is given in Chapter.4, which follows the description of the type of the experimental methods used in such type of measurements, Chapter .3.

In Chapter.2, a study of the most important electric characteristics of solid insulators which are intimately associated with their use as dielectrics, is presented.

In Chapter.5, the results obtained in the present work are presented.

Suggestion for further work, Chapter.8, follows Chapter.6 and Chapter.7, which contian the discussion and analysis of the obtained results and conclutions respectively.

CHAPTER TWO.

THEORETICAL TREATMENT

2.1 INTRODUCTION

The present chapter is mainly concerned with the response of dielectric material to the electric field. A dielectric material can react to an electric field because it contains charge carriers that can be displaced. This response or the interaction which occurs between the externally applied field and the atoms or molecules of the material is referred to as polarization (p).

The polarization phenomenon, however, can be pictured by the formation of dipole chains which line up parallel to the field and bind countercharges at the surface (Fig. 2-1), thus the polarization can be considered to represent the density of the neutralized surface charge. Alternatively, the polarization can be taken to be eqivalent to the dipole moment per unit volume of the material.

This latter interpretation of (p) provides an entrance from the macroscopic into the molecular world i.e. microscopic. However, before embarking on the main theme, it is useful to start the chapter with the definition of dielectric permittivity, a parameter which will be used frequently throughout this thesis.

2.2 DIELECTRIC PERMITTIVITY

It is well known that the capacitance of the condenser increases if the space between its conductors filled with a dielectric material. If, now, C_o is the capacitance of the condenser with the region between the conductors evacuated and C its capacitance when this region is filled with a dielectric, then the ratio:

$$\frac{C}{C_o} = \varepsilon_r \qquad \text{------- (2-1)}$$

is found to be independent of the shape or the dimensions

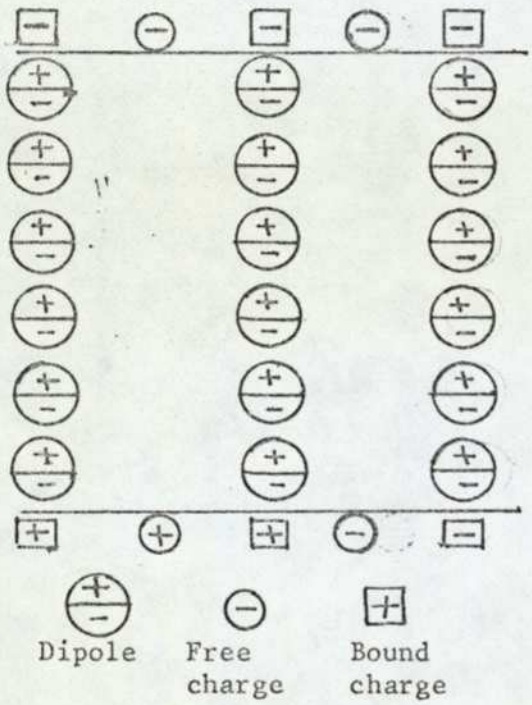

Fig. (2.1): Schematic representation of dielectric polarization (Von Hippel 1954).

of the conductors and is solely a characteristic of the particular dielectric medium used. ε_r is called the relative permittivity or the dielectric constant of the medium such that:

$$\varepsilon = \varepsilon_o \varepsilon_r \quad \text{-------} \quad (2\text{-}2)$$

where $\varepsilon_o = 8.854 \times 10^{-12}$ F.m^{-1} and is an electric constant which represents the permittivity of vacuum, whilst ε is the absolute permittivity of the material. Thus, a material having a dielectric constant of 2 in the c.g.s. system will have an absolute permittivity of $2 \times 8.854 \times 10^{-12}$ F.m^{-1}.

However, when an alternating voltage $V = V_o e^{j\omega t}$ of the angular frequency $\omega = 2\pi f$, is applying across the condenser ($C = \varepsilon_r C_o$) an alternating current, i, will flow its value being:

$$i = j\omega\varepsilon_r C_o V \quad \text{------} \quad (2\text{-}3)$$

provided that the dielectric is a "perfect" one. In general, however, an in-phase component of current equal to $V\omega\varepsilon'' C_o$ will appear corresponding to a resistive current between the condenser plates, such current is entirely due to the dielectric medium and is a property of it. The current i also has a component $V\omega\varepsilon' C_o$ - the charging or capacitive current - 90^o out of phase with alternating voltage.

In vector notation, the total current is the sum of the resistive current and the charging one, therefore,

$$i = j\omega (\varepsilon' - j\varepsilon'') C_o V \quad \text{-------} \quad (2\text{-}4)$$

where ε' is the measured dielectric constant of the dielectric material in the condenser and ε'' is its loss factor. The ratio $\varepsilon''/\varepsilon'$ represents the tangent of the loss angle δ, which is the phase-angle between

the total current i and the charging one.

2.3 MACROSCOPIC CONCEPT OF POLARIZATION

Insulators or dielectrics as pointed out in Chapter 1, are materials whose electrons are bound to the atomic structure by such strong forces that they are not free to move throughout the material under the influence of an applied electric field. The electrons can, however, be displaced very small distances relative to their nuclei whilst the atomic nuclei are displaced relative to one another. Although the distance moved is very small (10^{-10} - 10^{-11}m), since the displacement is limited by restoring forces which increase with increasing displacement, the centres of the positive and negative charges of these ~~non-polar~~ molecules are no longer coincident and the molecules are said to be polarised. If the material, on the other hand, is a polar one, a third process contributes to the polarizability (provided the dipoles are free to re-orientate). In the absence of an electric field, the permanent dipole moments of the molecules are distributed randomly in all directions, and change direction constantly because of the thermal motion of the molecules. When an electric field is applied, there is a tendency for the permanent dipoles to align themselves parallel to it. A net positive charge will be adjacent to the negative condenser plate and will neutralize some of the charge on it. Similarly, the negative charge will neutralize some of the charge on the positive condenser plate.

For an applied voltage V, the charge carried by the condenser ($C = \varepsilon_r C_o$) will be $Q = \varepsilon_r C_o V$).

Since the loss mechanism is not considered here, ε_r may be replaced by ε' (ε'' assumed zero, perfect dielectric), thus;

$$Q/\varepsilon' = C_o V \text{ ---------- (2-5)}$$

The implication is that, of the total charge Q, only a fraction Q/ε' contributes to neutralization of the applied voltage, the remainder $Q(1-1/\varepsilon')$ being bound charge neutralized by the polarization of the dielectric.

To obtain a clearer conception of the charge distribution and its effect, the total charge Q which is distributed over the plates of the condenser may be represented as a surface charge q_a per unit area and by introducing a new Vector D, the electric flux density, such as:

$$q_a \, dA = \bar{D} . \bar{ds} \text{ ---------- (2-6)}$$

where ds will be the area of a surface enclosing dA. Similarly, we allocate to the free charge density q_a/ε' a vector E, the electric field strength, by defining:

$$q_a/\varepsilon' \, dA = \varepsilon_o \bar{E} . \bar{ds} \text{ ---------- (2-7)}$$

and to the bound charge density a vector p, polarization as:

$$q_a(1 - 1/\varepsilon') \, dA = \bar{p} . \bar{ds} \text{ -------- (2-8)}$$

since:

$$q_a = q_a/\varepsilon' + q_a (1-1/\varepsilon')$$

we have from (2-6), (2-7) and (2-8):

$$q_a \, dA = \varepsilon_o \bar{E} . \bar{ds} + \bar{p} . \bar{ds} = \bar{D} . \bar{ds}$$

or in general:

$$\bar{D} = \varepsilon_o \bar{E} + \bar{p} \text{ -------- (2-9)}$$

But $\bar{D} = \varepsilon' \varepsilon_o \bar{E}$ for the dielectric, so that:

$$\bar{P} = \varepsilon_o (\varepsilon' - 1) \bar{E} \text{ ------ (2-10)}$$

From eq (2-9) $\bar{p}$ will have the same dimensions as $\bar{D}$, i.e. Coulomb meter^{-1}, whereas the electric field strength E can have a different physical meaning.

2.4 THE MICROSCOPIC CONCEPT OF POLARIZATION

On the macroscopic scale, the polarization p, was taken to represent the bound charges at the surface of the material such that:

$$P = \varepsilon_0 (\varepsilon'-1) \; E \quad \text{---------} \quad (2\text{-}11)$$

Alternatively, the polarization can be taken to be equivalent to the dipole moment per unit volume of the material. The dipole moment per unit volume may be thought of as resulting from the additive action of N elementary dipole moments $\bar{u}$,

$$P = N\bar{\mu} \quad \text{---------} \quad (2\text{-}12)$$

The average dipole moment of the elementary particle, furthermore, may be assumed to be proportional to the local electric field inside the dielectric. If this is denoted by E_{int}, being the value of the field acting on the dipole, then:

$$\bar{\mu} = \alpha \, E_{int} \quad \text{-------} \quad (2\text{-}13)$$

where α is called the polarizability of the dipole, i.e. is the average dipole moment per unit field strength. Substituting $(\bar{\mu})$ of eq (2-13) into eq (2-12) leads to a well known eq:

$$P = N \alpha E_{int} \quad \text{--------} \quad (2\text{-}14)$$

called Clausius' equation. This equation together with eq (2-11) are linking the macroscopically measured permittivity to three molecular paraments, the number N of contributing elementary particles per unit volume, their polarizability α, and the locally acting electric field E_{int}. This field will differ from the applied field E, owing to the polarization of the surrounding dielectric medium. It is the goal of the molecular theories to evaluate these parameters and thus to arrive at an understanding of the phenomenon polarization and its dependence on frequency

temperature, and applied field strength.

However, the polarizability α is defined in terms of dipole moment and its magnitude will be a measure of the extent to which electric dipoles are formed by the atoms and molecules. These may arise through a variety of mechanisms, any or all of which contribute to the value of α. Thus for convenience, the total polarizability will be regarded to be the sum of individual polarizabilities each arising from one particular model, i.e.:

$$\alpha = \alpha_e + \alpha_a + \alpha_o + \alpha_i \text{ ----- (2-15)}$$

where the terms on the right hand side are the individual polarizabilities which will now be discussed.

2.4.1. ELECTRONIC POLARIZATION (α_e)

An atom comprises a positively charged inner shell surrounded by electron clouds having symmetries determined by their quantum states. When a field is applied, the electron clouds are displaced slightly with respect to the positive cores, causing the atoms to take on an induced dipole moment Fig. (2-2a). This induced moment has all the characteristics of an assembly of dipoles produced by elastic displacement of electrons, which have natural frequencies equal, or higher than, those of visible light. The strength of the induced moment, μ_e for an atom is proportional to the local field in the region of the atom and is given by:

$$\mu_e = \alpha_e E_{int} \text{ -------- (2-16)}$$

where α_e is called electronic polarizability. However, when a large number of atoms or molecules are placed in an electric field, the microscopic mechanism of polarization is not as simple as the one described above. In

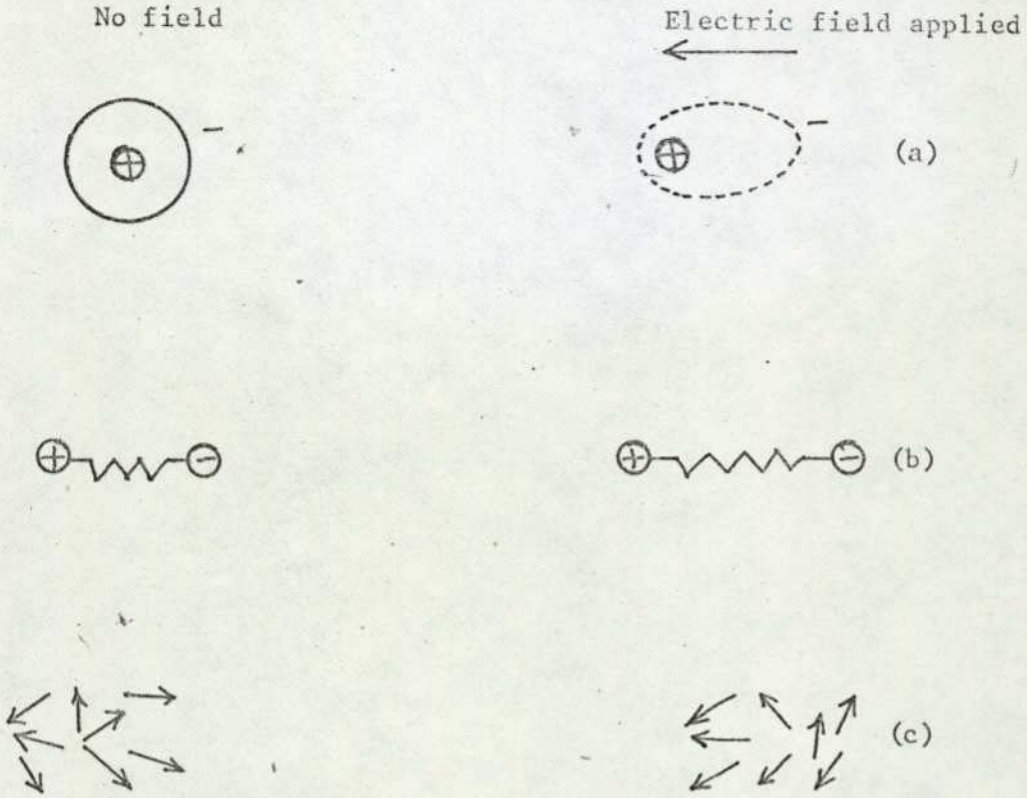

Fig. (2.2): Schematic representation of the four types of polarisation -

(a) electronic;
(b) atomic;
(c) orientation and
(d) space-charge.

addition to the electronic polarization, three other polarization mechanisms are distinguished: ionic or atomic, orientational, and space charge or interfacial polarization.

2.4.2 ATOMIC POLARIZATION (α_a)

When different atoms are present in molecules (as with polymers) the electrons involved in forming the bonds are displaced preferentially towards the stronger binding atoms, giving a bond moment. In an applied field the atoms are now immediately displaced relative to each other along its direction (Fig. (2-2b), giving an atomic polarization which for organic compounds is often only 5 - 10 per cent of the electronic polarization (since the interaction between electrons and nuclei varies as the distance between the nuclei changes, the atomic polarization will also contain a contribution from the electronic displacements relative to the nuclei). The atomic polarization is given by:

$$\mu_a = \alpha_a E_{int}$$

where α_a is the atomic polarizability of the molecules.

2.4.3 ORIENTATIONAL POLARIZATION (α_d)

This polarization is associated with dipolar substances. Here the molecules possess a dipole moment even in the absence of an applied field. Such a moment is not normally observed macroscopically because as a result of thermal agitation the molecules are orientated at random so that the average moment over a physically small volume is zero.

In the presence of an external field the dipoles experience a torque tending to orientate them is no longer zero (fig 2-2c).

To simplify the calculation of orientational polarization, which was first carried out by Debye (1929), it is assumed that the permanent electric moments P are independent of the temperature and applied field, that they are free to rotate and that the interaction energy between the dipoles is small relative to the thermal energy KT of each molecule. The potential energy of a dipole of moment μ in an electric field E is given by:

$$U = -\mu E \cos\theta$$

where θ is the angle between the dipole axis and the field E. In the absence of a field the number of dipoles $N(\theta)$ whose directions lie between angles θ and $\theta + d\theta$ with an arbitrary direction is proportional to the solid angle $d\Omega$ subtended by the elemental area $2\pi \sin\theta \, d\theta$ on a sphere of unit radius (Fig.2-3). When an electric field is applied along the z-direction then if the molecules possessed no thermal energy, they would all line up in the direction of the field acting on them. Because of thermal motion the number of dipoles corresponding to a solid angle $d\Omega$ must be weighted by the Boltzmann factor $\exp(-U/_{KT})$ so that:

$$N(\theta) = 2A\pi \sin\theta d\theta \exp\left(\frac{\mu E \cos\theta}{KT}\right) \text{ -------- } (2\text{-}17)$$

where A is a proportionality factor determined by the total number of dipole molecules per units volume.

The average moment of each molecule in the direction of the field is given by the ratio of the total moment due to orientation in the direction of the field to the total number of molecules:

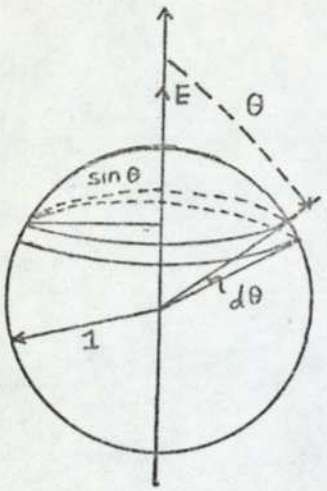

Fig. (2.3): Unit sphere model for calculating orientational polarization.

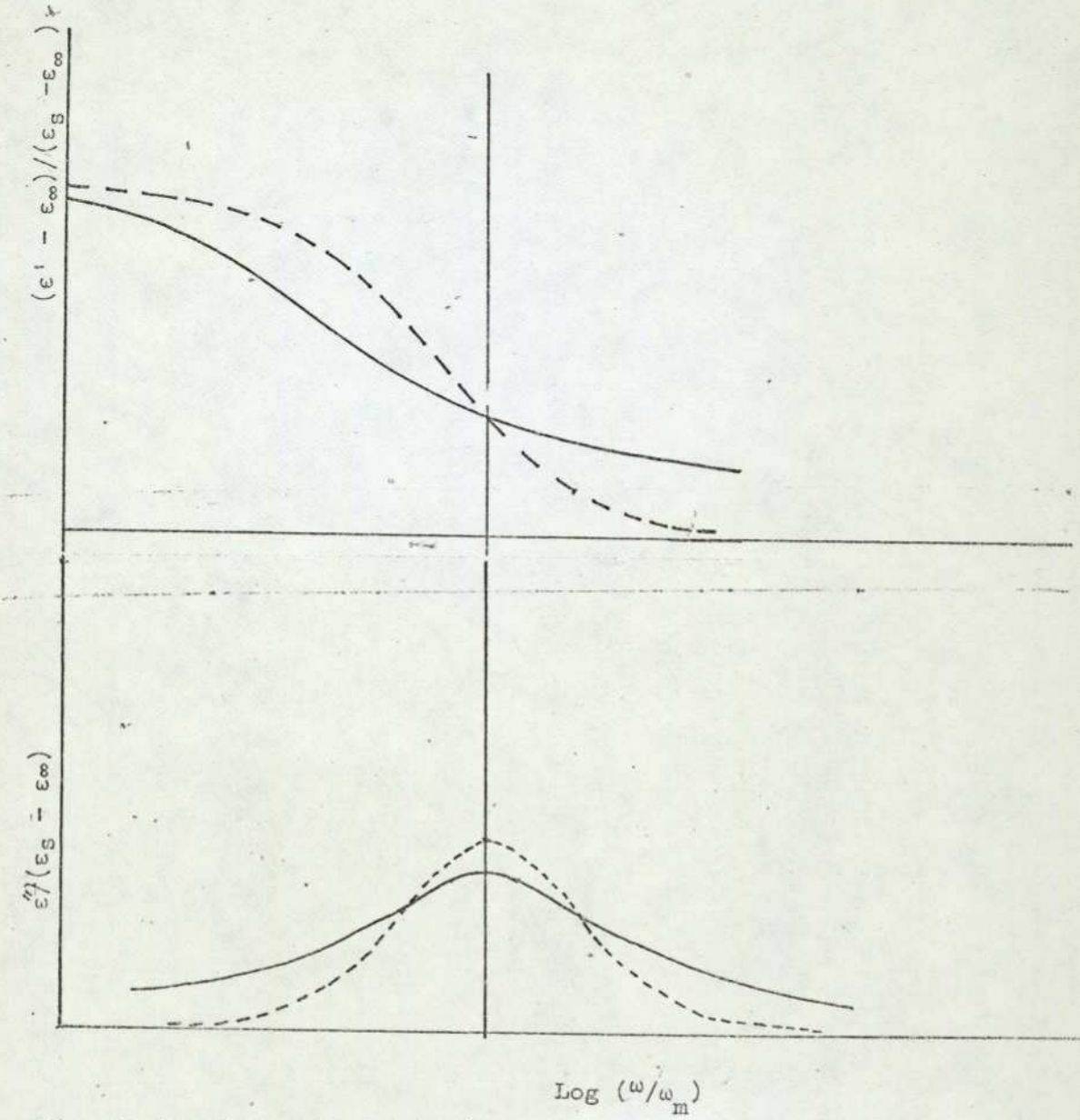

Fig. (2.4): Relaxation behaviour
- Polymeric material;
... Debye.

$$\mu_{av} = \frac{\int_0^{\pi} A 2\pi \sin\theta \exp\left(\frac{\mu E \cos\theta}{\kappa T}\right) \mu \cos\theta \, d\theta}{\int_0^{\pi} A \exp\left(\frac{\mu E \cos\theta}{\kappa T}\right) 2\pi \sin\theta \, d\theta}$$

The integrals give (see Von Hippel, p 148)

$\mu_{av} = \mu[\coth a - 1/a] = \mu L(a)$ -------- (2-18)

where $a = \mu E/\kappa T$. The function $L(a)$ is known as the Langevin function. From the practical point of view, even for highly polar molecules and fields, of the order of several hundred kilovolts per cm, the value of $a \ll 1$ and the Langevin function may be approximated to $a/3$ (Zaky, 1973), so that:

$$\mu_{av} = \frac{\mu^2 E}{3 \kappa T} = \alpha_o E_{int}$$

where α_o is the orientational polarizability.

By adding the above three polarizabilities, the total dipole moment per molecule is:

$$\mu = (\alpha_e + \alpha_i + \frac{\mu^2}{3\kappa T}) E_{int} \text{ -------- (2-19)}$$

This equation is known as the Langevin-Debye formula.

2.4.4 INTERFACIAL OR SPACE CHARGE POLARIZATION

It usually arises from the presence of electrons or ions capable of migrating over distances of macroscopic magnitude. Some of these charge carriers tend to become trapped and accumulate at lattice defects, impurity centres, voids, strains or at electrode surfaces and so distort the field and produce an apparent increase in the dielectric constant. Interfacial polarization is of particular importance in heterogeneous or multiphase materials. Due to the differences in the electrical conductivity of the phases present, charges move through the more conducting phases and build up on the surfaces that separate these from the more resistive phases. Effectively, each conducting

region will become polarized so that there is an apparent increase in the average moment of the molecules given by:

$$\mu_s = \alpha_s E_{int}$$

where α_s is the interfacial or space charge polarizability. Interfacial polarization, however, is of importance in practical dielectric measurements, since most commercial insulators such as plastic with fillers, polymer with plastic and sintered ceramics are usually heterogeneous and, therefore, special attention will be given to this subject in Chapter (5) and Appendix (E).

2.4.5 INTERNAL ELECTRIC FIELD

It was mentioned earlier that the internal electric field E_{int} is different from the externally applied field E and the relation between the two fields (see text books) is:

$$E_{int} = E \left(\frac{\varepsilon_r+2}{3}\right) \text{ -------- (2-20)}$$

substituting this value of the field in eq (2-11) and (2-14) gives:

$$P = \varepsilon_o(\varepsilon_r-1)E = \frac{1}{3} E(\varepsilon_r+2)\, N\, \alpha$$

or:

$$\frac{N\alpha}{3\varepsilon_o} = \frac{\varepsilon_r - 1}{\varepsilon_r+2} \text{ ---------- (2-21)}$$

If M is the molecular weight of the material and ρ the density, then the number of molecules per gram molecule No (Avogadro's number) is N M/ ρ and eq(2-21) was written as:

$$\frac{N_o\alpha}{3\varepsilon_o} = \frac{(\varepsilon_r-1)}{\varepsilon_r+2} \frac{M}{\rho} \quad m^3 \text{ ------ (2-22)}$$

This equation is known as the Clausius-Mosotti equation and the left hand term is sometimes referred to as the molar polarization. Eqs.(2.20-2.22) are considered as good first approximations for E_{int} values and approximately valid for ionic crystals and non-polar dielectrics.

2.5 DIELECTRIC IN ALTERNATING FIELDS

In the foregoing sections the permittivity has been calculated for the case where the applied field is steady, that is when the dielectric is in equilibrium with the field. The present section will discuss dielectric behaviour when the frequency of the externally applied alternating field is such that there is an observable lag in the attainment of equilibrium.

When a dielectric material is subjected to an alternating field the orientation of the dipoles, and hence the polarization will tend to reverse every time the polarity of the field changes. As long as the frequency remains low, the polarization follows the alternations of the field without any significant lag and the permittivity is independent of the frequency and has the same magnitude as in a static field. When the frequency is increased the dipoles will no longer be able to rotate sufficiently rapidly so that their oscillations will begin to lag behind those of the field. As the frequency is further raised, the permenant dipoles, if present, in the medium, will completely be unable to follow the field and the contribution to the static permittivity from this molecular process, the orientational polarization ceases. At still higher frequencies the relatively heavy positive and negative ions cannot follow the field variations so that the contributions to the permittivity from the atomic or ionic polarization ceases and only the electronic polarization remains.

The above effects lead to a fall in the permittivity of a dielectric material with increasing frequency, a phenomenon which is usually referred to as anomalous dielectric dispersion.

Dispersion arising during the transition from full atomic polarization to negligible atomic polarization is usually referred to as resonance absorption. This is beyond the scope of this thesis and will not be discussed. On the other hand, dispersion arising during the transition from full orientational polarization at low frequencies to negligible one at the high radio frequencies is referred to as dielectric relaxation.

2.5.1 DIELECTRIC RELAXATION

Relaxation phenomena are associated with the frequency dependence of the orientational polarization and hence with polar dielectric substances. Orientation polarization, however, involves atomic groups, and the forces opposing "rotation" of the molecular dipoles are more viscous than elastic (Baird, 1968). Thus, when a constant field is applied the dipolar polarization does not attain its full value immediately and the polarization decays over a finite time (t) after its removal, such that the rise and decay of polarization p is exponential of the form $P=P_0e^{-t/\tau}$ where (τ) is the relaxation time.

When an alternating electric field is applied, Debye relaxation behaviour occurs (Fig.2.4). At very high electrical frequencies the molecular dipoles have no time to change their orientation in keeping with the field since its period is much less than the relaxation time τ and the dielectric constant comprises only the contributions from the electronic and atomic polarization (ε_∞) whilst there

is no power loss. At very low frequencies, however, the period of the applied field is large compared with the relaxation time (τ) of the molecular dipoles, and the dipolar polarization is able to build up to its full extent. The static dielectric constant (ε_s) now contains the full contribution from the dipoles whilst the power loss is again zero because the polarization can keep in phase with the applied field. In between the two regions of constant relative permittivity a step occurs centred around the angular frequency, ω_m (equal to $1/\tau$). In this region, the dipolar polarization cannot keep in phase with the applied field, resulting in appreciable power loss with maximum value at ω_m.

The loss tangent tan δ also passes through a peak, but the maximum value occurs at a frequency slightly different from ω_m. The formula for ε' and ε'' may be written: (see almost all the text books)

$$\varepsilon'(\omega) = \varepsilon'_\infty + \frac{(\varepsilon_s - \varepsilon_\infty)}{(1+\omega^2\tau^2)} \text{ ---------- (2-23)}$$

$$\varepsilon''(\omega) = (\varepsilon_s - \varepsilon_\infty)\omega\tau/(1+\omega^2\tau^2) \text{ ------- (2-24)}$$

and:

$$\tan\delta = \frac{\varepsilon''}{\varepsilon'} = (\varepsilon_s - \varepsilon_\infty)\,\omega\tau/(\varepsilon_s + \varepsilon_\infty\omega^2\tau^2) \text{ ---(2-25)}$$

The maximum value of ε'', ε''_m occurs when $\omega = \omega_m = 1/\tau$

$$\varepsilon''_m = (\varepsilon_s - \varepsilon_\infty)/2 \text{ ---------- (2-26)}$$

The value of tanδ, $(\tan\delta)_m$, occurs at a slightly different frequency given by (Frolich, 1958).

$$\omega_m = \frac{1}{\tau}\sqrt{\varepsilon_s/\varepsilon_\infty} \text{ ---------- (2-27)}$$

and:

$$(\tan\delta)_m = (\varepsilon_s - \varepsilon_\infty)/2\sqrt{\varepsilon_s\varepsilon_\infty} \text{ ------ (2-28)}$$

With polymeric materials, for example, the pattern of behaviour is similar but the step in ε' and the peaks in ε''

and tan δ are spread out over a wider range of frequency (Fig. 2-4) whilst the peak height is lower than in eqs (2-26) and (2-28), indicating a distribution of relaxation times.

Although the reason for these deviations will be discussed latter in Chapter (6) when the different theories of dielectric relaxation will be examined to find out the causes for dielectric dispersion, there is still no harm to discuss some of these distribution theories briefly since their occurence before Chapter-6 is essential. Two common empirical distributions, the Fuoss-Kirkwood and the Cole-Cole plus that of Forlich Theory are given here:

(a) Fuoss-Kirkwood (1941)

The result of an intensive investigation on many polymeric materials led Fuoss-Kirkwood to assume a formula which is similar to that of Debye's eq., but differs in adding a new parameter (β) such that,

$$\varepsilon''(\omega) = \frac{\beta(\varepsilon_s - \varepsilon_\infty)\ (\omega\tau)^{\beta}}{1 + (\omega\tau)^{2\beta}}$$

The maximum value of ε'', ε''_m occurs when $\omega = \omega_m = \frac{1}{\tau}$ where τ is the most probable relaxation time and:

$$\varepsilon'' = \beta(\varepsilon_s - \varepsilon_\infty)/2$$

(b) Cole-Cole (1941)

On the other hand, Cole-Cole assumed on the basis of many experimental results another formula, i.e.

$$\varepsilon'(\omega) - \varepsilon_\infty = \frac{(\varepsilon_s - \varepsilon_\infty)\left\{1 + (\omega\tau_o)^n \cos(n\pi/2)\right\}}{1 + 2(\omega\tau_o)^n \cos(n\pi/2) + (\omega\tau_o)^{2n}}$$

$$\varepsilon''(\omega) = \frac{(\varepsilon_s - \varepsilon_\infty)(\omega\tau)^n \sin(n\pi/2)}{1 + 2(\omega\tau_o)^n \cos(n\pi/2) + (\omega\tau)^{2n}}$$

The maximum value of ε'', ε''_m occurs when $\omega = \omega_m = \frac{1}{\tau_o}$ where τ_o is the most probable time and:

$$\varepsilon_m'' = \frac{(\varepsilon_s - \varepsilon_\infty)}{2} \quad \frac{\sin(n\pi/2)}{1+2\cos(n\pi/2)}$$

In these equations β and n determine the widths of distributions and vary between 0 and 1 (values near 0 indicating a very wide distribution; values equal to 1 indicating a single relaxation time).

(c) Frolich (1948)

Instead of using β or n, Frolich assumed minimum and maximum relaxation times τ_1 and τ_2 and used a distribution function of the form:

$$f(\tau) = 1/\tau A \quad (\tau_1 < \tau < \tau_2)$$

where:

$$A = V/kT$$

$$f(\tau) = 0 \qquad (\tau_1 < \tau \quad \tau, < \tau)$$

The above distribution function - corresponding to an equal distribution of potential barriers over a range V, depends on temperature.

2.5.2 DIELECTRIC RELAXATION IN SOLID POLYMERS

Dielectric measurements on a great number of polymers have been done by many workers. As a result of their efforts, the nature of the relaxation processes have gradually become clearer. It now appears that the dielectric relaxation processes observed in solid polar polymer are usually called α, β & γ relaxations in order of appearance from the high temperature side.

The α- loss peak corresponds to the relaxation observed at highest temperature (at a given frequency) or the lowest frequency (at a given temperature). However, for polymers in the amorphous state α- relaxation region associated with the glass-transition (T_g) is observed around and above T_g and referred to as the primary or glass-rubber relaxation (McCrum, 1967). From a molecular

point of view, it has been widely accepted that the glass-rubber relaxation results from large scale conformational rearrangements of the polymer backbone (Ishida, 1961).

Such rearrangement occurs by a mechanism of hindered rotation around main chain bonds. The hinderance or frictional forces Brownian motions) can be described in terms of viscous or frictional forces which result from interactions of the moving segment with neighbouring molecules or with segments within the same chain (internal viscosity). The β and γ regions occur below T_g when the polymer is in the glass state, and the main chain is effectively frozen. These relaxation regions are ascribed to the side groups of the polymer molecules undergoing restricted rotation accompanied by local distortions of the main chain (Yamafuji, 1960).

However, at temperatures well above T_g, the shape of the α- absorption curve does not change but segments of amorphous polymer chains can easily jump from one equilibrium position to another and so called segmental motion is highly excited. That is to say, the temperature dependence of experimental relaxation time (τ) is generally assumed to take the Arrhenius form:

$$\tau = A \exp(\Delta H/RT)$$

where ΔH is apparent activation energy for the dielectric process and T is the absolute temperature. If (τ) is measured over a wide range of temperature, however, plot of $\log \tau$ against $1/T$ is often non-linear and ΔH derived by tangents at various temperatures on this plot, increases with decreasing temperature.

It is generally accepted that at frequencies and temperatures corresponding to a relaxation region, materials absorb energy and maximum loss occurs. The position of this loss peak at a given temperature, besides its dependence on frequency of the applied field also depends on some other parameters related to the sample structure, i.e.:

Molecular Weight

With amorphous polymers the temperature of maximum loss for the αrelaxation increases rapidly at first with increasing molecular weight but then levels off and remains virtually constant for molecular weight above 10.000 (Wurstlin, 1949). This can be explained by the plasticizing effect of chain ends, reduction in free volume and an increase in activiation energy occuring as molecular weight is increased up to about 10.000 and this effect becoming negligible thereafter. This increases in activation energy lengthens the retardation times and shifts the loss peaks to lower frequencies or higher temperatures. With polystyrene and polyvinyl acetate, the activation energy for theα-relaxation has been shown to pass through a maximum value as molecular weight increases and then to fall because the relaxing molecular volume is diminished, whilst the relaxation was affected by the width of the molecular weight distribution. (Kolesov,1967).

Crystallinity and Orientation

Increasing crystallinity will reduce the size of loss peaks associated with disordered regions and increase the magnitude of those arising from crystalline regions (Ishida, 1962). Furthermore, increasing crystallinity can

shift the position of the loss peak associated with chain segmental motion to higher temperatures and can also affect its shape (Curtis, 1961). Crystalline polymers shift the temperature of maximum loss still higher (Oakes, 1954). Raising crystallinity broadens the normalised loss peaks of the relaxation, particularly on the low frequency side giving rise to assymetry (Ishida, 1962).

Crosslinking:

Sufficient crosslinking will hinder segmental motion thus lowering the frequency of maximum loss or raising the temperature of maximum loss (Schmieder, 1953). Crosslinking also broadens the loss peaks for rubber (Mason, 1964) thus giving rise to wider distribution of retardation times, and it may also reduce the magnitude of the loss peak and the dielectric increment $(\varepsilon_s - \varepsilon_\infty)$.

Ageing

Ageing may change the dielectric behaviour of plastics owing to the action of light, ultra violet radiation, heat or outdoor weathering, arising from scission of chain molecules crosslinking or oxidation. These may introduce dipolar groups not previously present; they may cause ionic conductivity with a consequent rise in loss tangent at low frequencies and elevated temperatures, or they may cause a shift in retardation times with a consequent movement of the loss peak, possibly into a working range of frequency and temperature (Jackson, 1945). Thermal ageing of Polyvinyl chloride displaced the loss peak to higher temperatures, increased the activation energy and reduced the size of the peak owing to the formation of a wider distribution of retardation times (Bouvier, 1970).

Plasticizers

The addition of a plasticizer usually shifts the loss peaks due to segmental motion in amorphous polymers to lower temperatures at a fixed frequency or to higher frequencies at a given temperature (Broens, 1955) and sometimes broadens them as well. Plasticization also reduces the activation energy and relaxation times for both α and β relaxation. Non polar polymers containing various dipolar plasticizers showed loss peaks considerably larger than that for the pure material owing to dipolar orientation in the added plasticizer (Davies, 1967). The comparatively low activation energy found was attributed to the plasticizers being dispersed only in amorphous regions (Boyd, 1959).

Impurities

Impurities may markedly increase the dielectric losses and shift the α relaxation peak to lower temperatures (Ishida, 1964). At low frequencies the dielectric loss of water arises from ionic conduction, but at microwave frequencies relaxation occurs (Von Hippel, 1954). When absorbed by plastics it may increase the dc conductivity and introduce interfatial polarization, showing relaxation at low frequencies whilst augmenting dielectric losses already present at high frequencies, in addition to any plasticizing action. Thus, water shifts the relaxation peak of polymethyl methacrylate to lower temperatures and gives rise to an additional loss region (Scheiber, 1957).

Fillers

Many fillers are used for incorporation into plastics to improve mechanical properties, to reduce costs and, occasionally, to improve certain electrical properties.

Fillers may introduce dielectric loss through the relaxation of their own orientation polarization or, because of interfacial polarization arising from the two phase system. If the filler is relatively non-conducting and non polar the main effect of introducing it will be to change the relative permittivity (Deloor, 1956) without increasing the loss factor much but if the filler is relatively conducting the loss can be considerably increased because of interfacial polarization (Van Beek, 1967). Obviously, if the filler or polymer absorbs moisture, the effects may be even more serious and complex owing to increased conduction and interfacial polarization losses.

2.5.3 DIELECTRIC LOSSES

In discussing the losses which occur in a dielectric when it is subjected to an alternating field, we shall first consider the case in which the permittivity of the dielectric may be respresented by its static value, that is, the frequency of the applied field is sufficiently low to permit the permanent and induced dipoles to follow the field variations without any measurable lag. It will be assumed that the dielectric is ideal or perfect in the sense that its ohmic conductivity is zero. The relationship between the dielectric displacement density and the sinusoidally varying field intensity is given by:

$$D=\varepsilon_o\varepsilon_r E = \varepsilon_o\varepsilon_r E_o \cos\omega t = R_e \left\{\varepsilon_o\varepsilon_r E_o e^{j\omega t}\right\} \text{--------(2-29)}$$

The displacement or charging current density is, by definition:

$$J_d = \frac{dD}{dt} = R_e \left\{\varepsilon_o\varepsilon_r j\omega E_o e^{j\omega t}\right\} = -\varepsilon_o\varepsilon_r \omega E_o \sin\omega t$$
$$= \varepsilon_o\varepsilon_r \cos(\omega t + 90^\circ) \text{ ------- (2-30)}$$

So that the current density leads the field intensity by a temporal phase angle of 90^{o}. The energy absorbed per unit volume of the dielectric material (energy density) and per second is given by:

$$U = \frac{\omega}{2\pi} \int_{o}^{2\pi/\omega} J_d E dt \text{ -------- (2-31)}$$

substituting for J_d and E, we have:

$$U = -\frac{\omega}{2\pi} \int_{o}^{2\pi/\omega} \varepsilon_o \varepsilon_r \omega E_o^2 \sin\omega t \cos\omega t \, dt = 0 \text{ ------- (2-32)}$$

So that the dielectric does not absorb any energy from the field.

The next case is when the frequency of the alternating field to which the ideal dielectric is subjected is sufficiently high for the polarization to be frequency dependent. This frequency dependent leads to a complex permittivity:

$$\varepsilon^* = \varepsilon' - j\varepsilon'' \text{ ---------- (2-33)}$$

Hence, the corresponding displacement current density is:

$$J_d = R_e \{ \varepsilon_o (\varepsilon' - j\varepsilon'') j\omega E_o e^{j\omega t}$$

$$= \varepsilon_o \varepsilon' E_o \sin\omega t + \varepsilon_o \varepsilon'' \omega E_o \cos t \text{ ------- (2-34)}$$

Equation (2-34) shows that the displacement current now consists of two parts. The first part is the same as eq (2-30) and, therefore, does not lead to any energy absorption. The second part which is associated with ε'', is in phase with the applied field, and the corresponding energy density is:

$$U = \frac{\omega}{2\pi} \int_{o}^{2\pi/\omega} \varepsilon_o \varepsilon'' E_o^2 \cos^2 \omega t \, dt$$

$$= \frac{\omega \varepsilon_o \varepsilon'' E_o^2}{2} \text{ ---------(2-35)}$$

This energy appears as heat in the dielectric. Eq (2-35) shows that the energy density absorbed by the dielectric is proportional to ε'' and, consequently, ε'' is known as the

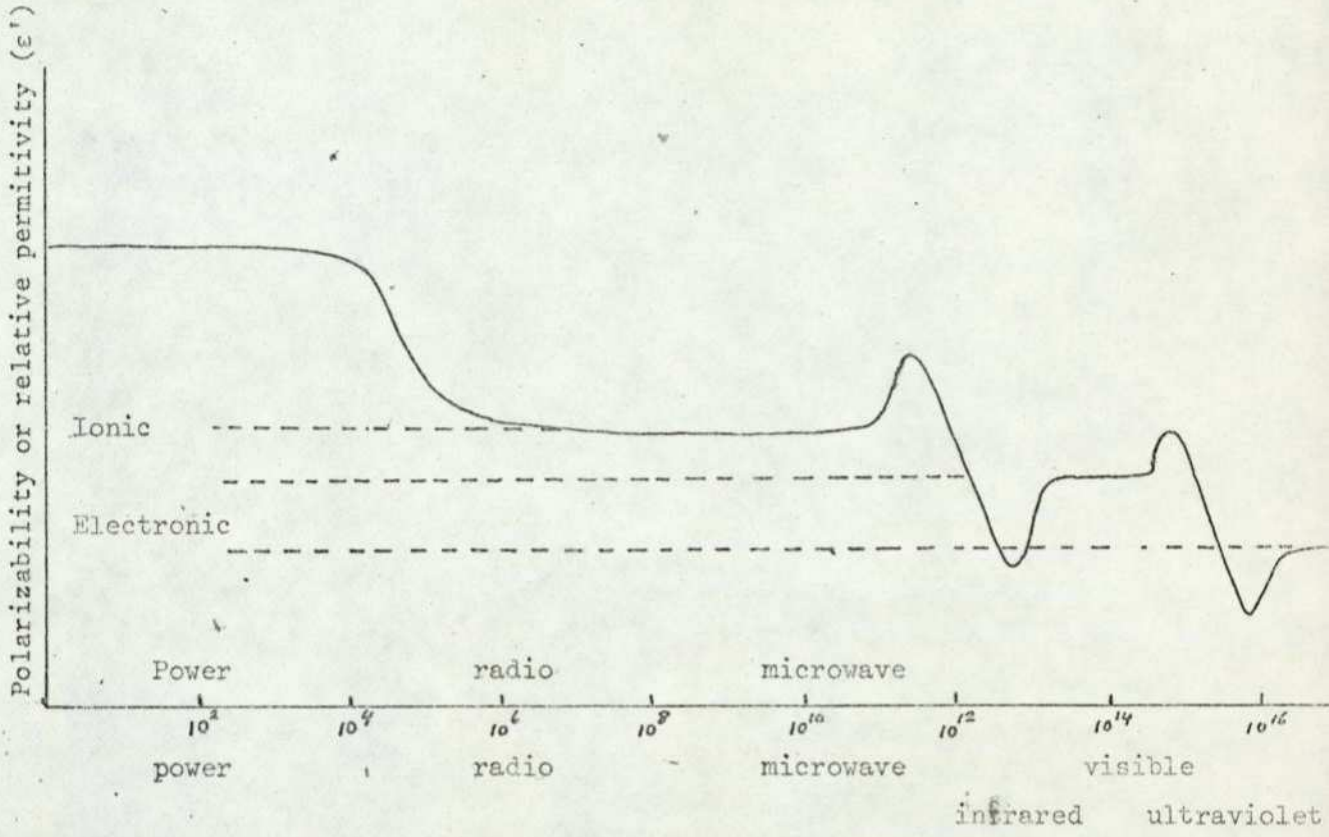

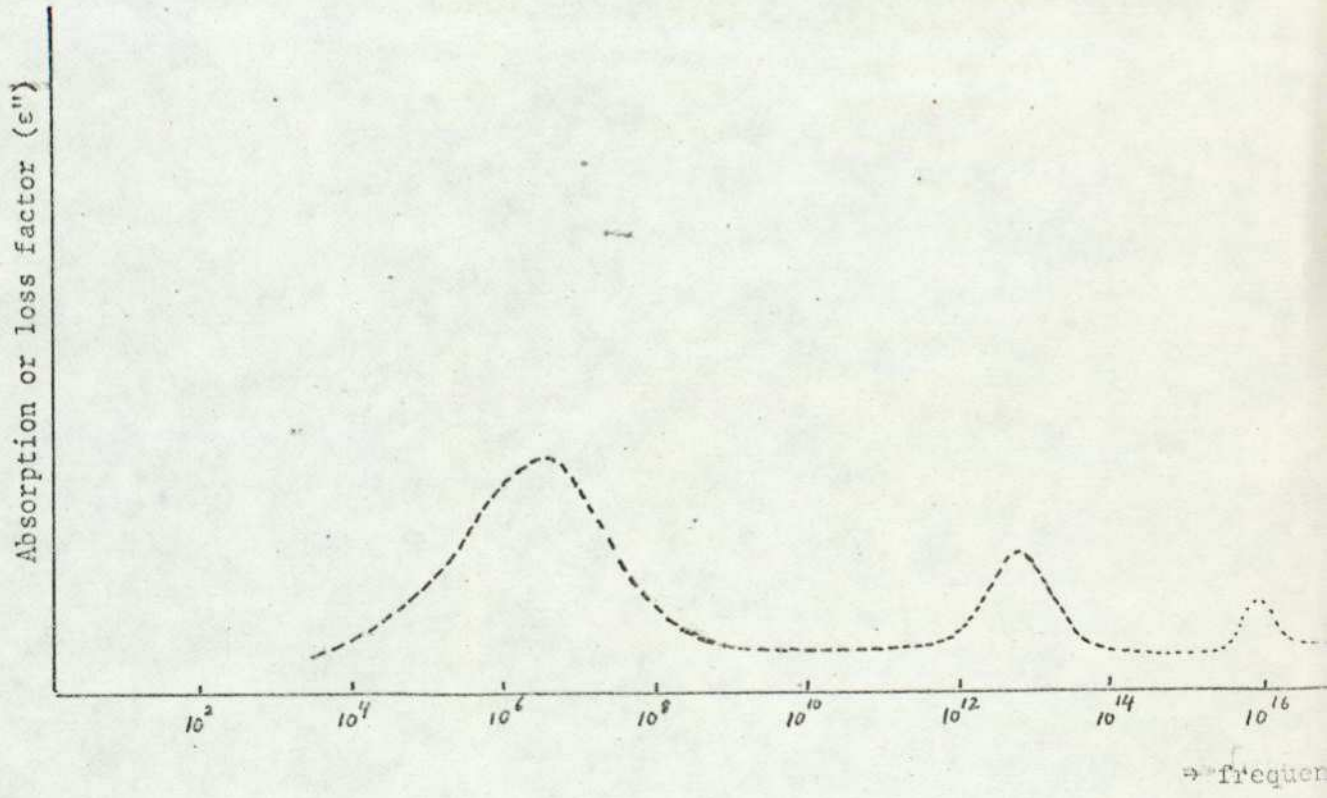

Fig. (2.5): Diagramatic representation of the variation of the permittivity and loss factor with frequency.

loss factor; the variation of ε'' with frequency gives the absorption characteristic or spectrum of the dielectric.

A knowledge of the dielectric loss of dielectric materials used for insulation or in the manufacture of condensers is of primary importance in high frequency electrical engineering problems. Excessive losses will not only reduce circuit efficiency but will cause undesirable heating which may lead to electrical or mechanical failure of the dielectric. Figure (2-5) summarizes the frequency dependence of ε' and ε'' for a dielectric having the three most important types of polarization.

In practice, it is found convenient to specify the absorption losses in a dielectric (at a given frequency and temperature) by the loss tangent. Thus, eq.(2-34) may be rewritten as:

$$J_d = \varepsilon_o \omega E_o |\varepsilon_r| \sin(\omega t - \delta)$$

where:

$$\sin \delta = \varepsilon''/|\varepsilon_r| \quad , \qquad \cos \delta = \varepsilon'/|\varepsilon_r|$$

and the loss tangent:

$$\tan \delta = \varepsilon''/\varepsilon'$$

where δ is the angle between the total displacement current J_d and its losses component.

CHAPTER THREE.

Experimental Methods

3.1 Introduction:-

The electric properties of a dielectric substances are usually described in terms of the complex dielectric permittivity $\varepsilon^* = \varepsilon' - j\varepsilon''$. For most materials this quantity is independent of the strength of the electric field over a wide range, but its value varies widely for different materials. For a specific material the dielectric constant is a function of the frequency of the applied voltage and also depends, in decreasing order, on other parameters, such as temperature, pressure..... etc.

Determination of dielectric constant can be made by measuring the response of the material to an externally applied electric field. The response can be obtained by a number of methods, which divide into two main categories namely: alternating current and direct current measurements. The choice of measurement technique is largely determined by the range of frequencies that are of interest for a given material. Table (3.1) summarizes the methods which are employed in particular regions within the large frequency range and shows that the lowest frequency obtainable with conventional bridges based originally on Weingarten's design (1955) could be as low as 5×10^{-2} Hz (Schieber, 1961). These methods however, have the disadvantage of being time consuming and also suffer from errors due to stray capacitance to earth. The latter can be made negligible in certain circumstances, or eliminated by an additional Wagner earth network, (Churcher and Dannutt, 1926). More recently, the availability of the operational amplifier led (Roberts, 1966) to use it in the bridge, to adjust the voltage and phase at various terminals, and to isolate voltage source from loads. By the use of a phase-sensitive detector, it was possible to establish a balance during the cycle time, thus reducing the time measurement substantially. Nevertheless this

Frequency Range Hz	Method
10^{-4} to 10^{-1}	d.c Transient measurements
10^{-2} to 10^{2}	Ultra low frequency bridge
10^{1} to 10^{7}	Schering bridge Transformer bridge
10^{5} to 10^{8}	Resonance circuits
10^{8} to 10^{9}	Coaxial line
10^{9} to 3×10^{10}	Cavity resonator Coaxial lines and waveguides

Table (3.1). Experimental Methods. (William's, 1967)

method is still not suitable for polymeric solid measurements, because in that case relaxation time, especially at low temperature is in general very long i.e. several hundred seconds, thus indicating that losses in the material will occur at frequencies below the region of 10^{-3} Hz. Hence the dielectric response of polymers at very low temperature cannot be measured by continous a.c. methods, and therefore a d.c. transient method is required. Accordingly, the classical bridge methods of measuring dielectric permittivity will not be given that much of consideration, since details of these methods can be found in the textbooks of (Von Hippel, 1954). (Smyth, 1955). (Daniel, 1967). etc, special emphasis will be given below to the direct current transient method, since its value and ease of operation have not been fully appreciated by many workers.

3.2 DC Step - Function Measurements (10^{-4} - 10^{-1} Hz):-

In principle, the simplest way of measuring the dielectric properties of a material, is to subject it to an electric field, and see how the polarization develops with time. Figure (3.1) gives a simple circuit to illustrate the method. Switch (S_1,a) is closed, the sample C_x reponds to the step voltage V giving rise to a transient charge current through C_x which is measured by the amplifier circuit. After charging equilibrium is attained switch (S_1,b) is closed and the transient discharge current is measured. Figure (3.2) shows typical charging discharging dielectric current after application and sudden removal of a step - voltage respectively. The measurement of charging and discharging currents demands an electrometer of very high input impedance, sufficient gain and time constant short compared with the time constant of the sample. The current in the circuit can be measured as a voltage across R_L which is equal and opposite to that across R_s. This can be achieved by feedback arrangement, which tends to degrade R_s by a factor equal to the amplifier gain, and ensures that the voltage drop is across the sample only.

The relation between these transient currents and a.c. dielectric behaviour has been known for a long time. When an alternating voltage V is applied to a capacitor with a dielectric filling the space between the plates, the resultant alternating current I is given by

$$I = I_L + I_c \qquad \ldots\ldots\ldots\ldots\ldots \quad (3.1)$$

as shown in Fig (3.3). The current I_c (equal to $j\omega C_s V$, where ω is the angular frequency equal to $2\pi f$) charges the capacitor to the required instantaneous voltage and leads the voltage by 90^o, as signified by the presence of ($i = \sqrt{-1}$) in form of $j\omega C_s V$, but the component I_L, in phase with V, arises when the polarization of the specimen cannot keep in phase

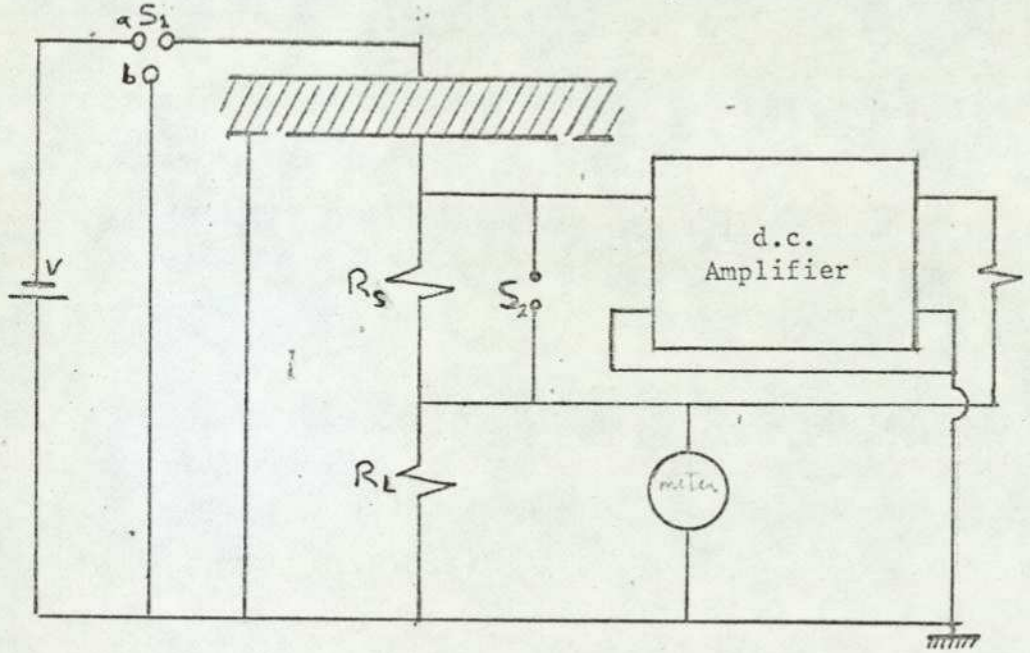

Fig. (3.1): Schematic Circuit of apparatus for investigating transient response of dielectrics subjected to step voltage.

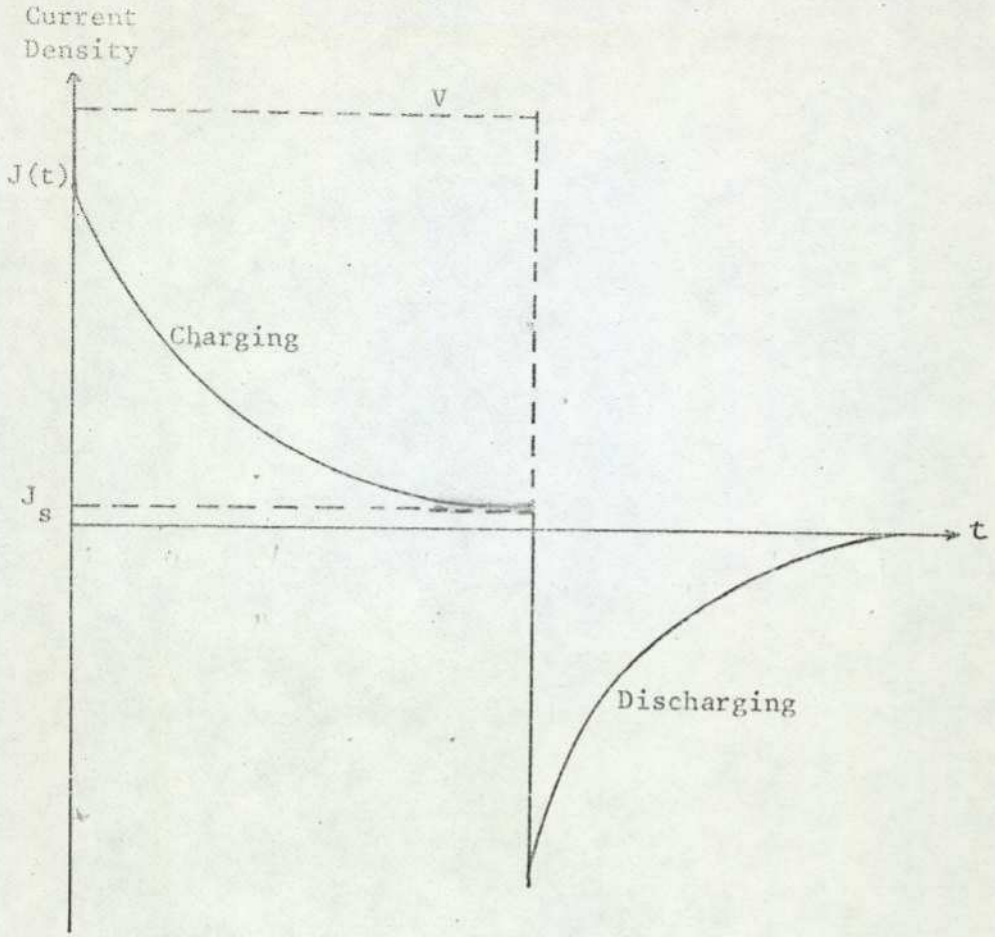

Fig.(3.2): Schematic diagram showing the charging discharging current of dielectric polymer after application and sudden removal of a step-voltage.

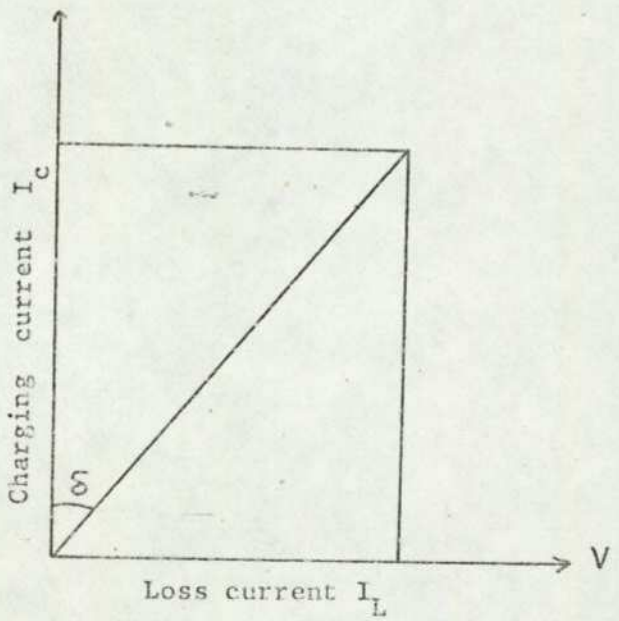

Fig.(3.3): Vector diagram for a capacitor with a dielectric filling the space between the plates.

with V and causes dissipation of energy as heat. The current component I_L will also contain a component due to the d.c. conductivity of the material. In practice I is proportional to $C_o V$ and may be written

$$I = j\omega(\varepsilon' - j\varepsilon'') C_o V \quad \ldots\ldots\ldots\ldots\ldots \quad (3.2)$$

where C_o is the value of the capacitance with air or a vacuum between the plates. In the other words $C_o = A/d\ \varepsilon_o$, where A is the area of the condenser, d the distance between the plates and ε_o denoted as the air permittivity. Hence

$$I = j\omega(\varepsilon' - j\varepsilon'') \frac{A}{d}\ \varepsilon_o V$$

or

$$J = j\omega\varepsilon_o\varepsilon' E + \omega\varepsilon_o\varepsilon'' E \quad \ldots\ldots\ldots\ldots\ldots \quad (3.3)$$

where J = I/A the current density and E the field strength between the plates is V/d V/m.

When a step voltage is applied to the same material, the direct current which flows behaves as shown in Fig (3.2). If i(t) represents the (reversible) part of the anomalous charging current, or the discharging current at a time t, after the application or removal of the steady voltage V, the i(t) (or the current response $\phi(t)$ per unit voltage) and the complex dielectric constant are related by the equations (Gross, 1941)

$$\varepsilon'(\omega) = \left[\frac{1}{C_o}\int_o^\infty \phi(t) \cos \omega t\, dt\right] + \frac{C_a}{C_o} \quad \ldots. \quad (3.4)$$

$$\varepsilon''(\omega) = \left[\frac{1}{C_o}\int_o^\infty \phi(t) \sin \omega t\, dt\right] + \frac{G}{\omega C_o} \quad \ldots. \quad (3.5)$$

Where C_a is the capacitance at very high frequencies, G is the steady - state d.c. conductance, and ω is the angular frequency. The first terms on the right-hand side of these equations represent the contributions to the dielectric constant and loss of the relaxation process in the material.

The second term on the righthand side of equation (3.4) gives the contribution to the dielectric constant of the virtually instantaneous electronic and atomic polarization, while that on the right-hand side of equation (3.5) gives the contribution to the loss of the d.c. conductivity of the material, $\phi(t)$ is known as the relaxation function of the material.

It should be remembered, however, that:-

a. The derivation of equation (3.4) and (3.5) was based on the assumption that the superposition principle (Baird. M.E, 1968) is valid. This states that each step change in voltage produces the same current as if it were acting alone and the total current at any time is then the algebraic sum of the currents appropriate to all the step changes. It is also assumed that the currents are proportional to the applied voltages. Thus in Fig(3.4) a step voltage is applied at t = 0 to a capacitor with a dielectric between the plates. After the initial surge a relatively small anomalous charging current I_c (not including the steady state current) is produced which may decay over a period of months. If, now, the capacitor plates are short circuited after a time t_o, an opposite discharging current $-I_d$ (of magnitude I_d) is produced which decays according to the same law. The discharging I_d may be represented at any time $t_1 > t_o$ in terms of the current $-I_c$ starting at $t = t_o$ and the positive charging current $+I_c$ extrapolated to $t = t_1$. According to the law of superposition;

$$-I_d(t_1) = -I_c(t_1 - t_o) + I_c(t_1) \quad \ldots\ldots\ldots \quad (3.6)$$

Obviously I_d is less than its correct value because the charging current $+I_c$ at $t = t_o$ is not yet equal zero.

b. In chapter one, it was mentioned that all materials conduct electricity, if only to an extremely slight extent. In this chapter,

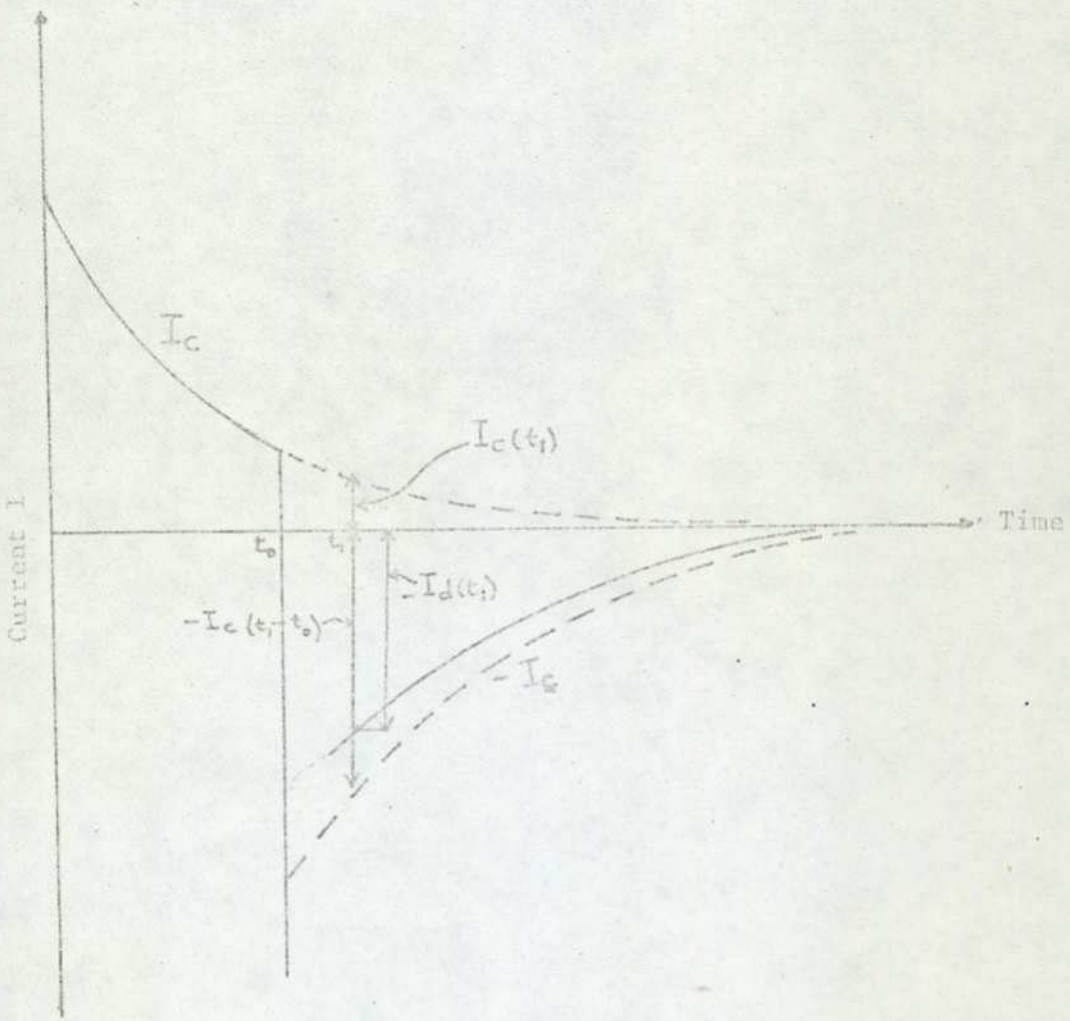

Fig. (3.4): Behaviour of the charging and discharging current, illustrating the law of Superposition Principle.

Fig (3.2) and equation (3.5) shows the existence of such conductivity in terms of the d.c. conduction current J_c, due to electronic or ionic carriers, and its contribution to loss factor ε''. Equation (3.5) refers to a dielectric, so that the current in the above equation can be defined as a displacement current, such that $J(t) = dD(t)/dt$ where $D(t)$ is the displacement current, $J(t)$ is the density current. Hence,

$$J(t) = J_D(t) + J_c \quad \ldots\ldots\ldots\ldots \quad (3.7)$$

where $J_D(t)$ is the current due to relaxation process in dielectric.

If, now, the conduction current behaves according to Maxwell's equation such that; the current carried by any kind of carriers is independently of time

$$\text{div } J_c = 0 \quad \ldots\ldots\ldots\ldots\ldots\ldots \quad (3.8)$$

Thus

$$D(t) = \int_o^t J_D(t)\, dt \quad \ldots\ldots\ldots\ldots \quad (3.9)$$

Equation (3.9) implies, therefore, that the superposition principle is valid and the contacts between the dielectric and the electrodes are ohmic (see chapter 4). In practice, however, contacts are not usually ohmic and this means that a part of the electronic or ionic carriers which contribute to conduction pile up at the electrodes and build up space charge which in turn oppose the flow of current (Daniel, 1967). Hence, J_c decreases with time until a value J_s is reached which corresponds to a steady state and obeys equation (3.8). In this case current may be seperated into three parts

$$J(t) = J_D(t) + J_i(t) + J_s \quad \ldots\ldots\ldots \quad (3.10)$$

where $J_i(t)$ represents the dielectric conduction current term due to space charge build up at the electrodes. This term lead to a polarization so that;

$$D(t) = \int_0^t (J_D(t) + J_i(t))\, dt \quad \ldots\ldots\ldots\ldots \quad (3.11)$$

Thus the time dependent parts of the current cannot be separated into the true displacement current and the current which builds up an interfacial polarization as long as all effects are linear. However, the build up of space charges at the electrodes implies non-linear behaviour of D(t) as a function of E(t) and invalidate the principle of superposition, so that the complication introduced by non-ohmic electrodes and interfacial polarization are serious in principle.

c. The switching at t = 0 is accompanied by a sudden change of ε_∞ E in the electric displacement and it is equivalent to the term C_a/C_o in equation (3.4). Theoretically this should last an infinitely short time, that is the current corresponding to it should be a delta function. In practice, the external circuit attached to the dielectric sample does not respond infinitely fast, and the switch surge lasts for some time.

Hence all time constants in the external circuit must be kept as short as possible (this will also be discussed in detail in chapter (4)).

d. The frequency-dependent complex dielectric constant and the time - dependent charge - discharge currents, equation (3.4) and (3.5) are related, such that

$$\varepsilon^*(\omega) = \varepsilon'(\omega) - j\varepsilon''(\omega)$$

$$= \varepsilon_\infty + \left\{ \int_0^\infty \phi'(t)\, e^{-j\omega t}\, dt \right\} - j\frac{G}{\omega C_o} \quad \ldots\ldots \quad (3.12)$$

where $\phi'(t) = \phi(t)/C_o$ and $\varepsilon_\infty = C_a/C_o$ is the high-frequency (unrelaxed) dielectric constant of the sample.

It is important to note from equation (3.12) that $\phi'(t)$ does not contain the contribution to observed charging current from the steady d.c. conductivity of the samples. The loss factor of the sample is thus separated into two components and hence the relaxation component of the complex dielectric constant from (3.12) is

$$\varepsilon^*(\omega) = \varepsilon_\infty + \int_0^\infty \phi'(t)\, e^{-j\omega t}\, dt \quad \ldots\ldots\ldots \quad (3.13)$$

For the real and imaginary part of dielectric constant

$$\varepsilon'(\omega) = \varepsilon_\infty + \int_0^\infty \phi'(t) \cos \omega t\, dt \quad \ldots\ldots\ldots \quad (3.14a)$$

$$\varepsilon''(\omega) = \int_0^\infty \phi'(t) \cos \omega t\, dt \quad \ldots\ldots\ldots\ldots \quad (3.14b).$$

Thus $\varepsilon'(\omega)$ and $\varepsilon''(\omega)$ can be obtained at any chosen value of ω if $\phi'(t)$ is known over the range $t = 0$ to ∞.

In practice, however, $\phi'(t)$ may be a complicated function of time. and the integration of equation (3.13) cannot be performed analytically. In these circumstances, the integration must be performed numerically at a given ω value. This may be done with the aid of a computer. If $\phi'(t)$ is known over its entire range of time, numerical integration of equation (3.13) will yield exact values for $\varepsilon'(\omega)$ and $\varepsilon''(\omega)$.

A less satisfactory procedure which avoids exact Numerical integration has been used in practice by postulating a certain form for the current decay function.

Hopkinson, (1901) found that many materials at a fixed temperature obey the following relation

$$\phi(t) = C_o A\, t^{-m} \quad \ldots\ldots\ldots\ldots\ldots \quad (3.15)$$

where A and m are constant for a given material. Using this expression for $\phi(t)$ in equations (3.4) and (3.5) gives

$$\varepsilon'(\omega) = \left\{ \omega^{m-1} A \Gamma(1-m) \cos ((1-m)\pi/2) \right\} + \frac{C_a}{C_o}$$

for $0 < m < 1$ ..... (3.16a)

and

$$\varepsilon''(\omega) = \left\{ \omega^{m-1} A \Gamma(1-m) \cos (m\pi/2) \right\} + \frac{G}{\omega C_o}$$

for $0 < m < 2$ ..... (3.16b)

where $\Gamma(1-m)$ is the gamma function, which has been calculated by some workers, see (Hodgman, 1958).

These relations have been known for some time but Hamon (1952) showed that the expression for ε'' could be reduce to a simple approximation.

Thus ε'' may be expressed in terms of the relaxation function $\phi(t_1)$ at a given time t_1 as

$$\varepsilon''(\omega) = \{ \phi(t_1/\omega C_o) \} + \frac{G}{\omega C_o} \quad \ldots\ldots\ldots\ldots \quad (3.17)$$

provided that ω and t_1 are related by the equation

$$\omega t_1 = \{ \Gamma(1-m) \cos (m\pi/2) \}^{-1/m} \quad \ldots\ldots\ldots \quad (3.18)$$

The expression on the right-hand side of equation (3.18) is almost independent of m in the range $0.3 < m < 1.2$ having the mean value 0.63 and so equation (3.17) may be written as

$$\varepsilon''(\omega) = (i(t)/\omega C_o V) + \frac{G}{\omega C_o} \quad \ldots\ldots\ldots\ldots \quad (3.19)$$

where

$$t = \frac{0.63}{\omega} = \frac{0.1}{f} \quad \ldots\ldots\ldots\ldots \quad (3.20)$$

However, the assumption in equation (3.15) cannot hold from t = 0 to ∞, since it would give D → ∞ if t → ∞ and m ≤ 1. Furthermore, substituting equation (3.15), in terms of decay function $Ke^{-t/\tau}$, where $K = \frac{\varepsilon_s - \varepsilon_\infty}{\tau}$, in equation (3.13) leads to an equation;

$$\varepsilon'' = \varepsilon_\infty + \frac{\varepsilon_s - \varepsilon_\infty}{1 + j\omega\tau} \qquad \ldots\ldots\ldots \quad (3.21)$$

which is the familiar equation for single relaxation process. In fact most of the materials, especially polymers, have broad distribution curve and obey Cole-Cole distribution accurately or approximately rather than the above Debye's equation (3.21). This raises a certain difficulty in accepting Hamon's approximation. This problem has been treated by Williams (1962), who expressed the decay function $\phi(t)$ from Cole-Cole approximation for characterizing relaxation time distribution. William's calculations result with

$$\omega t = \left[\Gamma(n) \sin (n\pi/2)\right]^{-1/(1-m)} = \chi 1$$

for $\omega\tau >> 1$

and

$$\omega t = \left[\frac{\Gamma(1-n) \sin (n\pi/2)}{n}\right]^{-1/(1+n)} = \chi 2$$

for $\omega\tau << 2$

where $n = 1 - \alpha$ and α is the factor determining the width of the distribution.

The values of $\chi 1$ and $\chi 2$ were evaluated by Williams for a range of n values. He found that $x\,1 = 0.62 \pm 0.03$ for n between 0 and 1, but $x\,2 \simeq 0.61 \pm 0.02$ for values of n up to 0.3 only. Thus for times $<< \tau_o$ the Hamon's approximation can be obtained for all n values, while for time $>> \tau_o$ it is valid for n values up to 0.3 only and τ_o is the most probable relaxation time. Hence, the very short time and high-frequency and the (very long time and low-frequency) behaviour of a dielectric meterial with a Cole-Cole distribution of relaxation times does conform with Hamon's

approximation. The most important region, however, is the actual dispersion region where $\omega\tau \approx 1$ and $t = \tau$. Then the previous theory does not apply. Williams used in this case values of $\phi(t)$ at various (t/τ) and n values, which had been tabulated by Cole-Cole and putting $(\varepsilon_s - \varepsilon_\infty/\tau)$ equal to unity.

Although, William's correction may give better results than Hamon's approximation, this method still unable to provide a direct calculation of ε' (see chapter one). Therefore, the fast fourier transform technique seems to be the right method to be adopted for ε' and ε'' evaluation.

3.3 D.C. Ramp Function Measurements (10^{-1} - 100 Hz) :-

Using equation (3.13) together with equation (D.5), a step voltage V applied at t = 0 gives

$$I = \varepsilon_\infty C_o V \delta(t) + \frac{V C_o (\varepsilon_o - \varepsilon_\infty) e^{-t/\tau}}{\tau} \quad \ldots\ldots\ldots \quad (3.22)$$

where $\tau = RC_o(\varepsilon_o - \varepsilon_\infty)$, C_o is the capacitance of the empty condenser in the parallel RC combination Fig (3.5); equivalent circuit for a parallel-plate condenser containing a Debye dielectric.

With the ramp voltage $V(t) = V\,t/T$, $0 < t < T$; $V(t) = 0$; otherwise, the current I(t);

$$I(t) = \frac{C_o V}{T}\left[\varepsilon_\infty + (\varepsilon_o - \varepsilon_\infty)\{1 - \exp(-t/\tau)\}\right] \quad \ldots\ldots \quad (3.23)$$

Accordingly, the step and ramp voltage could be used to provide satisfactory data on polymeric materials.

Davidson, Auty and Cole, (1951) have described apparatus which uses an applied ramp voltage. The ramp voltage has the advantage that the leading term in equation (3.23) may be made small compared with the

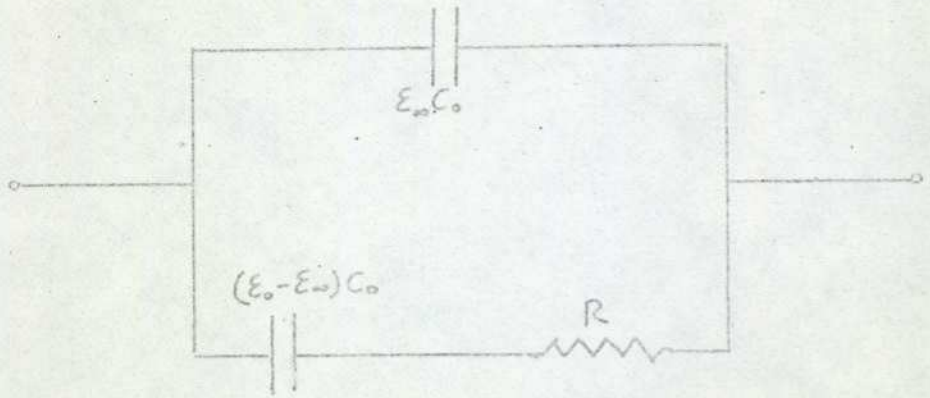

Fig. (3.5): Equivalent circuit for a parallel-plate condencer containing Debye dielectric.

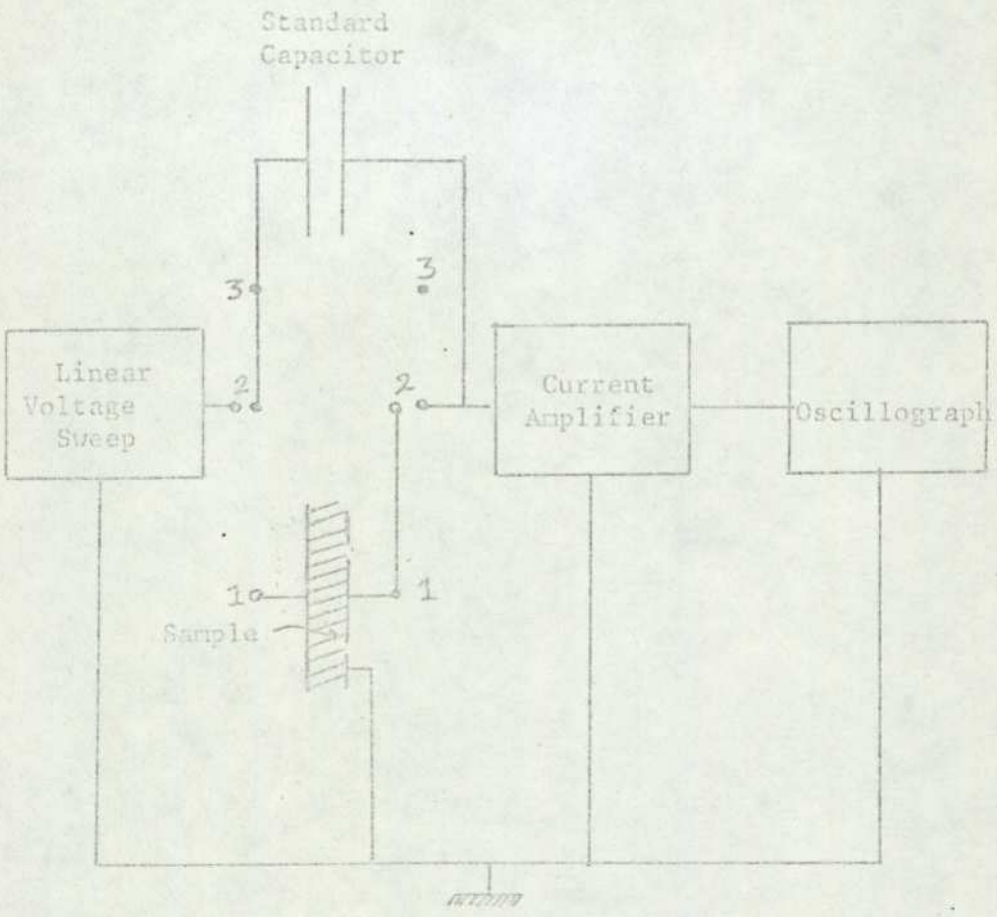

Fig.(3.6): Block diagram of apparatus for ramp-voltage studies of dielectric transients.

leading term in equation (3.22), and the second term in equation (3.23) is zero at t = 0, while the corresponding term in equation (3.22) is not. Thus large transients at short times are not as much of a problem as with the step voltage. The apparatus is intended for use over the time range 10^{-3} seconds to several seconds, corresponding to maxima in the dielectric loss in the range 10^{-1} to 100 Hz. Fig (3.6) shows the elements of the apparatus.

The ramp voltage is obtained by charging polystyrene dielectric condensers with the essentially constant plate current from a cathode - loaded tube. The maximum voltage obtainable is determined by a diode which stops the sweep by conduction. By combining dielectric condenser capacities of 1 pF to 10^{-4} μF with two different cathode resistors, ten sweep durations from 1.5 seconds to 5×10^{-5} seconds are possible. The current in the sample is amplified and feed to the horizontal plates of an oscillograph. To maintain the potential of the guarded electrode the same as the guard electrode, a feedback circuit is employed to reduce the input impedance of the amplifier.

However, in such measurements two problems are encountered which limit the time scale over which the apparatus may be used. To obtain a useful record, T must be long compared with τ. However, if T is very long, the current in the sample will be so small that measurable deflections on the oscillograph will not be possible. On the other hand, if τ is very short, the response time of the detector will be too long.

With a ramp voltage of 0 to 200 V, displacements on the oscillograph were sufficiently large to allow determination of the current to ± 2%.

Coming to the end of the section, we ought to mention that beside the above d.c. methods Reddish (1970) used a method in which he measured the charge on the condenser plates rather then the current through the

sample. This method has the advantage that the decay function is obtained directly and $q(t)$ is bounded at short times, while $\tau(t)$ is very large. However, the current seems easier to measure and more reliable since no prior assumption is required about the nature of the dielectric response (see chapter 1 and section 3.2).

3.4 A.C. Measurements For Frequencies Below 10^7 Hz):-

The vast majority of dielectric measurements employ alternating current methods. These methods are usually subdivided according to the frequency range used.

The frequency range between 10^{-2} and 10^7 Hz is the most convenient frequency range, where bridge methods may be used, in that the impedance of the capacitor containing the dielectric is balanced against a known combination of discrete resistances, capacitances, or inductances. Modern commercial bridge are usually variants of two types of basic circuit, namely the Schering bridge and the transformer ratio bridge. The Schering bridge designed by Scheiber, (1961) can be used for frequencies down to about 10^{-2} Hz, so that there is no frequency gap between direct and alternating current methods.

The most primitive form of Schering bridge is shown in Fig (3.7). It is a special case of a bridge with four arms analogous to the Wheatstone bridge originally used for direct current measurements. Such a bridge is balanced if an alternating voltage applied to opposite corners of the rectangle leads to zero voltage across the other pair of corner. When this condition is achieved an equation

$$Z_1^*(\omega)\, Z_4^*(\omega) = Z_2^*(\omega)\, Z_2^*(\omega) \quad \ldots\ldots\ldots\ldots\ldots \quad (3.24)$$

holds between the complex impedance of the four arms. Where $Z_1^*(\omega)$ is the impedance of the capacitor which contains the dielectric under investigation

and according to Appendix (c), $Z^*(\omega)$ is proportional to $\varepsilon^*(\omega)$ of the dielectric. Equating of the real and imaginary parts in equation (3.24) yields the complex dielectric constant of the dielectric as a function of $Z_2(\omega)$ to $Z_4(\omega)$ which are the impedances of components or combinations of components which may be known with high accuracy. On the basis of the simple circuit (3.7) one might suppose the bridge measurements could easily be carried out so as to give high precision. In practice, higher accuracy demands a skill in bridge design. The main reason for the difficulties of bridge design lies in the presence of "stray" impedances, inductances and capacitances between the different components and between the components and earth.

A Schering bridge for accurate work minimises strays by shielding and a guard circuit. This is, all stray capacitances and resistances go as far as possible to an earthed screen and are balanced out by an auxiliary circuit which enables the detector points to be brought close to earth potential. A well designed Schering bridge carefully operated may be used to measure small loss angles with and accuracy of $\pm 10^{-6}$ in increments of tan δ (Anderson, 1964).

Figure (3.8) shows the basic feature of a transformer ratio bridge. This bridge is, also, analogous to a Wheatstone bridge, but two arms consist of the two windings of a transformer. When a voltage is applied to the bridge the magnetic flux is common to both windings. This has the consequence that any stray admittance across the winding on the specimen side is "reflected" by the transformer to appear present on the standard side. In first approximation the strays cancel against their own reflection. Hence a transformer bridge is less affected by strays to earth than a Schering bridge. Later designs of this type of bridge use two transformers, thus isolating the bridge from the source and detector, as shown in Fig (3.9). Tappings on one or both transformers

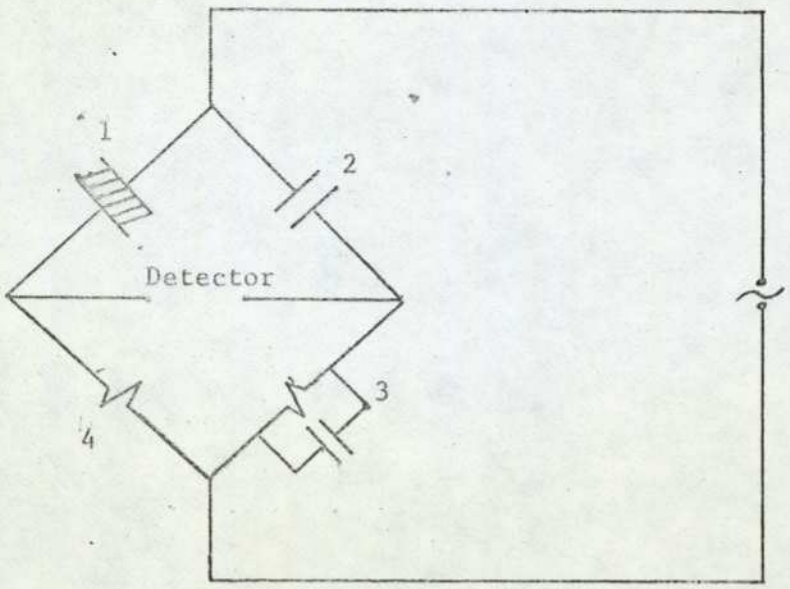

Fig. (3.7): Schematic Circuit of the simplest type of Schering bridge.

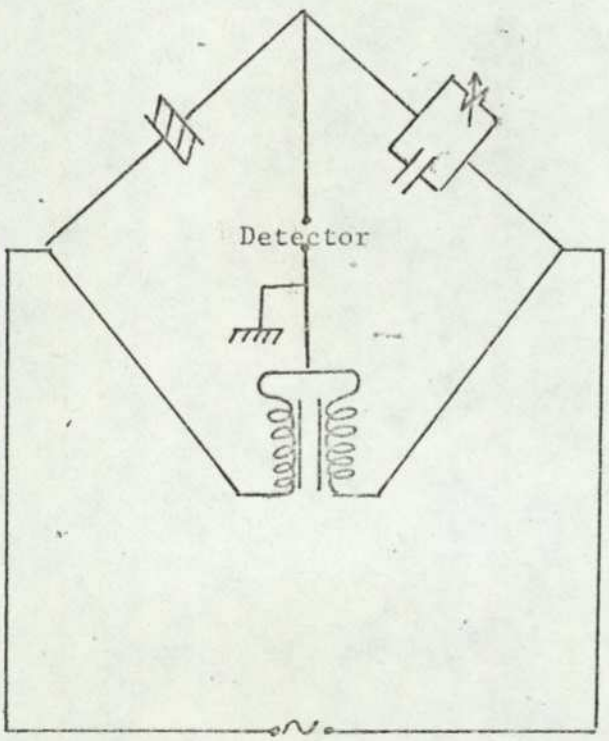

Fig. (3.8): Schematic Circuit of the simplest type of transformer bridge.

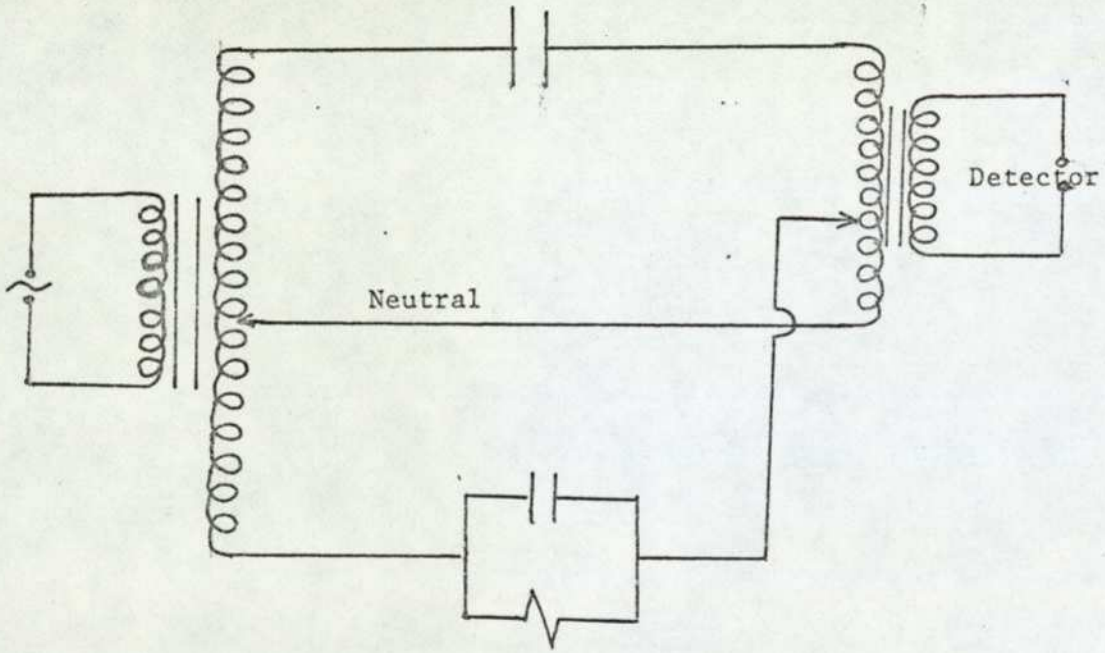

Fig. (3.9): Schematic circuit of a commerecial transformer ration bridge.

may be used to balance a wide range of values of the unknown against standards of moderate range. Strays to earth may be minimised by connecting shields of cables etc. to the neutral.

The accuracy of transformer ratio bridges may be as high as for Schering bridges, but the highest precision is likely to be confined to a less wide frequency range than for a Schering bridge. The upper frequency limit of the use of transformer ratio bridges is set by the inductance of the leads to the specimen. A limit of a few MHz is typical for the use of a commercial bridge with short leads, a capacitance $< 10^{-10}$ F and a permitted error of less than 2% in increments of tan δ (Daniel, 1967).

CHAPTER FOUR.

The Present Work

4.1 Introduction:-

The present work is mainly concerned with the designing and development of an accurate, fast and economic technique, (see chapter one), for the dielectric properties measurements at very low frequencies. Therefore, a d.c method was adopted and developed later to the extent such that the work can be divided into two parts:

The first involves the direct measurement of subsequent transient current. This current is then sampled and stored by an on-line computer which then proceeds to evalute its Fourier transform. On the other hand, the second method implies the application of the step response of an ideal low-pass filter to the dielectric sample and then follow the same procedure above. The method is called an ideal low-pass filter technique while the first is known as the step-voltage method. Both methods are now explained and discussed.

4.2 Step Voltage Technique

4.2.1 General Description:-

The whole apparatus used to measure the dielectric step response is shown diagramatically in Fig (4-1). The test-cell and electrometer amplifier were electrically screened from outside interference and each other by placing them in two separate aluminium boxes. The precaution was most important because the electrometer amplifier had a very high sensitivity of the order of 1 picoamperes. The test-cell unit was then placed in a controlled temperature environment that could be maintained at any temperature between - 10°C and 50°C to within ± 1°C. All leads entering and leaving the test-cell and electrometer compartment were co-axially screened.

The step voltage response was determined by applying a step voltage

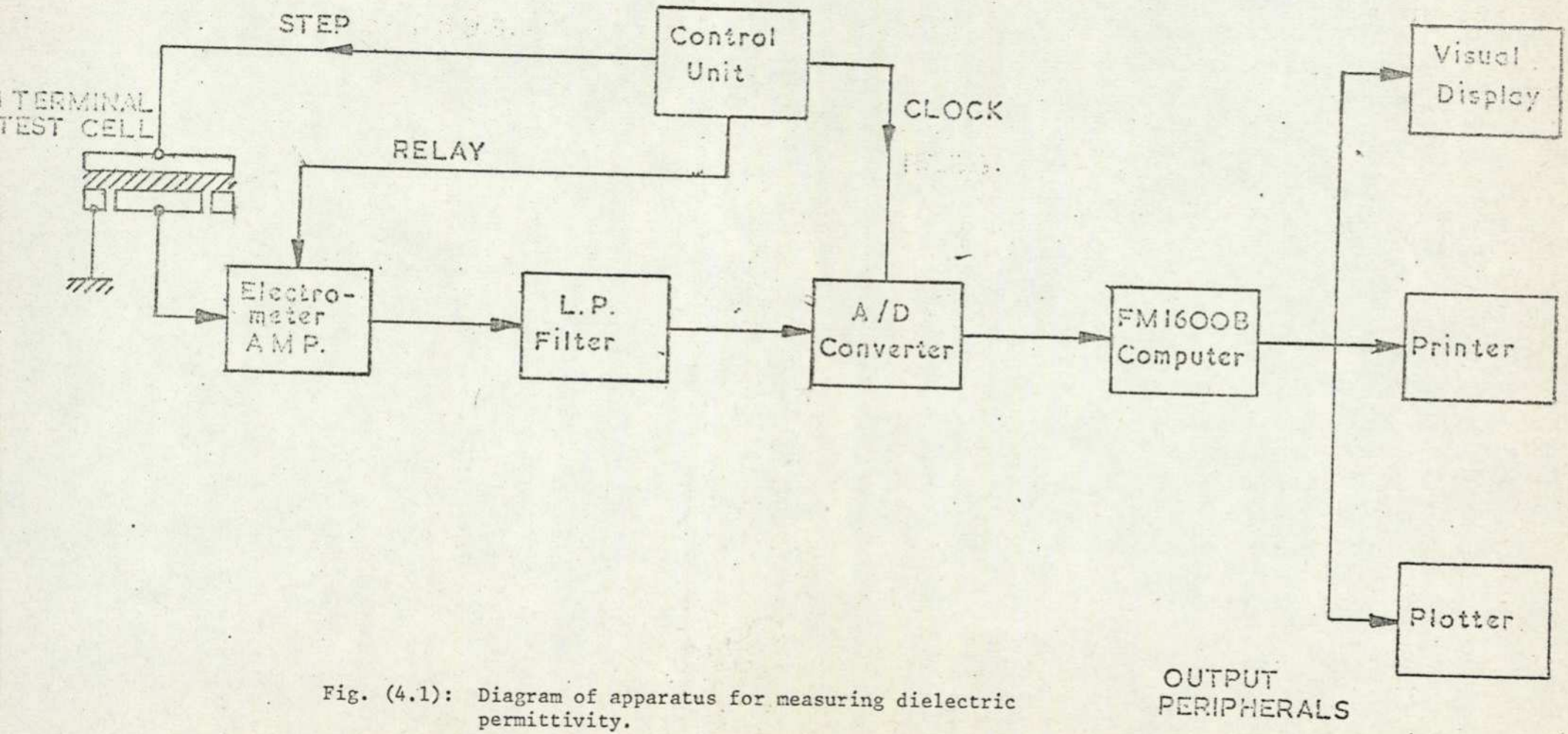

Fig. (4.1): Diagram of apparatus for measuring dielectric permittivity.

to the dielectric specimen and then measuring the current response. It was desirable that as much energy as possible should be transferred to the dielectric, so that an easily detected response was obtained. Thus it was necessary to maximise the area of the sample under the step while still observing firstly that the response (current) is linearly proportional to the step-voltage magnitude and secondly the charge saturation did not occur in the amplifier.

The latter is most important, since a traversal of this would introduce non-linearity into the system, making analysis of results most difficult. William's (1962), obtained good results for dielectric response to step voltage between 60 and 150 volts, and was able to confirm the linearity of the results. It was therefore decided to use step function of similar magnitude. The application of such step voltage to the dielectric sample of critical cross-sectional area and thickness (see sec 4.2.3) resulted in a large displacement current at the positive edge of the step. This displacement current was sufficient to saturate the input circuit of the electrometer amplifier causing it to remain "latched up" at full scale for some seconds after applying step voltage, thus rendering it incapable of measuring the true step response.

Consequently, it was necessary to devise a circuit that would protect the electrometer for the time required for the step voltage to rise up to its final value. A device was required that would either short-circuit the amplifier input or does not allow the output to swing up or down during that time, but that would be an open-circuit for time after that. The amplifier had an input impedance of 10^{12} Ω. The switching device had to satisfy the following conditions in having (1) an open-circuit impedance > 10^{12} (2) remotely controlled operation from outside the amplifier screening, and (3) relatively fast operation. Some make and break device, called the reed relay was used and found to satisfy the above

conditions quite adequately by connecting it across the amplifier's feedback resistance; sec(4.2.3).

The control unit basically produced the timing for the sequence of events, Fig (4.2), necessary to measure the step response. On receiving a trigger pulse, either manually or from the computer, it initiated the experiment by: (1) closing the relay to protect the amplifier, (2) producing a short delay (10ms) to allow the relay to close before (3) producing a high voltage step, (4) producing a trigger pulse to initiate sampling through the A.D.C. when the response started.

A circuit was required to obtain this sequence of events and a complete explanation of the circuit is given in sec (4.2.4).

The sampling rate is a most important variable in these measurements since it effectively band limits the response. By sampling theorem, "the sampling rate must be twice the highest frequency present in the sampled signal". Thus the response is band limited to half the sampling frequency, but if frequencies higher than this are present in the response, "aliassing" will take place in the Fourier spectrum of the sampled signal rendering every interpretation of the frequency spectrum quite meaningless. It is, therefore, necessary to band limit the response to half the sampling frequency and thus the response is passed through a low-pass filter before it is sampled. The implications of disobeying the sampling theorem in this experiment would be particularly damaging, since the quality of results depended on the correct interpretation of the Fourier transform of the step response. In practice it was found the effect of omitting the low-pass filter was not as severe as might have appeared, due to the band limiting effect of the electrometer amplifier. But the presence of the filter could be justified by it almost entirely eliminating noise associated with the response.

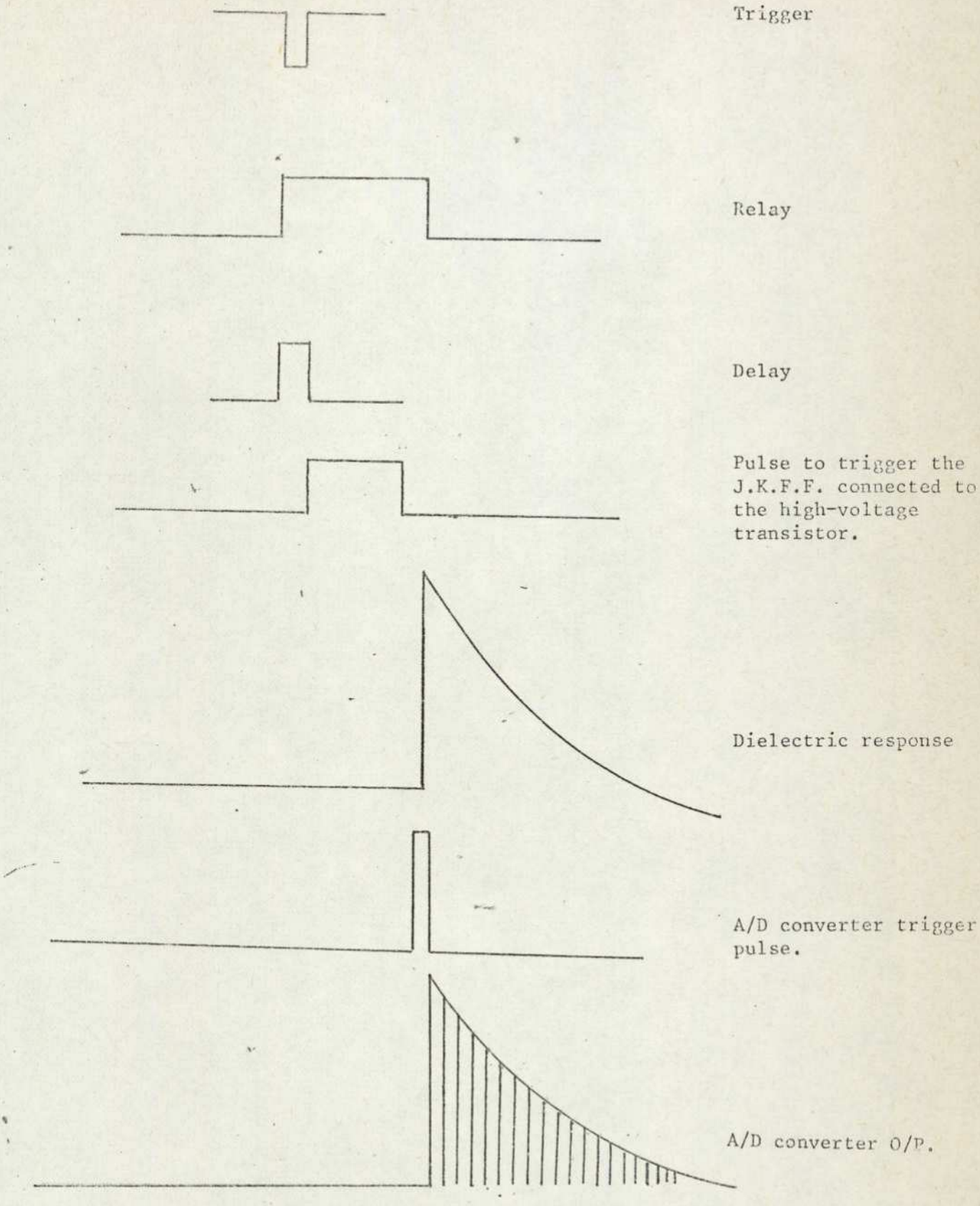

Fig. (4.2): Squence of events.

4.2.2 Test cell:-

Measurements of dielectric properties of material over a wide range of temperature are often difficult due to the lack of a simple cell which has a good response to cooling or heating. Such difficulties may be overcome by using elaborate cells, sometimes incomporating a thermostatically controlled air stream (see for example Van Turnhout 1975). Two simple cells have been used, their advantages include simplicity of construction, ease of operation and a good thermal response.

Fig (4.3) shows a three-terminal cell which we have used for solid dielectric materials (e.g. solid polymers). The disc sample, 50 mm diameter, is contained between the high potential electrode and the low potential electrode (43 mm diameter). The electrodes are insulated from the cell body by PTFE liners. The cell body together with the two electrodes were made in brass. The cell was constructed to avoid water condensation on the sample at very low temperature. Effectively, this changes the dielectric properties of the disc sample by introducing a new layer of different nature (see chapter 2). Later on, however, measurements were confined to range of temperature between 30°C to 50°C and therefore, there was no need to use the cell. Consquently a new one with large diameter giving easy response was used.

The new test-cell is shown in fig (4-4), the latter being an accurate full size drawing that was used for its construction. All critical dimensions i.e. the electrode diameter and thickness were machined to within .001" (see Wilding, 1973). The insulating parts of the cell were made of PTFE, that is because the PTFE had some particularly desirable insulating properties; It was easily machined and tapped. In fact, the electrical properties of the insulator are not very relevant here, since the insulating material does not come directly in contact with both electrodes and the upper electrode, through which the step voltage was

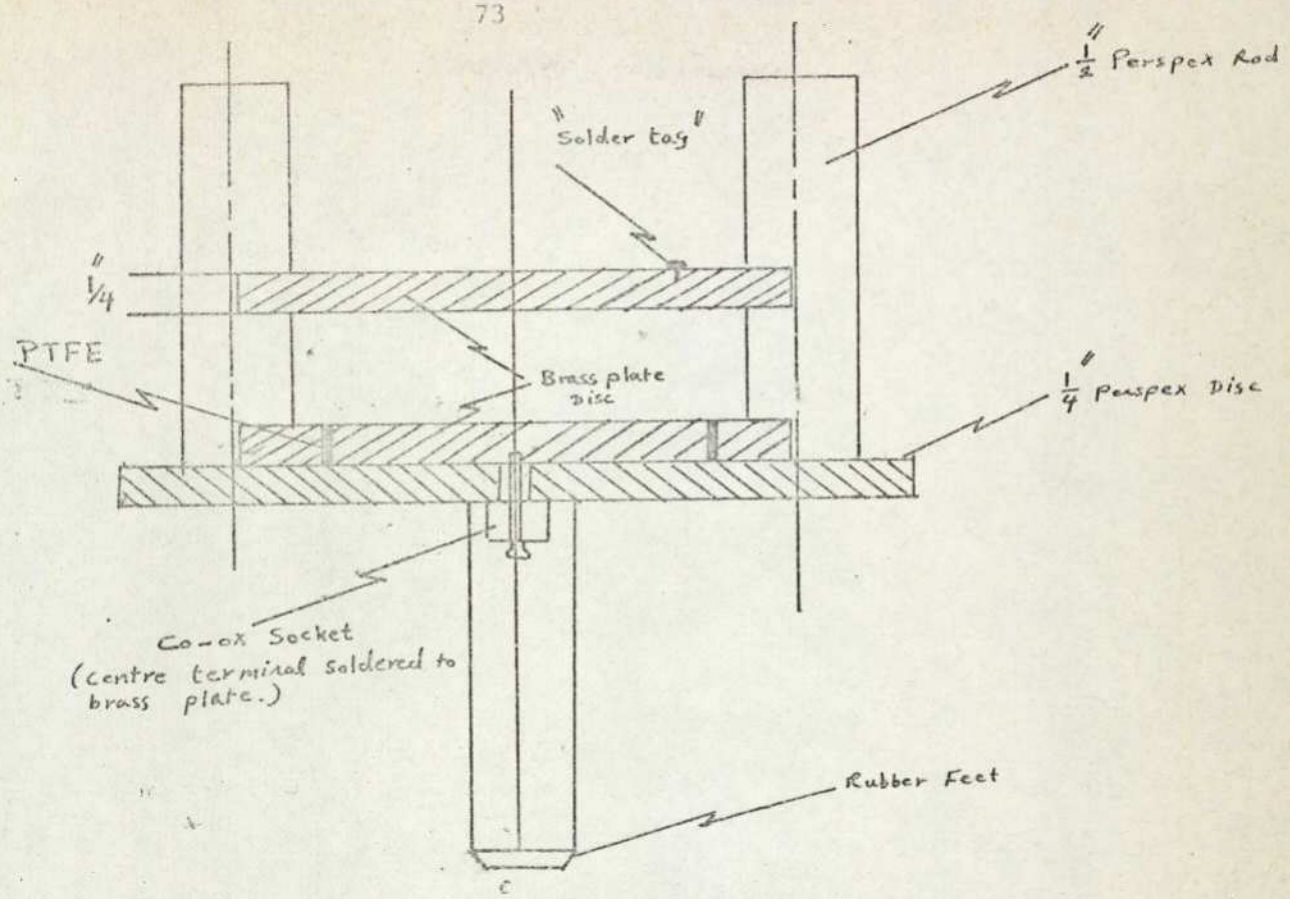

Fig. (4.4): Solid dielectric measuring Test-cell.

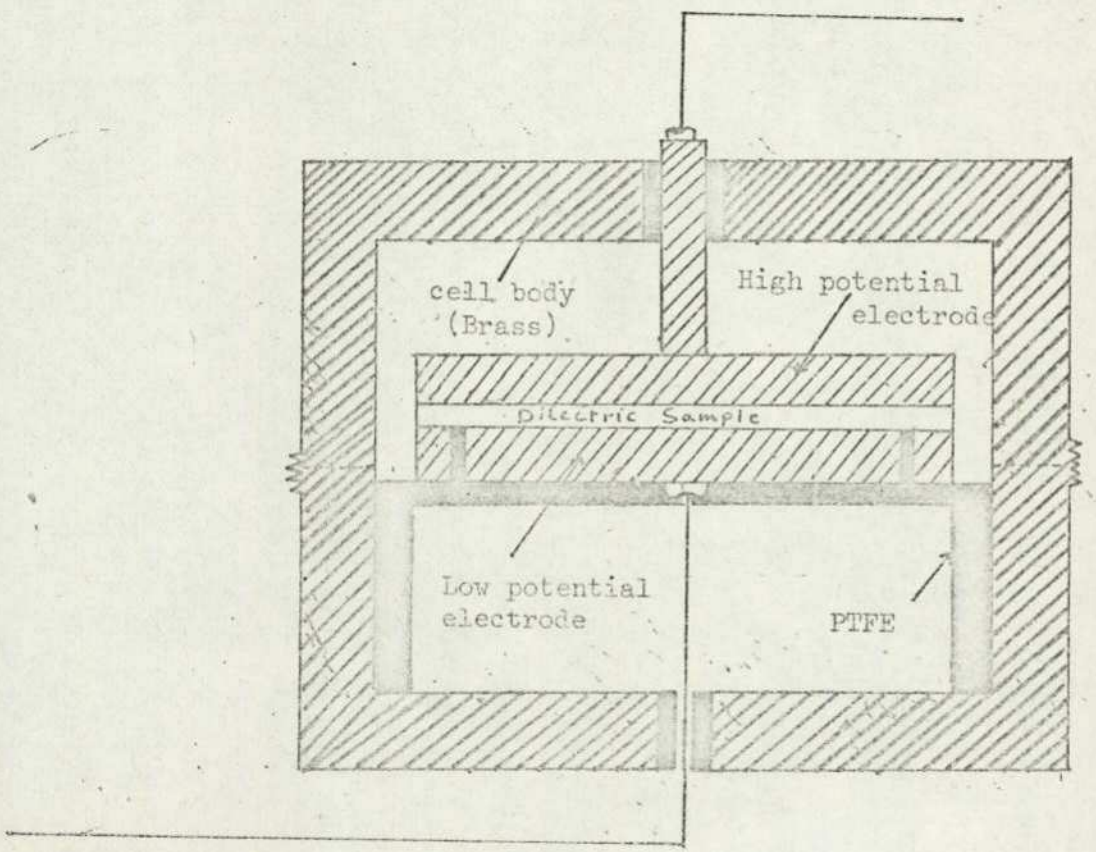

Fig. (4.3): The three-terminal Test-cell for Solid dielectric measurements.

applied to the dielectric, rested solely on the specimen.

The specimen was a disc 7 cm in diameter and typically 1.34 mm in thickness, and was machined to the same tolerance as the electrodes. This arrangement of dielectric specimen and test-cell is fairly normal and has been used by many experimenters, a detailed account of a more elaborate cell and an analysis of residual losses see (Scott and Harris, 1961).

The lower electrode consisted of a guarded electrode surrounded by a guard-ring which was earthed so that surface leakage currents and field fringing did not affect measurements which were taken from the guarded electrode. As a general rule the width of the guard-ring should be 10 times the electrode spacing in order to overcome the effect of field fringing (Von Hippel, 1958).

Connection was made to the guarded electrode via the inner conductor of a co-axial socket, the outer casing was connected to the guard-ring which was earthed via thick copper braid to the screen surrounding the cell. Co-axial cables connect the input of the amplifier directly to the guarded electrode. Fianlly a 3 lb weight was placed on top of the upper electrode, but separated from it by a PETF disc for insulation. This weight was used during all measurements and provided constant pressure to ensure an intimate contact between dielectric and electrode.

4.2.3 Picoammeter Design Techniques:-

From a study of earlier work, the current level to be measured in this type of work was not expected to be greater than about 10 PA and therefore an amplifier was required. It should be a high gain amplifier capable of detecting currents 10^{-12} A, i.e. a picoammeter and amplifying them sufficiently to give an out-put in the range of 0-10V, the range of the A.D.C. It was also desirable to be

stable over long periods of time, fast and it should generate the minimum of noise. The last two conditions were conflicting since both overall noise and speed of response were proportional to bandwidth, and some compromise had to be obtained.

Now in order to achieve sufficient sensitivity, past experimenters have often resorted to integrating the currents in order to overcome noise problems (Hyde, 1971). This technique unfortunately makes interpretation difficult and only if the transient currents were of the predicted shape would it suffice, but chapter (3) shows that such an assumption is invalid.

However, bandwidth of picoammeters can be more suitably expressed as a risetime for this application. This is defined as the time taken, t_r, for the output to change from 10% to 90% of its final value, in response to a step current input. Another alternative is to express the speed in terms of the time constant of an equivalent RC network. An approximate expression relating these is given by (Keithley, 1972).

$$t_r = \frac{.35}{f_{3dB}} = 2.2 \quad CR$$

where f_{3dB} is the 3dB bandwidth.

The straight forward method of measuring a current is to pass it through a sufficiently large resistor and monitor the voltage drop. This is known as the shunt method and requires a high input impedance voltage follower if the subsequent circuitry is not to load the resistor. The major problem concerns the capacitance present at the input which forms a CR circuit. So for a sensitivity of 1 V/PA, i.e. a 10^{12} Ω resistor and stray capacitance of 10 pf, the time constant would be 10 sec.

Another approach is to monitor this voltage drop with a vibrating capacitor electrometer. This can have a sensitivity of 10 mV with an 10^{16} Ω input impedance but sadly the instrument itself exhibits a

risetime of about a second (Evison, 1976).

The alternative is to use the "feedback" method. This, as the name suggests, places the high value resistor in the feedback loop of a high gain amplifier. This is illustrated in Fig (4.5). C_2 is the total effective capacitance across the input, and C_1 is self capacitance of the resistor R_1. The amplifier, gain K will need to be the electrometer-class namely having very small input bias currents so as not to swamp the current being measured.

The output e_o, expressed as a function of time in response to step current input of magnitude i, has been shown to be (Praglin and Nichols, 1960)

$$e_o = -\frac{iR_1}{1+1/K}\left\{1 - \exp\frac{-t}{R_1\left(\frac{C_2}{1+K} + C_1\right)}\right\} \quad \ldots\ldots\ldots (4.2)$$

Hence, for a sufficiently large K, the time constant is now unaffected by the input capacitance and is only dependent on the self capacitance of the resistor. Typically, this would be 1 pf - 10 pf, giving an improvement in time constant over the previous example from 10 sec to 1 sec.

This self capacitance can be minimised by the inclusion, in the feedback loop, of a compensation circuit as shown in fig (4.6). When this RC network has been adjusted so that

$$C_3 R_3 = C_1 R_1$$

then the new effective time constant has been shown by Praglin and Nichols to be

$$\frac{R_1 (C_1 + C_2)}{K + 1}$$

This implies that the response speed would now be virtually unlimited. Thus the circuit shown in Fig (4.6) was constructed and an amplifier that seemed idealy suited to this application was a "Computing Techniques

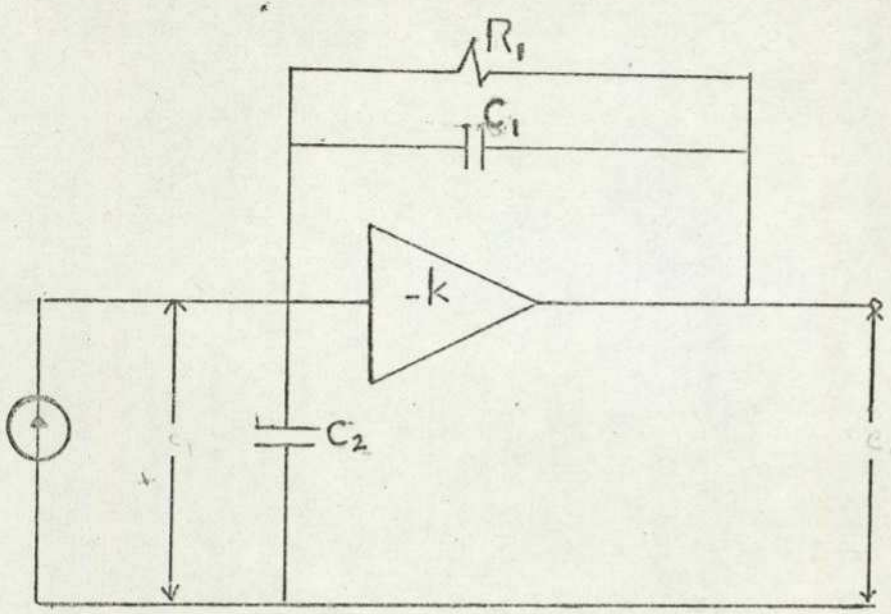

Fig. (4.5): Circuit using feedback (after Presley).

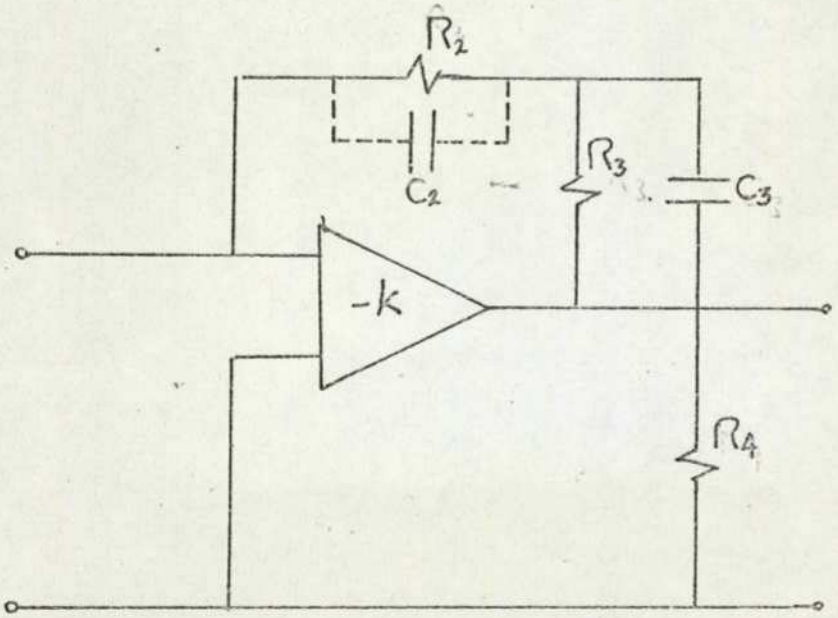

Fig. (4.6): Modified Picoammeter.

Electrometer Amplifier", type MF1-2. This device had the following desirable characteristics: an input impedance of 10^{12} Ω, open loop gain of 10^5, and an output voltage drift of less 1mV in 24 hours. The amplifier had an output range of ± 10V into a 2KΩ load. The feedback resistor R_f was a "Welmegox Type 3811" and had a value of 10^{12} Ω ± 1%.

To measure the risetime of the modified picoammeter it was necessary to apply a step current of very low magnitude. It was not practical to apply a square wave directly to the input of the picoammeter due to its high sensitivity. Therefore a triangular waveform was coupled to the input via a small capacitance, typically 5 pf. This capacitance and the input impedance of the amplifier resulted in an RC network, Fig (4.7), which differentiated the triangular wave giving a square wave of the right order of magnitude.

The above analysis however, assumed that the resistor's self capacitance can be lumped together as C_1, but in practice it is distributed, thus the component acts as a delay line and the final improvement was required to minimise this distributed capacitance. One approach by (Kendal and Zabielski, 1970) is to apply feedback to the middle of the resistor, thus making use of the distributed capacitance. With optimum adjustment, a fivefold improvement is risetime is claimed.

An alternative and perhaps sounder approach, has been given by (Presley, 1966). This method establishes an electric field to match the voltage gradient along the resistor. This is illustrated in Fig (4.8). The concept is to eliminate along the resistor, any stray capacitor to earth. In practice, this is achieved by mounting the resistor between two large metal plates. One is at earth potential (to match the virtual earth input), and the other is driven by the output of the amplifier.

Effectively, both modifications were not necessary, firstly, because the compensation network decreased the rise time of the picoammeter 1 sec to

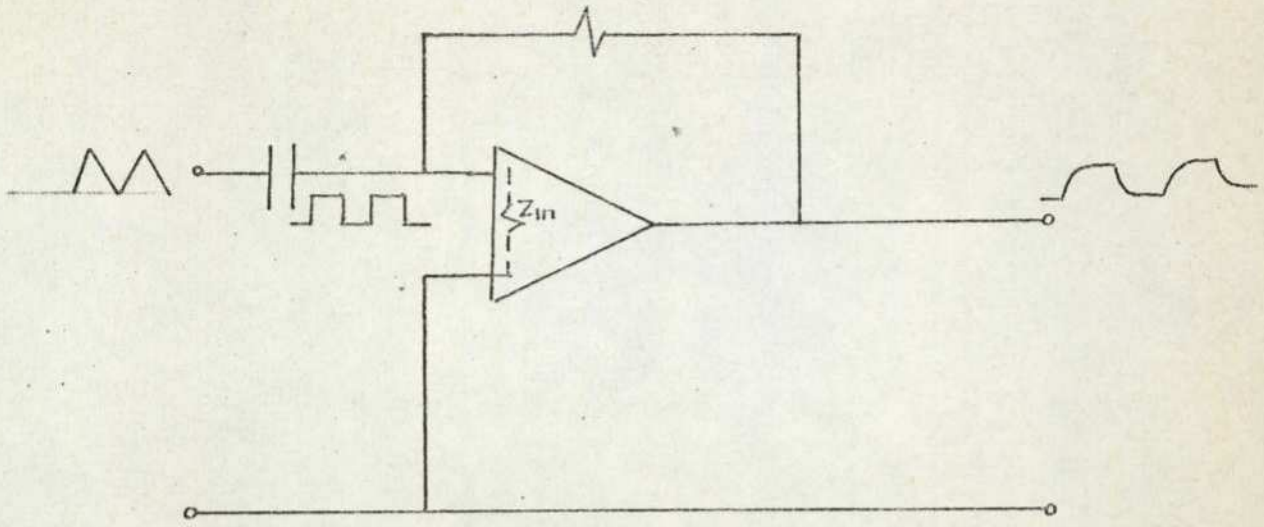

Fig. (4.7): Square wave testing circuit.

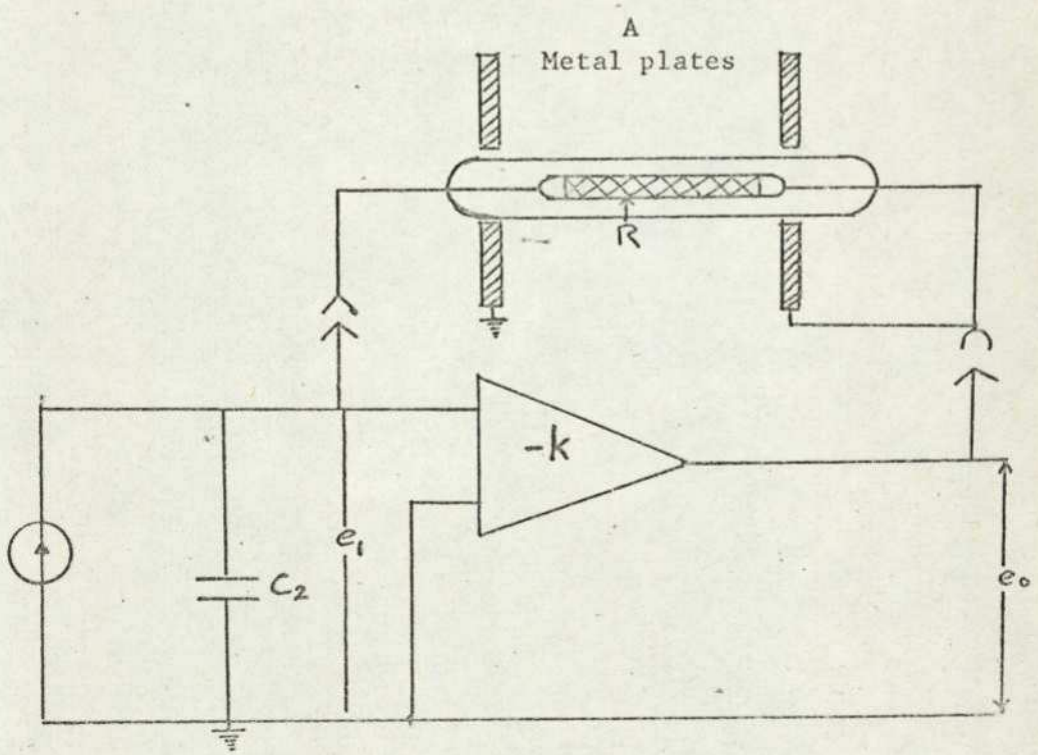

Fig. (4.8): Example of method used to reduced the distributed capacitance (Presley 1966).

10 m sec, see square wave response Fig (4.9), and this was an adequate improvement and secondly the dielectric relaxation times of polymeric solids are in general very long.

4.2.4 Protection Relay:-

It was mentioned earlier that a relay was used to protect the amplifier for the duration of the step-voltage rise. There were obvious problems in operating a relay in the vicinity of a very sensitive amplifier, these were due to electrostatic and/or electromagnetic coupling between the relay coil and input circuit of the amplifier. To a large extent these problems were overcome by positioning the relay as far as possible from the amplifier.

The relay used was a "Radio spares miniature reed-relay". Its contacts had an open-circuit resistance of 10^{13} Ω, this being the resistance of the glass bulb, in which it was sealed. This value is greater than the output impedance and many orders greater than the effective input impedance of the amplifier, thus the relay could be assumed to have a negligible effect, on the amplifier, when open-circuit. Fig (4.10) shows the circuit diagram of the whole test-cell and picoammeter units.

A zero off-set control is provided for the amplifier, this allows the output to be set to zero when there is no input current.

4.2.5 Low-Pass Filter:-

The necessity for using the low-pass filter sprang from the need to obey the sampling theorem and;

a - Eliminate the noise associated with amplifier

b - Bandlimit the response of the amplifier

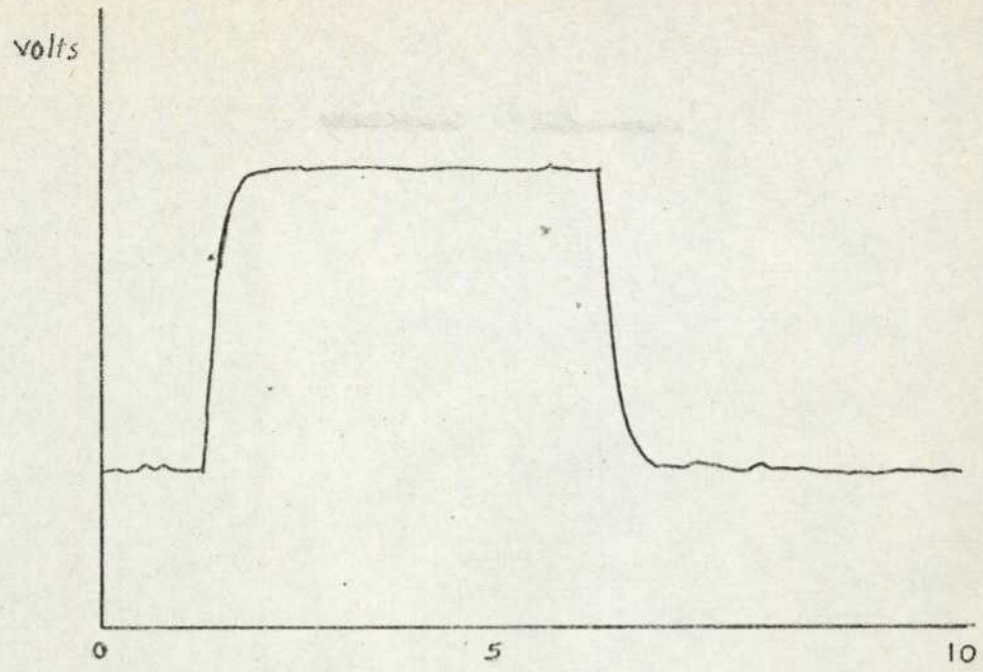

Square-wave response of unmodified Picoameter.

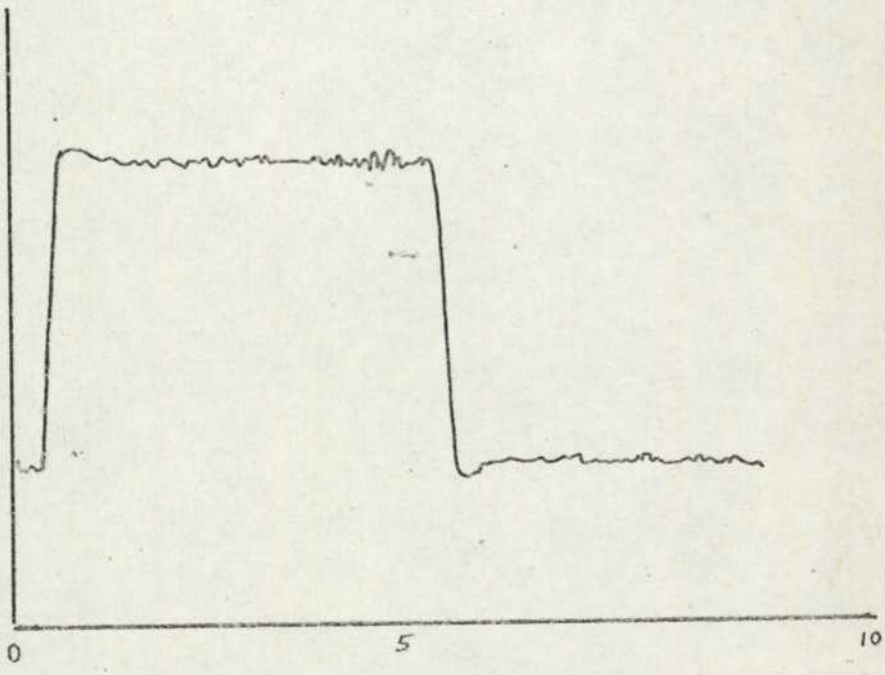

Fig. (4.9): Square-wave response of modified Picoameter (Rise-time increased by inertia of Pen Recorded.

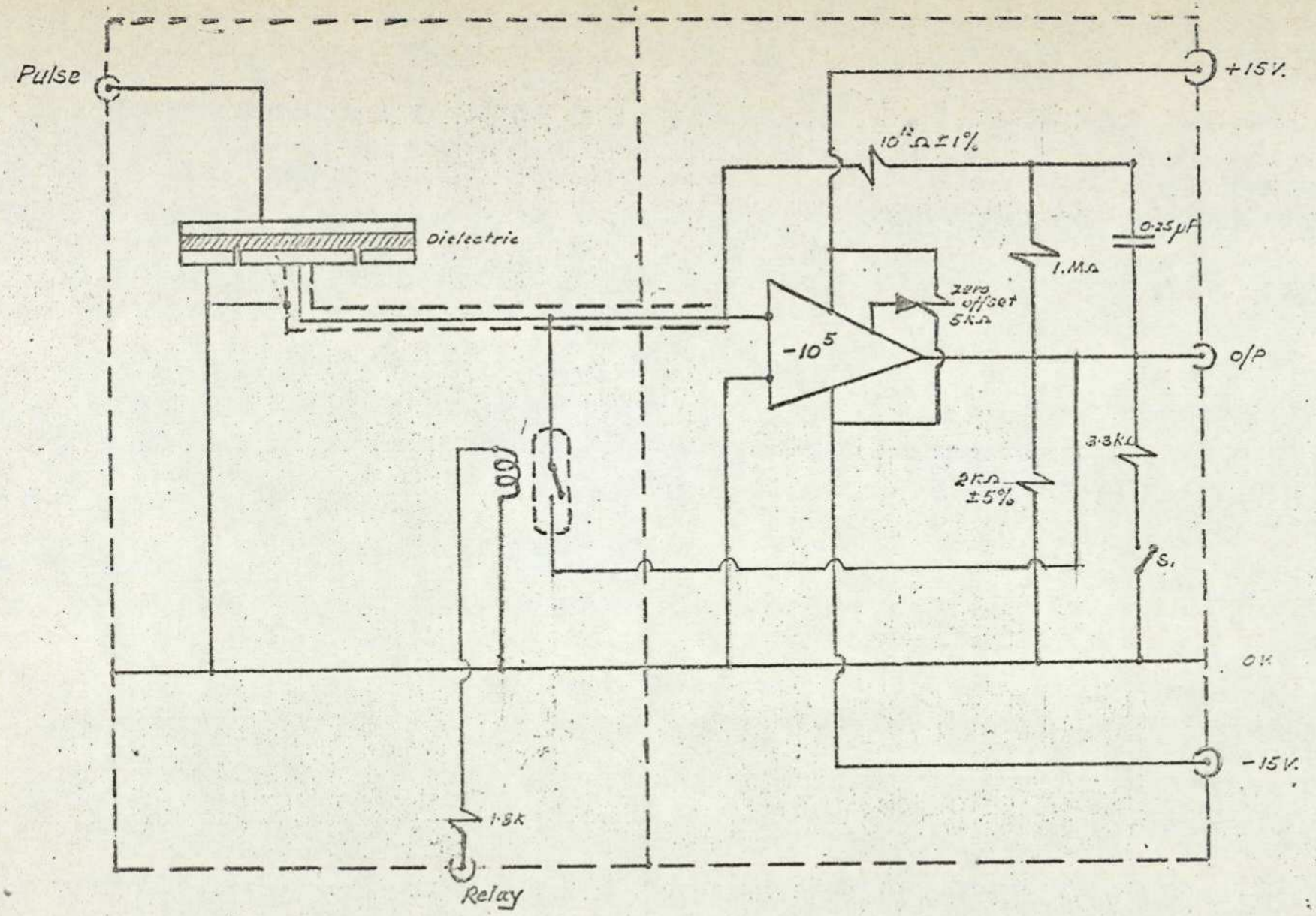

Fig. (4.10):· Test-cell and picoameter, (dashed lines represent Screening).

However, there are three major sources of noise

1 - Johnson noise current i_n, in the feedback resistor

2 - Amplifier current noise, i_a

3 - Amplifier voltage noise, ρ_a

The R.M.S. Johnson noise current is given by

$$i_n = \sqrt{\frac{4KT\ \Delta f}{R}} \qquad \ldots\ldots\ldots\ldots \quad (4.3)$$

where K is Boltzman's Constant, T is the absolute temperature, Δf is the bandwidth and R is the resistance.

This expression assumes that the picoammeter's bandwidth has a sharp cut off, but in practice it will have a 6 dB/octave roll off. Also the resistors used never reach their theoretical noise performance, so an empirical expression often used (Weinberger, 1971) is

$$i_n = \frac{2.2\pi}{2} \sqrt{\frac{4KT.\ 3.5}{R\ t_r}} \qquad \ldots\ldots\ldots \quad (4.4)$$

This expression, for a 10^{10} resistor and a risetime of 1 ms gives a noise current of about 10^{-13} A.

For current transient analysis, the R.M.S. value of the noise is less interest than the peak to peak value. It can be shown that the magnitude of the noise is less than $2\frac{1}{2}$ times the R.M.S. value for 99% of the time, so the following relationship is used.

$$I_{pp} = 5\ I_{R.M.S.} \qquad \ldots\ldots\ldots\ldots \quad (4.5)$$

The amplifier current noise depends on the particular amplifier and the overall risetime, but for modern electrometers, it would typically be 10^{-15} A, and can hence be ignored.

The amplifier voltage noise unlike the other sources of noise, is unlimited by the overall bandwidth and depends on the amplifier's open

loop bandwidth, This noise voltage can be expressed as an equivalent noise current, when it is referred to the input. A typical noise spectrum is shown in Fig (4.11).

Here F_o represents the bandwidth of the feedback resistor and the input capacitance, F_1 that of the overall picoammeter and F_4 that of the electrometer.

Now the total noise is given by the area under the curve and this noise spectrum raises several points. The first is that the spectrum is flat upto the limits of the electrometer, typically 1MHZ. Hence a filter is required on the output to limit this and its effects are shown for 2 different filters acting at a frequency F_2. It can be seen that a 6 dB/octave filter is insufficient and that a 12 dB/octave filter is essential.

Fig (4.12) shows the effect of an increase of input capacitance. This shows the importance of minimising this capacitance. Other sources of noise include electrostatic interference, microphonic effects and the picoammeter was very sensitive to mechanical vibrations, so great care was required to minimise all these effects in the apparatus.

Relaxation times of polymeric solids material are usually very long. Accordingly the maximum loss occurs at very low frequency and the sampling rate required to satisfy the sampling theorem is very low too. Therefore the high frequency components in the dielectric response should be eliminated and unlimited increase in bandwidth of the amplifier was not necessarily desirable.

The filter used to bandlimit the response was an active filter of 6th order, and its break frequency could be varied from 1 HZ upwards. It was quite adequate for bandlimiting the response but its square wave response tended to "overshoot", this was probably due to its higher order.

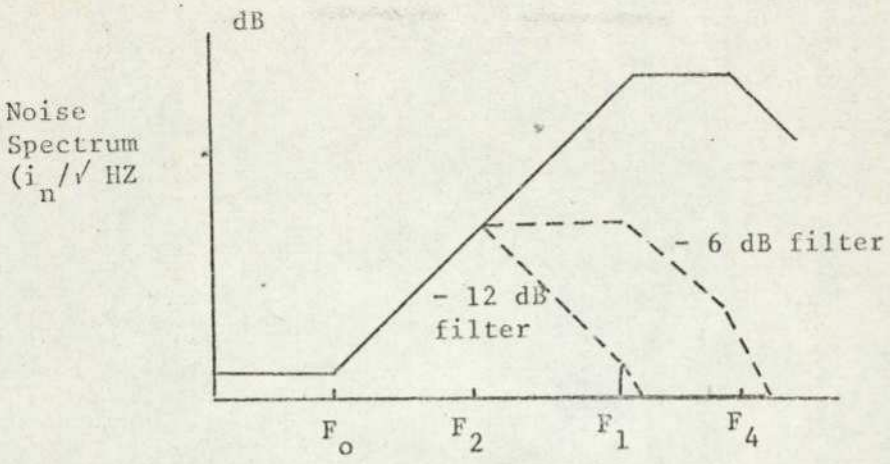

Fig. (4.11): Effect of post filtering on noise spectrum (after Evison).

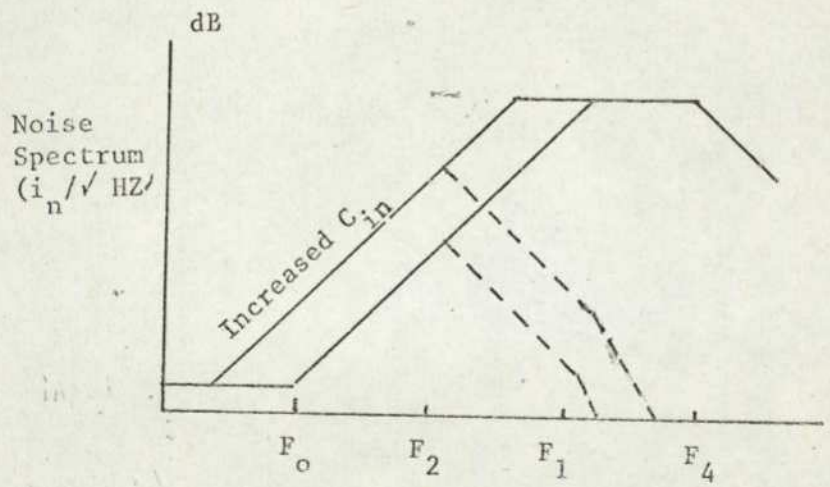

Fig. (4.12): Effect of input capacitance on the noise spectrum (after Evison).

4.2.6 Dielectric Samples:-

Choice of Polymer:-

It was mentioned earlier that d.c. instead of a.c. technique was adopted to evalute the variations of relaxation times of polymeric solid materials as a function of temperature at a given frequency.

Consequently, in the choice of a material to illustrate the above method, three characteristics were considered desirable.

1. It should have a principle relaxation region near room temperature. That is to say; the low frequency absorption region of some polymer - i.e. polyoxymethylene (William's, 1963) - occured at very low temperature i.e. - 83°C, and therefore a cryogenic apparatus is required which is not avaliable in our laboratory.

2. It should not depolymerise during moulding. Depolymerisation is a process of decomposition that takes place at high temperatures when long chain molecles of a polymer tend to break up. This results in a reduction in molecular weight of the polymer which changes its physical properties.

3. It should have been thoroughly studied previously to give a comparison of results.

These considerations led to the choice of polyvinyl actate (PVA_c) and the sample used was PVA_c 500,000 contained from B.D.H chemical Ltd (Wilding, 1973). It was easily moulded in a heated press, at 100°C into sheets of thickness 2 mm, from which 7 cm diameter were cut. The glass-rubber transition temperature. T_g, of PVA_c is 28°C, and it therefore exhibits a relaxation (Deutsch, Boff and Reddish, 1954) above this temperature. Consequently, it was studied well into this region at about 40°C, which incidentally, gives convenient comparison with the

results of (Saito, 1963). A thorough account of the dielectric properties of PVA_c and other polymers is given by (McGrum, Reed and Williams, 1967).

The sample disc was machined flat as accurate as possible and very slowly otherwise the heat generated by the machine tool melted the sample. The finished sample had a thickness of 1.34 mm.

4.2.7 The Control System:-

The circuit diagram of the control system is given in Fig (4.13). The operation of the system was triggered by a negative going edge pulse, derived either from a manual switch or directly from the computer. The negative edge triggered three monostables A, B and C simultaneously. Monostable A produced a pulse driving a transistor switch which operated the relay, B produced a short delay pulse before triggering the JK Flip-Flop which operated a high voltage transistor switch, C produced an inhibiting pulse that is longer than the relay pulse, and this stopped premature triggering of the A.D.C. due to any spurious pulses generated by the action of the high voltage transistor. Fig (4.13) also shows the waveforms associated with the components of the system.

SN74121 monostables in integrated circuit form were used which could produce pulse widths from a few nano-second up to 40 seconds. The pulse width is determined by an external timing circuit connected to the I·C and is given by

$$\text{Pulse width, } T = CR \log_e 2$$

where C and R are the values of capacitance and resistance in the timing circuit. B had a constant delay of 10 ms, while A and C had variable delays which could be selected by a ganged switch, the pulse widths were changed by a factor of 2 from 0.25, 0.5 and 1.0. For this reason

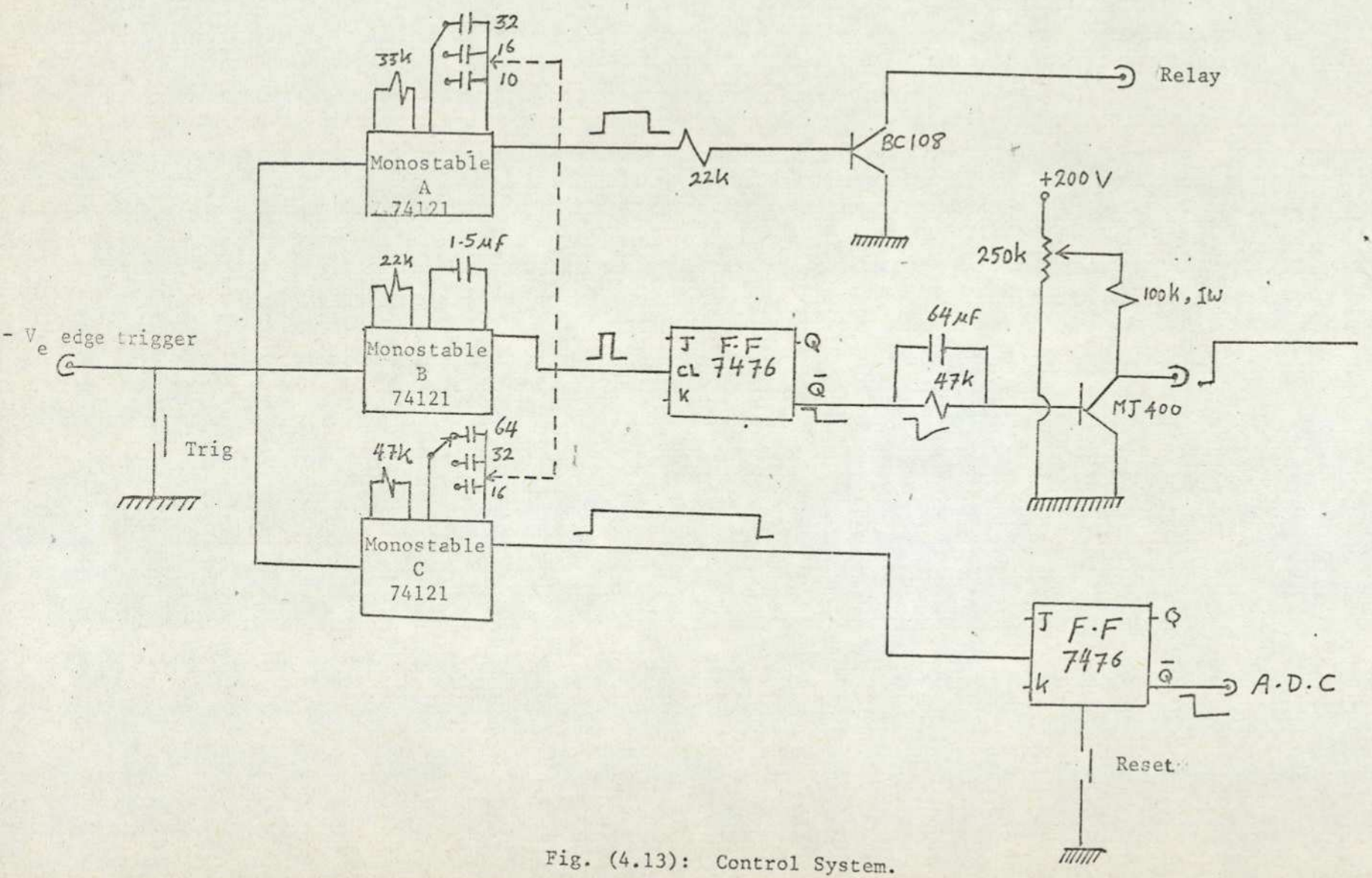

Fig. (4.13): Control System.

capacitors and not resistors were switched since preferred capacitance values are often multiples of two. The reed-relay was switched by a BC 108 transistor, this was entirely statisfactory since the relay had a coil resistance of 5 KΩ, and the transistor only had to pass a few milliamps. The transistor was switched on by + 5V logic level from monostable A. The series resistor acted as a current limiter.

The voltage step function was switched by a high voltage transistor, MJ400, for which $V_{cc\ max}$ = 325 V. The transistor was "on" all the time except for the duration being required for the dielectric sample to be subject to the step voltage, when it was switched "off" by a negative going pulse from the JK Flip-Flop. It remained "off" all the time until another negative going edge pulse change the state of the JK Flip-Flop. The RC coupling network was used to improve the switching times of the transistor. However, when the transistor was "on" all the high voltage appeared across the 100 KΩ collecter resistor, and when it was "off", the voltage appeared across the collecter and emitter. The H.T. voltage could be varied by a 250 KΩ potentiometer. Effectively a voltage step was obtained at the collecter, and this was connected with screened cable to the upper electrode of the test-cell.

The sampling rate was controlled by an external clock connected to the frequency divider Fig (4.14), and the trigger pulse merely applied the divider pulses to the A.D.C., in order to initiat sampling. All the gates were contained in one I.C, and the I.C's all operated from a stabilised supply of 5V, and the circuit current drain was 0.1 A. The whole system was constructed on electro-kit board, and the controls; pulse widths, pulse height, and the trigger switch were mounted on a panel for easy operation.

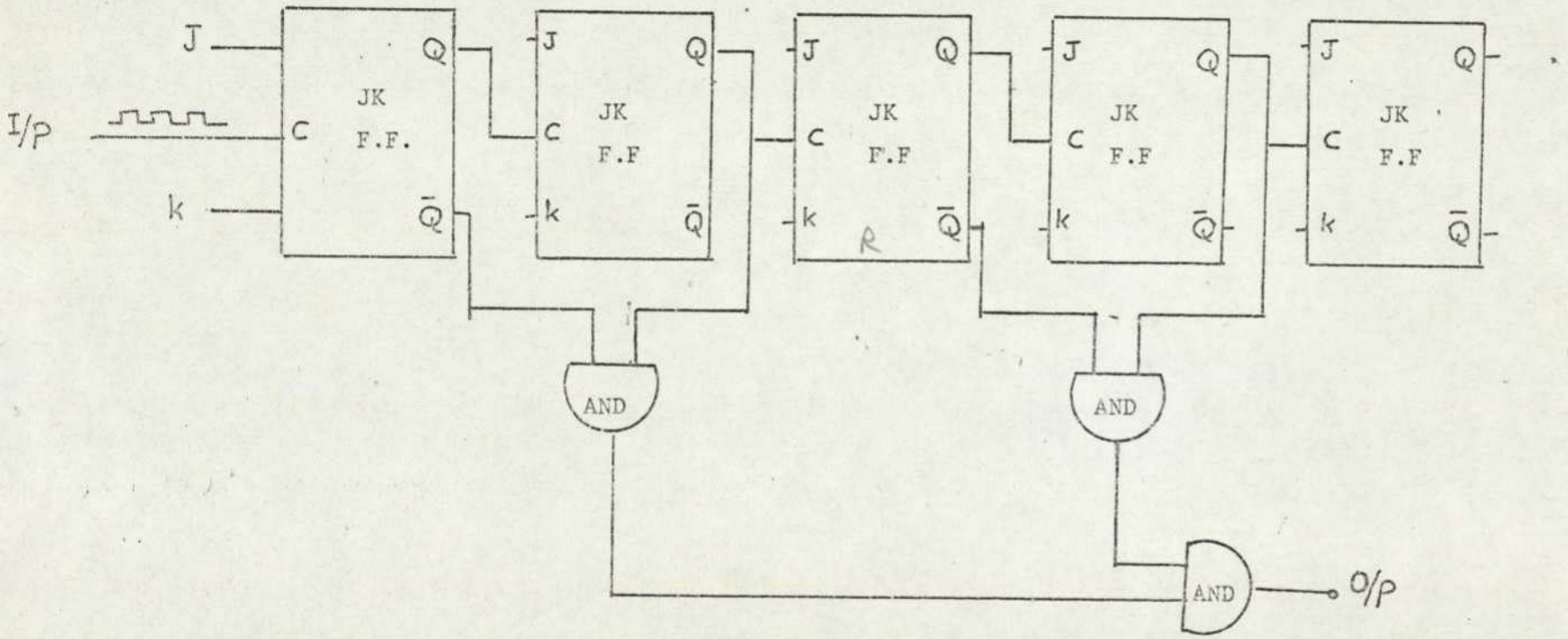

Fig. (4.14): Frequency divider.

4.3 Ideal Low-Pass Filter Technique

4.3.1 Introduction:-

Linear filters form a class of system which is of crucial importance in signal processing. Although in its most general sense the term "filter" implies any frequency selective device or processor, in practice it is generally reserved for a system which transmits a certain range (or ranges) of frequencies, and rejects others: such frequency ranges one called "passbands" and "stopbands" respectively. We shall see later that the ideal filter, which would introduce no attenuation of input signals falling within the passband, and infinite attenuation of signals in the stopband, is not attainable in practice.

Hence, an ideal low-pass filter is a linear system - see App (B) - which acts like an ideal distortionless system, provided that the input signal contains no frequency components above the "cutoff" frequency of the filter. Frequency components above this cutoff are completely blocked, and do not appear in the output.

However, the need for such an ideal low-pass filter may arises from:

a. It is always desirable in such measurements to maximise the area of the dielectric sample under the step voltage in order to get a large current easy to detect. The magnitude of such current, which is bound to saturate the amplifier, is mainly dependent on the rate of change of the applied step voltage (i.e. $i \alpha dv/dt$).

Consequently, a low-pass filter was required to cutoff high frequency components in step function, thus slowing the rate change of the applied step voltage and hence avoiding the amplifer's saturation. Effectively, the protection relay was eliminated and the control circuits reduced to the minimum.

b. Practically, it is impossible to build an ideal filter and RC network could be used for this purpose. Unfortunately, the using of such system wasn't without problems:

The most crucial one is, in the frequency range greater than its cutoff frequency the Fourier spectrum of the output of such system is quite similar to that of the real sample (see Fig (4.15). Thus, the final result was a mixture of the Fourier spectrum of both outputs and mainly due to RC network. Therefore, it was difficult to distinguish or seperate between the two spectra. Therefore;

The cutoff frequency of the RC network, determined from the relation $f_c = \frac{1}{2\pi RC}$, should be far greater than even the sampling frequency. That is because the Fourier spectrum of the dielectric's response to the applied voltage should be preserved to its own value without any attenuation. Hence, RC network with large cutoff frequency was required and saturation of the amplier raised again as the major problem. Accordingly, the RC network was avoided and the ideal low pass filter has to be used.

Ideal Low-pass Filter:-

Consider a system which has the following characteristic. f(t), the input to the system, has a Fourier spectrum $F(j\omega)$, see App (A-1), which is such that

$$F(j\omega) = 0 \quad |\omega| > \omega_c \quad \ldots\ldots\ldots\ldots \quad (4.6)$$

Then, the output g(t) will be equal to f(t) multiplied by a constant or be equal to (f(t) multiplied by a constant and delayed in time, this is (see App (B)).

$$g(t) = Kf(t-T) \quad \ldots\ldots\ldots\ldots\ldots \quad (4.7)$$

In this case, the output waveform will be the same shape as the input waveform and the system is said to be distortionless.

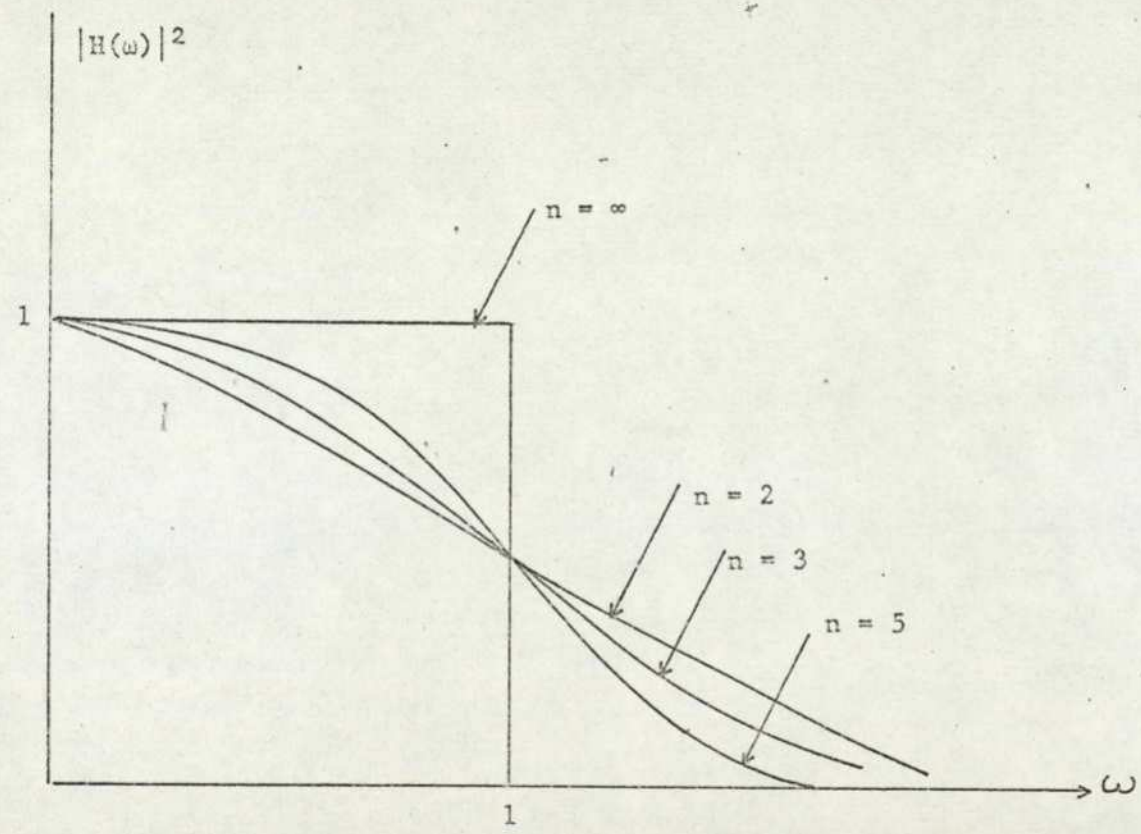

Fig. (4.15): Approximation to Ideal Low-Pass Filter characteristic (i.e. R.C. combination).

Now, consider the transfer function $H(j\omega)$ of such a distortionless system. If $t = 0$, then $g(t) = kf(t)$ and (see App (B-1))

$$H(j\omega) = k \quad -\omega_c \le \omega \le \omega_c \qquad \ldots\ldots\ldots\ldots \quad (4.8)$$

However, if the sytem delays the signal, then by using the time shift theorem, we have

$$H(j\omega) = k\, e^{-j\omega T} \qquad \ldots\ldots\ldots\ldots \quad (4.9)$$

Thus, the magnitude of $H(j\omega)$ is constant and its phase angle varies linearly with time if the system is distortionless. Hence, the transfer function for the network (filter), which passes, without distortion, signals whose Fourier spectrum is 0 for $|\omega| > \omega_c$, can be written as

$$H(j\omega) = \begin{cases} e^{-j\omega T} & -\omega_c \le \omega \le \omega_c \\ 0 & \omega > \omega_c \end{cases} \qquad \ldots\ldots\ldots\ldots \quad (4.10)$$

Thus, the transfer function $H(j\omega)$, such that $|H(j\omega)| = 1$ for $-\omega_c \le \omega \le \omega$, represent an ideal low-pass filter. It is illustrated in Fig (4.16).

Impulse Response:-

Impulse response of the ideal low-pass filter can be determined by applying eq. (A-2) and noting that $\delta(t) \to 1$, such that

$$h(t) = \frac{1}{2\pi} \int_{-\omega_c}^{\omega_c} e^{j\omega t} \, d\omega \qquad \ldots\ldots\ldots\ldots \quad (4.11)$$

Applying Euler's relation and eliminating the odd integraned, we obtain

$$h(t) = \frac{1}{2\pi} \left| \frac{e^{j\omega_c t} - e^{-j\omega_c t}}{jt} \right| \qquad \ldots\ldots\ldots\ldots \quad (4.12)$$

Then

$$h(t) = \frac{\omega_c}{2\pi} \sin \omega_c t / \omega_c t \qquad \ldots\ldots\ldots\ldots \quad (4.13)$$

This is of the form $(\sin x/x)$. Note that $h(t) \neq 0$ for $t < 0$. Thus the ideal low-pass filter is non-causal system.

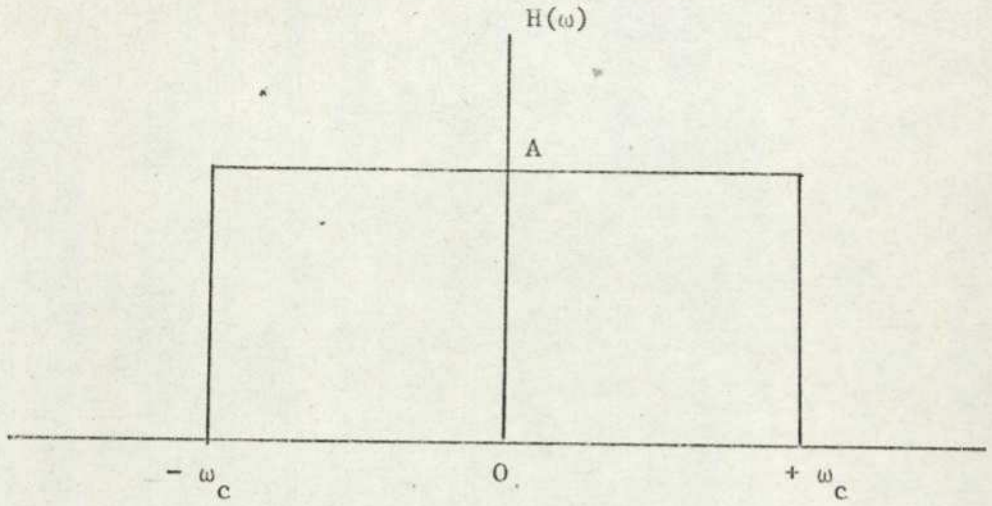

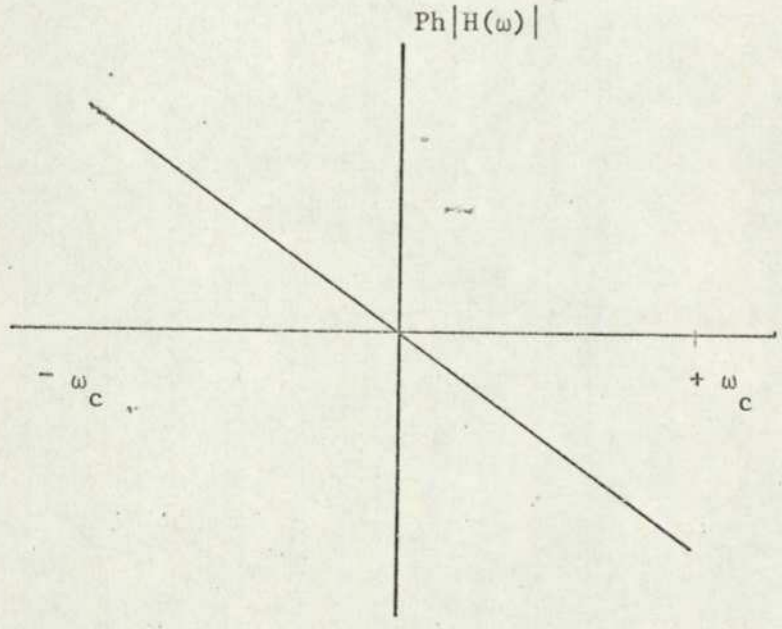

Fig. (4.16): Ideal Low-Pass Filter Characteristic.

Step Response:-

Refering to (App (B-2)), the time integration of Eq. (4.13) will give the step response of the ideal-low-pass filter $\alpha(t)$ where

$$\alpha(t) = \frac{\omega_c}{2\pi} \int_0^t \frac{\sin \omega_c t}{\omega_c t} \, dt \quad \ldots\ldots\ldots \quad (4.14)$$

hence,

$$\alpha(t) = \frac{1}{2\pi} \int_0^{\omega_c t} \frac{\sin X}{X} \, dx = \frac{1}{2\pi} \mathrm{Si}(\omega_c t) \quad \ldots\ldots \quad (4.15)$$

A plot of $\mathrm{Si}(\omega_c t)$ is given in Fig (4.17). Note that as $\omega_c t$ approaches infinity, $\mathrm{Si}(\omega_c t)$ approaches $\pi/2$, and that $\mathrm{Si}(\omega_c t)$ oscillates around this value. The maximum value of $\mathrm{Si}(\omega_c t)$ occurs at $\omega_c t = \pi$ and is given by

$$\mathrm{Si}(\pi) = 1.85194$$

Another useful fact is that, the unit step function can be considered as the sum of two waveforms. The first is simply a d.c. voltage of magnitude $\frac{1}{2}$ applied to the system at all time and the other is a unit step voltage from $-\frac{1}{2}$ to $+\frac{1}{2}$ applied at + = 0, Fig (4.18). Hence the new function g(t);

$$g(t) = \tfrac{1}{2} + \frac{1}{\pi} \mathrm{Si}(\omega_c t) \quad \ldots\ldots\ldots \quad (4.16)$$

represents the true ideal low-pass filter response to the step voltage. A plot of this function is shown in Fig (4.19). The time axis is in units of $\omega_c t$.

There are several important facts that should be mentioned. At t = 0 corresponding to the origin, g(t) is $\frac{1}{2}$ independent of the value of ω_c. In addition, for any fixed ω_c, g(t) oscillates about its final value 1. Note that (for t > 0) g(t) "overshoots" and "undershoots" its final value of 1. The maximum value of g(t) is

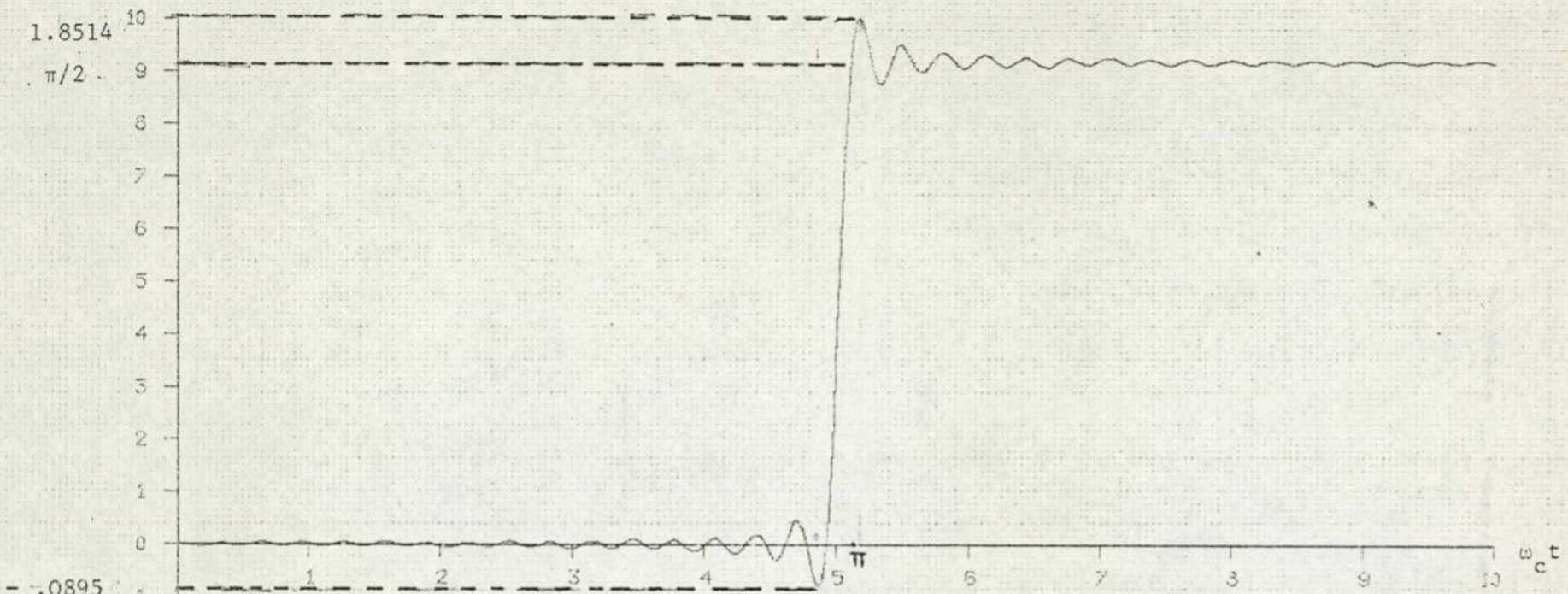

Fig. (4.17): Plot of $si(Y) = \int_0^Y \frac{\sin X}{X}\, dx$.

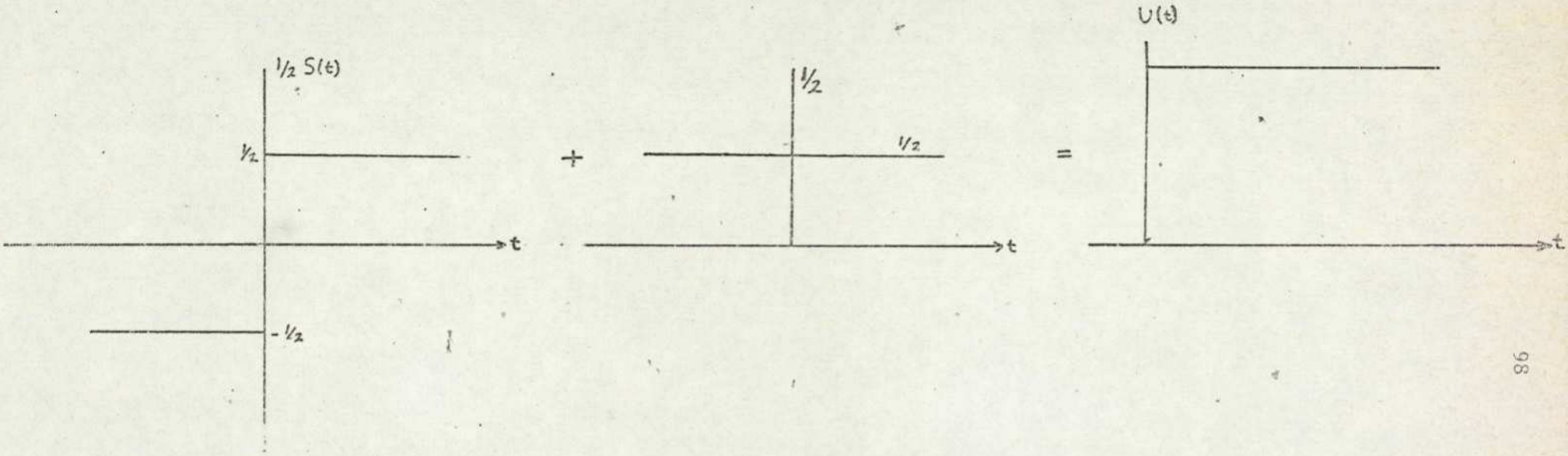

Fig. (4.18): Representation of U(t) as 1/2 (1 + S(t)).

$$g(t)\Big|_{max} = 1.0895$$

This occurs at $\omega_c t = \pi$ or, equivalently, at $t = \frac{\omega_c}{\pi}$. In addition for $t < 0$, $g(t)$ oscillates about zero. The minimum value of $g(t)$ is

$$g(t)\Big|_{min} = -0.0895$$

This occurs at $t = -\pi/\omega_c$

Comments:-

1. Defining the rise time t_r as from 0.1 to 0.9 of the amplitude gives:

$$\omega_c t_r = \pi \quad \text{or} \quad t_r = \frac{1}{2f_c}$$

2. The ripple frequency f_r is given by $f_r = \frac{1}{T}$ where;

$$\omega_c T = 2\pi$$

$$\therefore f_{rp} = f_c$$

3. The output response appears to begin even before the application of the step function. This is because of the idealized filter characteristics which cannot be obtained in practice.

4. The integral of (sin x/x) cannot be evaluated in closed form but, it can be evaluated by numerical means. This integral is written as

$$Si(\omega_c t) = x - \frac{x^3}{3.3!} + \frac{x^5}{5.5!} \quad \text{for } x \leq 10 \quad \ldots (4.17)$$

and

$$Si(\omega_c t) = \pi/2 - \left(\frac{1!}{x^2} - \frac{3!}{x^4} + \frac{5!}{x^6} + \ldots\right) \sin x$$

$$- \left(\frac{0!}{x^1} - \frac{2!}{x^3} + \frac{4!}{x^5} + \ldots\right) \cos x \quad \text{for } x \geq 10 \quad \ldots (4.18)$$

Hence, the computer was programmed to generated $(Si(\omega_c t) + \frac{1}{2})$ from equations (4.17) and (4.18). The obtained function was output through the General Input-Output Unit and the final result will be illustrate in chapter (5).

5. The most interesting thing about the function $\alpha(t)$ is that:

a) The ratio $\frac{f_c}{f_s}$, where f_s is the sampling frequency, could be varied such that;

$$\alpha(t) = \frac{1}{2\pi} \int_0^{\omega_c t} \frac{\sin x}{x}\, dx$$

$$= \frac{1}{2\pi}\, Si(\omega_c t)$$

Taking $t = kT$ where $k = 1, 2, 3 \ldots$

and $T = 2\pi/\omega_c$

Hence

$$\alpha(kT) = \frac{1}{2\pi}\, Si\left(2\pi k \frac{\omega_c}{\omega_s}\right) \quad \ldots\ldots\ldots\ldots \quad (4.19)$$

Refering to Fig (4.17), the peak occurs when $\sin x = 0$ i.e. $x = \pi$ therefore

$$\frac{\omega_c}{\omega_s}\, 2\pi k = \pi \quad \ldots\ldots\ldots\ldots \quad (4.20)$$

or

$$\frac{\omega_c}{\omega_s} = \frac{1}{2k} \quad \ldots\ldots\ldots\ldots \quad (4.21)$$

Obviously, the ratio ω_c/ω_s can take any value depending on the number of the points required for the peak to occur, i.e. k. In addition to that ;

b) For a given ratio f_c/f_s, f_s can be decreased or increased depending on how fast the function $Si(\omega_c t)$ is output. The speed, of outputing the function's samples, via the D/A converter, was dependent on the clocking rate of the clocking pulses, generated by a timing clock used for this purpose. Hence, the sampling frequency, which is equal to clocking frequency, can be varied by changing the latter and accordingly, the cutoff frequency will change, see equation (4.21). A programme,

written to initiate sampling of the dielectric response to the function $Si(\omega_c t)$ and output it at the same time, is shown in App (G).

CHAPTER FIVE.

Experimental Work and Results

5.1. Dielectric Measurements Requirements:-

It is easy in principle to apply to a specimen (i.e. dielectric sample) a voltage (i.e. step function) and generate a response. In practice, however the measurement of such response (charging, discharging current) demands:

1. Fast, High-gain and Low-noise Amplifier
2. Reliable Test-cell
3. The Usage of the Discharging Instead of the Charging Current
4. Other Requirements.

5.1.1 Fast, High-gain and Low-noise Amplifier.

It needs to be fast because switching at $t = 0$ is accompanied by a sudden charge of $\varepsilon_\infty E_o$ in the electric displacement (see Chapter 3). Theoretically this should last an infinitesimal time, that is the current corresponding to it (i.e. through a perfect capacitor) should be a delta function. In practice, the amplifier attached to the dielectric sample does not respond infinitely fast, mainly due to the presence of the stray capacitance across the feedback resistance and the switch surge lasts for some time.

The usage of such a slow rise time amplifier would mean a slow recovery time, resulting in a superimposed output response. Thus the detection of the true dielectric response would be delayed and errors would be introduced in the measurements.

However, the effect of the stray capacitor was almost eliminated using the technique described in Chapter (4) and hence, the rise time was reduced to the minimum (10 m sec).

The high-gain was required because relaxation times of polymeric solid materials are, in general, very long. Therefore, the resulting output response (current) of such material, due to voltage application, should be measured for a long time (i.e. 500 secs). After such a long time the magnitude of the current becomes very small (i.e. in the range of 10^{-15} A) and therefore a very high-gain amplifier is required. A feedback arrangement was adopted for this purpose and a feedback resistance of 10^{11} Ω was used. The adoption of such an arrangement was not just to obtain a high-gain amplifier but also to reduce the input impedance of the amplifier (see Chapter 4). The latter was necessary to ensure that the full polarizing voltage appears across the specimen, when the input impedance of the amplifier is considerably less than the instantaneous effective resistance of the sample.

Apart from the obvious problem of noise in the same band as the small input signal a low-noise amplifer should be used since sampling at low-rate (e.g. 1 Hz) is required due to the fact that at normal temperature the maximum loss, represented by the peak in ε'' - log f curve, occurs at a very low frequency. Thus, the presence of high-frequency components (i.e. short-time responses, peak-to-peak noise) in the output response resulted in aliasing which makes the interpretation of the results the most difficult. Hence the existence of such high-frequency components is undesirable. However, the peak-to-peak noise, mainly due to the earth circulation and pick up were reduced

to minimum by using a one earth system (i.e. floating the power supplies, etc.) and a low-pass filter to extract the rest of these noises and to remove all the short-time components in the output decay function before it is sampled.

5.1.2 Reliable Test-Cell.

The test-cell plays a very important role in these measurements and using a reliable one could facilitate the whole process to a very great extent. This cell should satisfy the following:

a. Three-terminals test-cell: A test-cell consisting of two electrodes could be used but the addition of an earthed guard-ring surrounding the lower electrode will make sure that the surface leakage currents and field fringing did not affect measurements taken from the guarded electrode. As a general rule the width of the guard-ring should be 10 times the electrode spacing in order to overcome the effect of field fringing. If this condition is satisfied the electric flux will be normal to the electrodes in the vicinity of the guarded electrode, and hence the electrode will "see" a piece of dielectric of an area equal to its own.

b. The material under test should fill a capacitor so that it makes perfect contact with perfectly clean electrodes, that it fills the capacitor without leaving voids. In practice, the absence of such conditions will introduce (i) non-ohmic electrode (see Chapter 3) and (ii) the building up of space charge at the electrode surfaces.

The existence of either (i) or (ii) will result in non-linear behaviour of D as a function of E and invalidate the principle of

superposition (see Chapter 3), so that the complications introduced by non-ohmic electrode and interfacial polarization are serious in principle.

Originally, it was hoped to deposit or evaporate a thin layer of metal onto the surface of the dielectric, and then make a division between the guard-ring and the guarded electrode using a photo-etch technique. Unfortunately, the evaporation process required a temperature above the melting point of the polymer. Nevertheless, the test cell being used in the present measurements, Fig. (4.3) was tested at Bangor University, using a General Radio Bridge Model 1621. Table (5.1) illustrates the testing results.

5.1.3 Discharging Instead of Charging Current.

For $\varepsilon''(\omega)$ and $\varepsilon'(\omega)$ evaluations the discharging current should be used instead of the charging current for the following reasons:

a. The experimentally determined dielectric absorption is a measure of energy dissipation in the medium and, in practice, most systems will show energy losses from processes other than dielectric relaxation. Usually these will be in charging current measurement related to the d.c. conductivity of the medium. Assuming a homogeneous medium of conductivity $\delta(\text{ohm}^{-1}\ \text{cm}^{-1})$ the Joule heating arising from the conductivity contributes a loss factor ε''(conductances) so that the observed value of frequency f Hz is :

$$\varepsilon''\ (\text{total}) = \varepsilon''(\text{dielectric} + \varepsilon''(\text{conductance})$$

$$\varepsilon''\ (\text{total}) = \varepsilon''d_i + \frac{\delta(\omega)}{\varepsilon_o \omega} \qquad \ldots\ldots\ldots \quad (5.1)$$

Frequency of the Applied Field	Capacitance (pf)	Conductivity $(Ohm)^{-1}$	ε'' x A/d
20 HZ	28.282	3.143×10^{-11}	2.33×10^{-2}
100 HZ	28.05	1.37×10^{-10}	2.46×10^{-2}
1 KHZ	27.771	1.207×10^{-9}	2.17×10^{-2}
10 KHZ	27.5	1.28×10^{-8}	2.3×10^{-2}
29.8 KHZ	27.35	3.63×10^{-8}	2.19×10^{-2}

NOTES.

a. Leakage resistance at 1 KHZ > 10^{16} ohm

b. ε'' x A/d was calculated from

$$\delta(\omega) = \omega\varepsilon_o\varepsilon''$$

c. It was not possible to go below 20 HZ due to difficulty associated with bridge balancing.

Table (5.1): Measurements taken with a General Radio Bridge (Model 1621) on test cell with dielectric sample (PVAC)

With higher values of δ(i.e. at high temperatures), the corresponding loss factor will persist to higher frequencies and correspondingly larger at lower frequencies (Davies, 1969).

Hence, the use of charging current will introduce errors in dielectric measurements while the discharging current measurements give a clear way of separating the loss due to relaxation from the loss due to d.c. conductivity (see Chapter 3).

b. In the presence of the d.c. conductivity there are difficulties of convergence associated with the evaluation of $\varepsilon^*(\omega)$

for a rising step voltage and a negative going step is required.

c. Effectively the discharging current is the mirror image of the charging current (after substraction of the steady-state current) and when the latter decays to its minimum value (i.e. when the polarizaing step-voltage applied for a sufficient time, see Fig. (3.4).

5.1.4 Other Requirements.

a. It is always necessary to keep strict control of polarization and depolarization times to ensure that samples were thoroughly depolarized at the beginning and the end of each experiment.

b. A zero offset control should be provided for the amplifier since this allows the output to be set to zero when there is no input current (i.e. at the beginning of each experiment).

c. A "noise-free" cable carrying graphite on the polyethylene under the screening braid should be used to connect the guarded electrode to the input of the d.c. amplifier or electrometer. Long connecting leads between test-cell and amplifier are most susceptible to microphonic pick-up and introducing extra capacitance to the sample and the amplifier's input capactances. Thus, slowing down the amplifer response and leading to errors in the dielectric measurements.

d. Dielectric sample should be left at the chosen temperature for sufficient time in order to attain equilibrium in temperature distribution over the whole parts of the sample.

5.2 Step-Function Technique Measurements

5.2.1 Preliminary Work.

It is always desirable, before any measurement on the dielectric specimen can be carried out using the whole set up, to check up the function of each part of the system separately.

5.2.1.1 Amplifier Test.

It was shown earlier in Chapter (4) that the amplifier response to square pulses was quite adequate (see Fig. 4.9) and its rise time was reduced to 10 m sec by using the modification technique described there. Therefore, the amplifier is reasonably fast and functioning correctly.

5.2.1.2 Test-cell Check.

Refering to Appendix (5), Eq. (E.8), shows that it is not possible to distinguish between the effects of interfacial and orientational polarizability by a sole measurement of the real part of relative permittivity. That is because the variation of ε' with frequency is precisely the same as that for the case of Debye relaxation. On the other hand Equation (E.9) gives a clear way to distinguish between the two polarizabilities by observing the variation of ε'' with frequency such that, ε'' tends to infinity as ω tends to zero. In the Debye case ε'' drops towards zero as the frequency is lowered.

Consequently, measurements on test-cell containing the dielectric sample were carried out, see section 5.1.2, to observe the variation of ε'' with the frequency of the applied voltage.

The smallness of the difference between the value of ε'' at 20 HZ and that at 29.8 KHZ, (see table (5.1)), proves without doubt that the interfacial polarization is not a major problem. Hence the sample is a homogenous medium and the test-cell is a reliable one.

5.2.1.3 Fast Fourier Transform Program Test.

Testing of the F.F.T program function was done by evaluating the F.T. of the pulse $f_T(t)$ shown in Fig. (5-1a). This pulse can be considered as the sum of the unit step advanced by T seconds and the negative unit step delayed by T seconds Fig. (5.1b). From Appendix A, we have

$$U(t) \leftrightarrow \pi\delta(\omega) + \frac{1}{j\omega} \quad \ldots\ldots\ldots\ldots\ldots\ldots \quad (5.1)$$

using the time shift theorem, we have

$$U(t - T) \leftrightarrow e^{-j\omega T} \{ \pi\delta(\omega) + \frac{1}{j\omega} \} \quad \ldots\ldots\ldots \quad (5.2a)$$

and

$$U(t + T) \leftrightarrow e^{j\omega T} \{ \pi\delta(\omega) + \frac{1}{j\omega} \} \quad \ldots\ldots\ldots \quad (5.2b)$$

Before proceeding further let us evaluate $f(x)\ \delta(x)$; i.e., the product of the impulse and ordinary function. Distribution theory shows that if $f(x)$ is continuous at $x = 0$, we can write;

$$f(x)\ \delta(x) = f(0)\ \delta(x)$$

Applying the above relation to Equation (5.2) yields

$$U(t - T) \leftrightarrow \pi\delta(\omega) + \frac{e^{-j\omega T}}{j\omega} \quad \ldots\ldots\ldots\ldots \quad (5.3a)$$

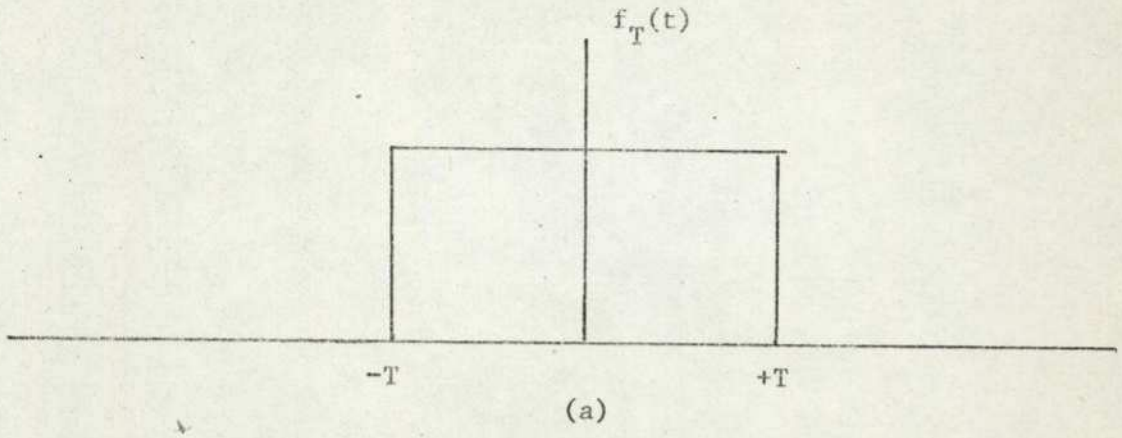

(a)

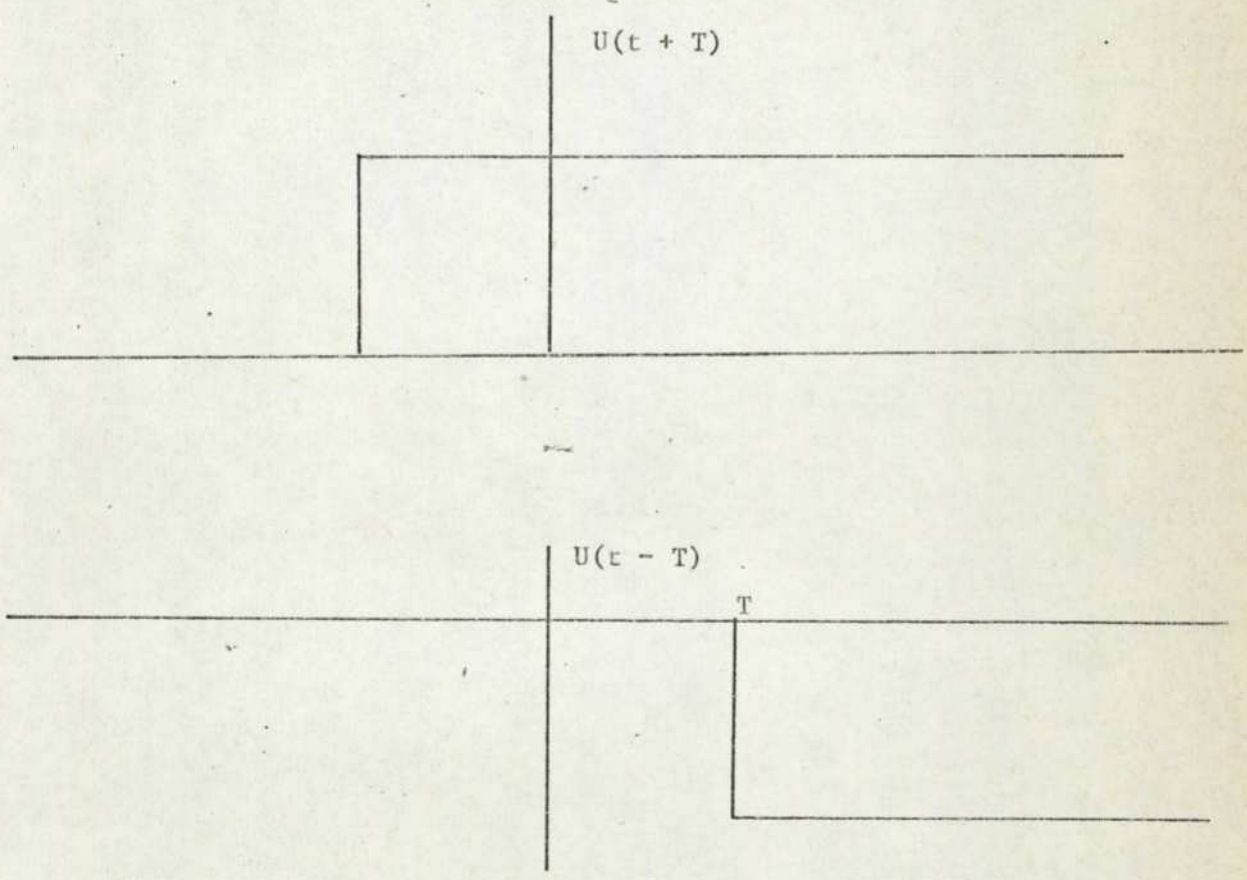

(b)

Fig. (5.1): (a) Pulse $f_T(t)$.

(b) Two function which, when added, yield $f_T(t)$.

and

$$U(t + T) \leftrightarrow \pi\delta(\omega) + \frac{e^{j\omega T}}{j\omega} \quad \ldots\ldots\ldots\ldots \quad (5.3b)$$

Now

$$f_T(t) = U(t + T) - U(t - T)$$

Then applying F.T. linearity property we have

$$f_r(t) \quad \frac{e^{j\omega T} - e^{-j\omega T}}{j\omega} = 2\frac{\sin(\omega T)}{\omega} = 2T \text{ Sinc } (\omega T) \ldots\ldots \quad (5.3c)$$

Accordingly, a narrow rectangular pulse was taken from the high voltage transistor output, through the A/D converter, to the computer. The pulse and its F.T., in real and imaginary forms, are shown in Fig. (5.2). The reason for this complex F.T. spectrum is that the rectangular pulse is unlike $f_T(t)$ far from symmetrical about $t = 0$ and could therefore only be synthesised from both sin and cos terms. Hence, the results including the imaginary part, $(\cos \omega T - 1)/\omega$, makes it clear that the F.T. program is functioning correctly. However, the distortion occurs in Fig. (5.2b) due to the small d.c. voltage associated with transistor output (see Fig. 5.2a).

5.2.2 Direct Measurements.

5.2.2.1 R.C. Network Direct Measurements:-

Although, it was shown that most of the fundamental parts of the system were functioning correctly, it is still important to make sure that the measured step response is in fact due to relaxation occuring in the dielectric sample or its RC equivalent, and not in some other parts of the system.

This easily could be checked by:

- Recording the step response of the test-cell with and without the dielectric sample. For the case without dielectric, an air gap

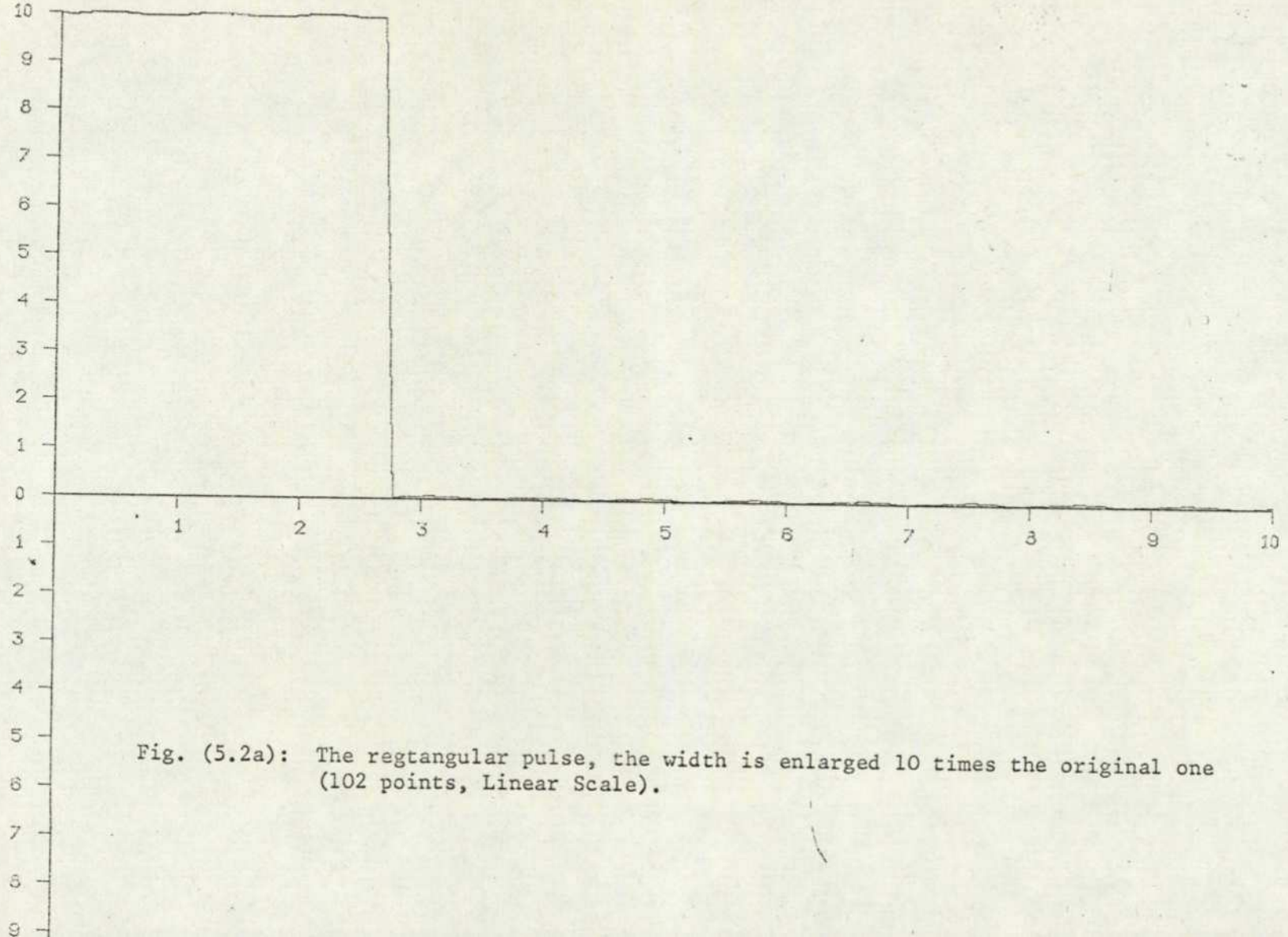

Fig. (5.2a): The regtangular pulse, the width is enlarged 10 times the original one (102 points, Linear Scale).

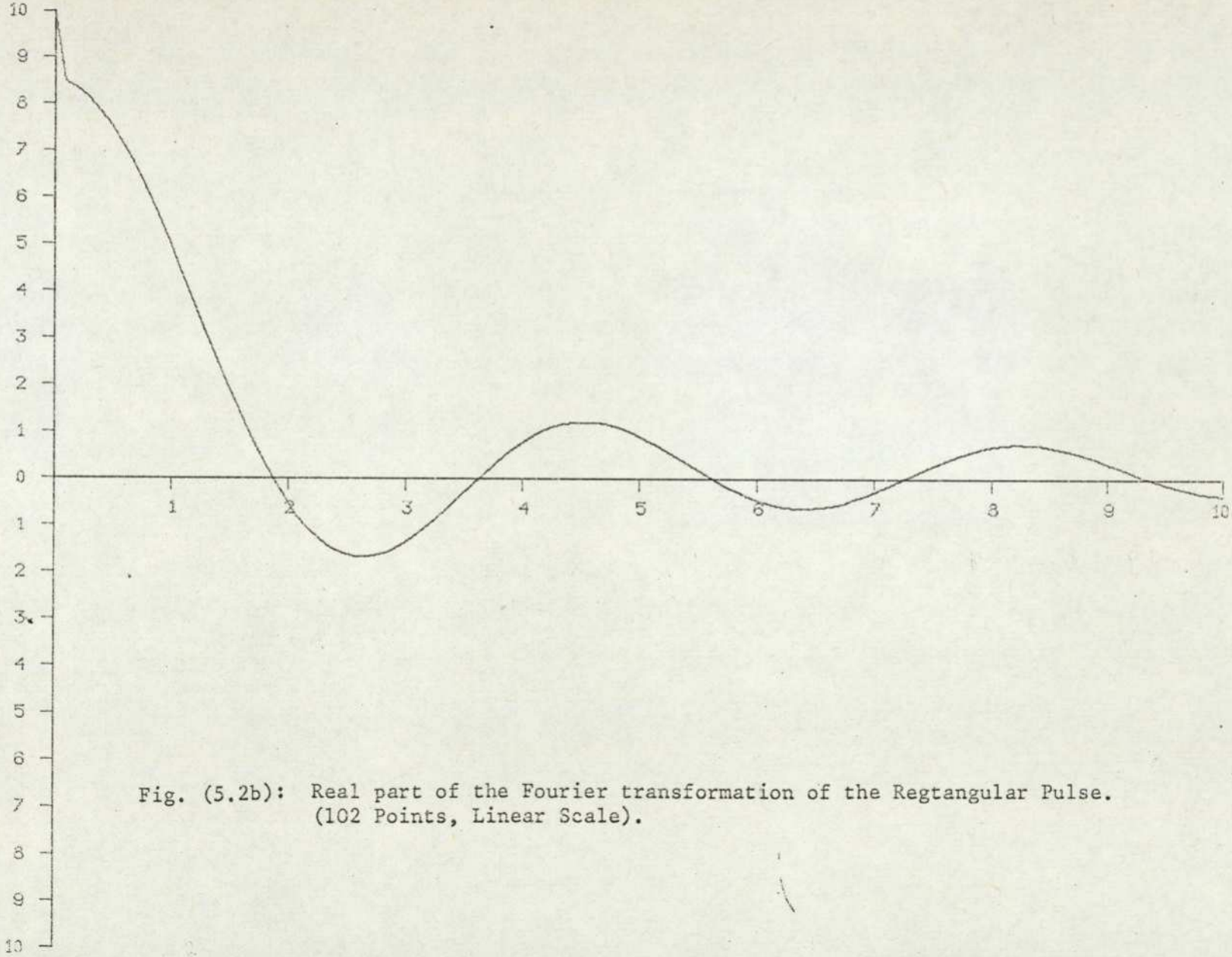

Fig. (5.2b): Real part of the Fourier transformation of the Regtangular Pulse. (102 Points, Linear Scale).

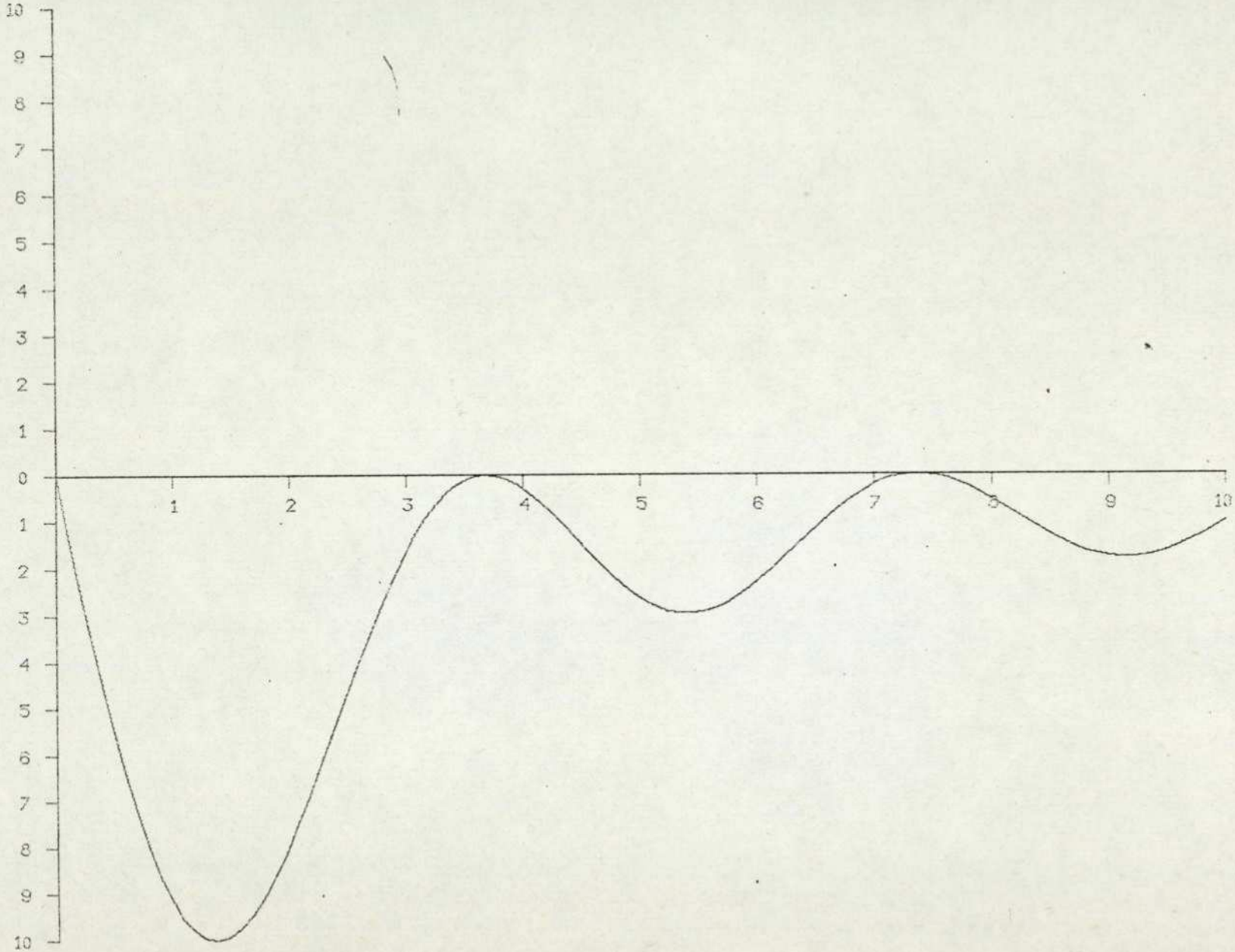

Fig. (5.2c): Imaginery Part of the fourier transformation of the Regtangular pulse (102 points, linear scale).

equal to the thickness of the sample could be formed with insulting spacers between the guarding and the upper electrodes.

However, the immediate dying of the response due to the usage of the relay gave insignificant result and therefore the following procedure was then adopted.

- A series RC combination (parallel combination is not suitable since the d.c. voltage appears across the amplifier's input resistance after $t > o$ and tends to saturate the amplifier) provides a good test to the whole system. The use of such arrangement could be attributed to:

1. The frequency corresponding to maximum energy loss (f_m) can be easily calculated from knowing the RC value such that:

Refering to equation (C.2), App. (C), we have

$$Z = R + \frac{1}{J\omega C}$$

or

$$Y = \frac{1}{Z} = \frac{j\omega C}{1 + jR\omega C} = \frac{j\omega C + R^2\,\omega^2\,C^2}{1 + R^2\,\omega^2\,C^2} \quad \ldots\ldots \quad (5.4)$$

By definition, a capacitor containing a dielectric of relative permittivity $\varepsilon_r = \varepsilon' - j\varepsilon''$, has an admittance,

$$Y = j(\varepsilon' - j\varepsilon'')\omega\, C_o \quad \ldots\ldots\ldots\ldots\ldots\ldots \quad (5.5)$$

Therefore, From equations (5.4) and (5.5) we have

$$\varepsilon' = \frac{C}{C_o}\,\frac{1}{1 + R^2\,\omega^2\,C^2} \quad \ldots\ldots\ldots\ldots\ldots\ldots \quad (5.6a)$$

and

$$\varepsilon'' = \frac{C}{C_o}\,\frac{CR\,\omega}{1 + \omega^2\,R^2\,C^2} \quad \ldots\ldots\ldots\ldots\ldots\ldots \quad (5.6b)$$

Taking $\frac{d\epsilon''}{d\omega}$ and making it equal to zero (maximum energy loss), we have

$$\frac{d}{d\omega}\left\{\frac{R^2\,\omega}{1+\omega^2\,R^2C^2}\right\} = 0$$

This results in

$$\hat{\omega} = \frac{1}{RC}$$

or

$$\hat{f} = \frac{1}{2\pi RC} \qquad \ldots\ldots\ldots\ldots\ldots\ldots \qquad (5.7)$$

Therefore, for certain values of R and C the whole system could be checked by comparing the calculated frequency with the experimental one

2. The output step response of the RC network is a time function f(t) such that :

$$f(t) = \begin{cases} 0 & t < 0 \\ e^{-\beta t} & t > 0 \end{cases}$$

where β is real and postive. Thus f(t) is 0 for $t < 0$, becomes 1 for $t = 0+$ (i.e. just greater than zero), and then decays exponentially. To obtain the F.T. of such function we substitute for f(t) in equation (A.1), App (A).

$$F(j\omega) = \int_0^\infty e^{-\beta t}\; e^{-j\omega t}\, dt = \frac{-1}{\beta + j\omega}\; e^{-(\beta + j\omega)t}\Big|_0^\infty$$

or

$$F(j\omega) = \frac{1}{\beta + j\omega} \qquad \ldots\ldots\ldots\ldots\ldots\ldots \qquad (5.8)$$

Multiplying equation (5.8) by $(\beta - j\omega)$ and putting $F(j\omega) = R(\omega) + j\,X(\omega)$, we obtain

$$R(\omega) = \frac{\beta}{\beta^2 + \omega^2} \qquad \ldots\ldots\ldots\ldots\ldots\ldots \qquad (5.9a)$$

and

$$X(\omega) = -\frac{\omega}{\beta^2 + \omega^2} \quad \ldots\ldots\ldots\ldots\ldots\ldots\ldots\ldots \quad (5.9b)$$

The plot of f(t) and the magnitude of $R(\omega)$ and $X(\omega)$ are given in Fig. (5.3).

Therefore, comparing the theoretically predicted shapes of $R(\omega)$ and $X(\omega)$ with the experimental results gives a good check for the system's reliability.

Having justified the usage of RC network as an easy way to check the function of the whole system, we connected an RC network to the amplifier as shown in Fig. (5.4).

The values of R and different capacitors (e.g. $R = 10^{12}\ \Omega$, C = 15, 10 and 5.6 pf) were chosen to be close to the values of those associated with the dielectric sample.

A 50 volts rising step function was applied, but measurements at different sampling rates were taken when the external voltage was suddenly removed. The resulting output response, however, was filtered of frequences above the Nyquist folding frequency and was therefore virtually noise-free. Hence no cumulative averaging was required. Fig. (5.5) shows a typical inverted step-response of the RC network plotted by the computer. These transients were Fourier transformed by the computer and the results, in real and imaginary parts were plotted. Fig. (5.6) shows the F.T. of the output step-response of an RC network consisting of 15 PF capacitor and $10^{12}\ \Omega$ resistance.

It should be noted that in Fig. (5.6):

a - The graphs are plotted on a logarithmic frequency scale. This was done to get more meaningful results.

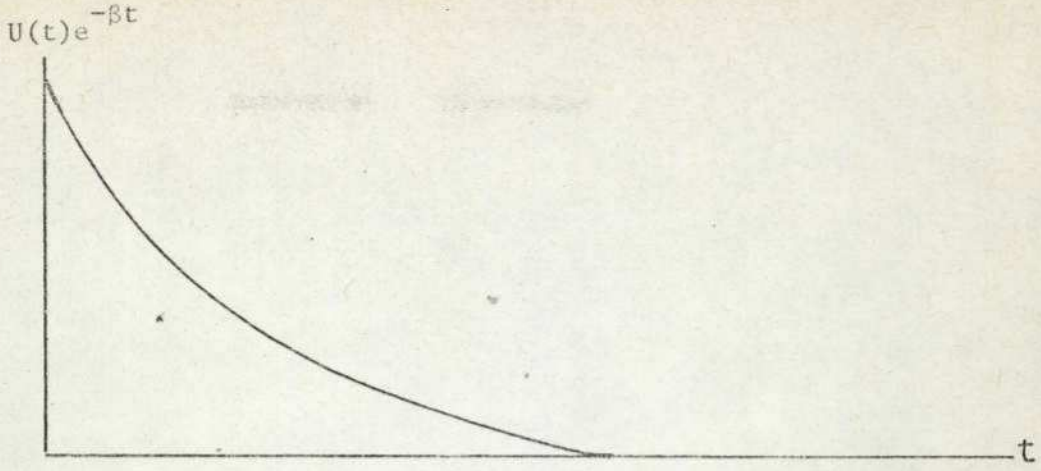

(a)

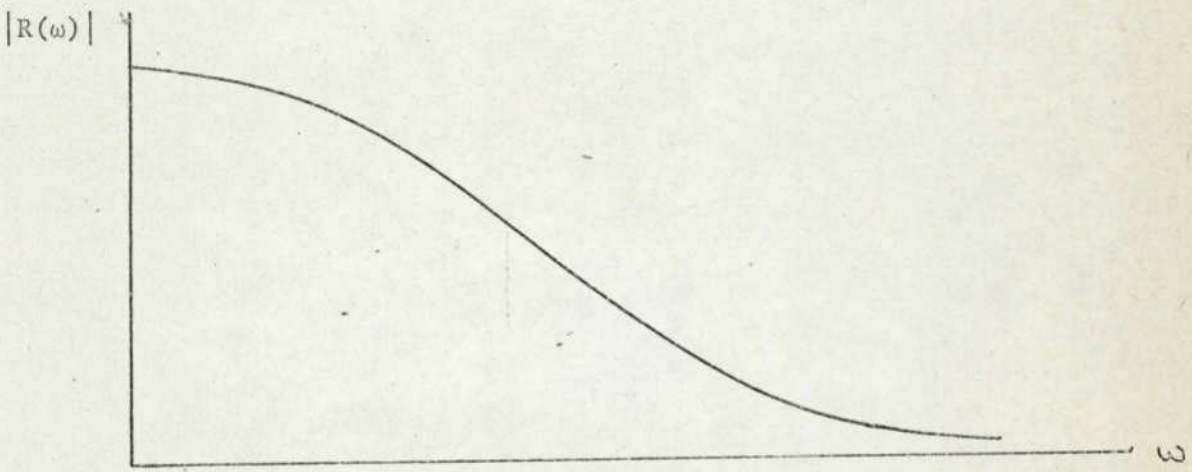

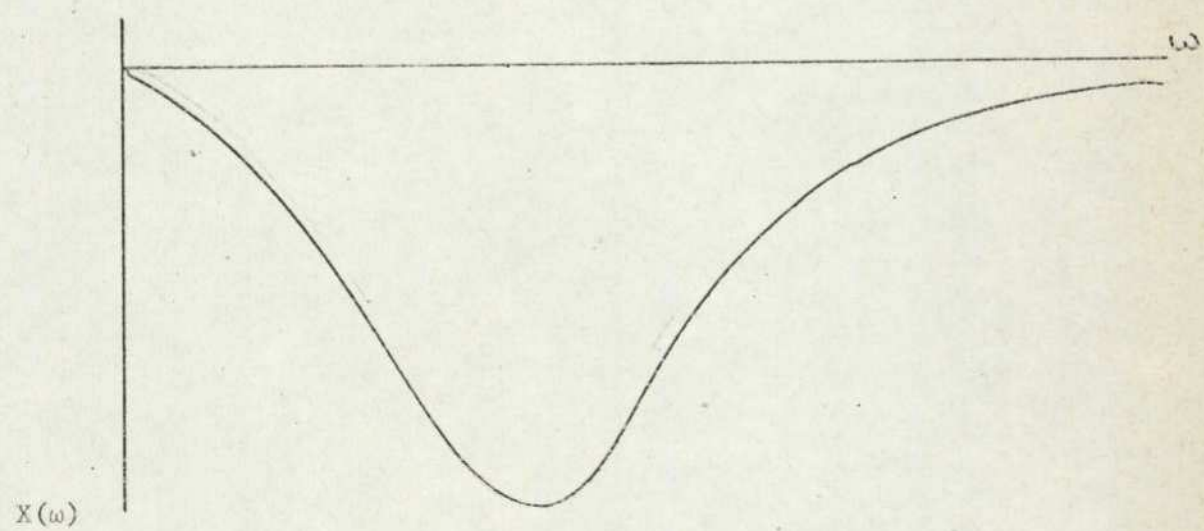

(b)

Fif. (5.3): a) Plot of $f(t) = U(t)\, e^{-\beta t}$;
b) Magnitude of its F.T parts, $R(\omega)$ and $X(\omega)$.

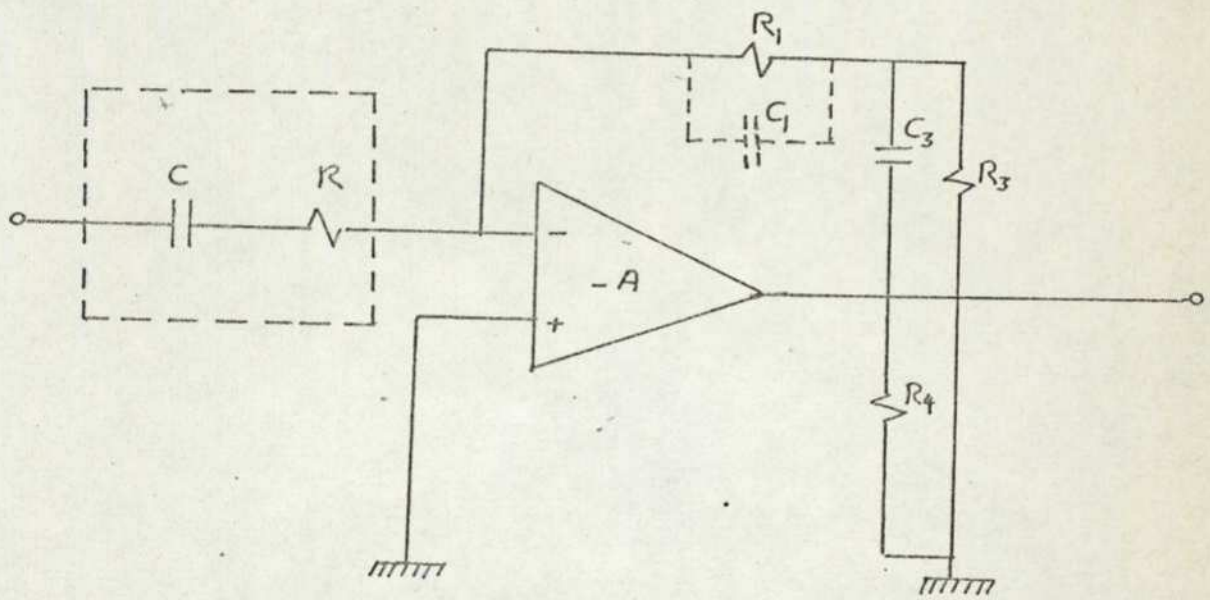

Fig. (5.4): Arrangement for R.C. network direct measurements.

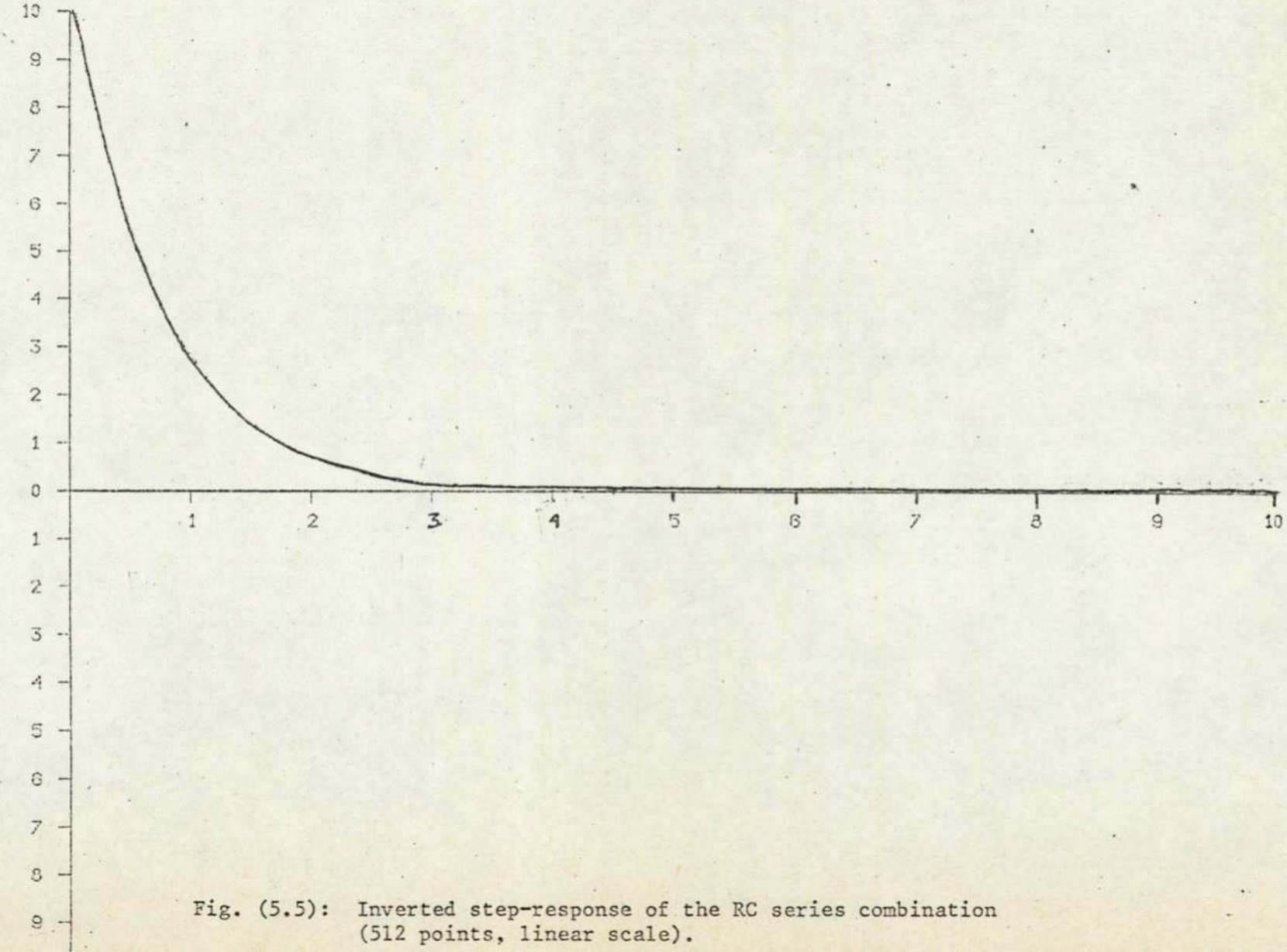

Fig. (5.5): Inverted step-response of the RC series combination (512 points, linear scale).

b - Fig.(5.6a) represents the variation of ε' with the frequency i.e. ε' - log f while ε'' - log f is plotted in Fig. (5.6b).

c - Only 512 points out of the 1024 original points were plotted in both curves. This was done to get clearer results.

d - Measurements were taken at sampling rate 1 Hz. Thus, the 10 X Divisions in both curves are equivalent to 1/2 Hz. This was calculated from,

The frequency equivalent to X_{th} divisions =

$$\frac{\text{Number of points represented by the } X_{th} \text{ division}}{1024} \times \text{sampling frequency}$$

e - Maximum loss, represented by the peak in Fig. (5.6b), occurs at frequency, fm = 1.0131×10^{-2} Hz. This was calculated from finding;

No. of points represented by the X_{th} division =

$$10^{\frac{X}{10}} \text{ Log (No. of points being plotted on the curve)}$$

Examining Fig. (5.6b) shows that fm occurs at 3.75 Divisions, therefore

No. of points represented by 3.75 Division = $10^{.375 \log (512)}$

= 10.370000 points

and

$$fm = \frac{10.370}{1024} \times 1 \text{ Hz} = 1.010000 \times 10^{-2} \text{ Hz.}$$

The above value is in a fair agreement with the theoretical fm = 1.0160×10^{-2} Hz calculated from Eq. (5.7).

f - It is noticeable that the first point of ε' - log f curve is not consistent with the rest of the curve. This occured frequently and it is difficult to investigate owing to the very low frequency represented

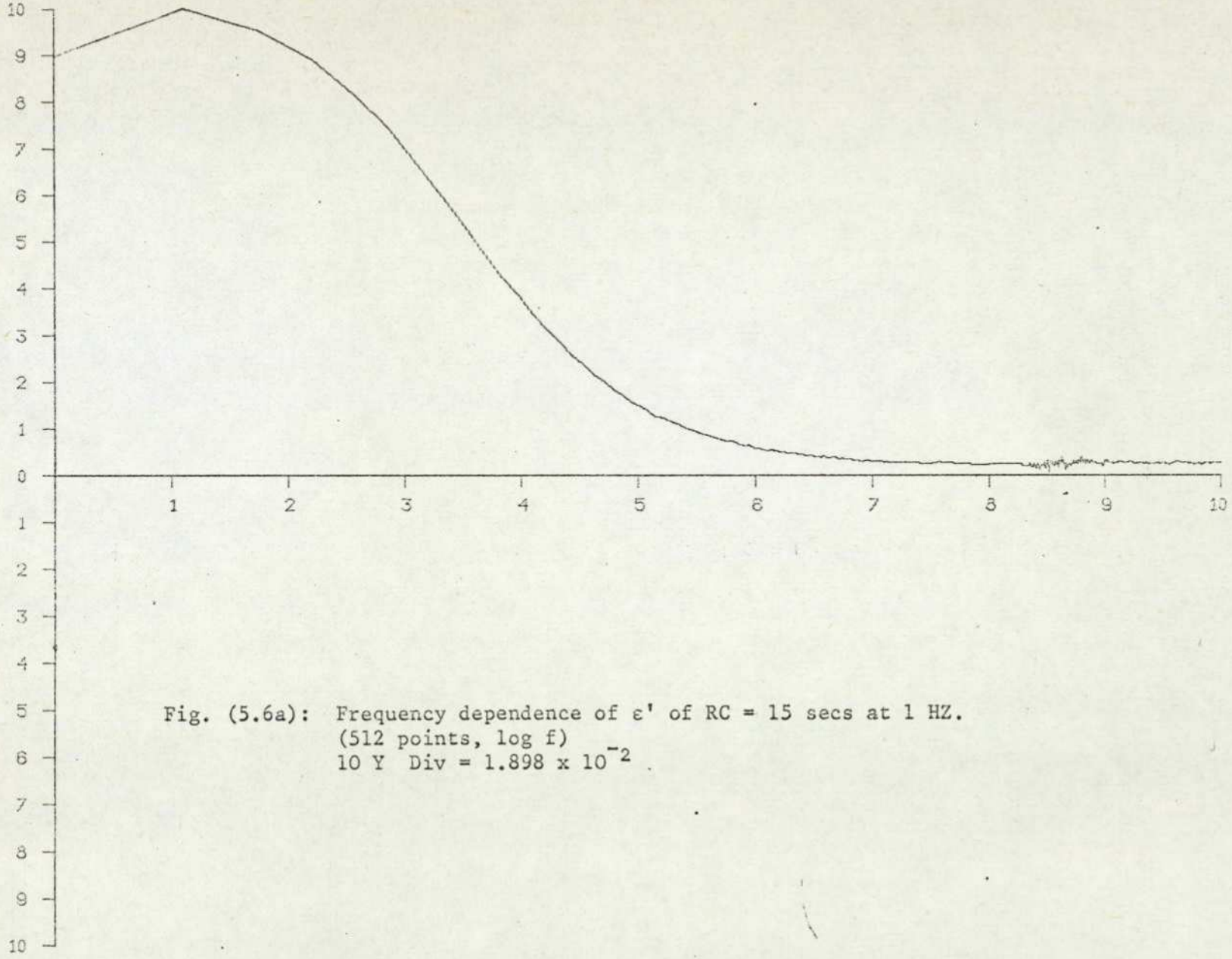

Fig. (5.6a): Frequency dependence of ε' of RC = 15 secs at 1 HZ.
(512 points, log f)
10 Y Div = 1.898×10^{-2}

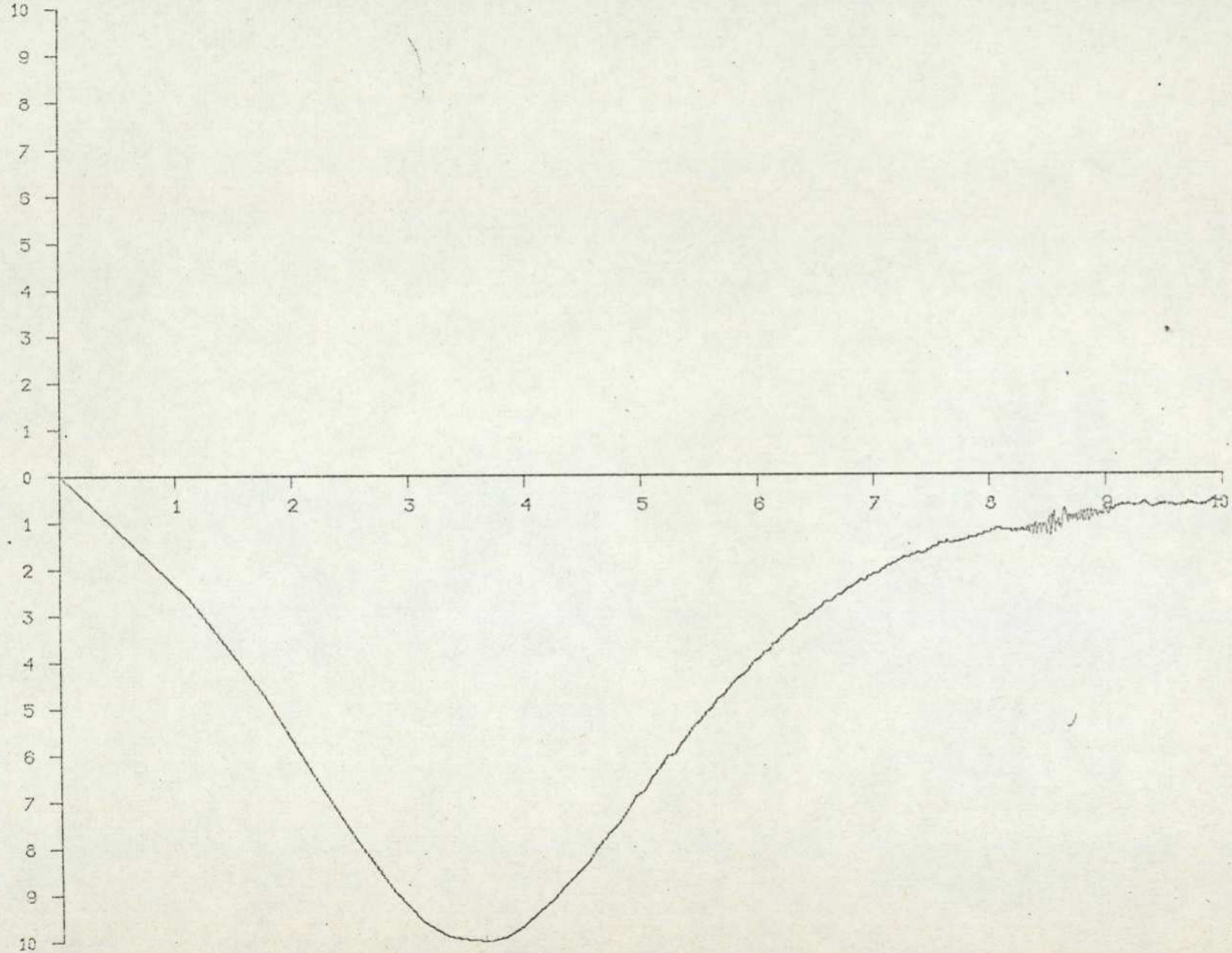

Fig. (5.6b): Frequency dependence of ε" of RC = 15 secs at 1 HZ.
(512 points, log f)

10 Y Div = 9.320×10^{-3}

by the first point, but was taken to be produced by the necessity to time - limit the total sampling period and the impossibility of exactly setting the d.c. offset in the amplifier. Hence, the response never reaches quite its theoretical value of zero during the experiment.

g - In Fig. (5.6a) ε_s, defined as the part of ε' at very low-frequency is equivalent to the 10 Y Divisions 1.9000×10^{-1}. ε_∞, defined as the part of dielectric permittivity occurs at high-frequency, is calculated from the above curves and found to be equivalent to 5.9000×10^{-2}. Although, the final points of the ε' - log f curve do not necessarily represents ε_∞ exactly but they seem to take a constant value beyond the 8th division.

Now, if the relaxation associated with the RC network is a Debye's relaxation type ($\omega_m \tau = 1$) then, the corresponding ε'_m and ε''_m of ε' and ε'' are obtained by introducing $\omega\tau = 1$ in Eqs. (2.23) and (2.24) respectively:

$$\varepsilon'_m = \frac{\varepsilon_s + \varepsilon_\infty}{2} \qquad \ldots\ldots\ldots\ldots\ldots\ldots \quad (5.11a)$$

$$\varepsilon''_m = \frac{\varepsilon_s - \varepsilon_\infty}{2} \qquad \ldots\ldots\ldots\ldots\ldots\ldots \quad (5.11b)$$

Using the above values of ε_s and ε_∞ in the above Eqs, we have

$$\varepsilon'_m = 9.85 \times 10^{-2}$$

$$\varepsilon''_m = 9.14 \times 10^{-2}$$

Fig. (5.6) shows that the corresponding values of ε'_m and ε''_m are equivalent to 9.6×10^{-2} and 9.32×10^{-2} respectively.

It is clear that ε'_m and ε''_m values calculated from Eq. (5.11) are in a good agreement with those found experimentally and hence, the relaxation is of Debye's type.

Although consistency between theoretical treatments and the above experimental results was found in many aspects, it was still necessary to carry out more measurements on different RC combinations. The reliablity of the system will be then proved by given different - correct results for these different RC networks.

Accordingly, measurements using different RC values (15, 10 and 5.6 secs) were carried out. The output step-response was sampled at a rate of 2 Hz in each case (i.e. different from the previous rate 1 Hz for RC = 15 secs). Fig. (5.7) shows only the imaginary parts of the F.T spectrum of the output step - responses for these three networks. It is obvious that the three peaks occur at three different positions along the f - axis. A good agreement between the calculated and the experimental (f_m) was obtained in each case and Table (5.2) illustrates such an agreement.

5.2.2.2 Dielectric Material Direct Measurements: -

Having made sure that the whole system functioned correctly, we replaced the RC network by a real dielectric sample (PVAC). Dealing with RC network measurements is not, however, a difficult problem. That is because the resistance R and C values are assumed to be constants (i.e. they are not function of either the applying voltage frequency nor the temperature). When it comes to the dielectric materials, the story becomes quite different. Capacitors and resistances associated with these materials are both functions of frequency and temperature (i.e. the resistivity $\delta \propto \lambda^{T}$ and ω and their values change as these parameters change.

Also, applying a step-function, containing both very high and very low-frequency components, to the dielectric sample will be accompanied

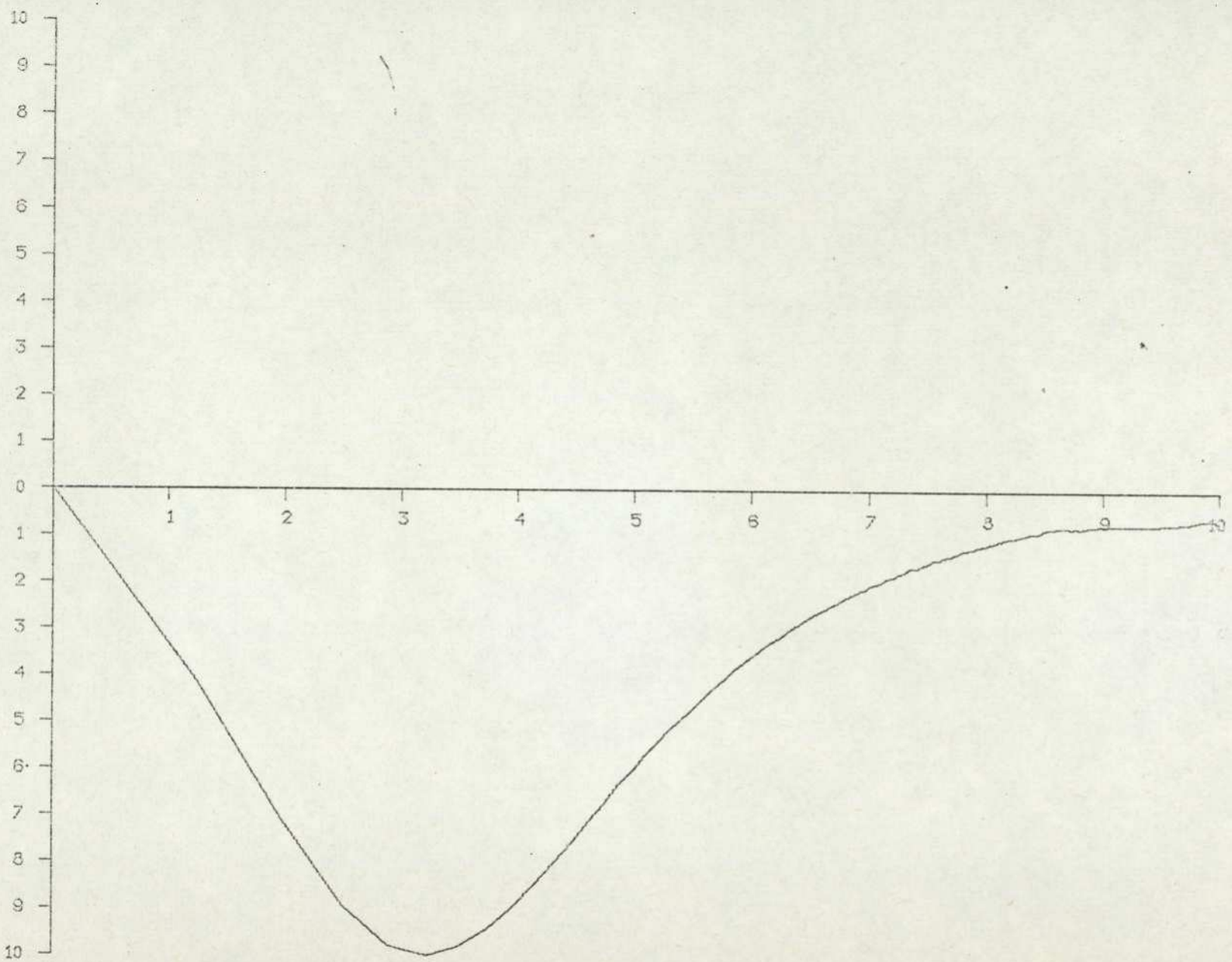

Fig. (5.7a): Frequency dependence of ε" of RC = 15 secs at 2 HZ (256 points, log f).

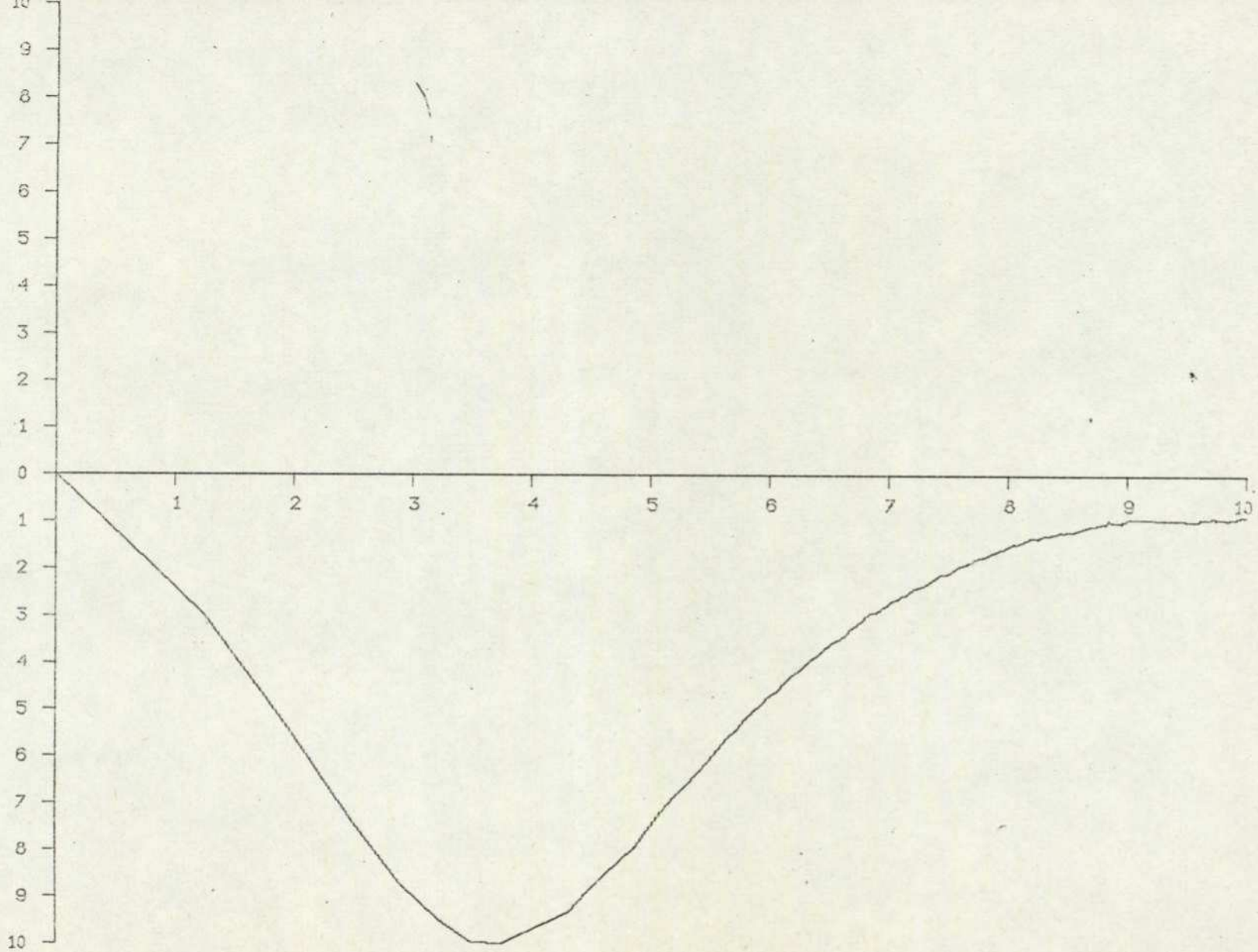

Fig. (5.7b): Frequency dependence of ε" of RC = 10 secs at 2 HZ (256 points, log f).

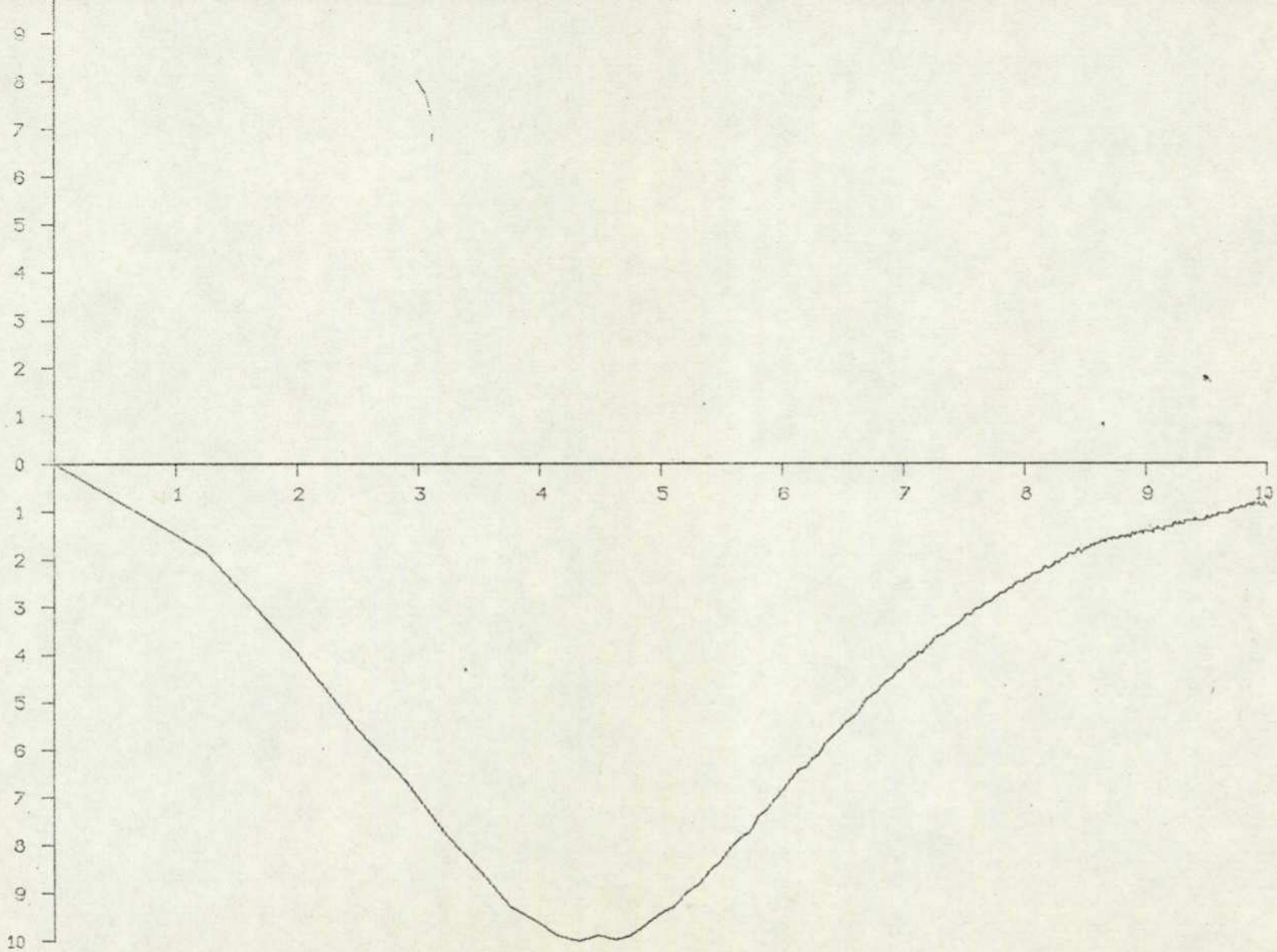

Fig. (5.7c): Frequency dependence of ε" of RC = 5.6 secs at 2 HZ (256 points, log f).

at t = 0, by a huge output response (current) which tends to saturate the amplifier if not causing damage to it.

Consequently, a relay was connected across the feedback resistance, see chapter 4, to protect the amplifier and to bypass the input to the amplifier during the initial short-time transient.

Measurements on PVA_c were, then, carried out and the results in real (ε' - log f) and imaginary (ε'' - log f) forms were obtained following the same procedure adopted in RC measurements. These results are presented

Figure Number	RC (sec)	Sampling Frequency (Hz)	Theoretical Frequency (Hz) ($f_m = \frac{1}{2\pi RC}$)	Experimental Frequency (Hz) f_m
(5 - 6) b	15	1	1.06×10^{-2}	1.01×10^{-2}
(5 - 7) a	15	2	1.06×10^{-2}	1.08×10^{-2}
b	10	2	1.59×10^{-2}	1.56×10^{-2}
b	5.6	2	2.84×10^{-2}	2.37×10^{-2}

Table (5.2) Comparison between the theoretical maximum frequency f_m - calculated from 1/2 πRC - and the experimental f_m.

in Fig. (5.8) and (5.9). The main features of these results are :

a - The shape of both curves (ε' - log f) and (ε'' - log f) are in a bad agreement with those predicted by theory (see Fig. (2.4)).

b - The peak corresponding to maximum energy loss associated with the ε'' - log f curve does not seem to be much affected when the sampling rate changes (i.e. from 1 Hz to 5 Hz) but the shape of both curves seem

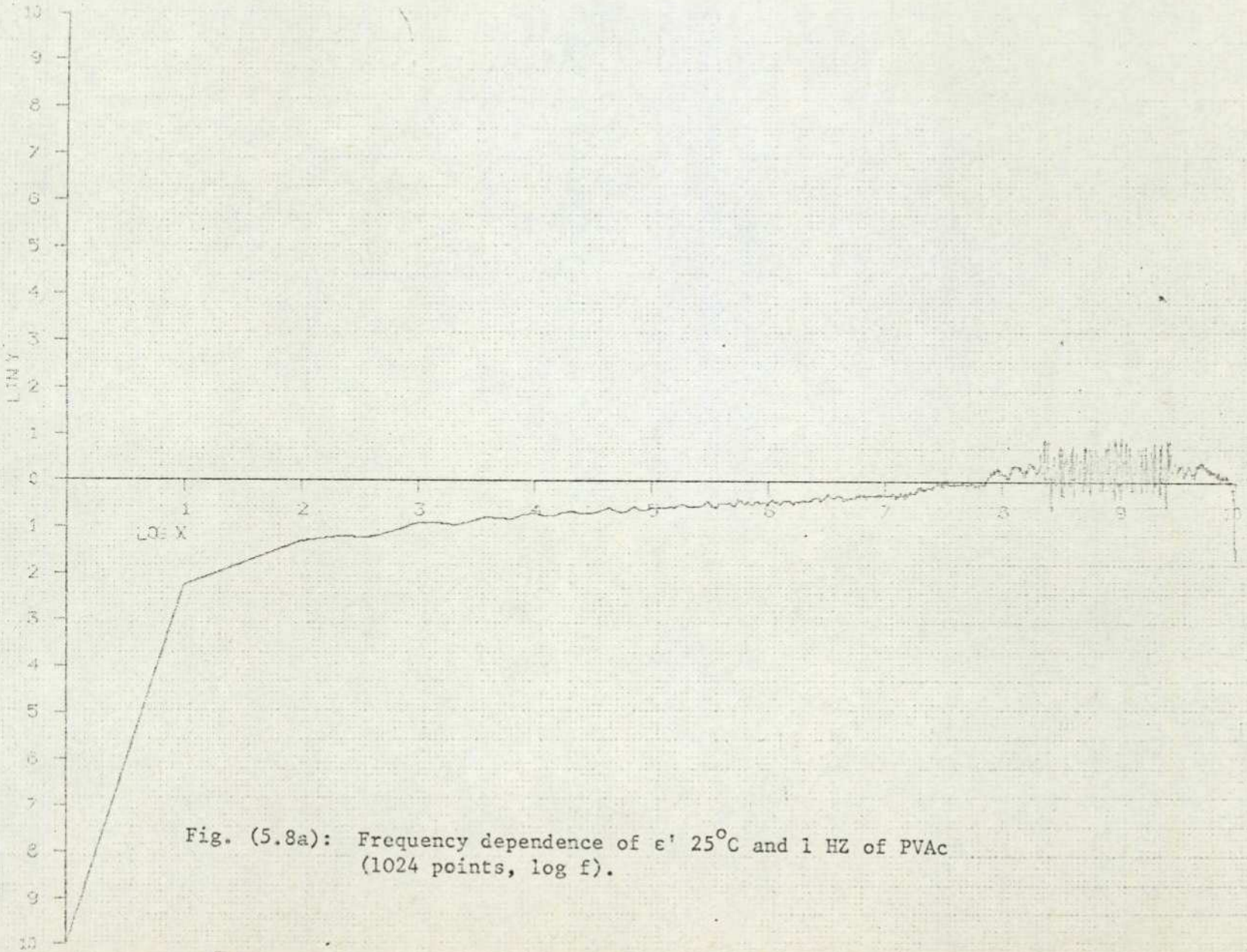

Fig. (5.8a): Frequency dependence of ε' 25°C and 1 HZ of PVAc (1024 points, log f).

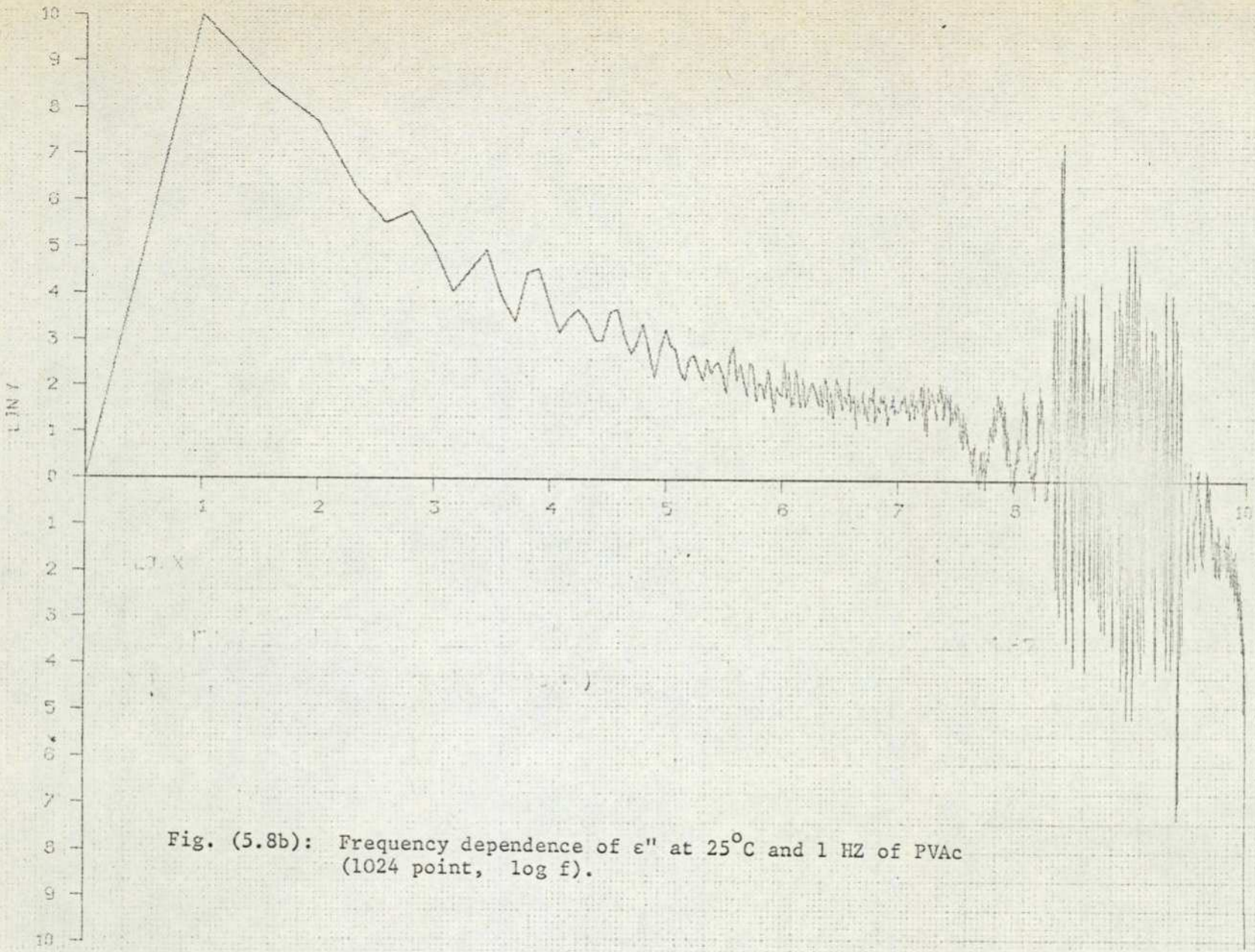

Fig. (5.8b): Frequency dependence of ε" at 25°C and 1 HZ of PVAc (1024 point, log f).

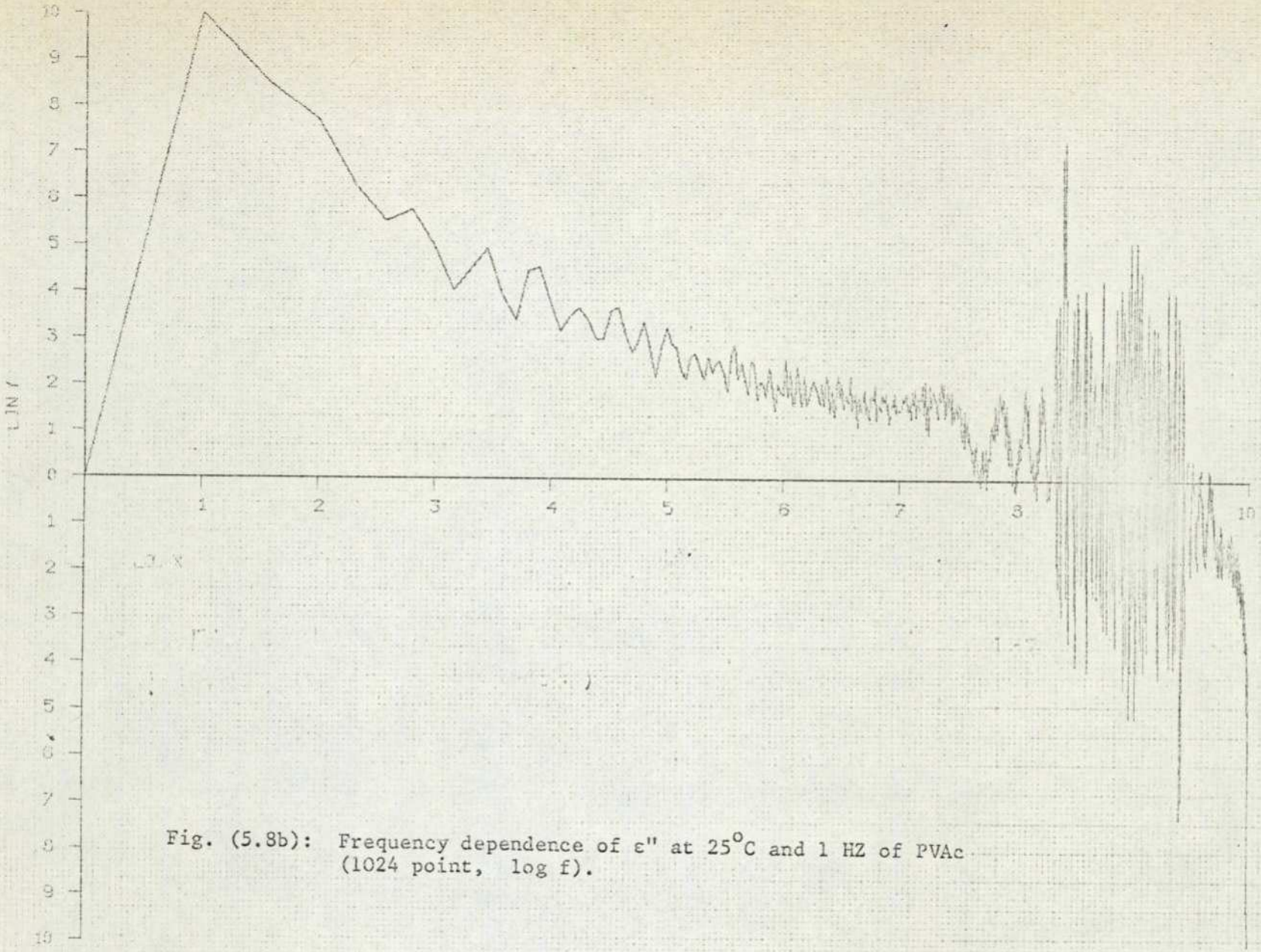

Fig. (5.8b): Frequency dependence of ε" at 25°C and 1 HZ of PVAc (1024 point, log f).

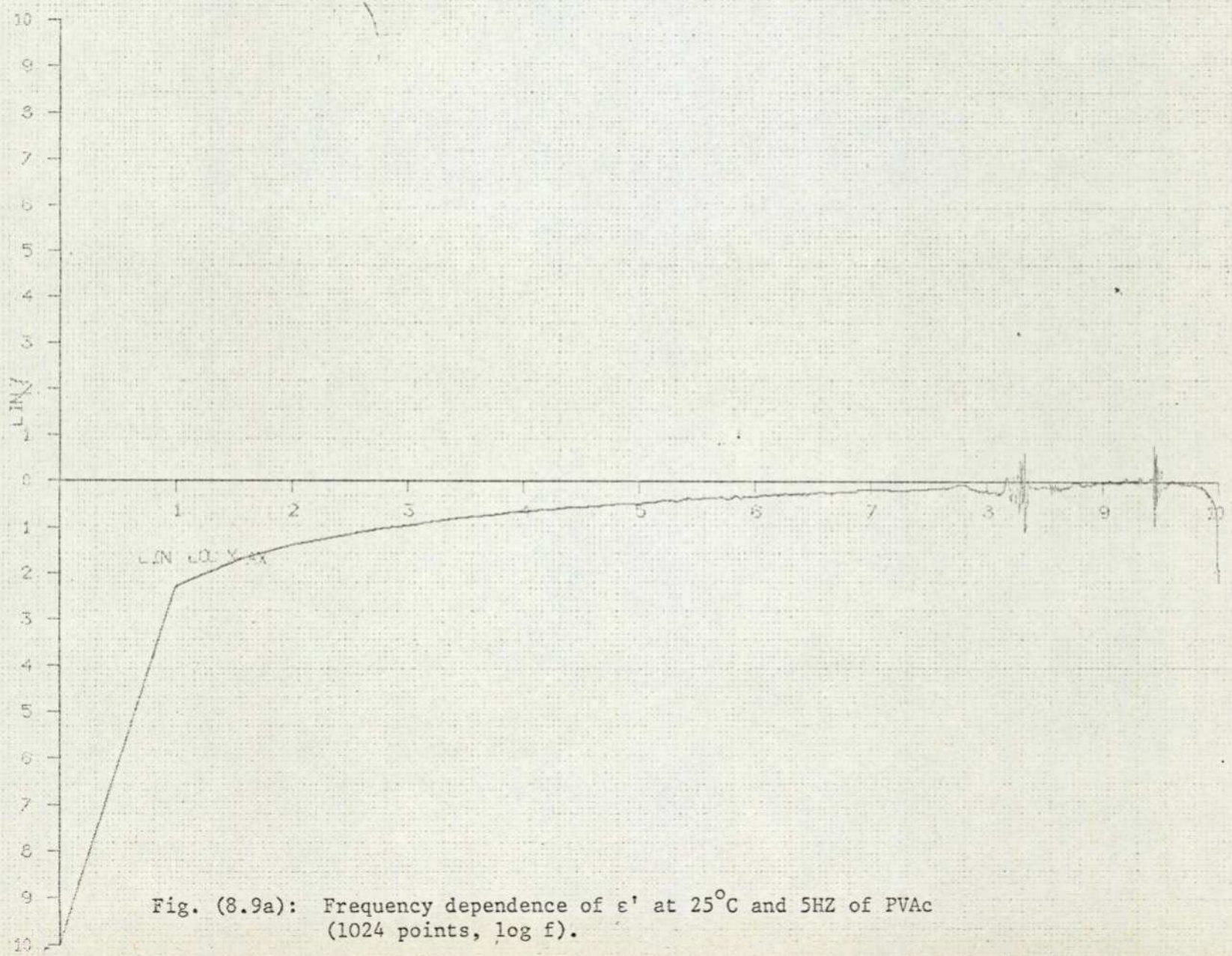

Fig. (8.9a): Frequency dependence of ε' at 25°C and 5HZ of PVAc (1024 points, log f).

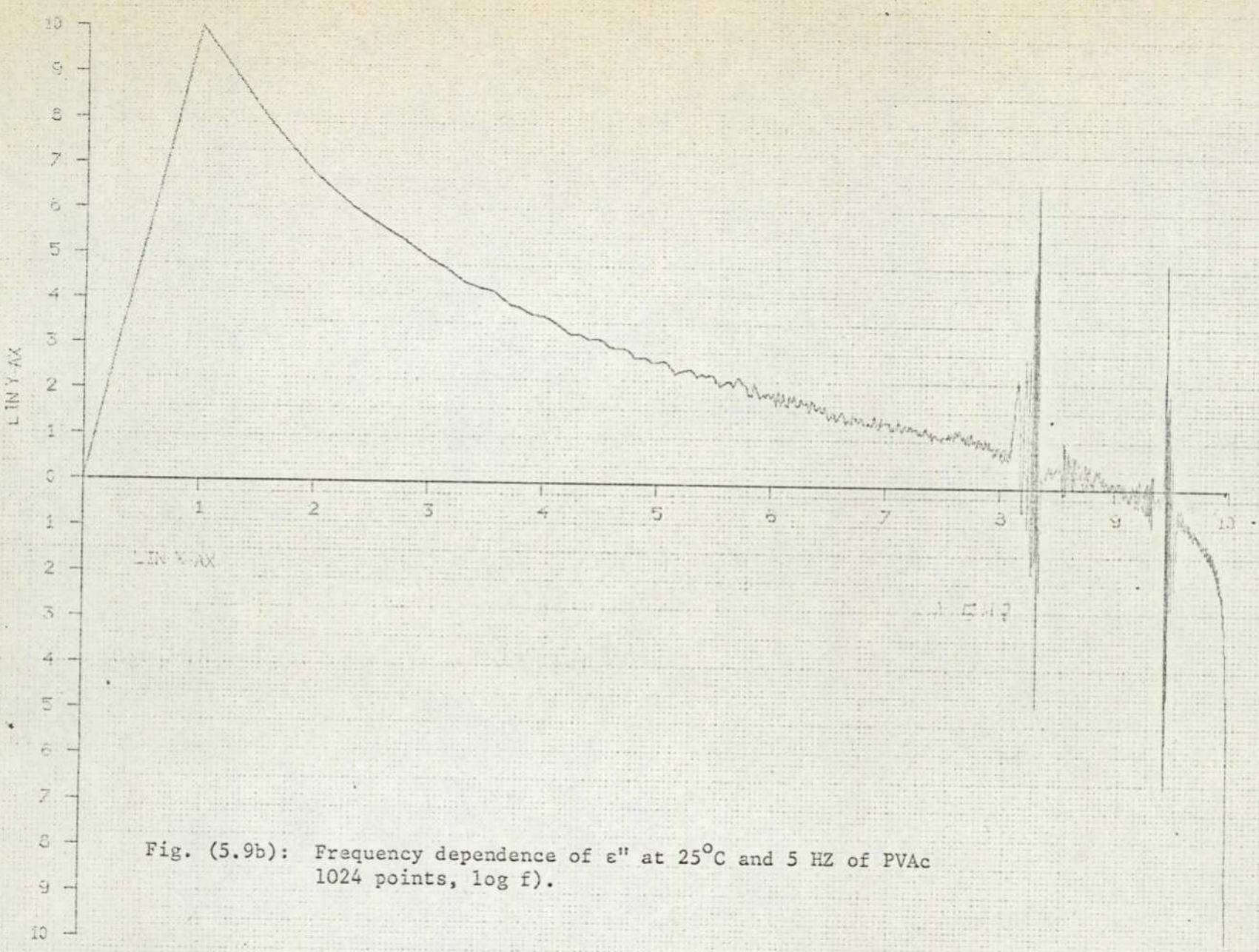

Fig. (5.9b): Frequency dependence of ε" at 25°C and 5 HZ of PVAc 1024 points, log f).

to improve (i.e. less distortion) and the peak becomes clearer, see Fig. (5.9b), compared with the one before, Fig. (5.8b), with increasing the sampling frequency.

c - It was also found that, replacing the sample or heating it did not mean that much and, the peak seemed to occur always, at the same position along the f - axis.

A considerable amount of effort was spend to find out the reasons behind these deviations. Naturally, it was thought at the beginning that the whole problem was mainly due to the new presence of the relay in the system. But, the occurence, of (1) the aliasing, defined as a distortion in the frequency spectrum, at high-frequency side with these results and (2) the high-frequency and fixed position peak, indicates that the presence of high-frequency (above Nyquist's frequency) components in the output response and the peak is a fake one mainly due to the dominating effect of high-frequency (short-time) response.

The question now is, how is it possible for these high-frequency components to exist in the output response when a low-pass filter with cut-off frequency as low as 1 Hz is being used.

Earlier, in Chapter 4, it was mentioned that the low-pass filter, being used to bandlimit the output response, is of a high-order and its square wave response tended to "overshoot" due to its high order. Thus, the low-pass filter output overshoots at the beginning owing to the fast rising of the amplifier output and since the sampling of data always starts at the same time the relay becomes an open circuit, the first part of the output response is included and hence measurements are subjected to errors.

The problem can not be solved, however, by removing the low-pass

filter since this introduces aliasing in the output results owing to disobeyance the sampling theorem, but it may be overcome by smoothing down the output response or by starting to sample data some time later (i.e. 1 sec after the relay becomes an open circuit). The first was adopted at the beginning and achieved by:

a) Connecting a capacitor (39 PF) across the feedback resistance as shown in Fig. (5.10). Effectively, this increases the time constant of the amplifier thus slowing down the rising rate of its output response. The output response was noise-free and there was no need for the low-pass filter to be used. Measurements on the dielectric sample (PVAc) at room temperature were taken and the results in real and imaginary parts, after being Fourier transformed the dielectric sample step-respone, were obtained as shown in Fig. (5.11).

The occurrence of the peak in Fig. (5.11b) at frequency, fm = 2.21×10^{-2} Hz, for greater than the expected one for the PVAc sample at room temperature and slightly different from that for the RC network ($\frac{1}{2\pi RC} = 4.1 \times 10^{-2}$) made it clear that the response was mainly due to the RC network across the amplifier and further measurements were not necessary.

b) Slowing down the changing rate of the applied step voltage ($\frac{dv}{dt}$) using the arrangement shown in Fig.(5.12). Effectively, this reduces the output response (current) magnitude, see App. D, and slows down the rate of its changing. The RC value (1 sec) was selected to ensure that the cut-off frequency of its low-pass filter is far greater than the expected frequency associated with the maximum loss in the dielectric sample being used at a given temperature. That was done to preserve the magnitudes of the real and imaginary parts of the dielectric step-response from being attenuated by the filter.

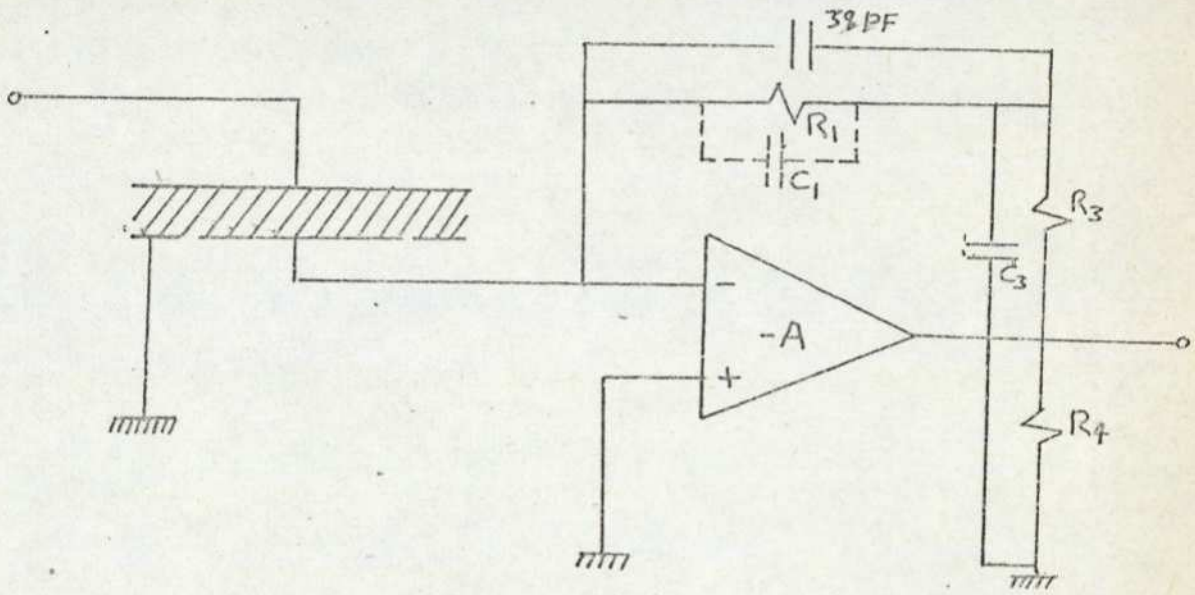

Fig. (5.10): The amplifier with the capacitor (39PF) connected across.

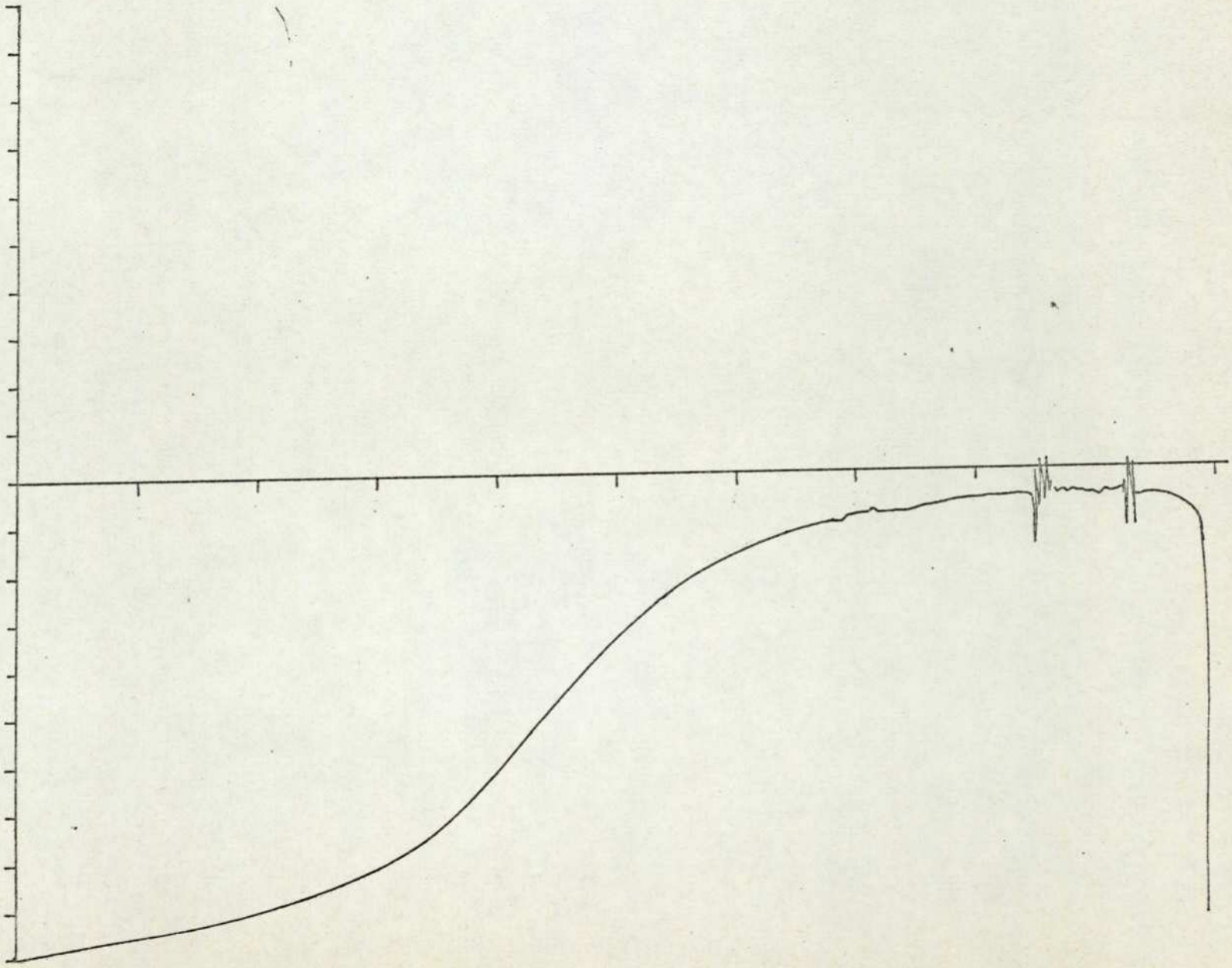

Fig. (5.11a): Frequency dependence of ε' at 25°C and 1 HZ of PVAc using the arrangement Fig. (5.10).

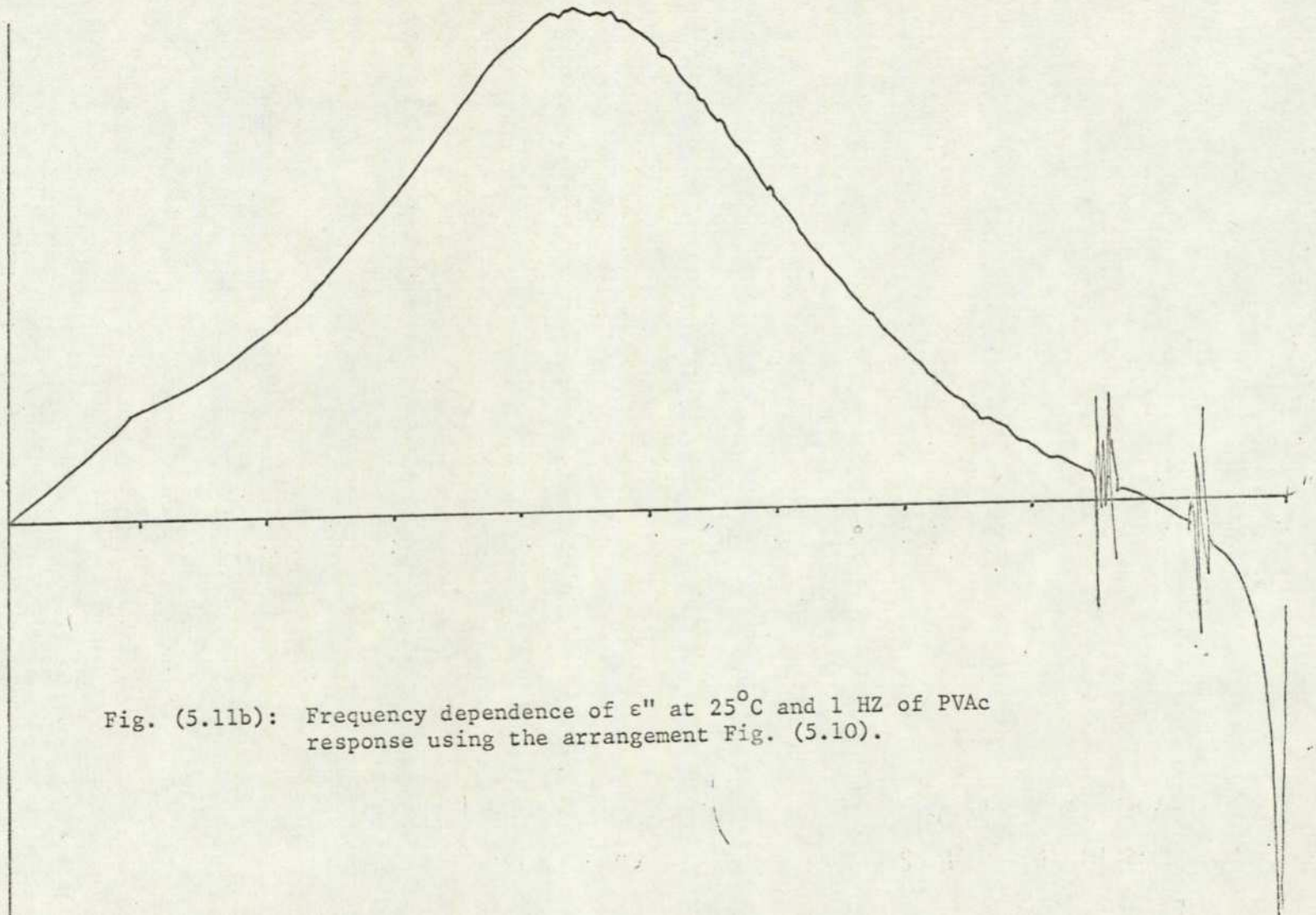

Fig. (5.11b): Frequency dependence of ε" at 25°C and 1 HZ of PVAc response using the arrangement Fig. (5.10).

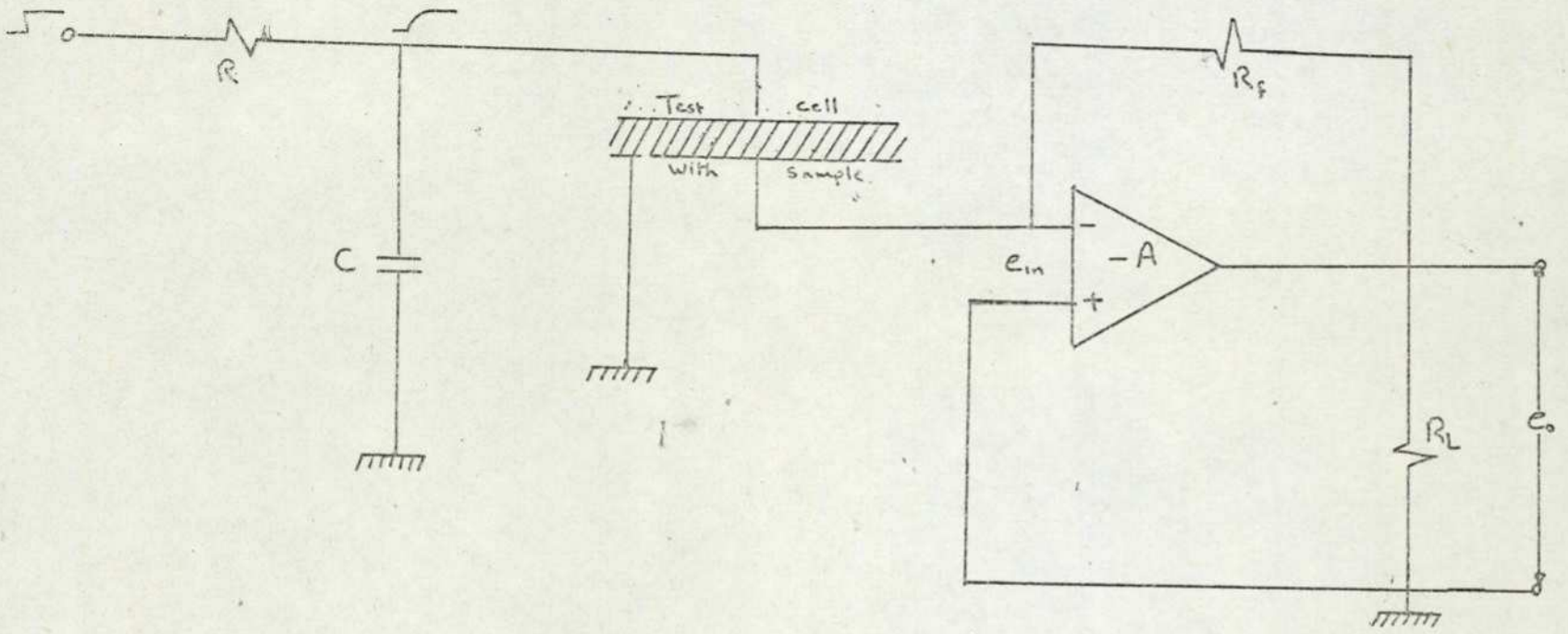

Fig.(5.12): Arrangement with R.C. network to eliminate the high frequency components in the applied step function.

Measurements were taken and Fig.(5.13) shows the obtained results in real and imaginary forms respectively. Fig. (5.13b) shows that the peak occurs at frequency, fm = 0.156 Hz which is just equal to that calculated from $\frac{1}{2\pi RC}$ = 0.159 Hz; the filter cut-off frequency.

Further measurements using different RC values ended with similar conclusion and confirmed that the whole response was entirely due to the low-pass filter being used.

Having done all that and to get more clear idea about what was happening, we decided to start the experiment from the very beginning. The amplifier being used was replaced by a new one namely, Keithley amplifier, Model 60 B and connected its output to a chart recorder instead of A/D converter. The dielectric sample (PVAc) step-response was measured then and recorded at different temperatures. Fig. (5.14) shows some of the plot results for ε'' derived from the discharging current I(t) measurements, using the Hamon approximation.

$$\varepsilon'' = \frac{I(t)\, d_s}{2\pi f\, \varepsilon_o\, A_s\, V} \qquad \ldots\ldots\ldots\ldots\ldots\ldots \quad (5.12)$$

where V is the step-voltage applied to the sample and f is the effective frequency given by $0.63/2\pi t$. The corresponding values of t, f and ε'' plotted in Fig. (5.14a) and (5.14b) are shown in table (5.3).

It should be noted from Fig. (5.14) that the first two points in both curves, corresponding to t = 1 sec are not consistent with the rest of the curves. It is clear that the deviation of the first point at 40^{o}C is far greater than that at 22^{o}C. It is also, noticable that the peak, corresponding to maximum dissipation of energy in the dielectric sample, occurs at frequency fm = 1.1×10^{-2} at 22^{o}C and shifts towards higher frequency fm = 1.0×10^{-2} in Fig. (5.14b) at 40^{o}C. The corres-

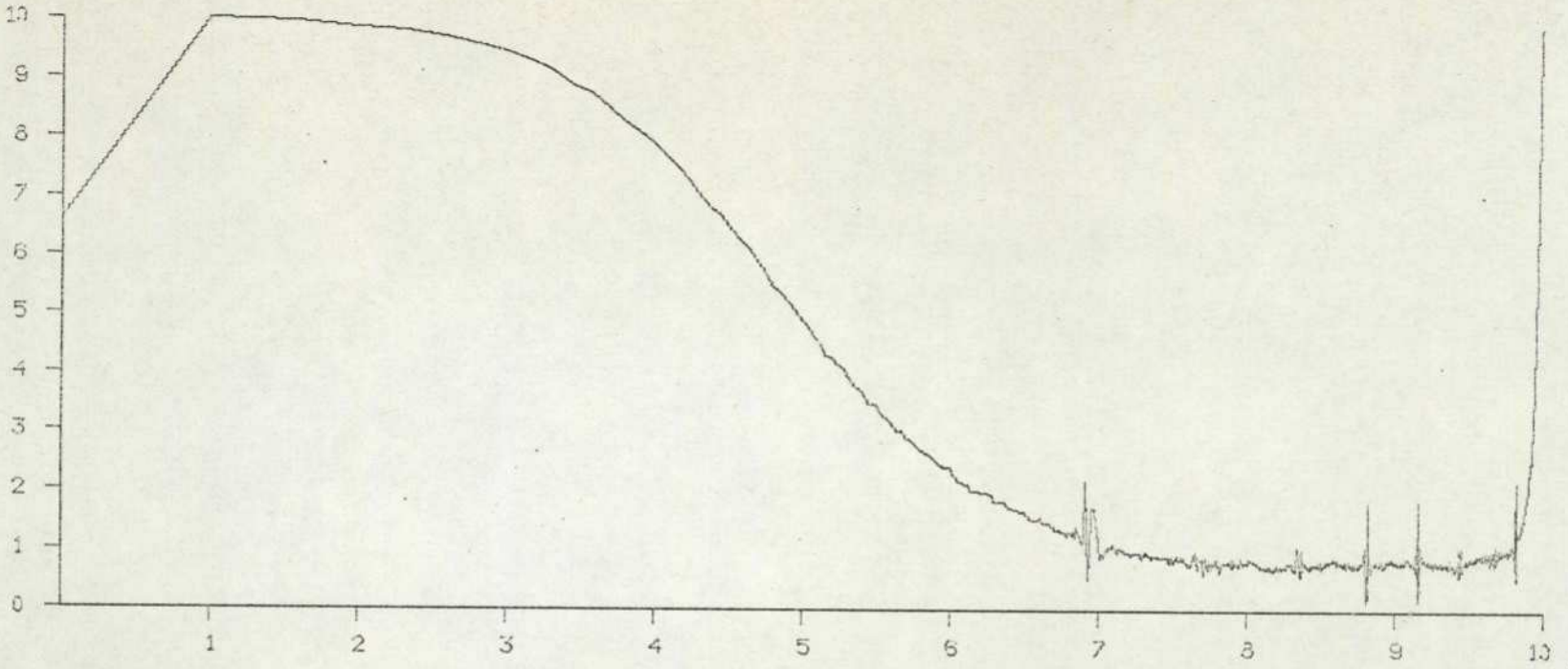

Fig.(5.13a): Frequency dependence of ε' at 5HZ using the arrangement shown in Fig. (5.14).

CALIBRATION
START ADDRESS 4000
10Y DIV.= -0.580506 E - 2
10X DIV.= +0.695152 E + 1

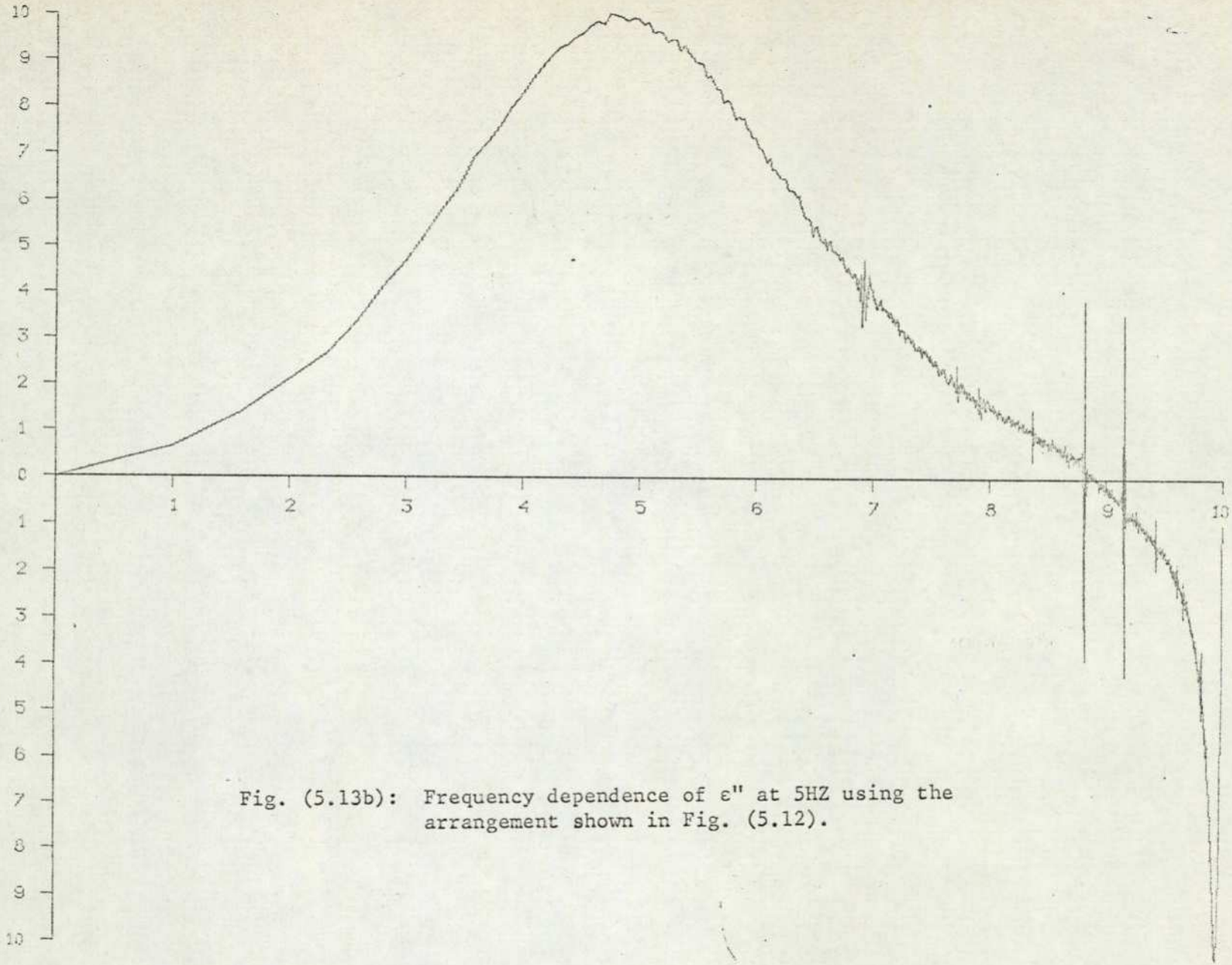

Fig. (5.13b): Frequency dependence of ε" at 5HZ using the arrangement shown in Fig. (5.12).

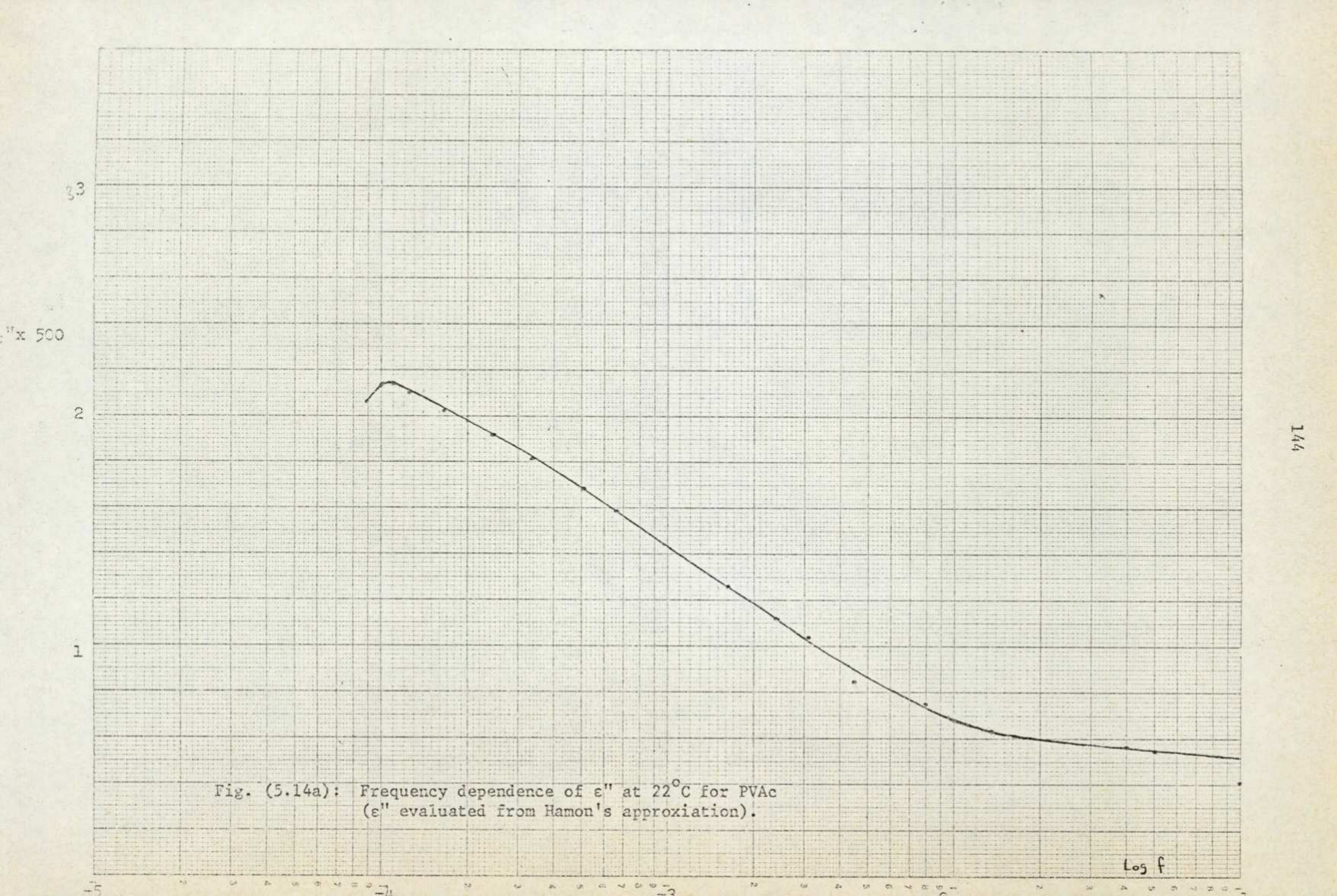

Fig. (5.14a): Frequency dependence of ε" at 22°C for PVAc (ε" evaluated from Hamon's approxiation).

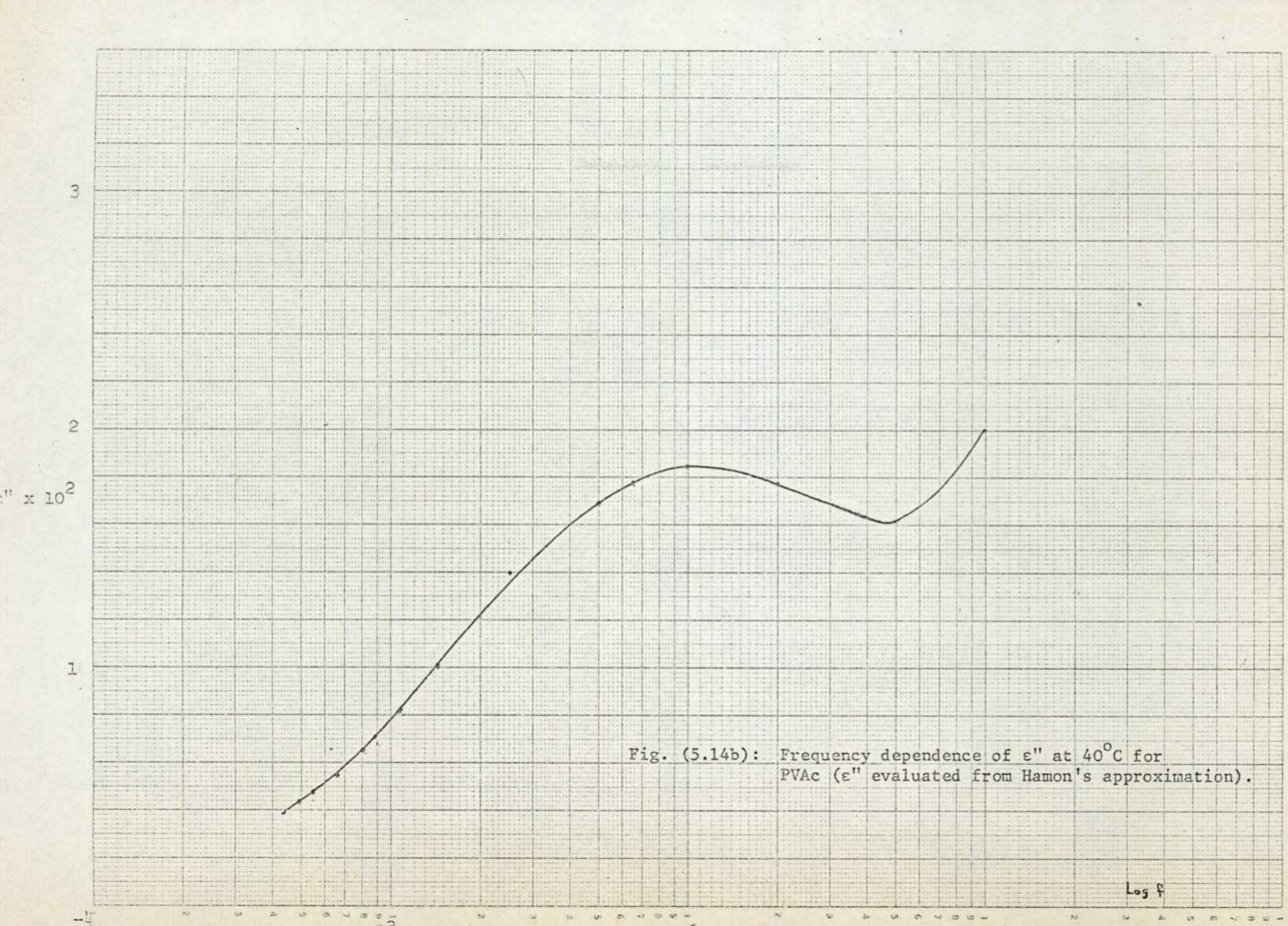

Fig. (5.14b): Frequency dependence of ε" at 40°C for PVAc (ε" evaluated from Hamon's approximation).

T = 22		T = 40	
$f = \frac{0.63}{2\pi t}$	$\varepsilon'' \times 10^{-3}$	$f = \frac{0.63}{2\pi t}$	$\varepsilon'' \times 10^{-2}$
1.000267×10^{-1}	0.813	1.000267×10^{-1}	1.99
5.000×10^{-2}	1.10	5.00×10^{-2}	1.62
4.00×10^{-2}	1.13	2.00×10^{-2}	1.78
1.33×10^{-2}	1.25	1.00×10^{-2}	1.83
8.6×10^{-3}	1.5	6.684×10^{-3}	1.77
4.445×10^{-3}	1.68	5.013×10^{-3}	1.68
3.077×10^{-3}	2.00	3.34×10^{-3}	1.53
2.353×10^{-3}	2.2	2.50×10^{-3}	1.40
1.905×10^{-3}	2.4	2.0×10^{-3}	1.21
1.60×10^{-3}	2.5	1.432×10^{-3}	1.00
1.212×10^{-3}	2.7	1.114×10^{-3}	0.81
9.758×10^{-4}	2.9	9.115×10^{-4}	0.68
8.165×10^{-4}	3.06	8.3554×10^{-4}	0.644
6.56×10^{-4}	3.16	6.684×10^{-4}	0.514
5.48×10^{-4}	3.28	5.570×10^{-4}	0.44
4.94×10^{-4}	3.34	5.0×10^{-4}	0.39
3.961×10^{-4}	3.48		
3.306×10^{-4}	3.6		
2.837×10^{-4}	3.7		
2.485×10^{-4}	3.84		
1.99×10^{-4}	3.94		
1.66×10^{-4}	4.0		
1.246×10^{-4}	4.2		
1.1083×10^{-4}	4.3		
9.977×10^{-5}	4.27		
9.072×10^{-5}	4.138		

Table (5.3) :- The variation of PVAc energy loss ε'', calculated from discharging current measurement using Hamon approximation, with frequency at two different temperatures 22°C and 40°C.

ponding average times (τ_o) at both temperatures (22°C and 40°C), calculated form $\tau_o = \frac{1}{2\pi fm}$, are 1435.99 and 15.9112 secs respectively.

In view of the above results, it becomes obvious that the triggering of the A/D converter to initiate sampling should be delayed some time after the application of the step-voltage in order to exclude the first part of the response. Actually we have shown in Appendix (F) that this delay does not effect the results that much, especially when the dielectric response is measured at low temperature and sampled at low-rate. It was also shown that the values of ε' and ε'' obtained from the high-temperature response measurements are subjected to errors due to the presence of e^{-aT} term, see Eq. (F.10) in App (F) where a and T are given there, and the correct values of ε' and ε'' could be obtained from dividing the experimental values by e^{-aT}. The error magnitude could be however, minimized by shortening the interval between the application of the step-voltage and triggering the A/D converter (T) for those measurments taken at high temperatures. This can be done simply by adjusting the values of the timing-components (capacitors and resistance connected with monostable C see chapter 4, section 4.2) to give the required delay time (i.e. 2 seconds for those measurements taken at 34, 36 and 38°C and 1 sec for those at 40, 42 and 44°C). The sequence of events for the modified control system is shown in Fig. (5.15).

Having done that, we replaced the Keithley instrument by the previous amplifier and connected its output, through the low-pass filter, to the A/D converter input.

Measurements at different temperatures were required thus, at the beginning of each experiment we made sure that (1) the output of the amplifier was set-off to zero, (2) the sample was left at the chosen temperature for at least one hour, (3) the sample was subjected to

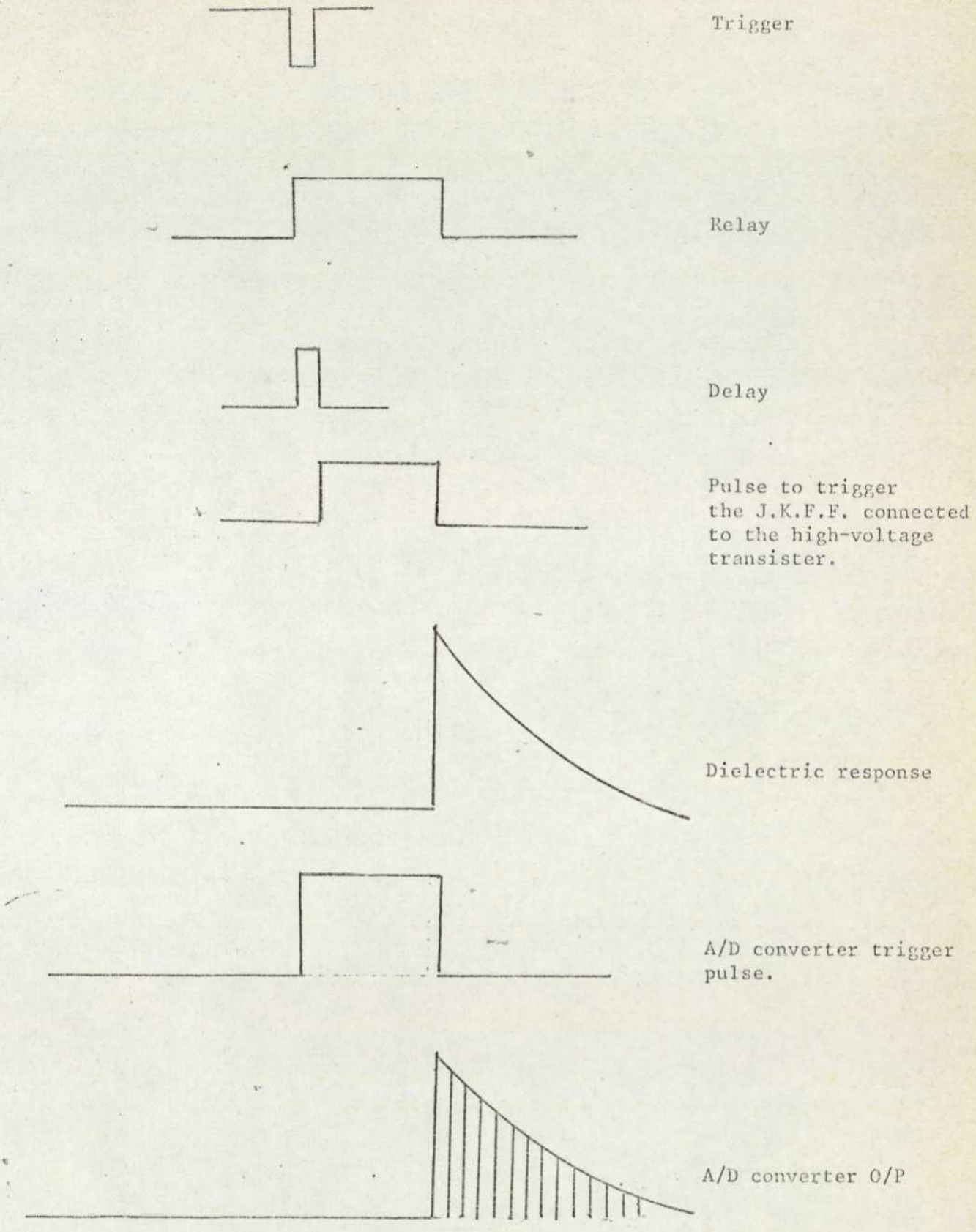

Fig. (5.15): The new squence of events.

the polarizing voltage for at least 30 τ_o seconds where τ_o is the expected average relaxation time at a given temperature, the same time was given to the sample to depolarize before a new experiment could take place and (4) the electrodes were clean enough and the sample was in good electrical contact with both of them.

With the above conditions being satisfied, the dielectric step-response was measured, filtered from high-frequency components, sampled after the required delay time and Fourier transformed by the computer. The results in real and imaginary parts for PVAc dielectric sample (1.34 mm in thickness and 7 cm in diameter) at different temperatures, namely 44, 42, 40, 36 and 34^{o}C, were obtained and plotted in Fig. (5.16).

Examination of these results shows:

a) The value of ε', Fig. (5.16a), falls from a higher to lower level as the frequency increases. This drop in ε', which is termed the "dielectric increment" occurs because dipolar segments of the molecule can change their average orientation in response to the applied field at low frequencies and thus contribute to polarization and hence to the value of ε'. At higher frequencies they are unable to follow the alterations of the field due to the hindering effect of collisions with neighbouring molecules and hence make no contribution to ε'. Thus, the dielectric constant comprises only the contributions from the electronic and atomic polarization ε_∞.

b) The rate of change of ε' with the frequency is greatest at the frequency at which the peak in ε'' value occurs, Fig. (5.16b). This is because the polarization cannot keep in phase with the applied field, resulting in appreciable power loss with maximum value at ω_m (see chap. 2).

c) The absorption process observed in these measurements is only

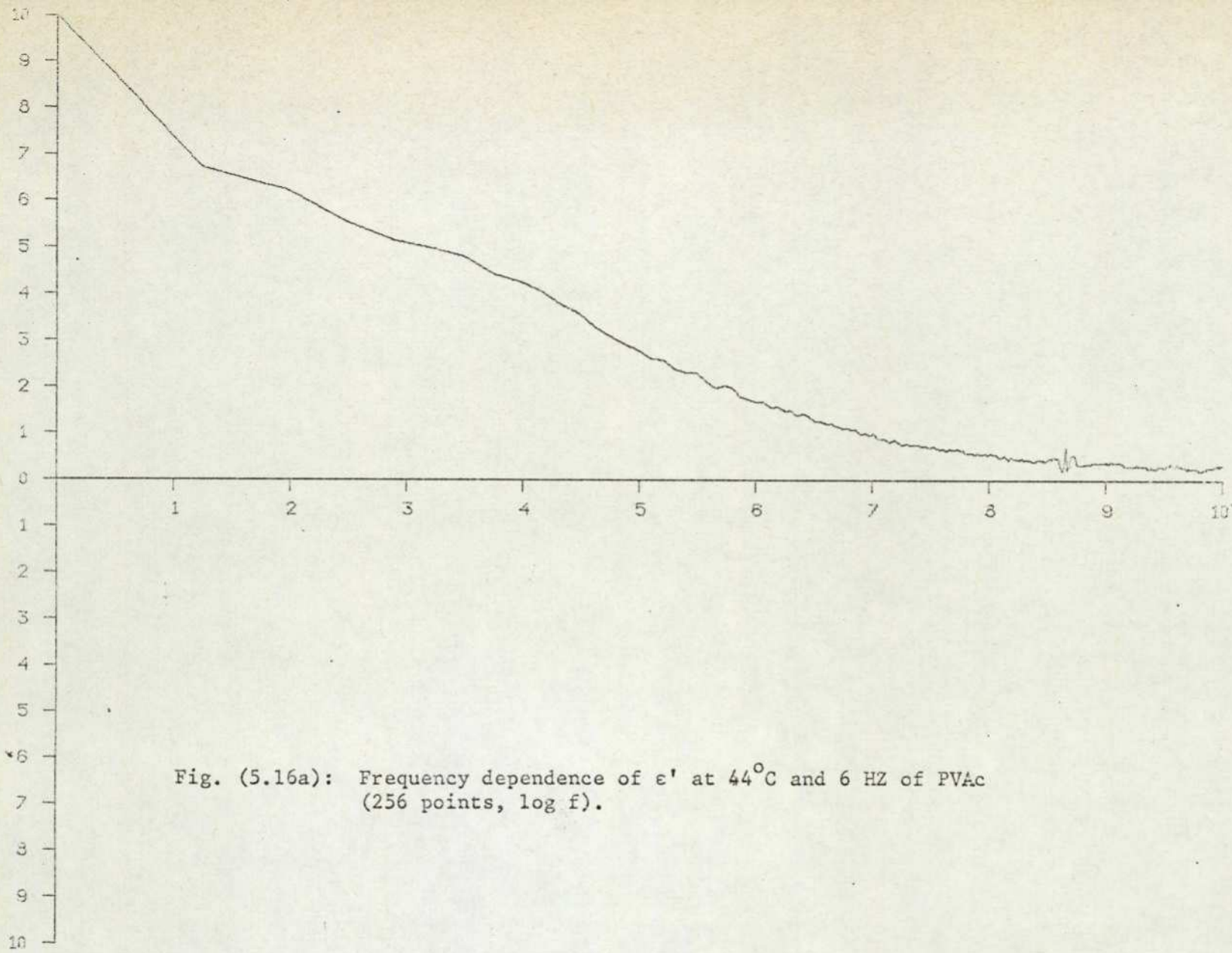

Fig. (5.16a): Frequency dependence of ε' at 44°C and 6 HZ of PVAc (256 points, log f).

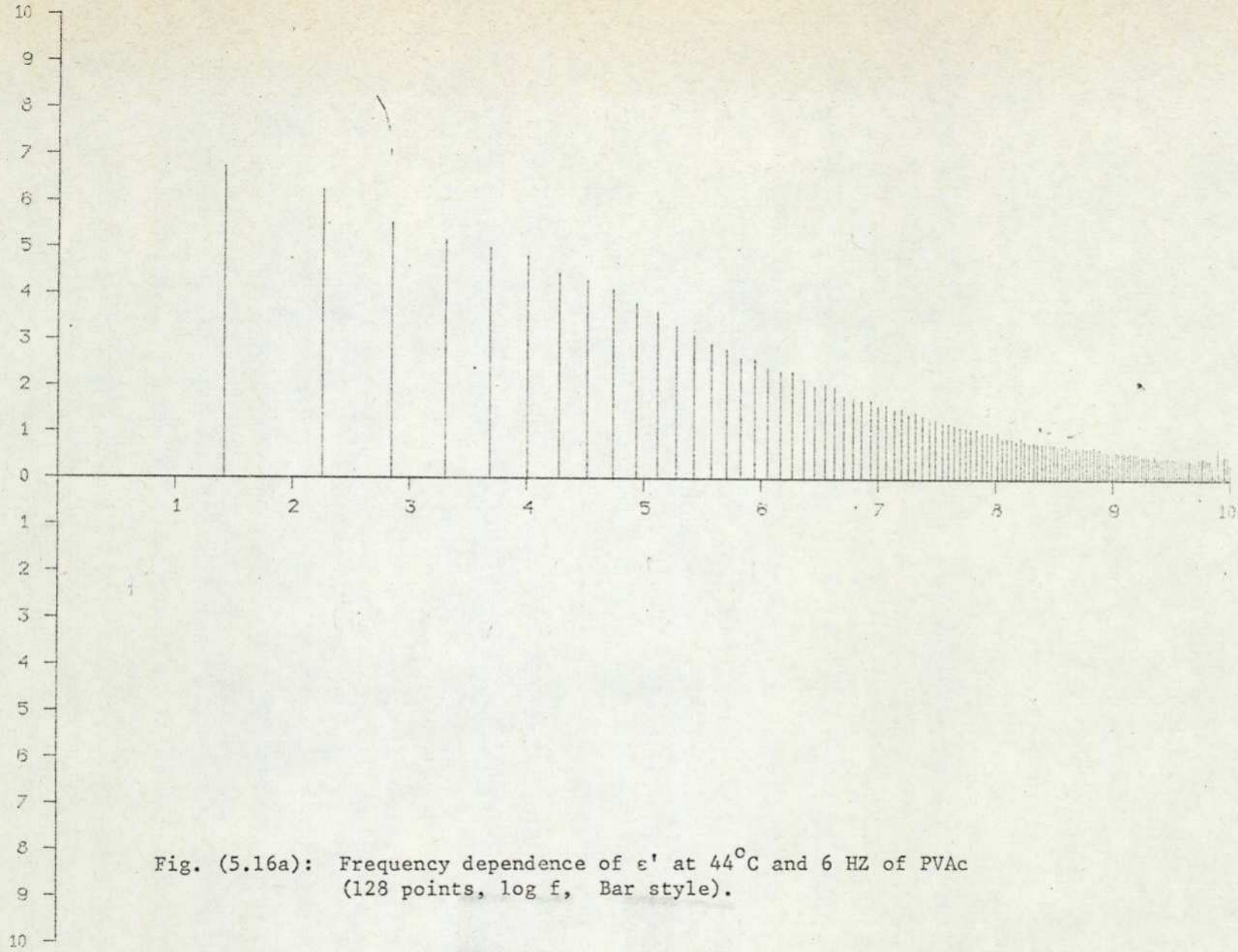

Fig. (5.16a): Frequency dependence of ε' at 44°C and 6 HZ of PVAc (128 points, log f, Bar style).

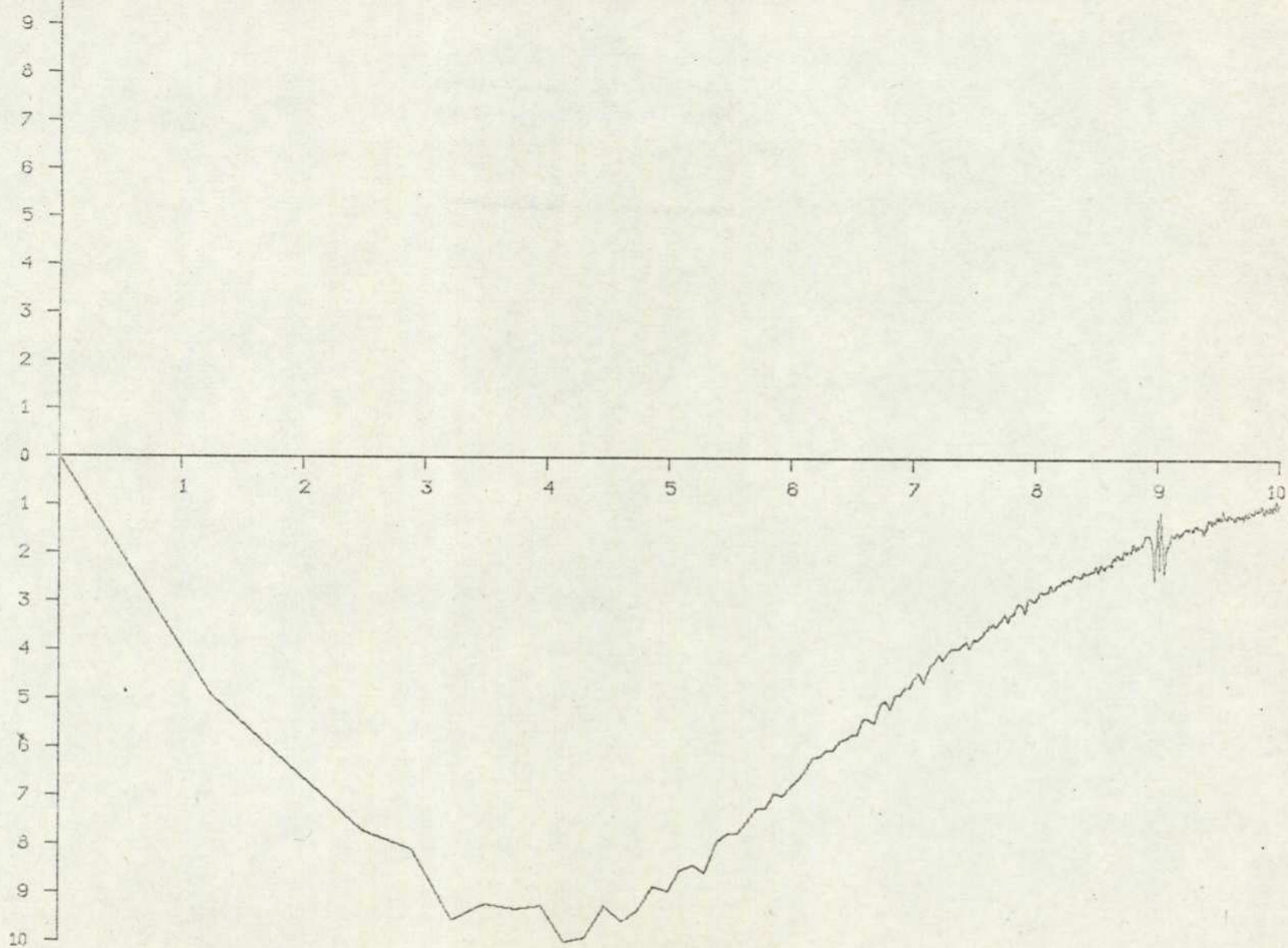

Fig. (5.16b): Frequency dependence of ε" at 44°C and 6 HZ of PVAc (256 points, log f).

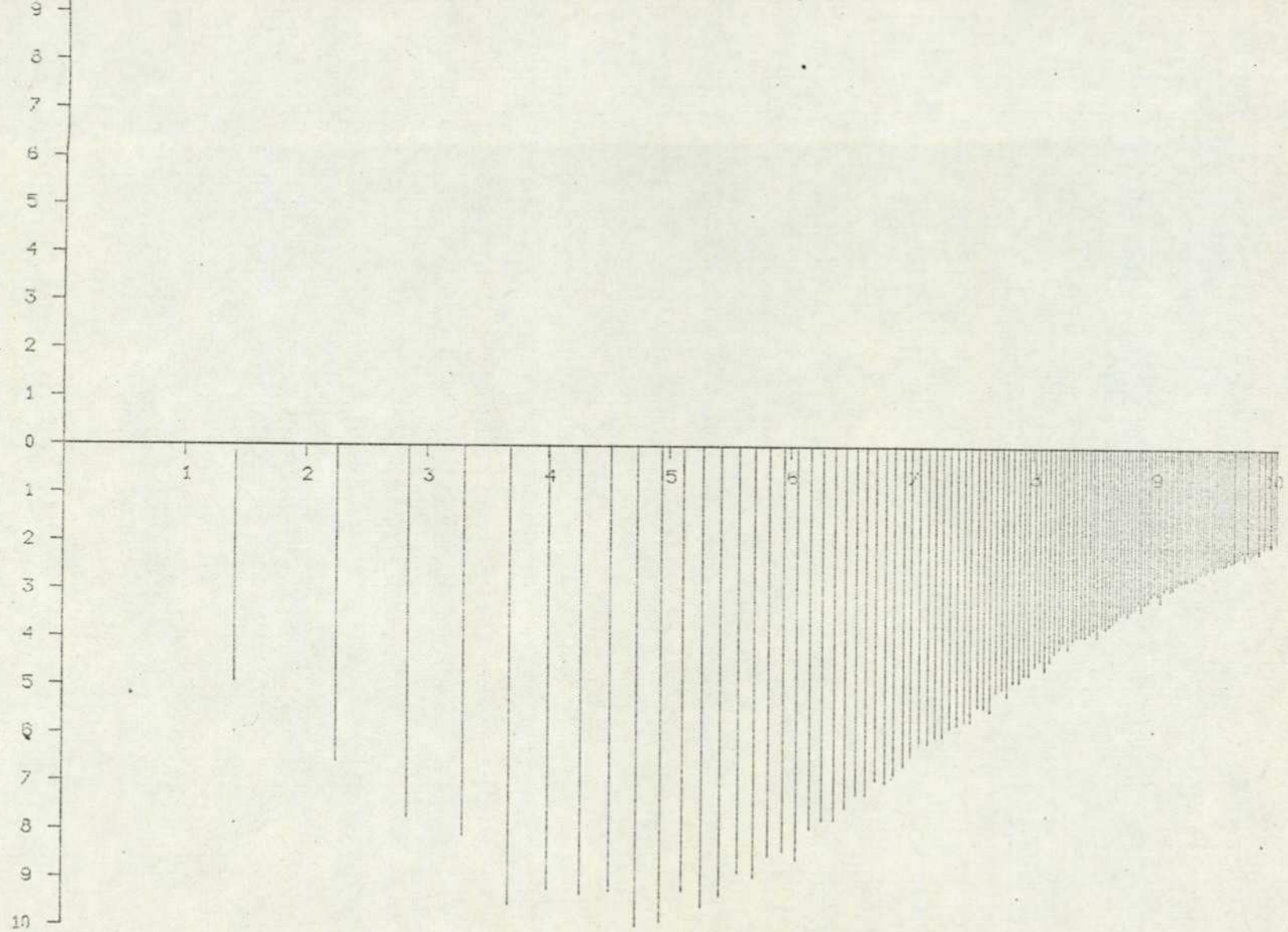

Fig. (5.16b): Frequency dependence of ε" at 44°C and 6 HZ of PVAc (128 points, log f).

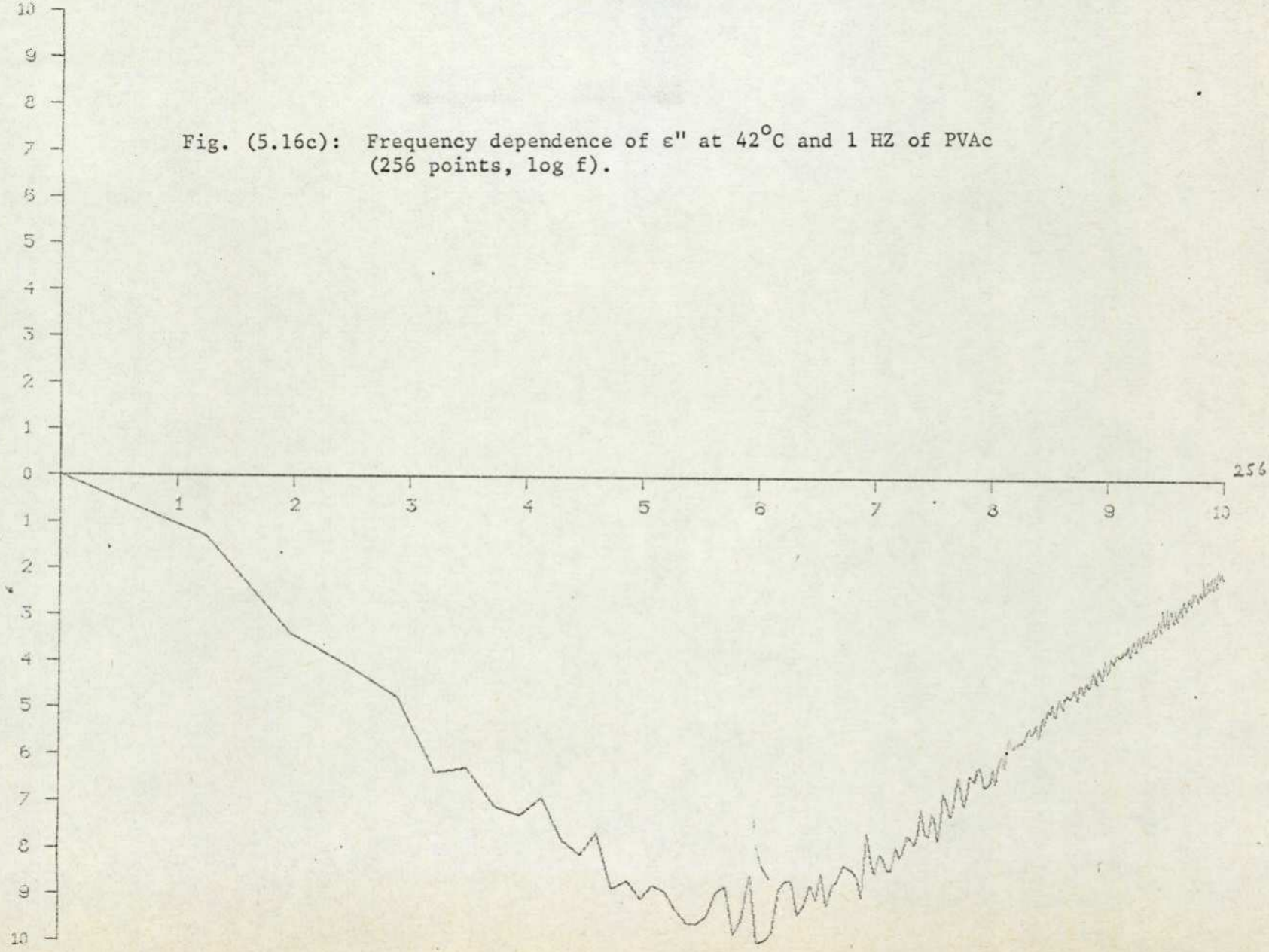

Fig. (5.16c): Frequency dependence of ε" at 42°C and 1 HZ of PVAc (256 points, log f).

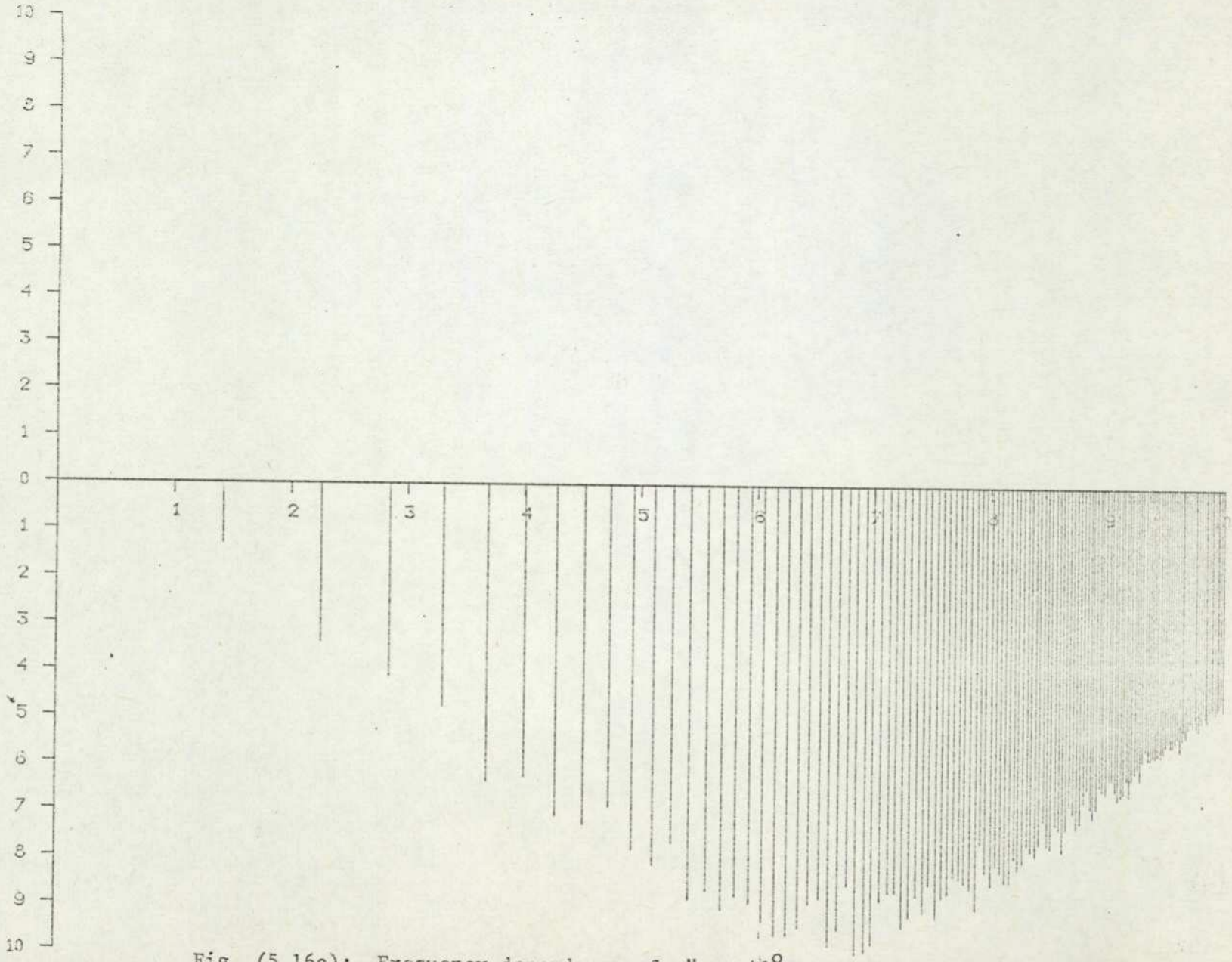

Fig. (5.16c): Frequency dependence of ε" at 42°C and 1 HZ of PVAc (128 points, log f).

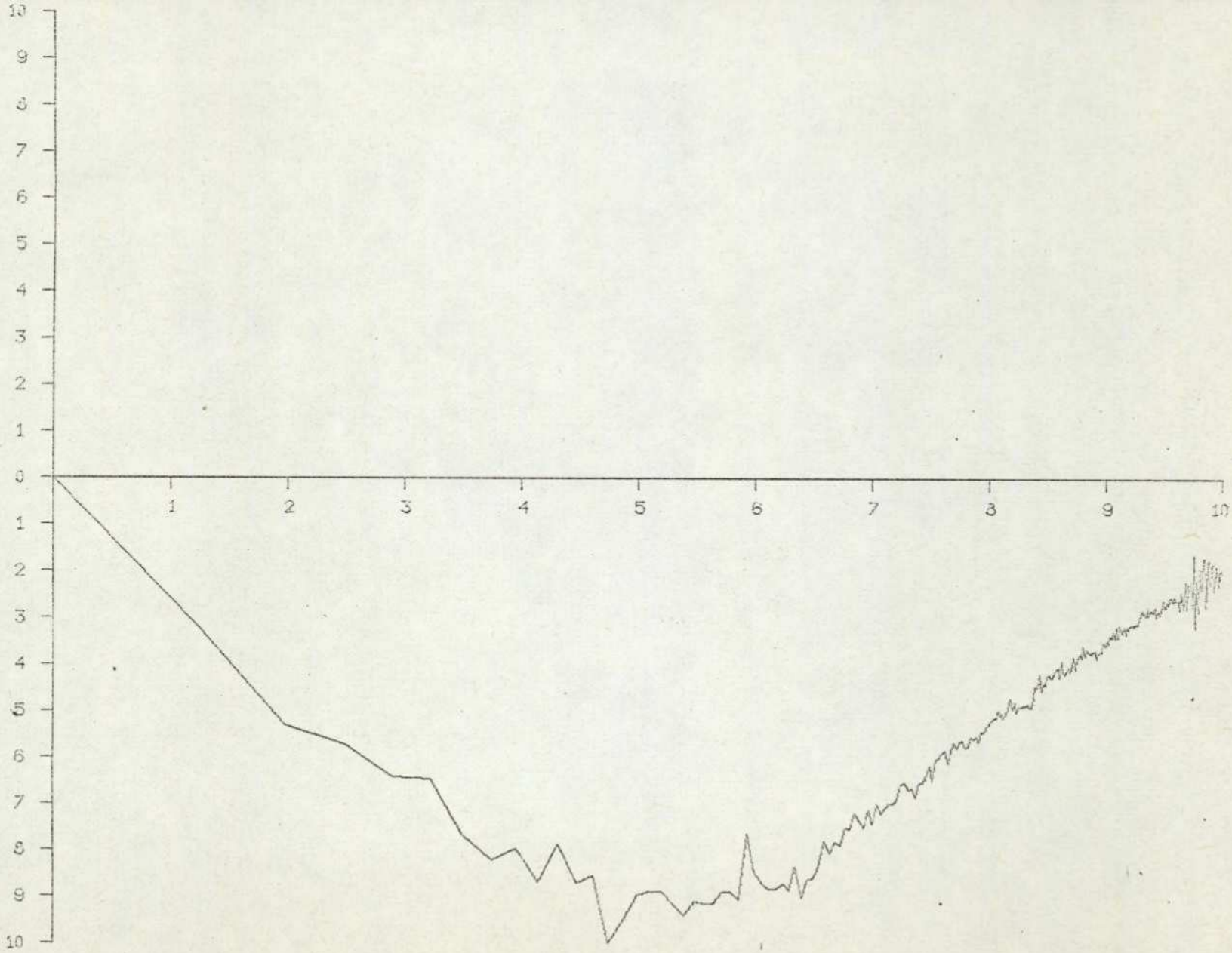

Fig. (5.16d): Frequency dependence of ε" at 40°C and ½ HZ of PVAc (256 points, log f).

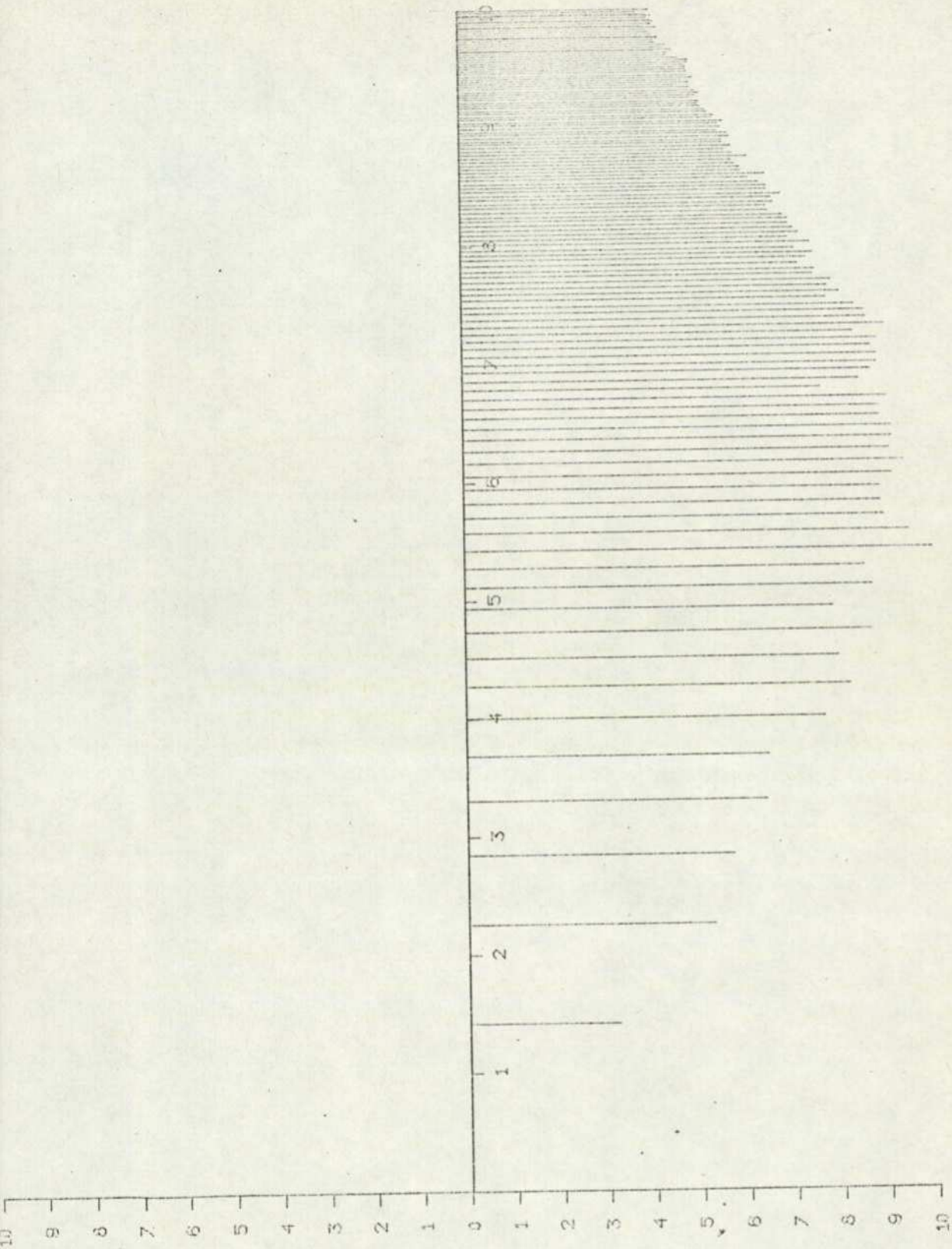

Fig. (5.16d): Frequency dependence of ε" at 40°C and ¼ HZ of PVAc (128 points, log f).

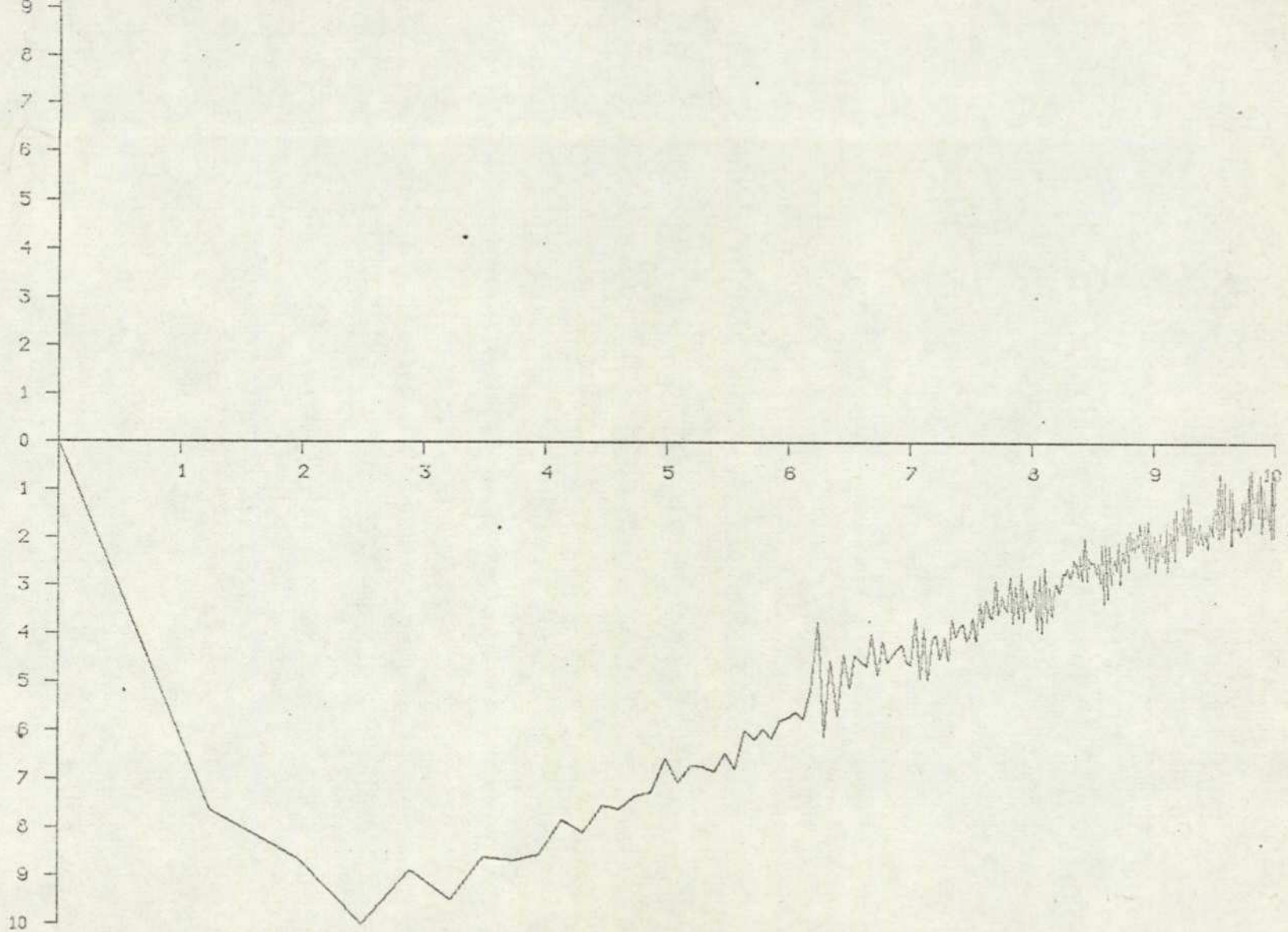

Fig. (5.16e): Frequency dependence of ε" at 36°C and ½ HZ for PVAc. (256 points, log f).

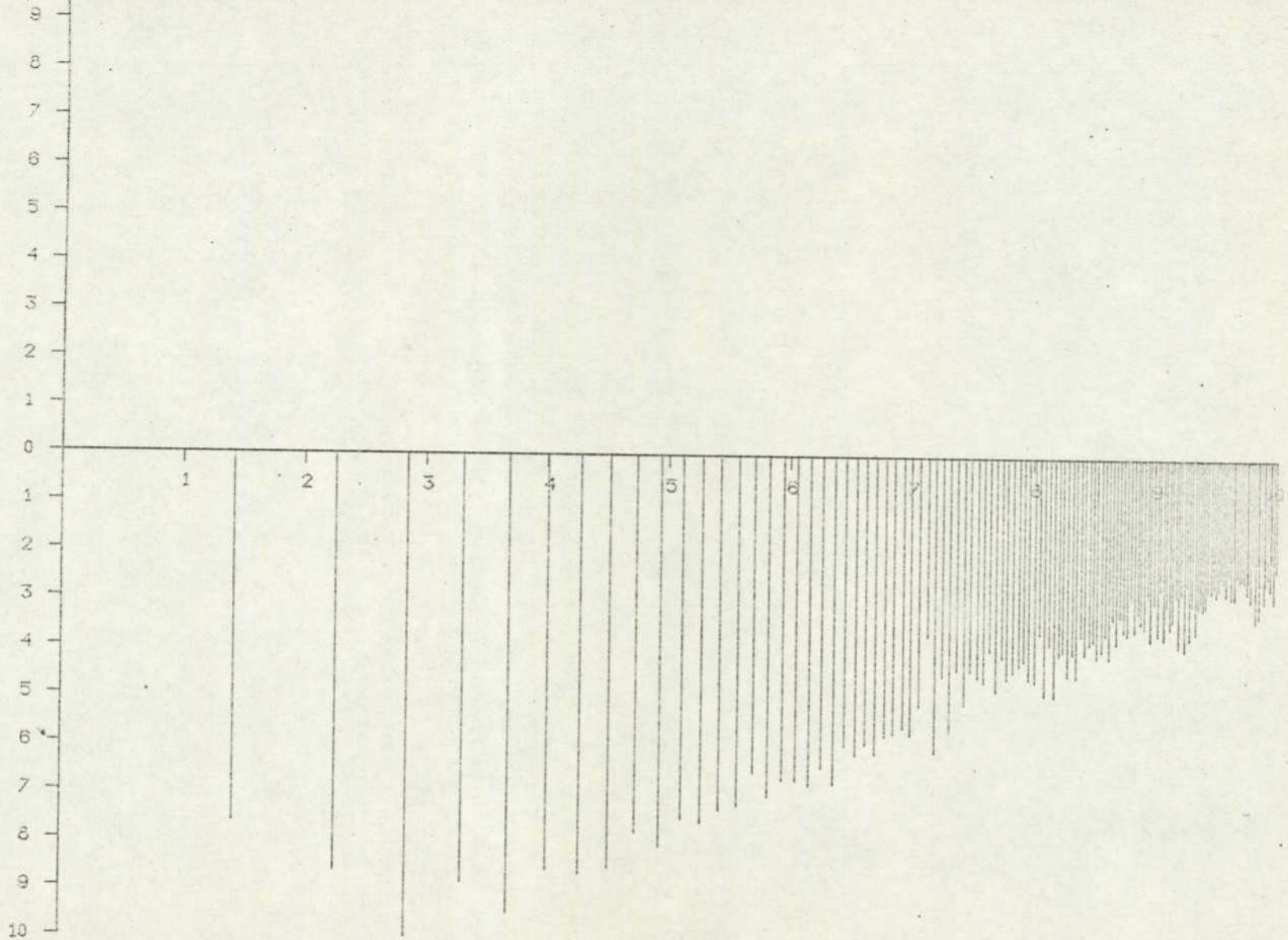

Fig. (5.16e): Frequency dependence of " at 36°C and ½ HZ for PVAc (128 points, log f).

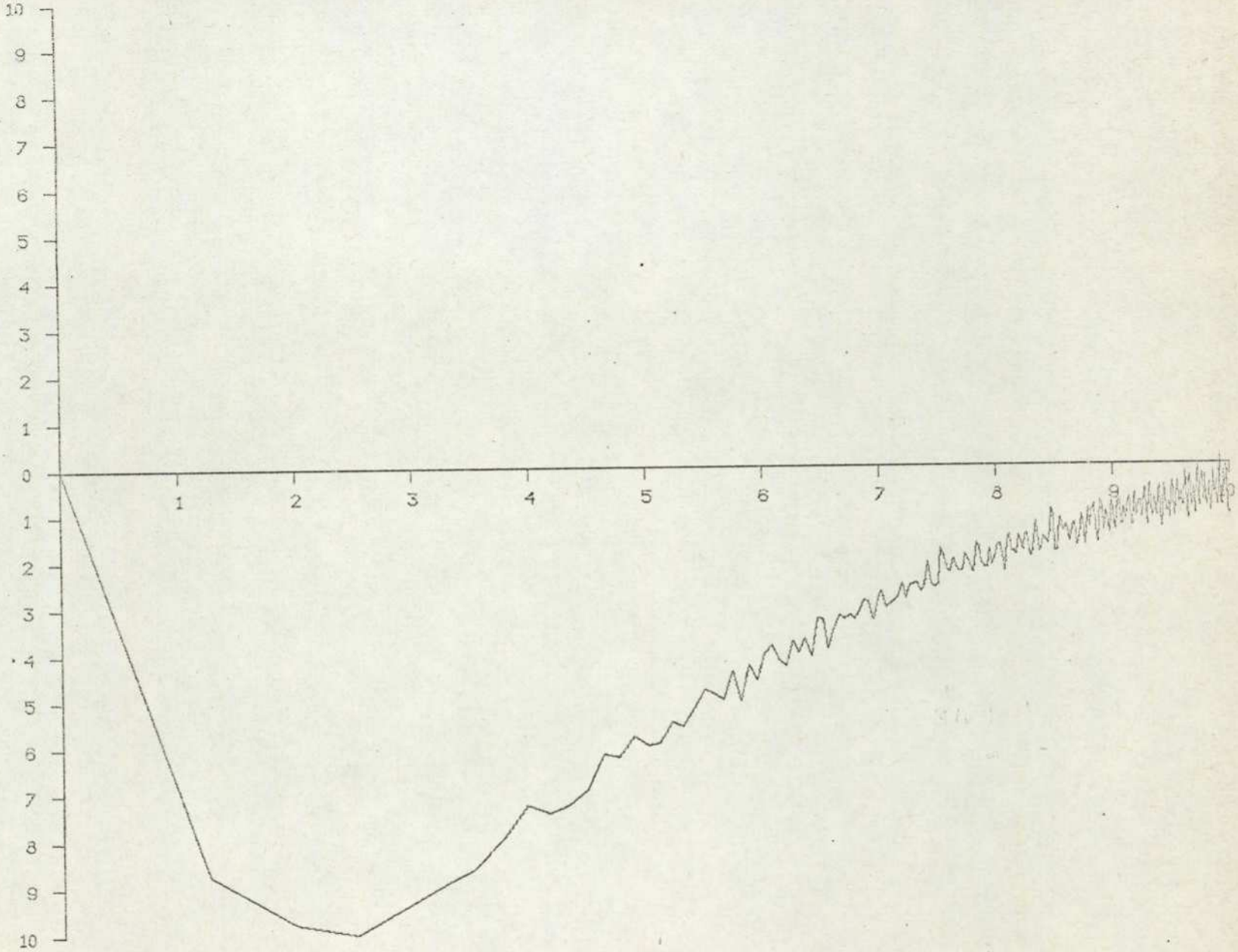

Fig. (5.16f): Frequency dependence of ε" at 34°C and 3/8 HZ for PVAc (256 points, log f).

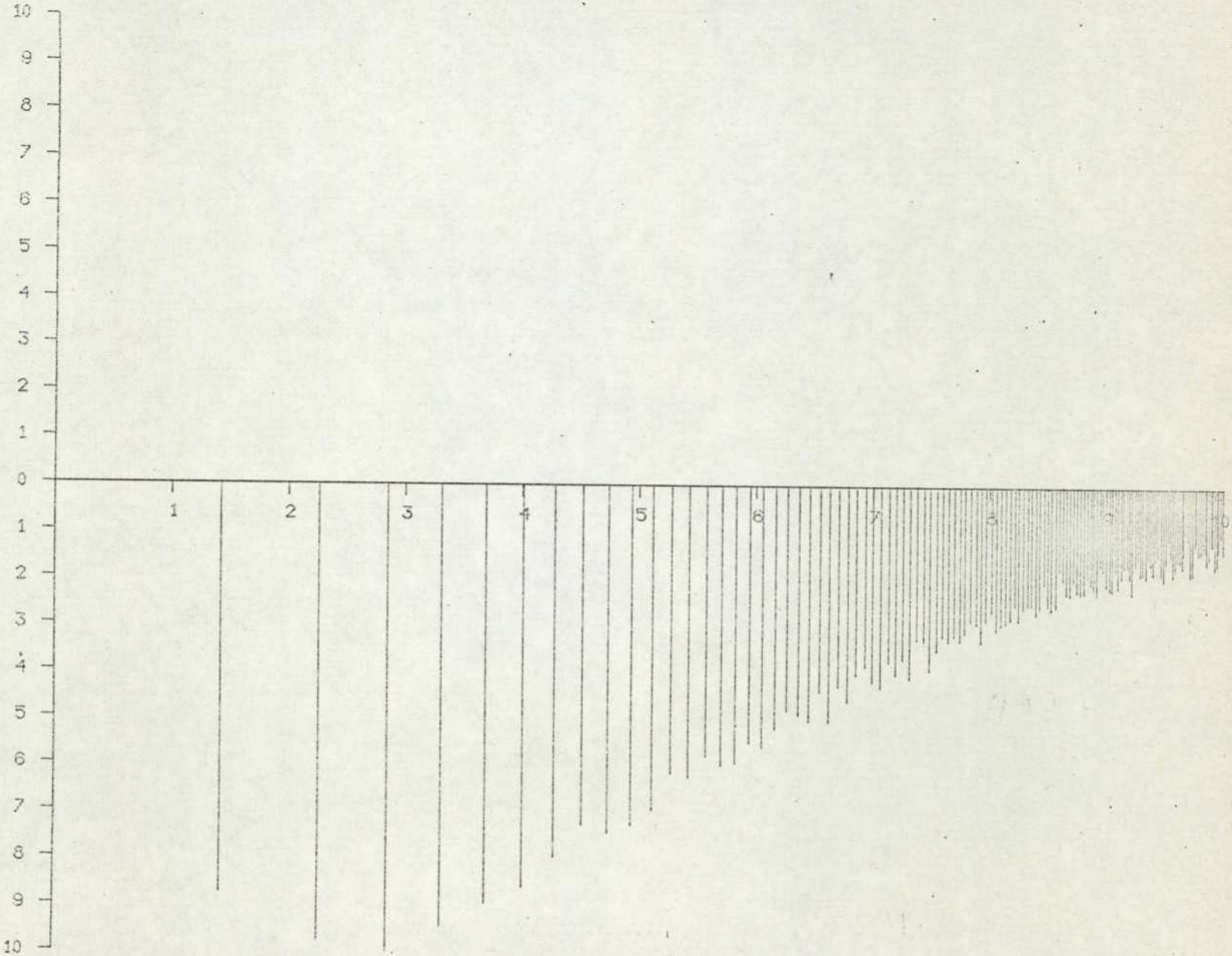

Fig. (5.16f): Frequency dependnce of ε" at 34°C and 3/8 HZ for PVAc (128 points, log f).

that which can be observed at temperatures above T_g (glass transition, 28°C) namely the α - absorption (see chapter 2).

d) The loss peaks are clearly observable in these results and occur at frequencies corresponding to relaxation regions where materials absorb energy and maximum loss occurs. The positions of these peaks are clearly dependent on temperatures at which measurements were taken.

e) The shape of the α-absorption curves does not seem to change as the temperature increases but the curves become narrower (due to convergence of relaxation time) at high temperatures. The curves seem to be slightly non-symmetrical, being broader on the high frequency side.

f) The magnitude of loss becomes higher at higher temperatures. This is because the magnitude of $(\varepsilon_s - \varepsilon_\infty)$ is dependent on the total dipole moment, and only slightly dependent on temperature, so the total change of permittivity from low to higher frequency likewise the total area under the ε'' - log f curve remains approximatly the same- However, at certain frequency f_o, ε'' decreases strongly as the temperature decreases, since τ increases and hence also $\omega_o\tau$ strongly increases with decreasing temperature.

g) The results appear to be very similar to the dielectric loss curves obtained for PVAc by Saito (1962), Fig. (5.16g), especially in their temperature - frequency locations. This is illustrated in Table (5.3a), which shows the temperature - frequency locations of loss maximum fo PVAc obtained by Saito and this author.

h) The average relaxation time (τ_o) for the PVAc sample obtained from these measurements at 40°C, 13.914372 sec seems to be close to that obtained from Hamon's approximation method, 15.911246 sec, at the

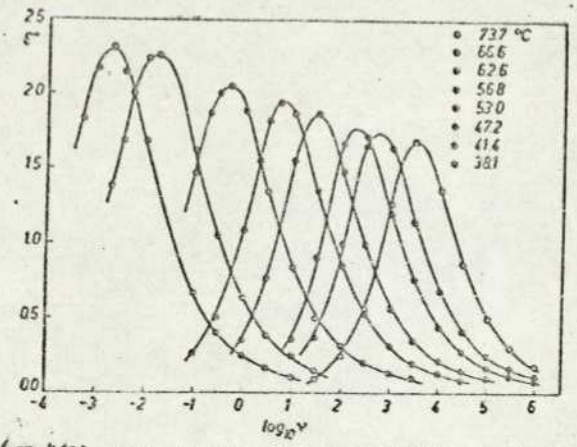

Fig (5-163):. Dielectric absorption curves of PVAc at various temperatures

Figure's Number	Temperature T C	Experimental fm(Hz)	Experimental Relaxation Time τ (sec)	Temperature at which the other's results were measured (C)	τ from other* experimental results (sec)
(5.16)					
b	44	5.20×10^{-2}	3.06	47.1	0.33
c	42	2.71×10^{-2}	5.87		
d	40	1.144×10^{-2}	13.9	41.4	10.3
e	36	2.48×10^{-3}	64.1	38.1	32.9
f	34	1.46×10^{-3}	109.0		

* Rough estimations, from Saito (1962) measurements, of τ at different temperatures.

Table (5.3a); The relaxation times of PVAc at different temperatures.

same temperature Fig. (5.14b). This difference could be attributed to the inaccuracy associated with the latter method (see chapter 1).

i) Results are plotted on the logarithmic scale with different patterns namely, normal and Bar pattarns. The position of the maximum loss becomes clear in the second pattarn since only 128 points were plotted in each curve.

5.3 Non-Causal Method Measurements.

5.3.1 General Introduction: -

Earlier in this chapter it was mentioned that the RC network was used to slow down the rising rate of the dielec- step-response by filtering the high frequency components in the applied step-function. Inspection of the results showed that with a value of RC chosen to prevent amplifier saturation the overall response was dominated by the RC distortion, in consequence the dielectric relaxation peak could not be observed.

In an attempt to gain more insight into the nature of the dominating effect of the RC distortion and perhaps to overcome this problem we may treat the above method and its results theoretically.

Assuming S1 and S2, Fig. (5.17), are linear systems having $h_1(t)$ and $h_2(t)$ impulse responses respectively, we can write, in the absence of loading effects,

$$g_1(t) = h_1(t) * U(t) \quad \ldots\ldots\ldots\ldots\ldots \quad (5.13)$$

where $g_1(t)$ represents the system S1 response to the Unit step U(t), and

$$g_2(t) = h_2(t) * g_1(t) \quad \ldots\ldots\ldots\ldots\ldots \quad (5.14)$$

where $f_2(t)$ represents the system S2 response to $g_1(t)$.

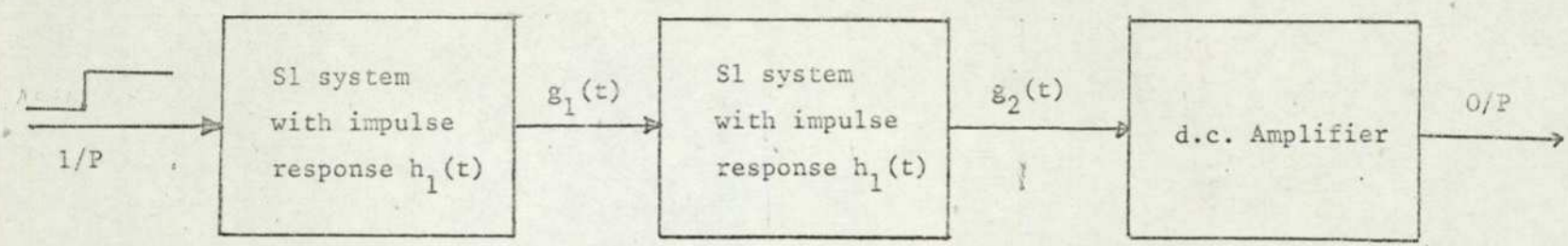

Fig. (5.17):- System S1 and S2 with their transfer function $h_1(t)$ and $h_2(t)$.

Now, if S1 is an RC network whose transfer function is given by,

$$H(j\omega) = \frac{1}{1 + j\omega RC} \quad \ldots\ldots\ldots\ldots\ldots\ldots \quad (5.15)$$

then using Eq. (A.2), we have

$$h_1(t) = \frac{1}{2\pi} \int_{-\infty}^{\infty} \frac{1}{1 + j\omega RC} e^{-j\omega t} \, d\omega \quad \ldots\ldots\ldots \quad (5.16)$$

Multiplying Eq. (5.16) by $\frac{1 - j\omega RC}{1 - j\omega RC}$, employing Euler's relation and eliminating the odd integrand, we have the well known impulse response

$$h_1(t) = \frac{1}{RC} e^{-t/RC} \quad \ldots\ldots\ldots\ldots\ldots\ldots \quad (5.17)$$

Making use of known relation between impulse and step-response, see App. (B.2), we have

$$g_1(t) = \int_0^t h(t) \, dt = 1 - e^{-t/RC} \quad \ldots\ldots\ldots \quad (5.18)$$

Thus

$$g_2(t) = h_2(t) * (1 - e^{-T/RC}) \quad \ldots\ldots\ldots\ldots \quad (5.19)$$

In the frequency domain, this becomes

$$G_2(j\omega) = H_2(j\omega) \, \mathcal{F} \, (1 - e^{-t/RC}) \quad \ldots\ldots\ldots\ldots \quad (5.20)$$

or

$$G_2(j\omega) = H_2(j\omega) \, \mathcal{F} \, 1 - H_2(j\omega) \, \mathcal{F} \, e^{-t/RC} \quad \ldots\ldots\ldots \quad (5.21)$$

Equation (5.21) shows that the F.T of the system step-response consists of two parts; the first represents the F.T of the dielectric step-responce and second part is a superimposition of the F.T of both impulse-responses of the system S2 and of the RC network.

Accordingly, as a result of this second term of Eq. (5.22) RC distortion can be expected and by trivial analysis it can be shown that

(for large value of ω) this second part of Eq. (5.21) becomes the dominating term. This is in agreement with the observed results.

Therefore, in order to eliminate the RC distortion it is necessary either to remove the system S1 or replace it by a new one which does not impose any delay time on the components of the step-function passing through it i.e. a phaseless system with a transfer function such as

$$H(j\omega) = \begin{cases} 1 & -\omega_c < \omega < \omega_c \\ 0 & \omega > \omega_c \\ 0 & \omega < \omega_c \end{cases} \quad \ldots\ldots\ldots\ldots \quad (5.22)$$

Substituting in Eq. (5.17), the value of $H(j\omega)$ in Eq. (5.22) we have

$$h_1(t) = \frac{1}{2\pi} \int_{-\omega_c}^{+\omega_c} e^{-j\omega t} \, d\omega \quad \ldots\ldots\ldots\ldots\ldots \quad (5.23)$$

Hence the impulse response required is

$$h_1(t) = \frac{1}{\pi} \frac{\sin \omega_c t}{t} \quad \ldots\ldots\ldots\ldots\ldots\ldots\ldots \quad (5.24)$$

and the step-response is,

$$g_1(t) = \frac{1}{\pi} \int_0^t \frac{\sin Y}{Y} \, dY = \frac{1}{\pi} \, Si(\omega_c t) \quad -\infty < t < +\infty \ldots \quad (5.25)$$

The value of Si(t) cannot be obtained exactly for finite limits. However, Si(t) oscillates about $\pi/2$ and approaches this value as t approaches infinity (see Chapter 4).

Making use of the above value of Si(t), we have

$$\lim_{t \to \infty} \left\{ g_1(t) \right\} = \frac{1}{2} \quad \text{and} \quad \lim_{t \to -\infty} \left\{ g_1(t) \right\} = -\frac{1}{2} \quad \ldots\ldots\ldots \quad (5.26)$$

Making use of Eq. (5.14), in the frequency domain;

$$G_2(j\omega) = H_2(j\omega) . \mathcal{F} \, Si(\omega_c t) \quad \ldots\ldots\ldots\ldots\ldots\ldots \quad (5.27)$$

Eq. (5.27) shows that the F.T of the dielectric response to $g_1(t)$ is likewise the F.T. of the dielectric step-response - $\mathcal{F} \, Si(\omega_c t)$ is equal to the F.T of the unit step-function (i.e. $\frac{1}{j\omega}$) for $-\omega_c < \omega < \omega_c$ - provided that the transfer function of the system S1 is a real constant (i.e. S1 is an ideal low-pass filter).

Unfortunately, the ideal filter does not represent a physically realisable device because its impulse response, begins before the instant at which the impulse is delivered (see Chapter 4 , 4.3.2). The reasons for this difficulty are two fold: firstly, we have assumed a filter with an infinitely sharp "cut-off", that is, one which transmits equally all frequencies up to ω_c, and rejects completely all higher ones. Secondly, we have implied no phase shift in those components transmitted, because $H(j\omega)$ has been put equal to a real constant.

5.3.2 Advantages of Non-Causal Method:-

Although it seems that we have ended with the same result, i.e. Eq. (5.27), as if we had been dealing with the step-voltage directly applied to the dielectric sample, the ideal low-pass filter technique still has many advantages over the other methods. These are -

1. The computer may be used to generate the desired function (i.e. $\int \frac{\sin x}{x} dx$), to output it later through the D/A converter and to

'sample simultaneously the dielectric response due to the above function. This means that (a) the control system (b) the pulse generator (to provide sampling frequency) (c) the relay and (d) the frequency divider when it is necessary to sample at low rate all become redundant and therefore this reduces the size of the whole set-up considerably. This may entail lower cost and reduces the size of the experimental errors.

2. It is very suitable for an on-line computing technique measurements. The computer can be made to perform almost the whole operations; to output the required stimulus, to trigger the A/D converter to initiate data sampling, to sample the output response, to process the input data and finally to plot the results. Hence, a mini-computer with certain peripherals (i.e. A/D, D/A converters, real time clock .... etc) could be used and a small set-up for dielectric measurement could easily be devised, and more importantly the method is suitable for realisation as a special microprocess instrument.

3. It was shown in Chapter (4), Eq.(4.21), that the ratio of the sampling frequency, f_s, to the filter's cut-off frequency, f_c, is always constant. Thus f_c can take any value depending on the value of f_c predetermined by the operator. Consequently, measurements on the dielectric at any temperature and within any frequency range can be easily carried out.

4. At the beginning of this chapter, it was mentioned that applying a step-function to the dielectric was accompanied, at $t = 0$, by a sudden change of $\varepsilon_\infty E$ in the electric displacement and therefore a very fast amplifier was required. Alternatively, if a slow amplifier is employed then an obviously undesirable fake peak will be introduced (see Fig. (5.8)). In the present technique, and due to the linearity of the system, the output response will contain only those frequencies

present in the applied input function. Therefore, the use of a very fast response amplifier and the relay is not essential.

5.3.3 Direct Measurements of Ideal Low-Pass Filter Response

5.3.3.1 Preliminary Work :-

For the reasons mentioned below the following were done before any RC network or dielectric response measurements were taken :

a. Practically, no realisable filter can achieve an infinitely sharp cut-off, nor can it fail to introduce a phase shift which implies, more or less, a delay imposed upon all components passing through the filter. Two RC filters connected in tandem, for instance, double the time delay but sharpen the shape of the cut-off region. Thus the price paid for the achievement of an infinitely sharp cut-off, such as assumed for the ideal filter, is an infinite time delay. The way out of this problem is to evaluate the integral (5.25) by numerical means (see chapter 4, 4.3.2) and hence the computer was programmed, (see program No.2, App G), to evaluate Si(t) from both Eq. (4.17 and 4.18) for different values of t. Fig. (5.18) shows the output results plotted by the computer.

b. The values of the function Si(t) being calculated were in Floating Point Format. To output these data, through the D/A converter, they have to be converted into Fixed Point Format and normalised to the maximum and minimum values of the D/A converter output (i.e. ± 5 volts). Program No. 3, App. G, was therefore written for this purpose.

c. Owing to the use of a phaseless filter and hence the occurence of its response before the application of the step-function (i.e. at t = 0) the dielectric response due to this part of the filter step-response sampled at this time (i.e. $\frac{-t}{2} \leq T < 0$) - where t is the time required to

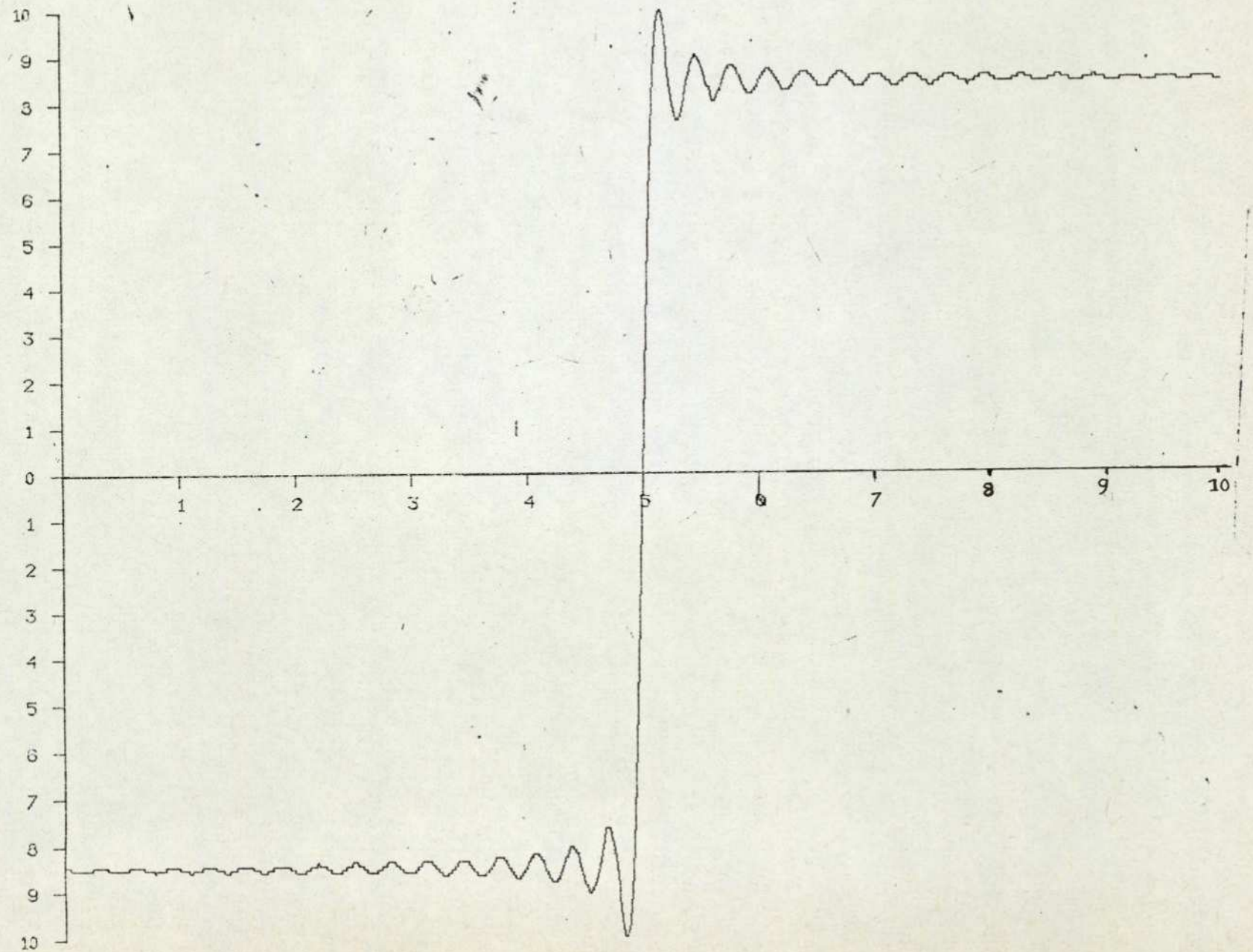

Fig. (5.18): The response of the Ideal Low-Pass filter to the step function ploted by the computer.

output the whole function si(t) - should be transfered to the location immediately following the location of the last sampled data of the dielectric output due to the filter step-response occuring at $T = \frac{t}{2}$.

That was done to avoid the occurence of the non convergent F.T. resulting from employing the integration limits ± t. Hence, Program No. 4, was written to cyclicly shift the required data to their new locations and to allow integration from 0 to t (i.e. t = the time required to sample 1024 data).

d. Program No. 4 was designed to instruct the computer to output the function Si(t) values and sample their output dielectric response at the sametime. However, sampling at slow rate (i.e. 1/4 Hz) means 4 secs should pass before another new values output. During this time the GIPOP unit output tends to decay to zero and when a new value is output, there will be a sudden jump from zero to this new value. This introduces a high frequency component in the dielectric response likewise the applying of a step-function. Therefore the GIPOP output should be kept constant at the old value until the new one is output. That was done by outputting the old value 400 times/sec. That was the maximum number of times the computer was capable of and it was found quite satisfactory.

5.3.3.2 RC Series Combintion Measurements:-

Having done that and to make sure that the whole system was functioning correctly, we connected an RC network to the amplifier (see Fig. (5.10)) and the filter step-response was then applied. The resulting RC network response was filtered, sampled at 4.22 Hz and 1024 samples were taken. Fig. (5.19) shows a typical RC network response as plotted by the computer. These responses were then F.T. by the computer and the results in real and

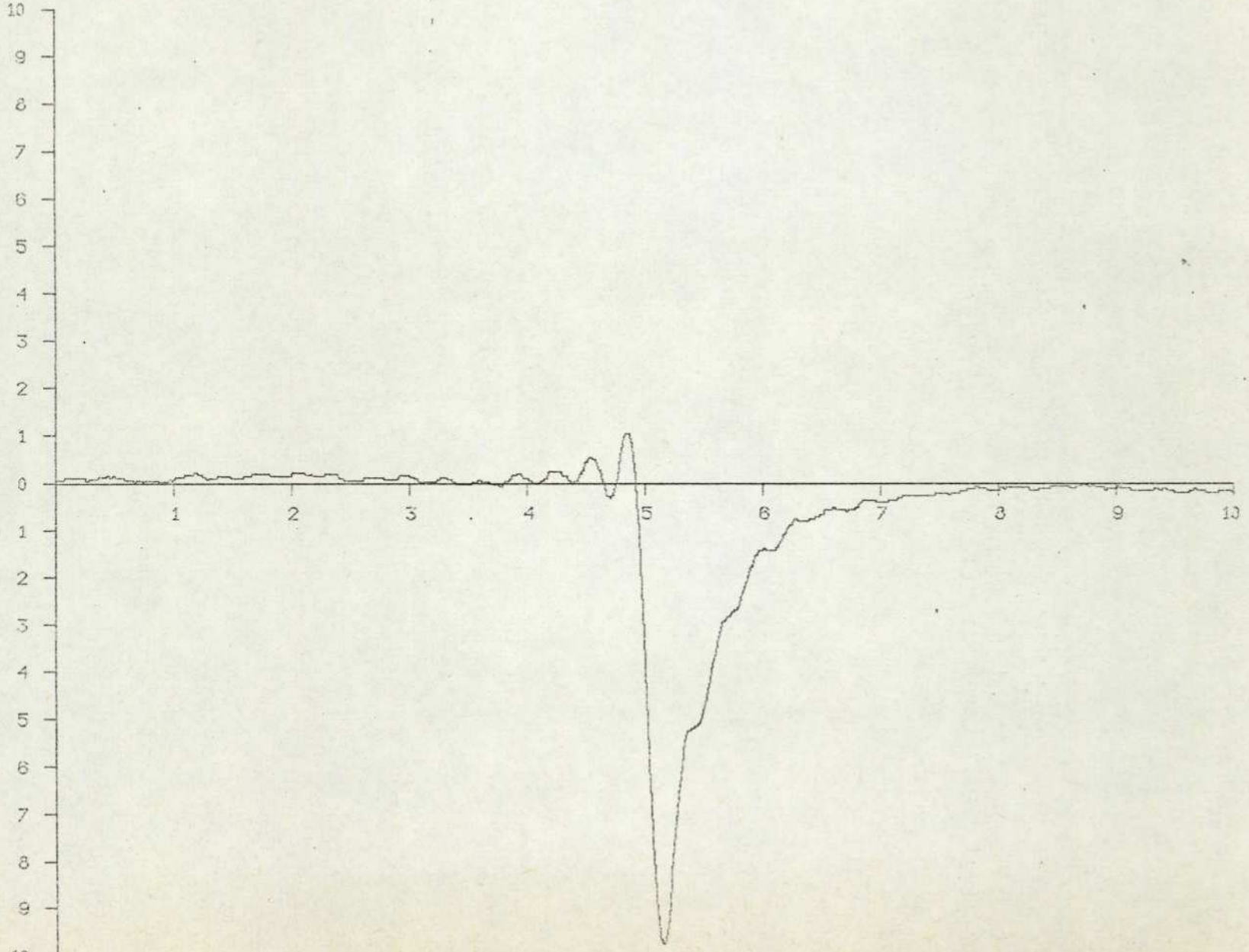

Fig. (5.19): A typical response of an RC network to the function $G(\omega_c t)$; (Fig. (5.18).

imaginary forms were plotted in Fig's (5.21, 22, 23). It should be noted that :

a. Fig. (5.20) represents the real and imaginary parts of the F.T. of the RC (5.6 sec) network response to the filter step-response sampled at 2.13 and 4.26 Hz respectively. The graphs were plotted on a logarithmic scale and contain either 32 or 1024 data points. The latter, i.e. Fig. (5.21 b), was plotted to show the filter cut-off frequency.

b. Figs. (5.21) and (5.22) illustrate the real and imaginary parts of the F.T. of he RC networks, 10 and 15 secs, responses to the filter step-response sampled at 4.27 Hz.

c. The loss peak are clearly observable in these results and tend to shift towards lower frequencies with increasing the RC values. A good agreement between the values of the maximum frequencies associated with these peaks and the calculated ones, $f_m = 1/2\pi RC$, is obtained. Table (5.4) illustrates such an agreement.

d. The filter cut-off frequency is clearly sharp and occuring always at the same position on the different curves. With the sampling rate (4.27 Hz) being used, the cut-off frequency found to be equal to 1.38×10^{-1} Hz. Thus, the ratio, f_s/f_c, is 31 in fair agreement with the ratio $f_s/f_c = 32$ being assigned for the filter.

e. The shape of the curves is in a good agreement with those predicted by theory, see Fig. (4.2).

f. The type of relaxation can be easily shown, see section 5.2.2.1, to be a Debye's relaxation type.

5.3.3.3 Dielectric Sample (PVAc) Measurements:-

In view of the above results

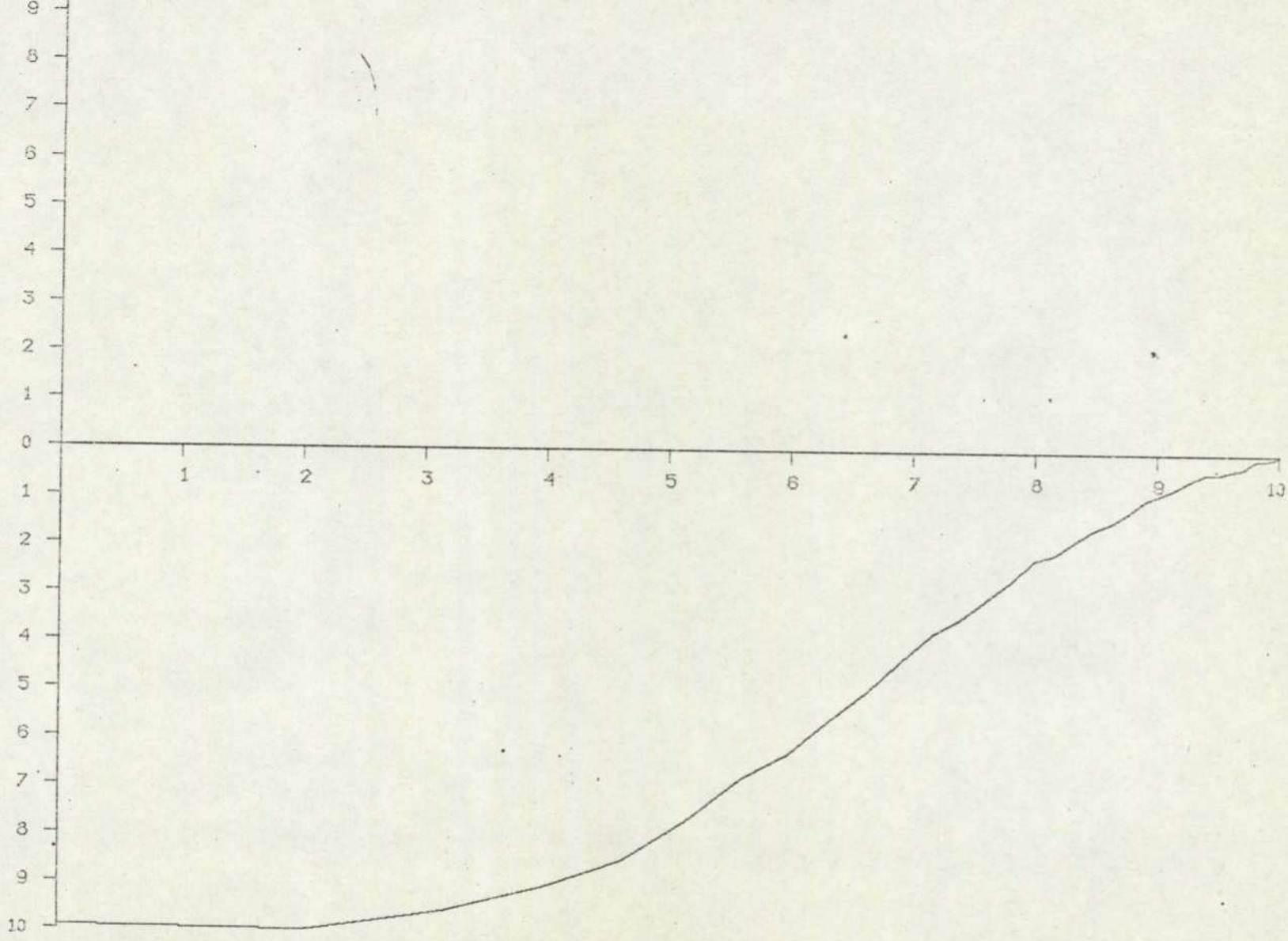

Fig. (5.20a): Frequency dependence of ε' of the RC = 5.6 at 2.13 HZ (32 points, log f).

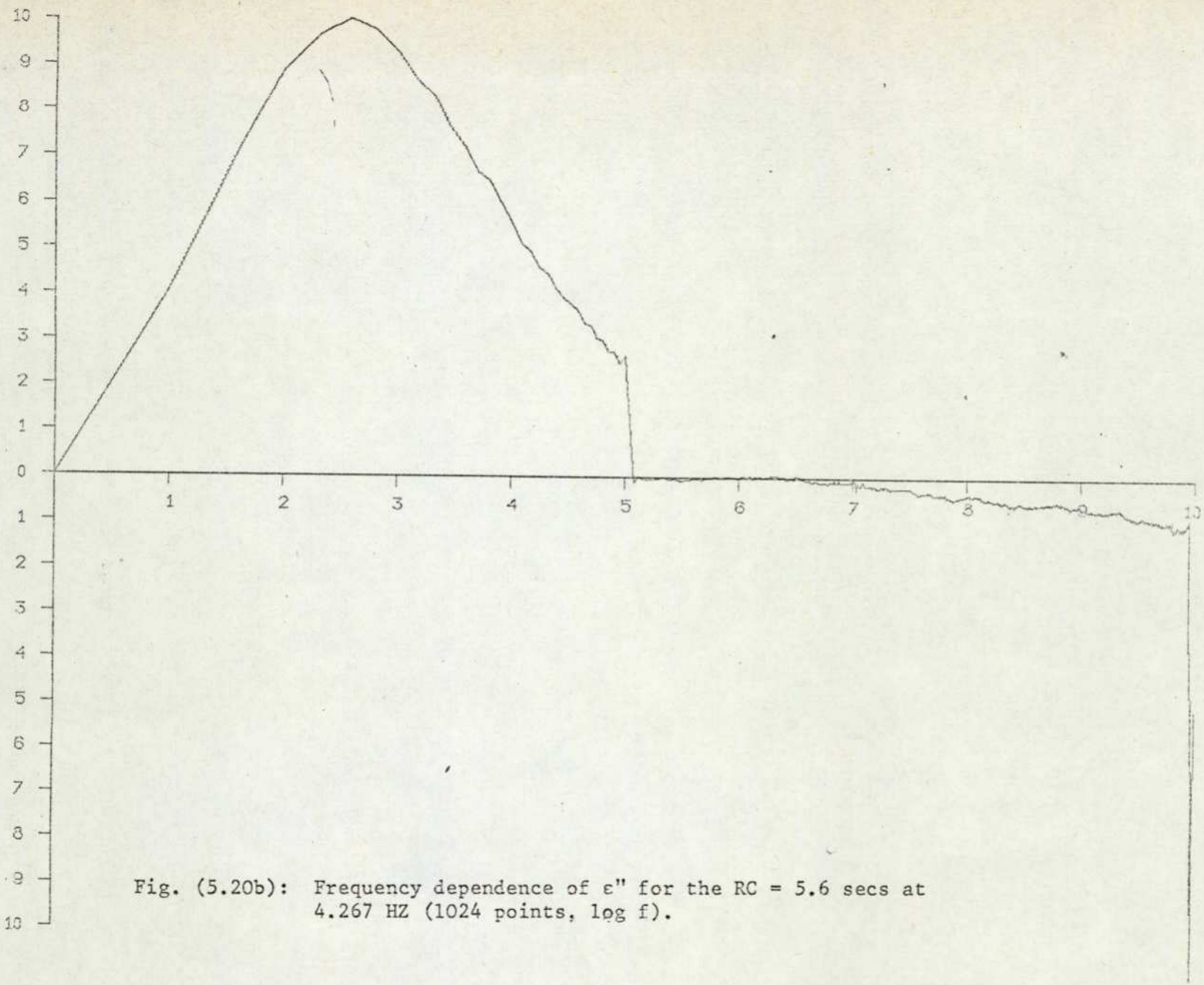

Fig. (5.20b): Frequency dependence of ε" for the RC = 5.6 secs at 4.267 HZ (1024 points, log f).

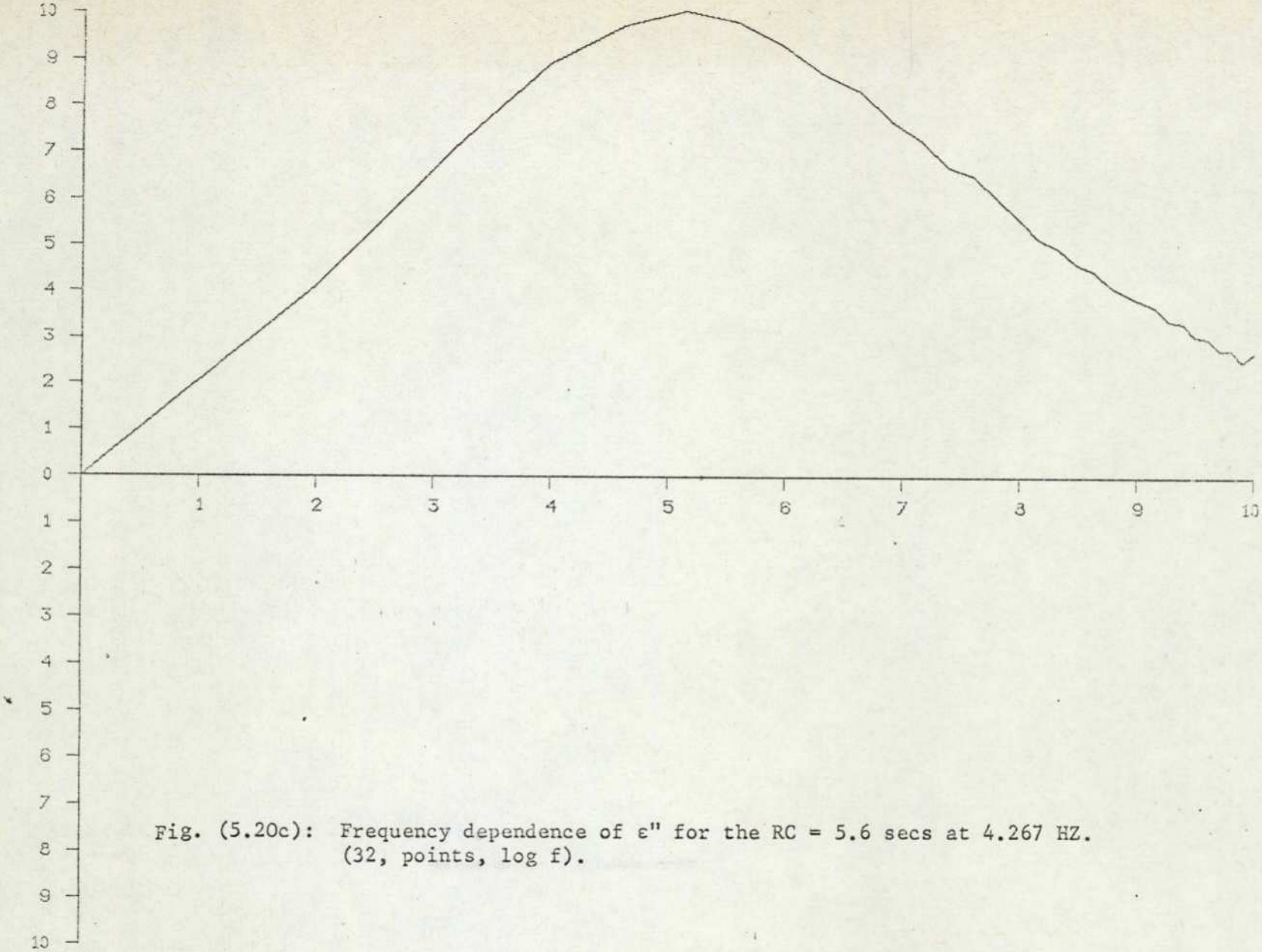

Fig. (5.20c): Frequency dependence of ε" for the RC = 5.6 secs at 4.267 HZ. (32, points, log f).

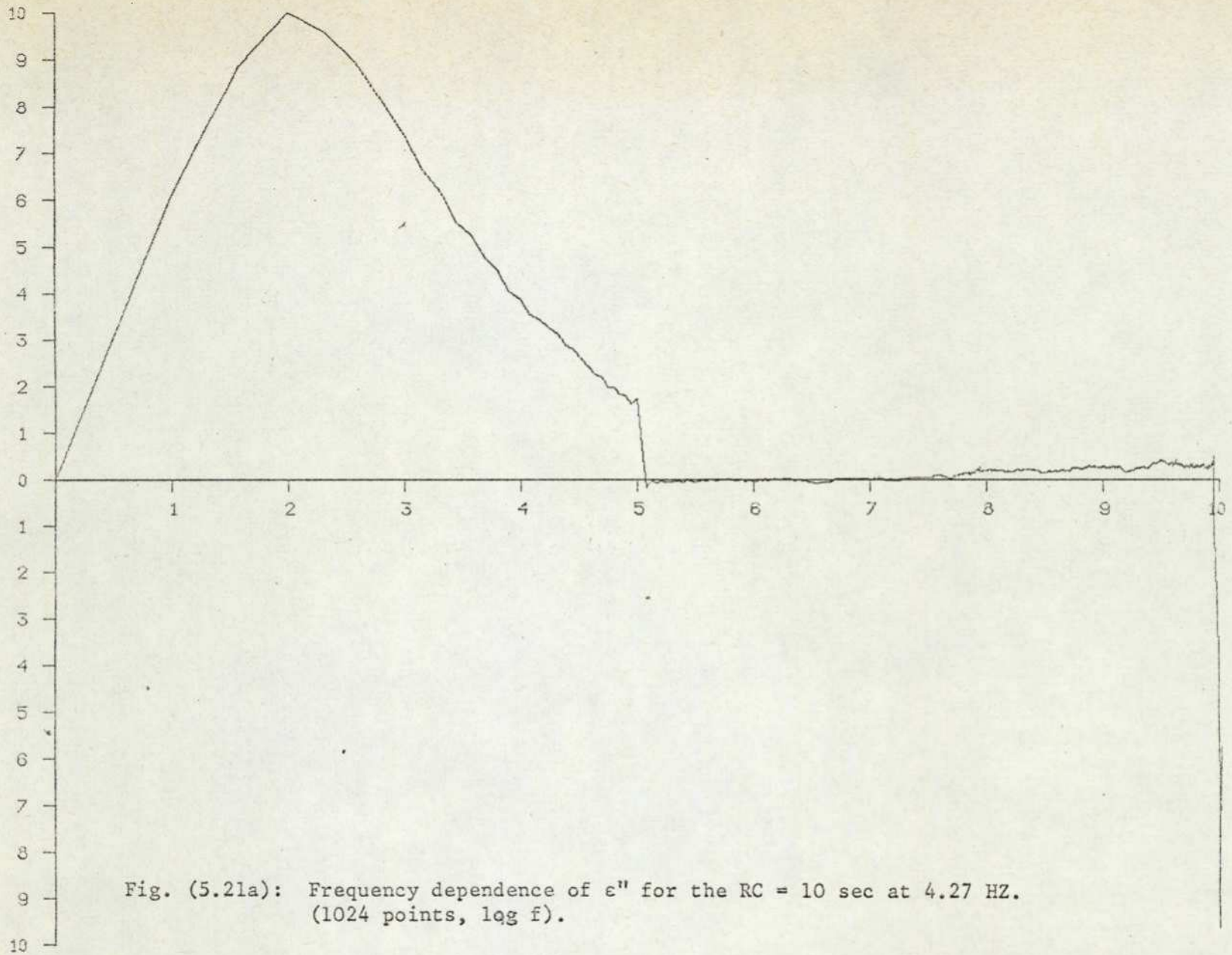

Fig. (5.21a): Frequency dependence of ε" for the RC = 10 sec at 4.27 HZ. (1024 points, log f).

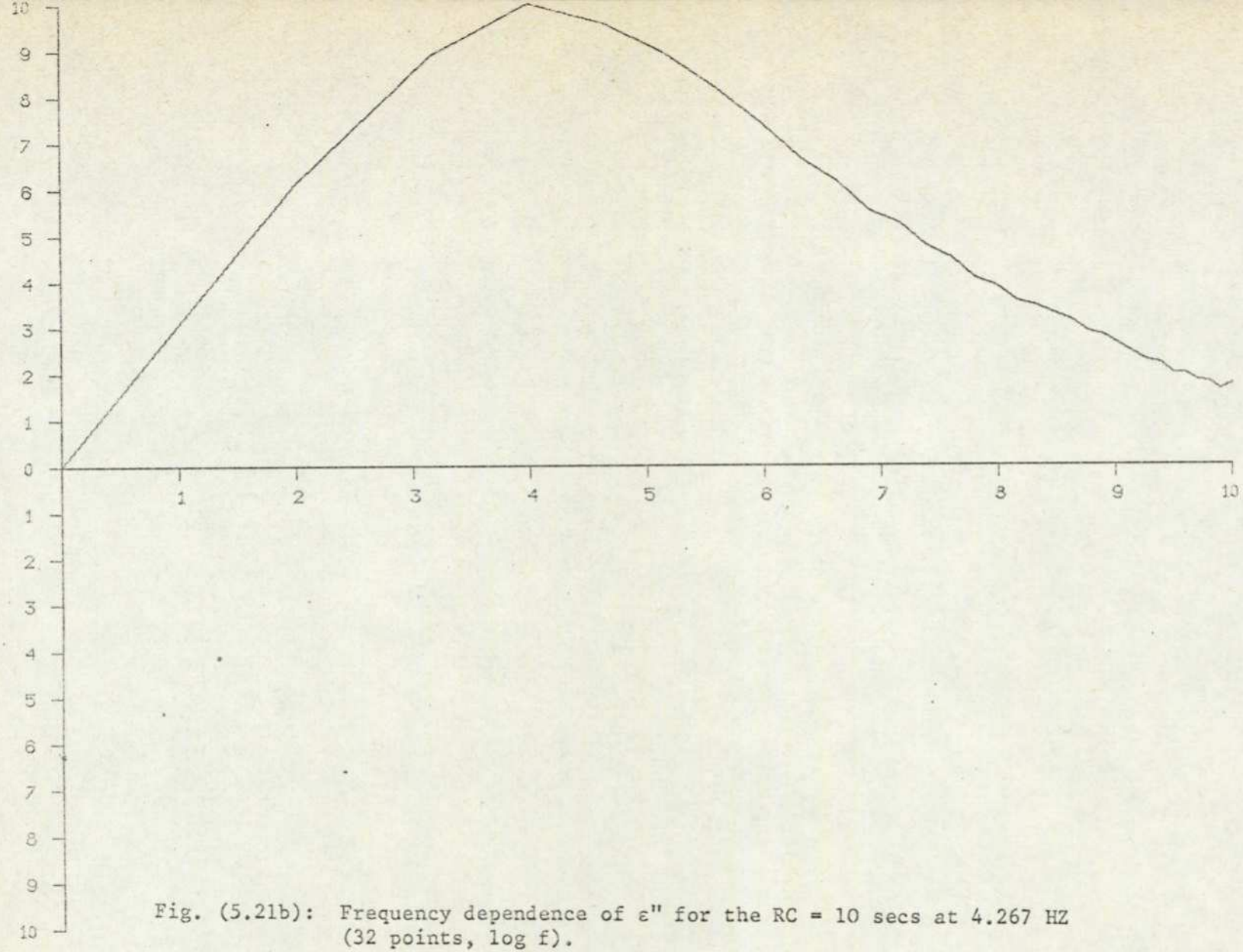

Fig. (5.21b): Frequency dependence of ε" for the RC = 10 secs at 4.267 HZ (32 points, log f).

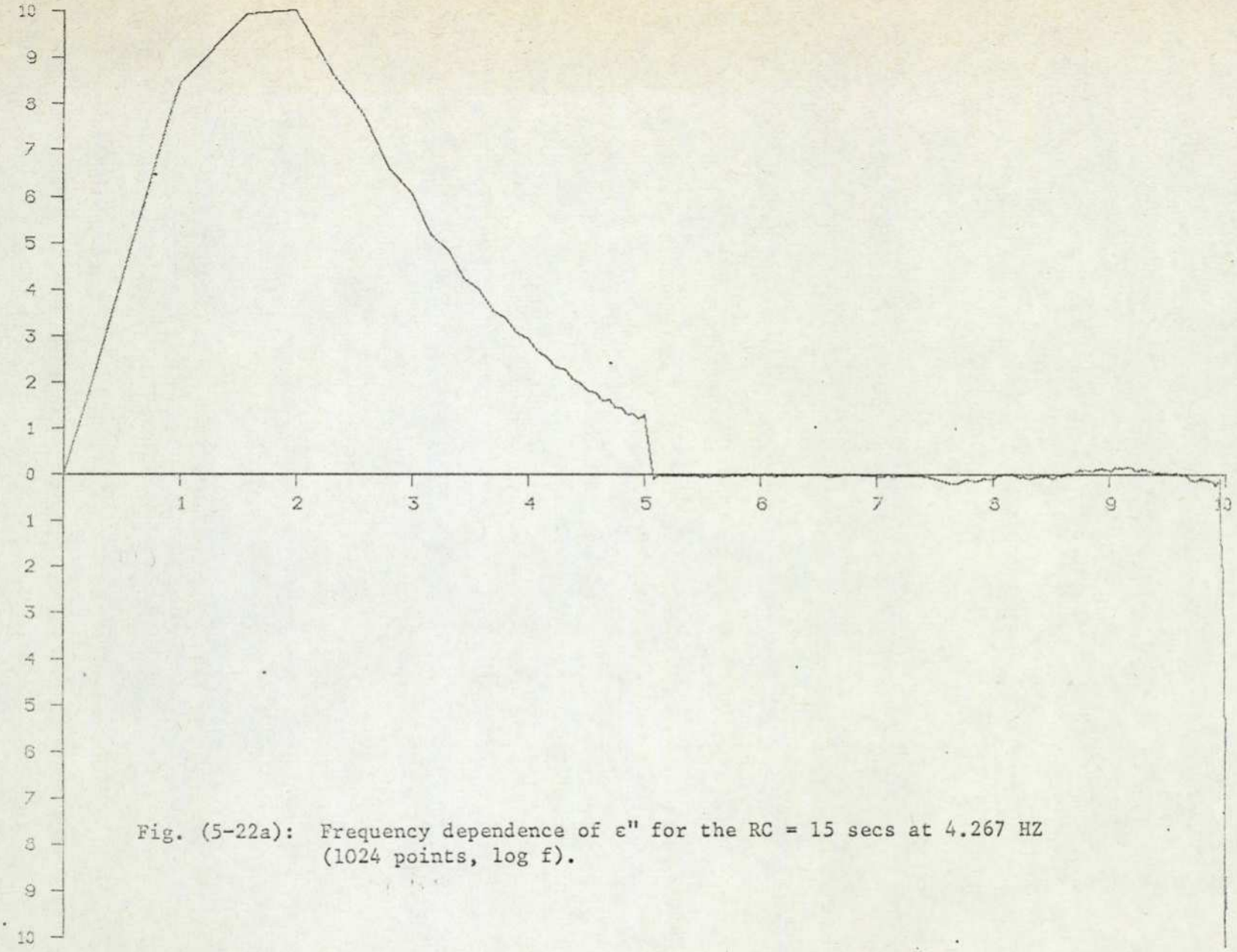

Fig. (5-22a): Frequency dependence of ε" for the RC = 15 secs at 4.267 HZ (1024 points, log f).

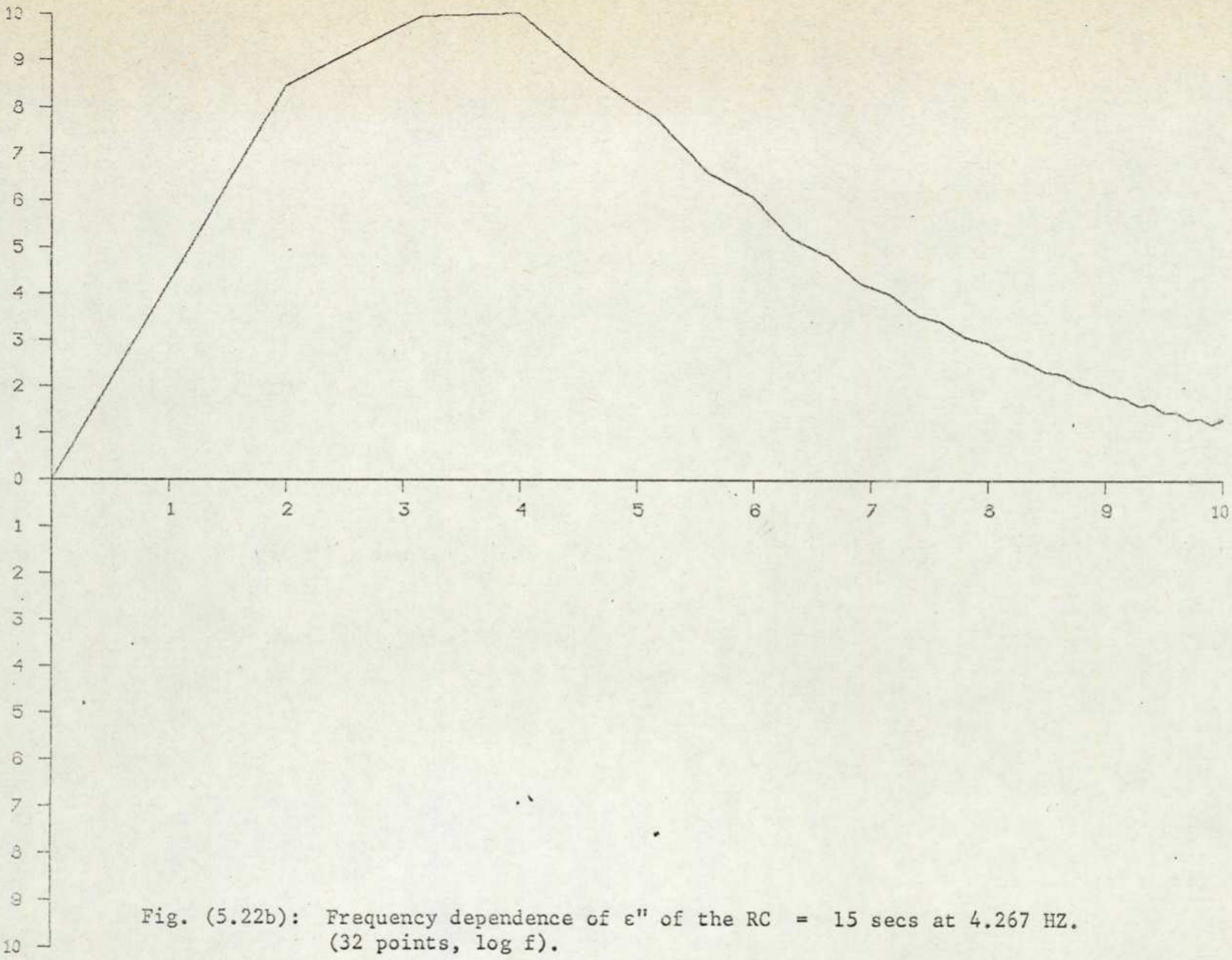

Fig. (5.22b): Frequency dependence of ε" of the RC = 15 secs at 4.267 HZ. (32 points, log f).

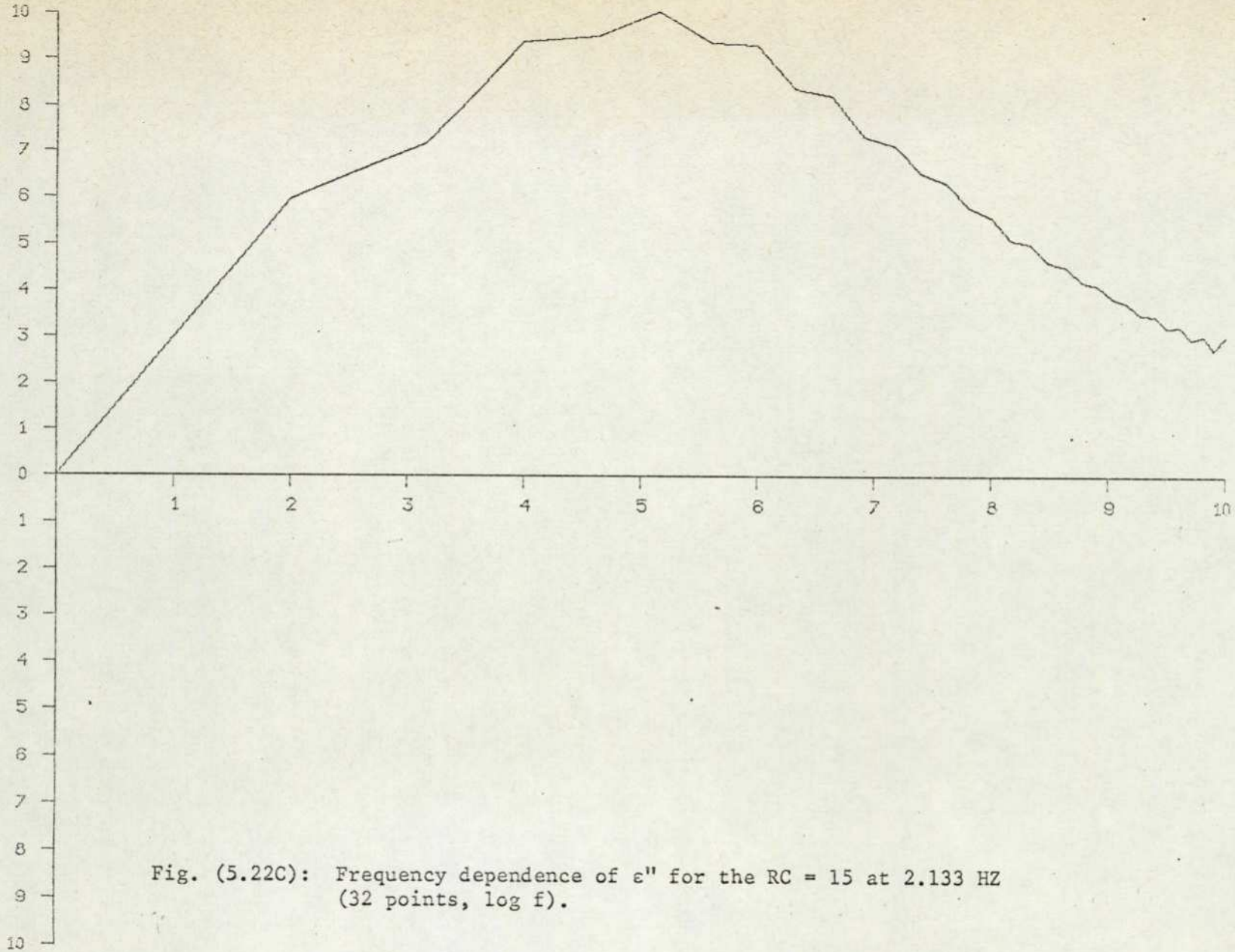

Fig. (5.22C): Frequency dependence of ε" for the RC = 15 at 2.133 HZ (32 points, log f).

Figure's Number	RC (sec)	Sampling frequency (Hz) f_s	Experimental f_m (Hz)	Calculated f_m = 1/2 RC (Hz)	Experimenal cut-off frequency f_c (hz)	$\frac{f_s}{f_c}$
(5.20 c)	5.6		2.57×10^{-2}	2.8×10^{-2}		
(5.21 b)	10	4.27	1.67×10^{-2}	1.6×10^{-2}	1.38×10^{-1}	31.0
(5.22 b)	15		1.17×10^{-2}	1.06×10^{-2}		
(5.22 c)	15	2.13	1.17×10^{-2}	1.06×10^{-2}	6.9×10^{2}	31.0

Notes: a. Theoretically ; $\frac{\omega_s}{\omega_c} = 2K$, where K = 16 (see Chapter 4)

b. Sampling frequency was calculated by dividing 1024 over the time required for the clock to output the function $G(\omega_c t)$.

Table (5.4) : Comparison between Experimental results and those calculated for different RC combinations at different sampling rates.

the system seemed to function correctly and hence the method was quite satisfactory. Therefore, measurements on PVAc dielectric sample were carried out straight away after making sure that : (a) the amplifier output was set to zero at the beginning of the experiment; (b) the sample was left at the chosen temperature for at least one hour; (c) the electrodes were in a good electrical contact with the sample (d) the dielectric sample was thoroghly depolarized before the sampling of the dielectric response to the filter step-response started. That was necessary because the computer was instructed to output a (- 5) volts (i.e. equal to the value of the first point of the function Si(t) before outputting the function values, hence the dielectric response due to this - 5 volts should be excluded. The computer keeps outputing the - 5 volts as long as the bit 0 of the handswitch is OFF.

With the above conditions being satisfied, the bit 0 was put ON and the computer started outputting the function Si(t) values. The presence of stepwise progression, imposed by the zero - hold D/A convertor (Fig. (5.23), with the function Si(t) resulted in high frequency components dielectric response. Therefore, it was necessary to filter the response from these high-frequency component before being sampled and Fig. (5.24) shows the new set-up. A typical dielectric response to the function Si(t) is shown in Fig. (5.25). These responses were then F.T. and the results, in real and imaginary part, were obtained, Fig. (5.26). It should be noted that in Fig. (5.26);

a. Fig. (5.26 a) represents the real part of the F.T. of the dielectric response to the function Si(t) taken at 46^{o}C and sampled at 6.96 Hz.

b. Fig. (5.26 b,c,d,e) represent the imaginary parts of the F.T. of the dielectric responses to the function Si(t) taken at different

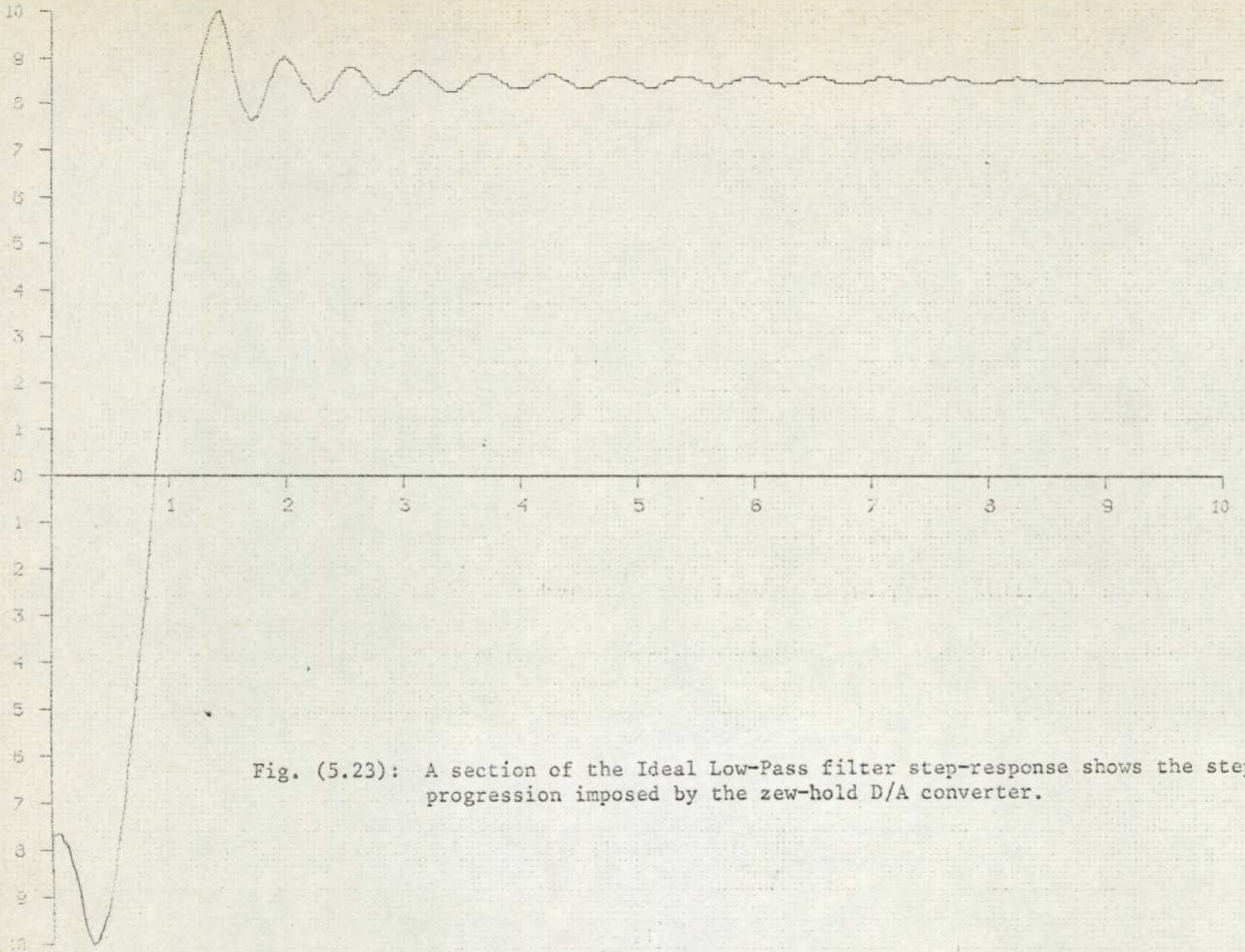

Fig. (5.23): A section of the Ideal Low-Pass filter step-response shows the stepwise progression imposed by the zew-hold D/A converter.

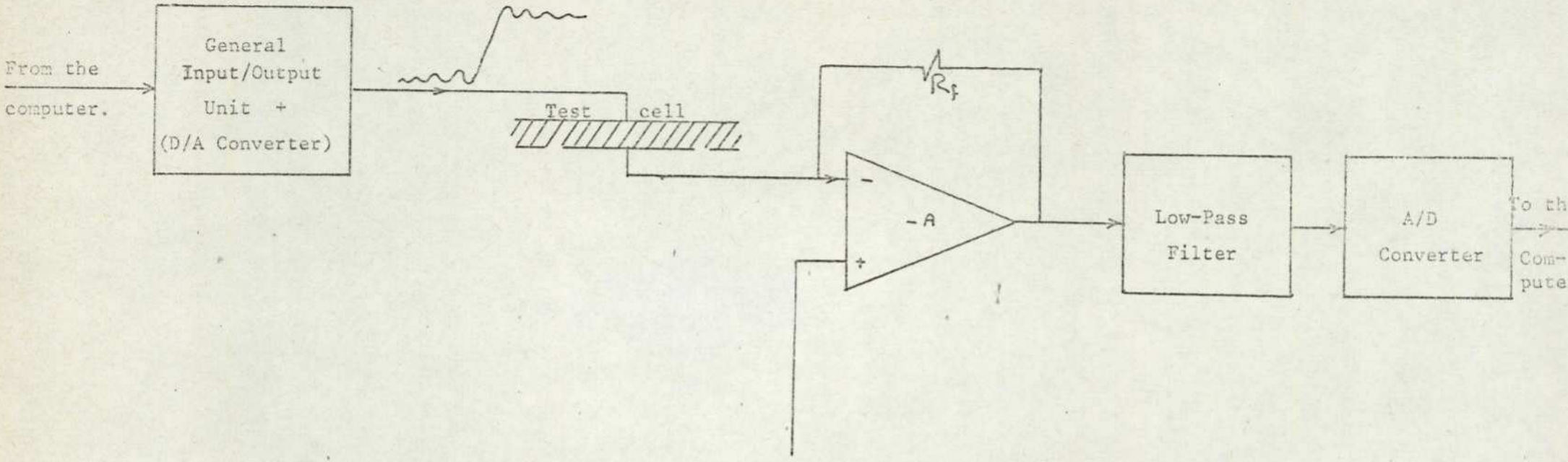

Fig.(5.24): Final set-up for dielectric measurements using Ideal Low-Pass Filter technique.

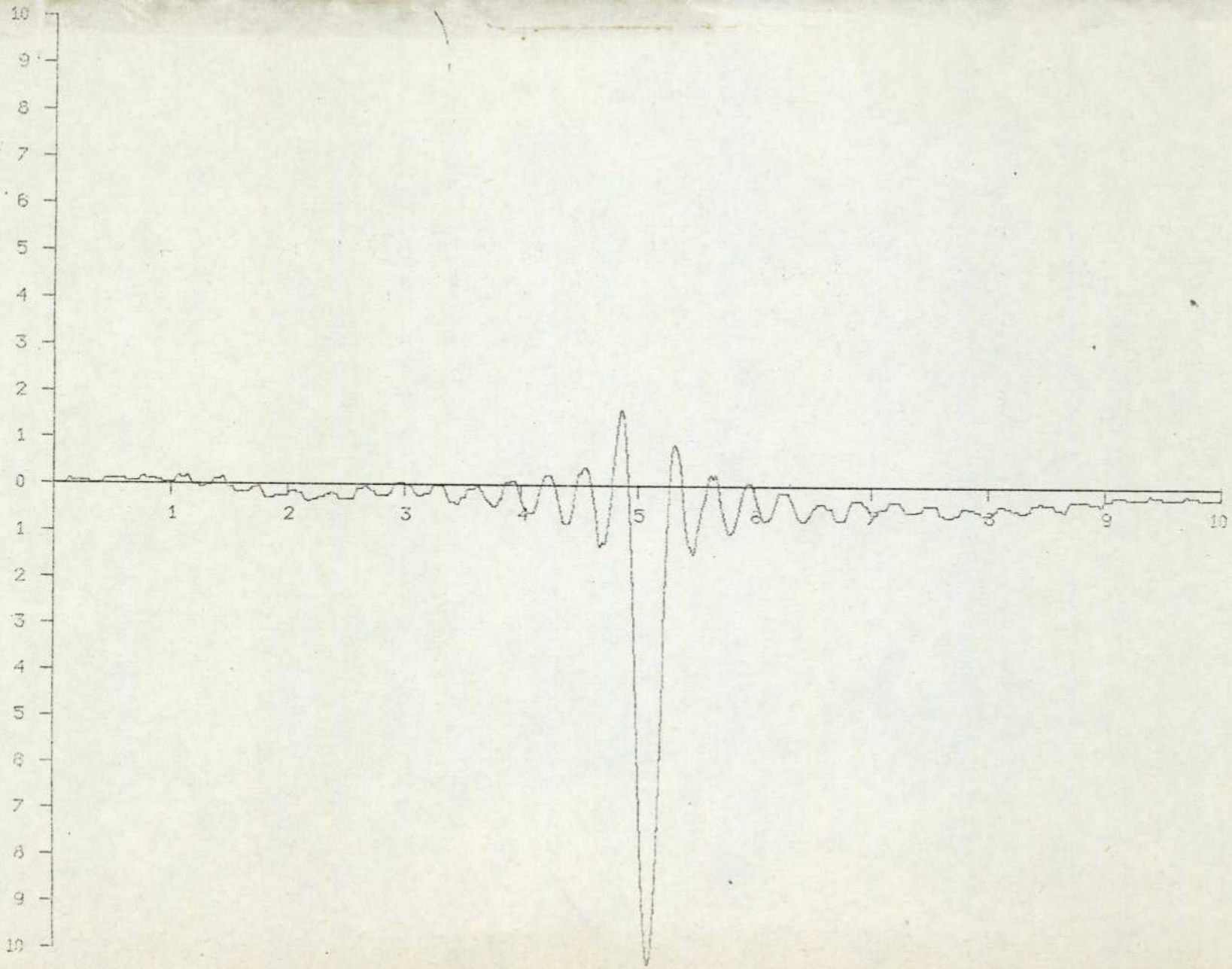

Fig. (5.25): Typical response of the PVAc dielectric sample to the applied function $Si(\omega_c t)$ plotted by the computer (sampling frequency = 6.96 HZ, 1024 points).

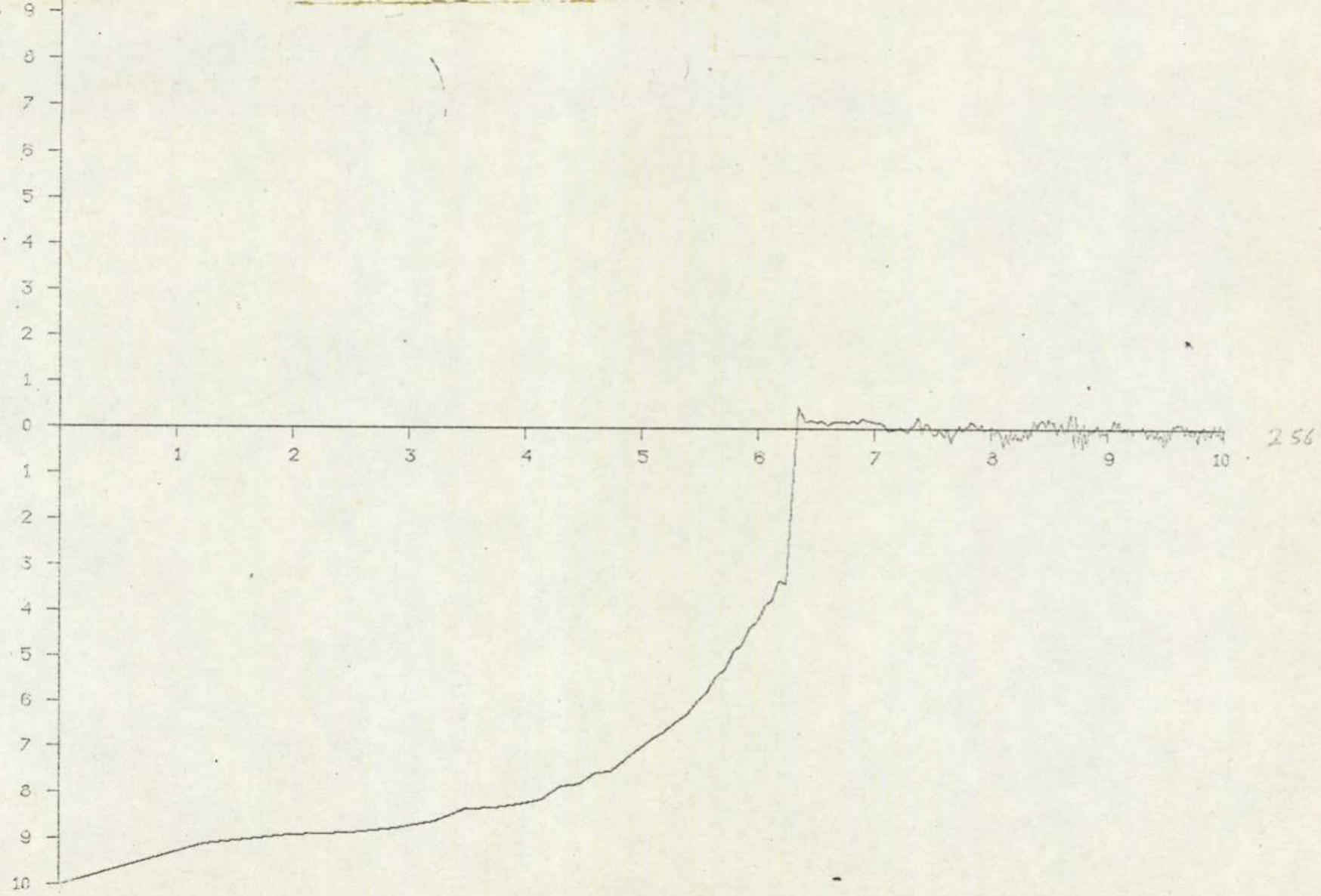

Fig. (5.26a): Frequncy dependence of ε' at 46°C and 6.96 HZ for PVAc (256 points, log f).

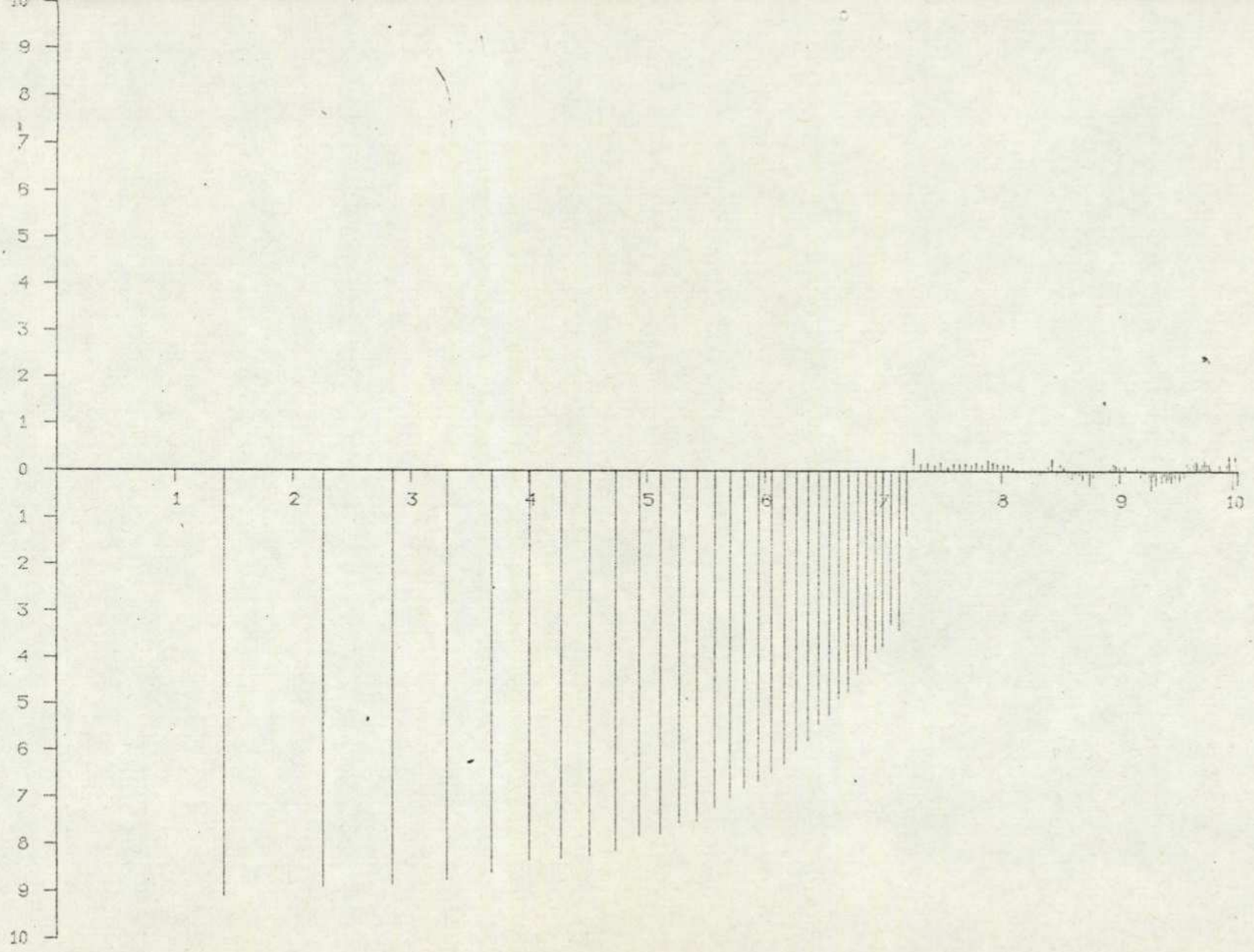

Fig. (5.26a): Frequency dependence of ε' and 46°C and 6.96 HZ for PVAc (128 points, log f).

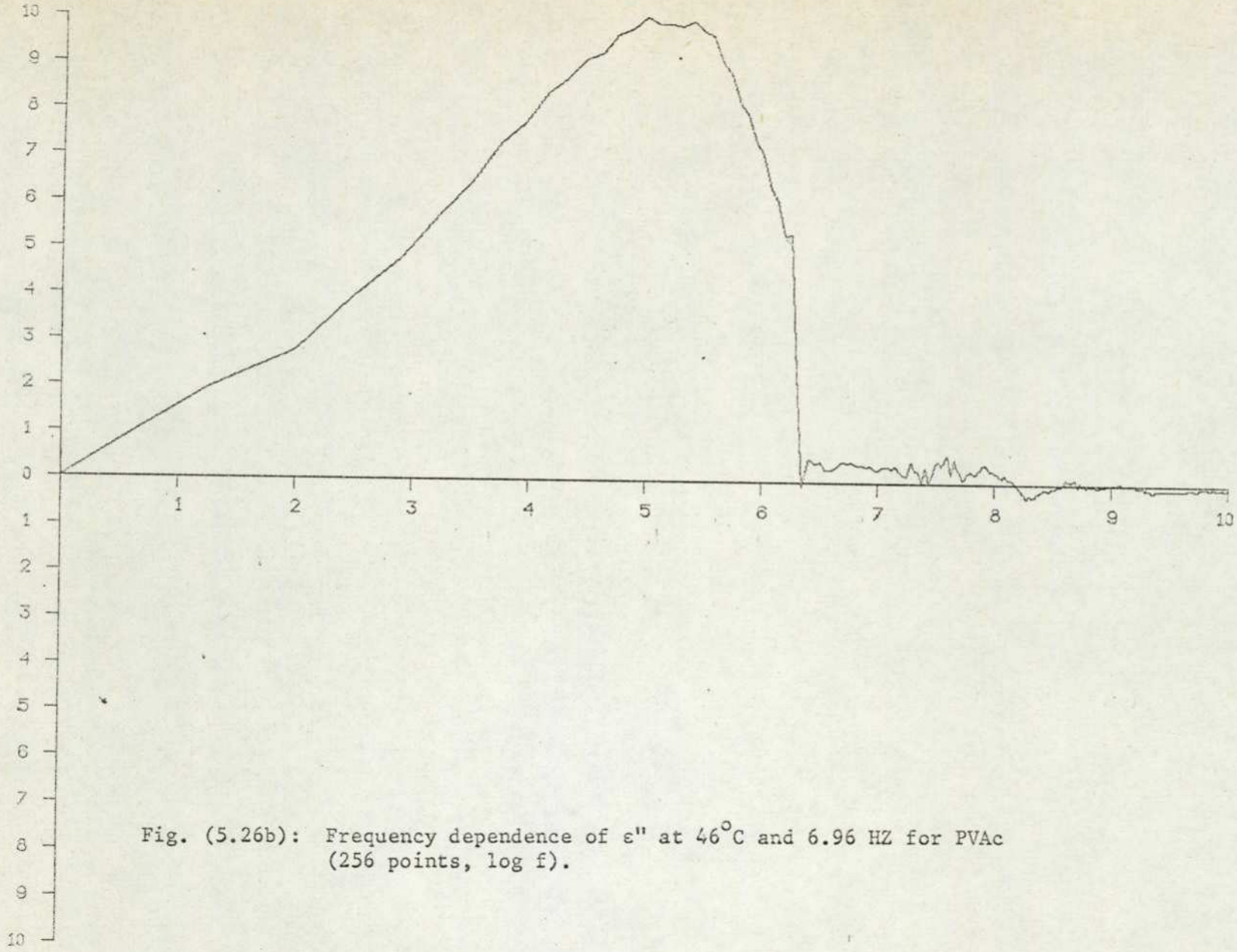

Fig. (5.26b): Frequency dependence of ε" at 46°C and 6.96 HZ for PVAc (256 points, log f).

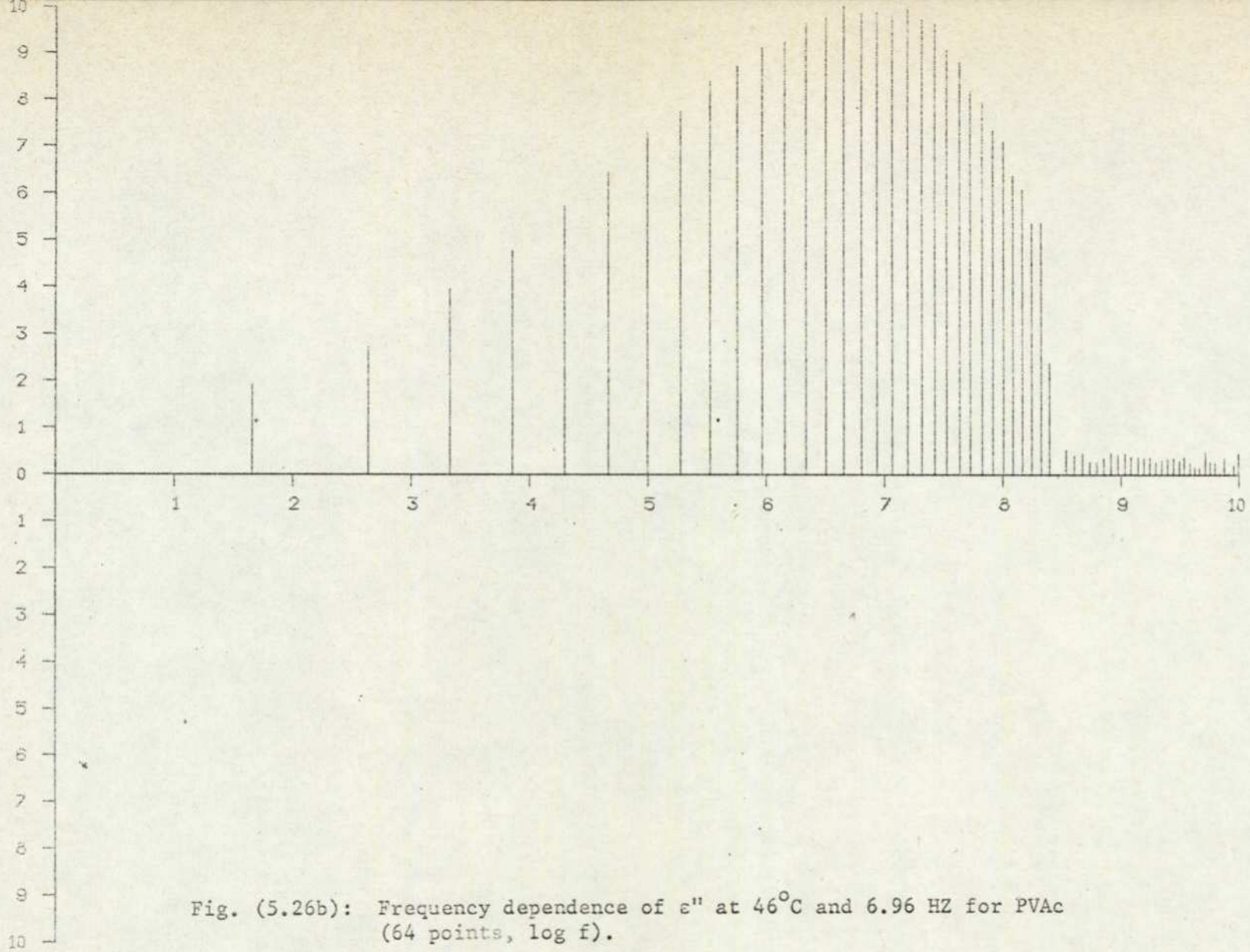

Fig. (5.26b): Frequency dependence of ε" at 46°C and 6.96 HZ for PVAc (64 points, log f).

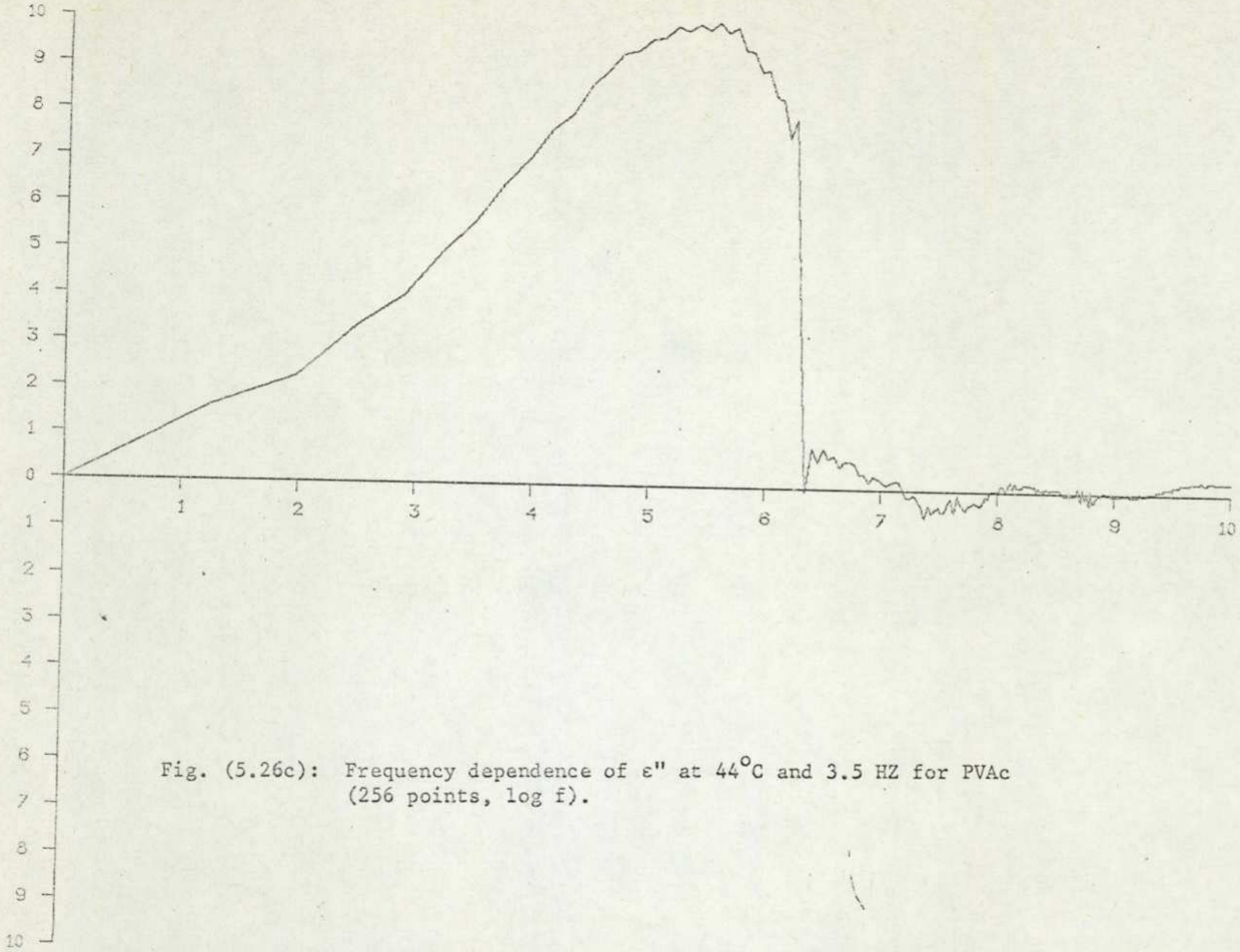

Fig. (5.26c): Frequency dependence of ε" at 44°C and 3.5 HZ for PVAc (256 points, log f).

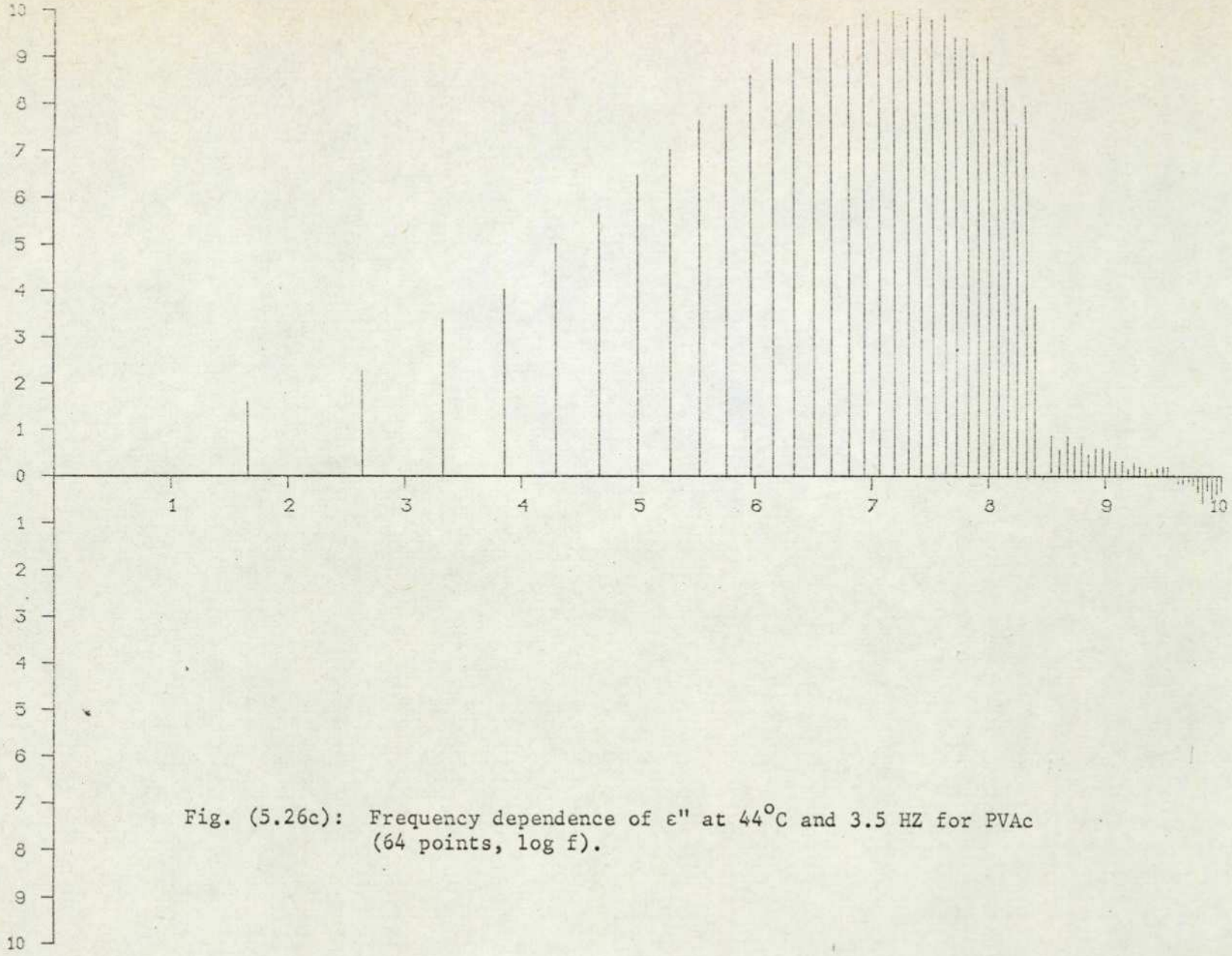

Fig. (5.26c): Frequency dependence of ε" at 44°C and 3.5 HZ for PVAc (64 points, log f).

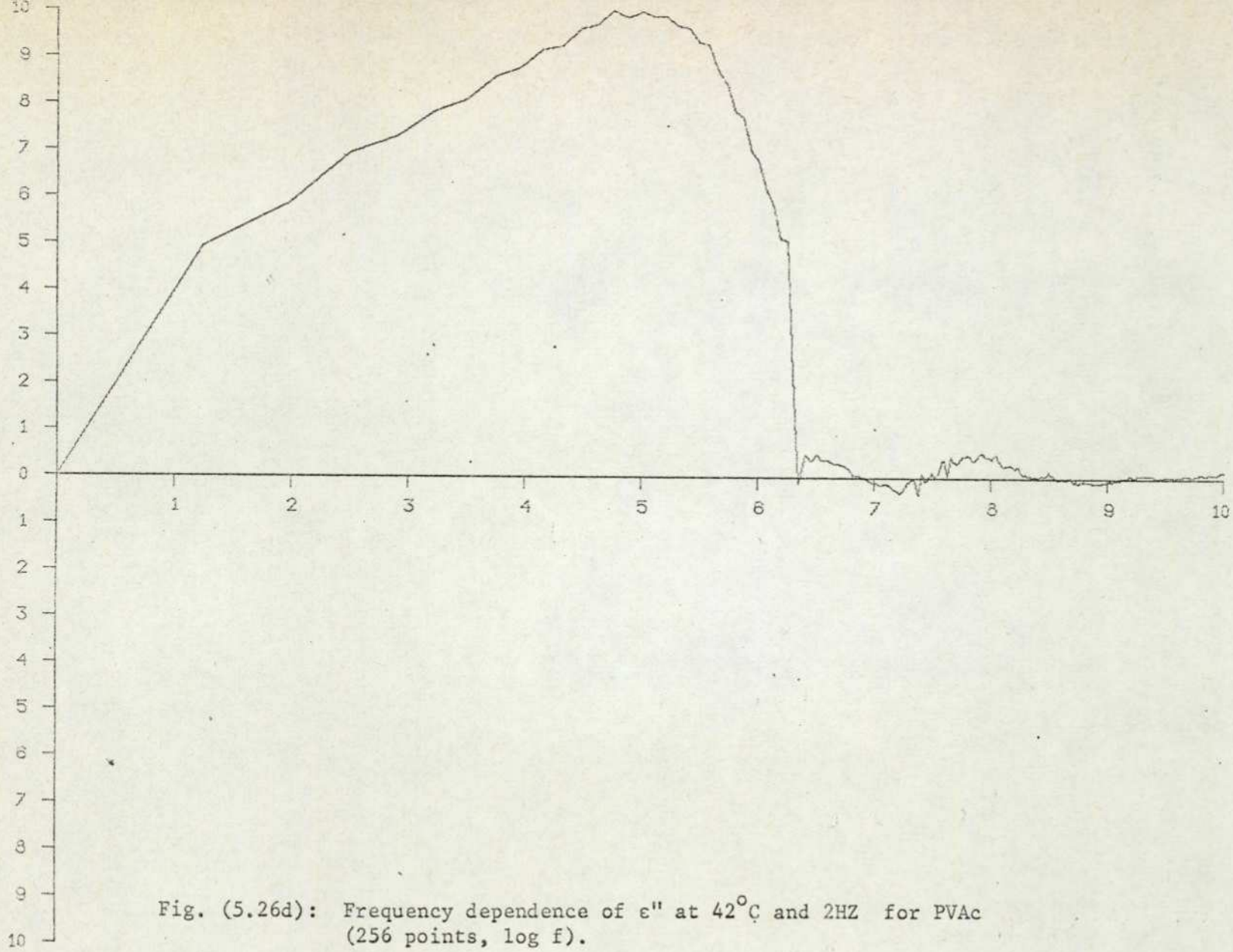

Fig. (5.26d): Frequency dependence of ε" at 42°C and 2HZ for PVAc (256 points, log f).

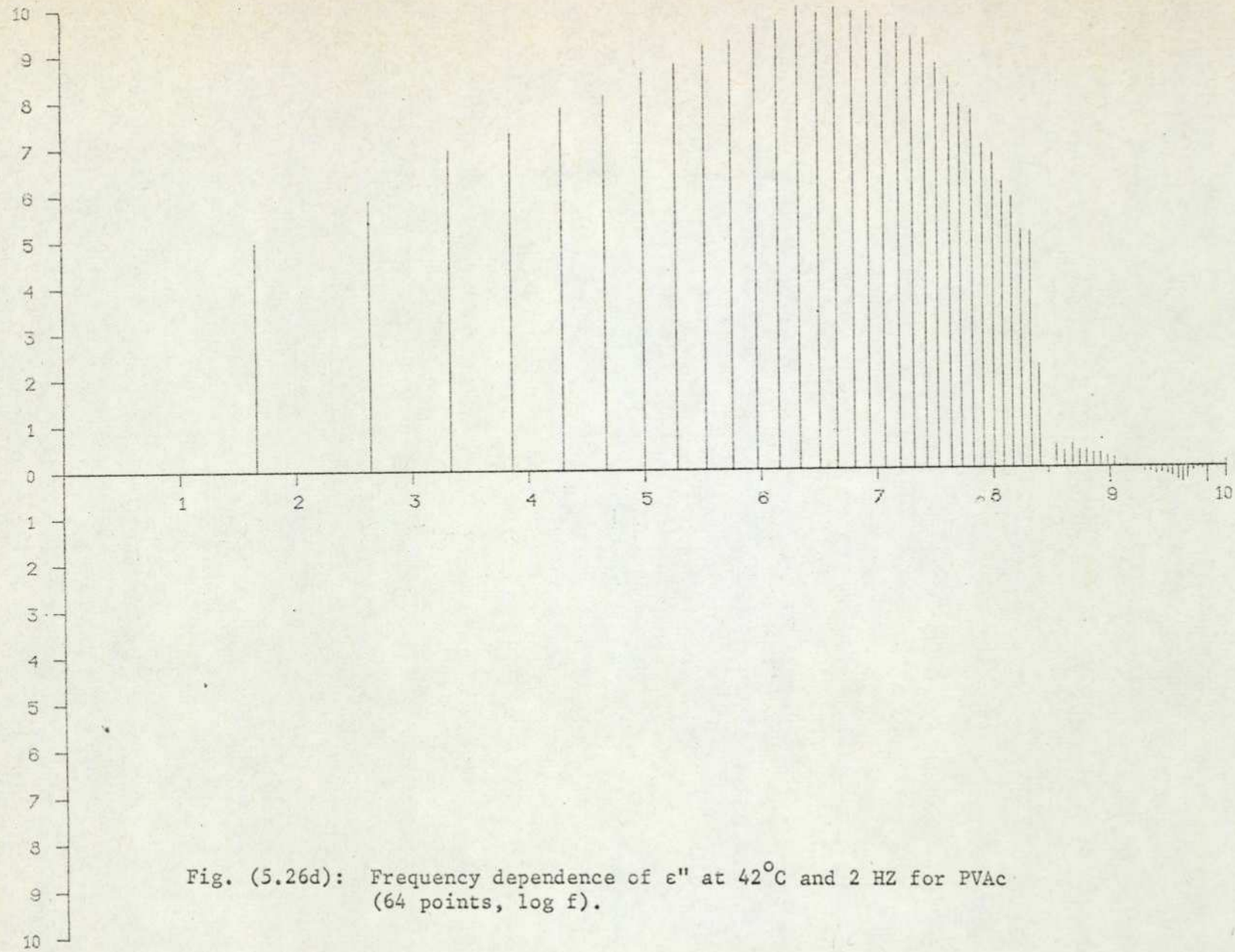

Fig. (5.26d): Frequency dependence of ε" at 42°C and 2 HZ for PVAc (64 points, log f).

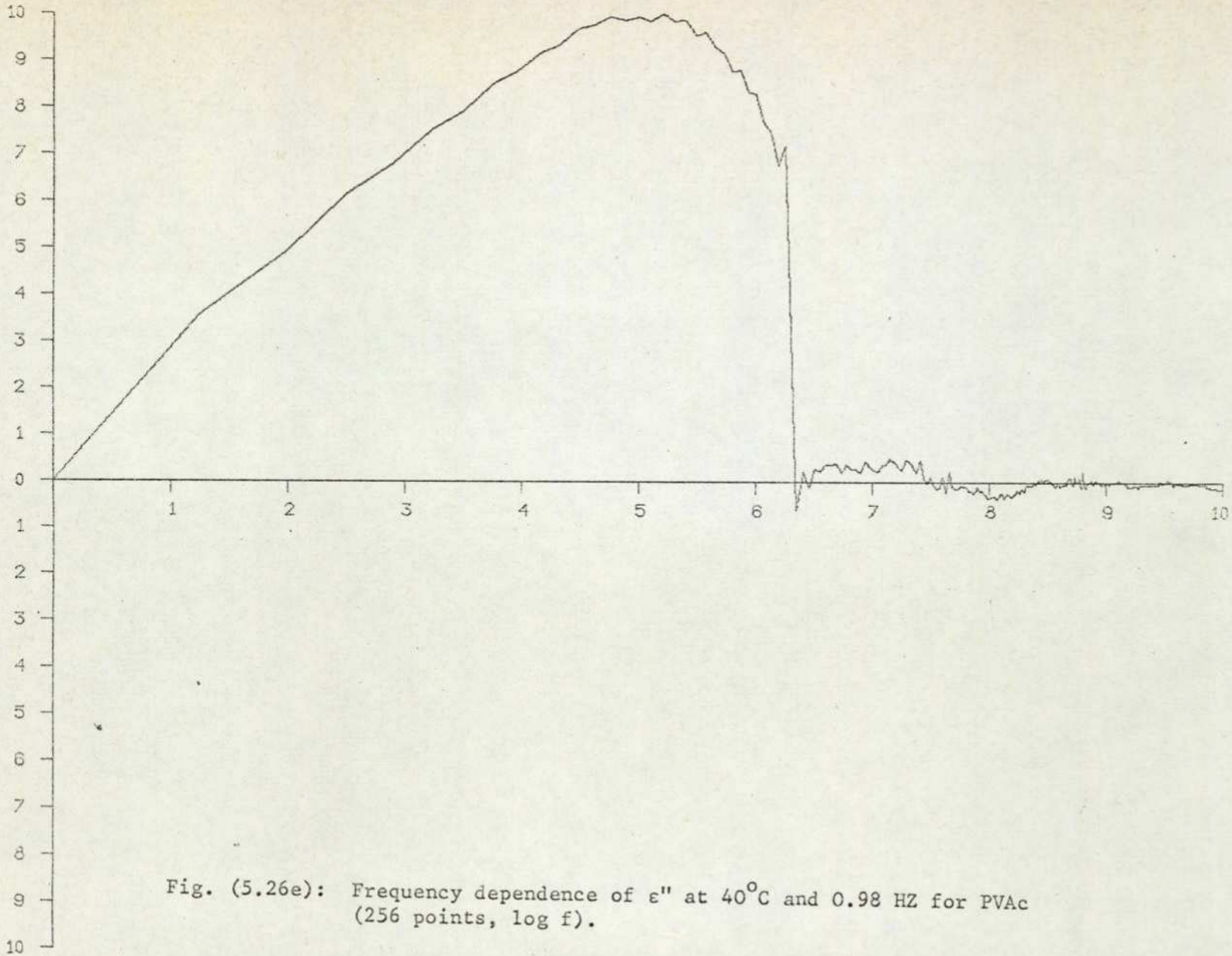

Fig. (5.26e): Frequency dependence of ε'' at $40^{o}C$ and 0.98 HZ for PVAc (256 points, log f).

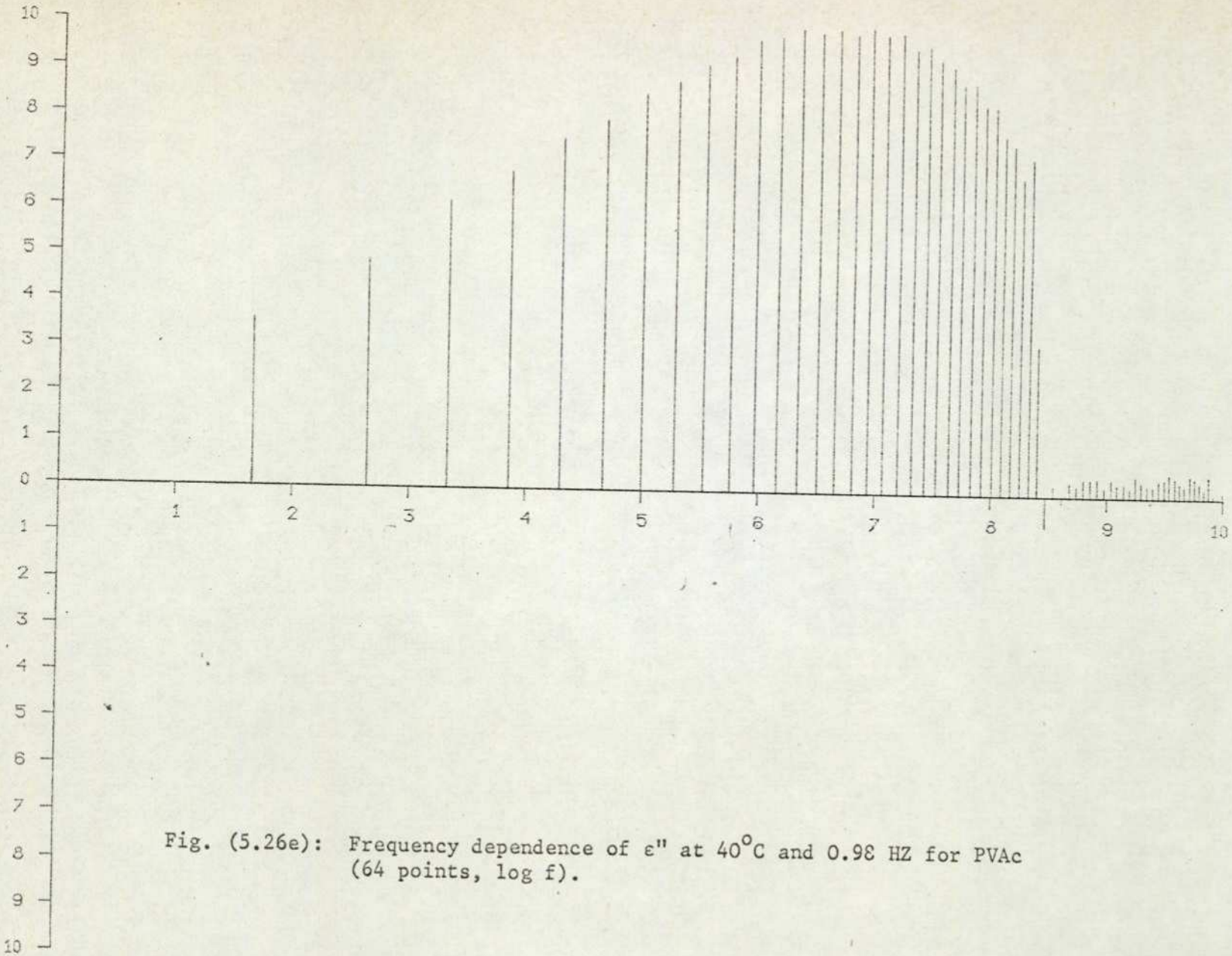

Fig. (5.26e): Frequency dependence of ε" at 40°C and 0.98 HZ for PVAc (64 points, log f).

temperatures (i.e. 46, 44, 42 and 40^{o}C) and sampled at different rates.

c. These graphs were plotted on a logarithmic frequency scale and each of them presented in two patterns namely, the Normal and Bar patterns. The reason for inclusion of the latter was explained before.

d. The value of ε', Fig. (5.26 a), clearly falls from a higher to a lower level as the frequency increases. The rate of change of ε' with frequency is greatest at the frequency at which the peak in ε'' value occurs, Fig. (5.26 b).

e. The absorption process observed in these measurements is only that which can be observed at temperatures above T_g (glass temperature, 28^{o}C) namely the α-absorption (see chapter 2).

f. The loss peaks are clearly observable in these results and occur at frequencies corresponding to relaxation regions where materials absorb energy and maximum loss occurs. The positions of these peaks are clearly, see Table (5.5), depending on temperatures at which measurements were taken.

g. The shape of the α-absorption curves does not seem to change as the temperature increases but the curves become narrower (due to convergence of relaxation time) at higher temperatures. Surely, the latter feature of these results made it certain that these results are due only to the dielectric sample and nothing else.

h. The results appear to be very similar to the dielectric loss curves obtained, for PVAc, earlier in this chapter, section 5.2.2.2, especially in their temperature frequency locations and also, that the magnitude of loss becomes higher at higher temperature. Table (5.5) shows the temperature frequency locations of loss maxima in both measurements.

Figure's number	Temperature T c	Experimental f_m (Hz)	Experimental relaxation time	Frequency f_m from Table (5.3)	Relaxation Time from Table (5.3)	Difference between the two relaxaion times
(5.22)						
c	46	1.15×10^{-1}	1.4	--	--	--
d	44	6.3×10^{-2}	2.53	5.2×10^{-2}	3.06	0.53
e	42	3.17×10^{-2}	5.01	2.7×10^{-2}	5.87	0.86
f	40	1.62×10^{-2}	10.1	1.14×10^{-2}	13.91	3.81

Table (5.5): Comparison between the relaxation times, measured with different techniques, of the same dielectric sample (PVAc) and at the same temperatures.

i. The sharp cut-off frequency (f_c) of the filter is quite clear and those data occuring at frequencies beyond f_c are completly rejected. The distortions that occur after f_c are due to quantization errors in these measurements. In this measurement the ratio f_s/f_c is also equal to 32.

CHAPTER SIX.

Discussion and Analysis

6.1 General Introduction;

It has been shown in Chapter (5) that, the experimental results from both methods (i.e. step-function and Non-Casual) are similar to each other and to those obtained by previous workers.

However, the differences in the locations of the maximum losses in both results may be attributed to the time truncation errors associated with Fourier Transformations of the dielectric responses. This can be shown as follows:

Clearly any set of experimental data will only describe a finite range of time and therefore errors will arise due to cutting-off of the Fourier Integral at both small and large values of time. The magnitude of such errors will depend on the time range of the avliable data such as;

a. Short-time Cut-off:-

we have from Equation (D.5);

$$\varepsilon^* = \frac{1}{C_o V_o} \int_a^\infty i(t)\, e^{-j\omega t}\, dt \quad \ldots\ldots\ldots\ldots \quad (6.1)$$

Assuming a single time constant, i.e., $I(t) = \frac{1}{\tau_o} e^{-t/\tau_o}$, we have

$$\varepsilon^* \propto \frac{1}{\tau_o} \int_a^\infty e^{-t/\tau_o}\, e^{-j\omega t}\, dt \quad \ldots\ldots\ldots\ldots \quad (6.2)$$

$$\varepsilon' \propto \frac{1}{1 + \omega^2 \tau_o^2} \left\{ e^{-a/\tau_o} (\cos \omega_a - \omega\tau \sin \omega_a) \right\} \ldots (6.3)$$

$$\varepsilon'' \propto \frac{\omega \tau_o}{1 + \omega^2 \tau_o^2} \left\{ e^{-a/\tau_o} (\cos \omega_a + \frac{\sin \omega_a}{\omega\tau}) \right\} \ldots (6.4)$$

b. Long-time Cut-off;-

Buy putting a = 0 Eq. (6.1) becomes;

$$\varepsilon^* \propto \frac{1}{\tau_o} \int_o^b e^{-t/\tau_o} \; e^{-j\omega t} \; dt \qquad \ldots\ldots\ldots \quad (6.5)$$

and gives,

$$\varepsilon'' = \frac{1}{1 + \omega^2\tau_o^2} \left\{1 - e^{-b/\tau_o} (\cos\omega b - \omega\tau \sin \omega b)\right\} \ldots \quad (6.6)$$

and

$$\varepsilon'' = \frac{\omega\tau_o}{1 + \omega^2\tau_o^2} \left\{1 - e^{-b/\tau_o} (\cos \omega b + \frac{\sin \omega b}{\omega\tau}\right\} \ldots\ldots \quad (6.7)$$

Inspection of Eq. (6.4) shows that the peak shifts to lower frequencies as (aω) increases. On the other hand, Eq. (6.7) indicates that distortion increasing and the peak shifting to high frequencies as (bω) becomes smaller. This is in agreement with the experimental results. To be more precise, let us examine the results obtained, at 40°C, from both methods. Table (5.5) shows that; the resultant peaks, in the measurements taken with both methods, occur at frequencies 1.14×10^{-2} Hz and 1.62×10^{-2} Hz, respectively. The reasons for this difference are i) in the step-function measurement the sampling of the data was delayed 1 sec after the applying of the step-function ii) the sampling rate(1 HZ) used in the non-causal measurement was higher than that ($\frac{1}{2}$ Hz) used in the step-function method and hence the time range (b) was shorter. Therefore the delay process does more than simply eliminating the high frequency components in the dielectric response. It introduces errors of different amount (i.e. depending on the amount of the transient censored from the beginning which is arbitray and variable) in the dielectric measurements by a) shifting the peaks associated with maximum loss in the dielectric measurements to lower frequencies and b) reducing the magnitude of ε' and ε'' values (see App. F).

In assessing former methods it is necessary to bear in mind:

a. The necessity of employing the delay process in the step-function technique to avoid problems arising from the dominating effect of the high-frequency dielectric response (see Chapter 5).

b. The need for utilising of the crude approximation (Hamon's) in the absence of the digital computer, which besides its restricted regime of validity and ill-defined accuracy, has the disadvantage that it yields independently only the imaginary part of the response.

c. The need to employ a different method, for measurements above 1 Hz, from the d.c. method (step) which does not produce reliable results above the 10 Hz.

d. The including of energy losses due to another processes with the one due to dielectric relaxation in the a.c. method technique which, besides its disadvantage of being time consuming, does not produce reliable results below 1 Hz.

In contrast the non-causal method has the advantage of being;

1. Fast, economic and accurate (see Chapter 1).

2. Very suitable for the on-line computer technique (see Chapter 5).

3. Having a dielectric response containing only these frequencies present in the applied input function (filter step-response) hence, the delay process is not required and then the errors associated with it will be eliminated.

4. Capable of covering a wide range of frequency and hence measurements over a wide range of temperature could be taken.

5. Capable of producing the real and the imaginary parts of the dielectric response.

Therefore, in view of the above desirable features characterising

the non-causal method, it becomes worthwhile to devise a special instrument working on the same basis to perform dielectric measurements.

This digital instrument (i.e. Microprocessor computer) connected together with;

1. Test-cell
2. Fast Amplifier

and a number of peripherals such as ;

1. A/D converter
2. D/A converter
3. Real time clock
4. Floppy disc
5. Paper tape reader
6. V.D.U.
7. Plotter

will produce a powerful instrument to perform the dielectric measurements. The F100-L microprocessor computer which is becoming available now has the advantage of being; (a) real-time system (b) having 16 bit word length (c) having 32 K address range (d) encapsulated in a single 40-pin Dual-in-line package (e) requiring a single 5 volts supply only (f) having a general purpose an Interface Set of three LSI chips which replaces the large amounts of TTL circuits that are often required for interfacing to other microprocessor and the most important that (g) having a special processing unit to perform the F.F.T. Thus, F100-L seems to be suitable for this purpose. Fig. (6.1) shows the configuration of the new instrument to perform the dielectric measurements.

6.2. Results Analysis:-

Generally, in polar polymers, two or three

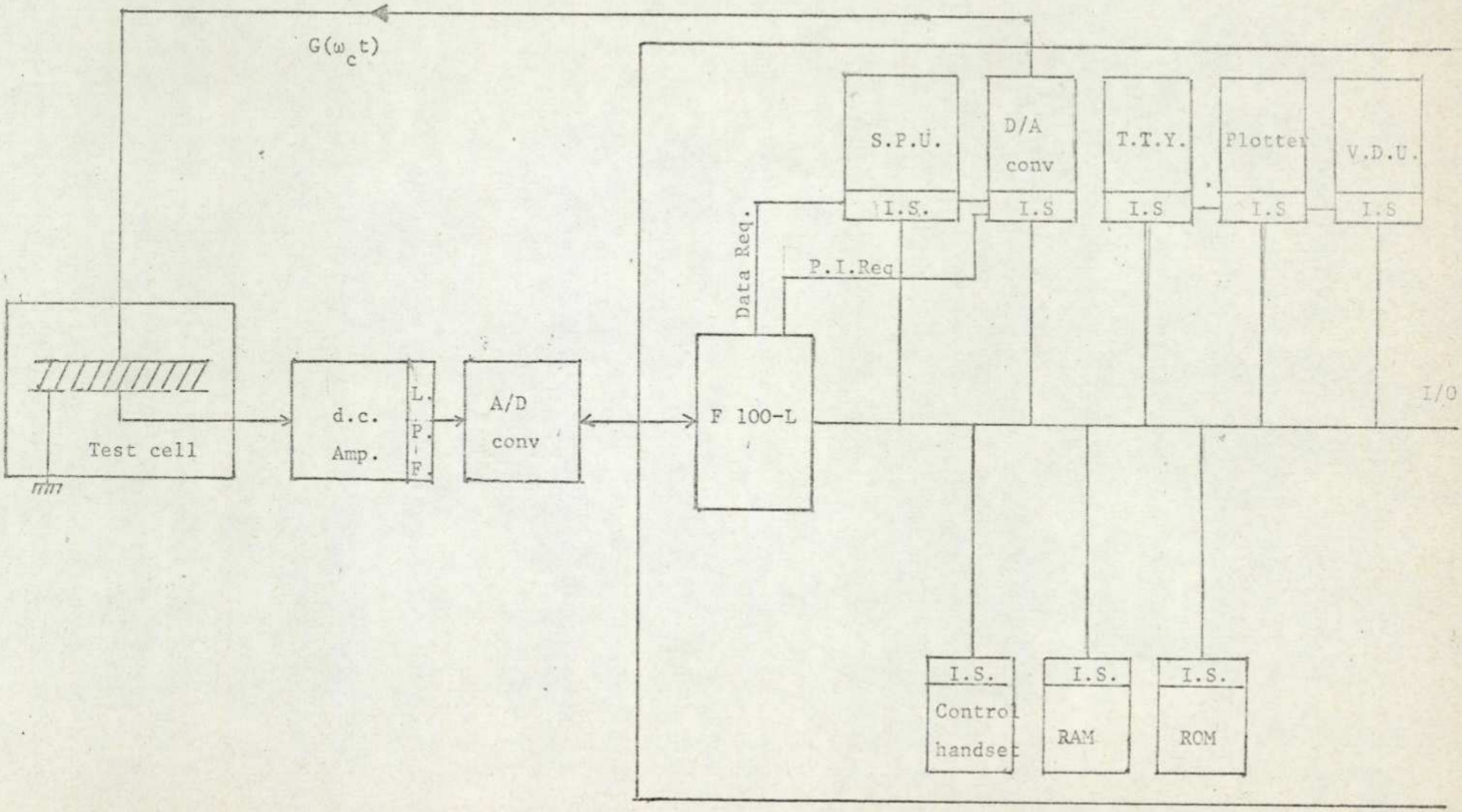

Fig. (6.1):- The new digital instrument for dielectric measurements.

dielectric absorption (dispersion) processes are observed, when measured over the wide temperature range. The dielectric absorption process observed in the present study is only that which can be observed at temperatures above T_g and is due to the orientation of polar segments of main chains (see Chapter 2).

We shall discuss the properties of the dielectric, PVAc, α-absorption in the following points:-

1) Determination of average relaxation time:-

An example of the experimental results is shown in Fig's (5.16) and (5.26) where the dielectric absorption curves are obtained over fairly wide range of frequency and the loss peaks are clearly observed. The relaxation time (τ) was calculated from the following relation

$$\tau = \frac{1}{2\pi f_m} \qquad \ldots\ldots\ldots\ldots\ldots\ldots \quad (6.8)$$

where f_m is the frequency at which the loss maximum occurs. The absorption curves are rather fairly flatter than the Debye absorption curve (for single relaxation time system, see Fig. 2.4). The broadening of the absorption curves can be related to the distribution of the relaxation times. Hence, the relaxation time obtained from Eq.(6.8) should be called the average relaxation time.

2) Apparent activation energy:-

To examine the temperature dependence of τ, it is generally assumed, see Chapter 2, that this temperature dependence of experimental relaxation (τ) to take the Arrhenius form ; $\tau = A \exp(\Delta H/RT)$, where ΔH is apparent activation energy for the dielectric process and T is the absolute temperature. If the relaxation times are measured over a wide range of temperature, however, plot of

log τ against 1/T gives rise to a straight line and ΔH is determined from its slope. In the present study, however, the temperature dependence of τ for the polymer system (PVAc) is not ruled by the Arrhenius equation, i.e. plot of log f_m against 1/T is non-linear (Fig.6.2). Hence ΔH should be derived by tangents at various temperatures on this plot and increases with decreasing temperature. In the range of high temperature and short relaxation time, the change of ΔH with temperature seems to be slow and ΔH can be taken as constant (i.e. 26.5 k cal/mol)

3. Distribution of the relaxation Time ;-

The dependence of ΔH on the temperature, Fig. (6.2), has been reported by many workers. Ferry and his collaborators (1962) found that, the Arrhenius equation in the form

$$\ln a_T = \frac{\Delta H}{R}\left(\frac{1}{T} - \frac{1}{T_o}\right) \quad \ldots\ldots\ldots\ldots \quad (6.9)$$

where a_T is the ratio of the relaxation time at temperature T ~~to~~ that at temperature T_o, is usually applicable to relaxation in polymers occuring at temperature below the glass transition (β and γ relaxations). On the other hand they found that; for the great majority of relaxations, ln a_T is a simple function of T and the Williams, Landel and Ferry (WLF) semi-empirical relationship, see below Eq. (6.10), is nearly always applicable to the glass-rubber relaxation of amorphous polymers. This relaxation is:

$$\text{Log } a_T = - \frac{C_1 (T - T_g)}{C_2 + T - T_g} \quad \ldots\ldots\ldots\ldots \quad (6.10)$$

where a_T is the ratio of the relaxation time at temperature T to that at the glass temperature T_g.

To determine the values of the parameter C_1 and C_2 in WLF-equation,

Fig. (6.2): The frequency-temperature locations of dielectric loss maxima for the α-relaxation of PVAc.

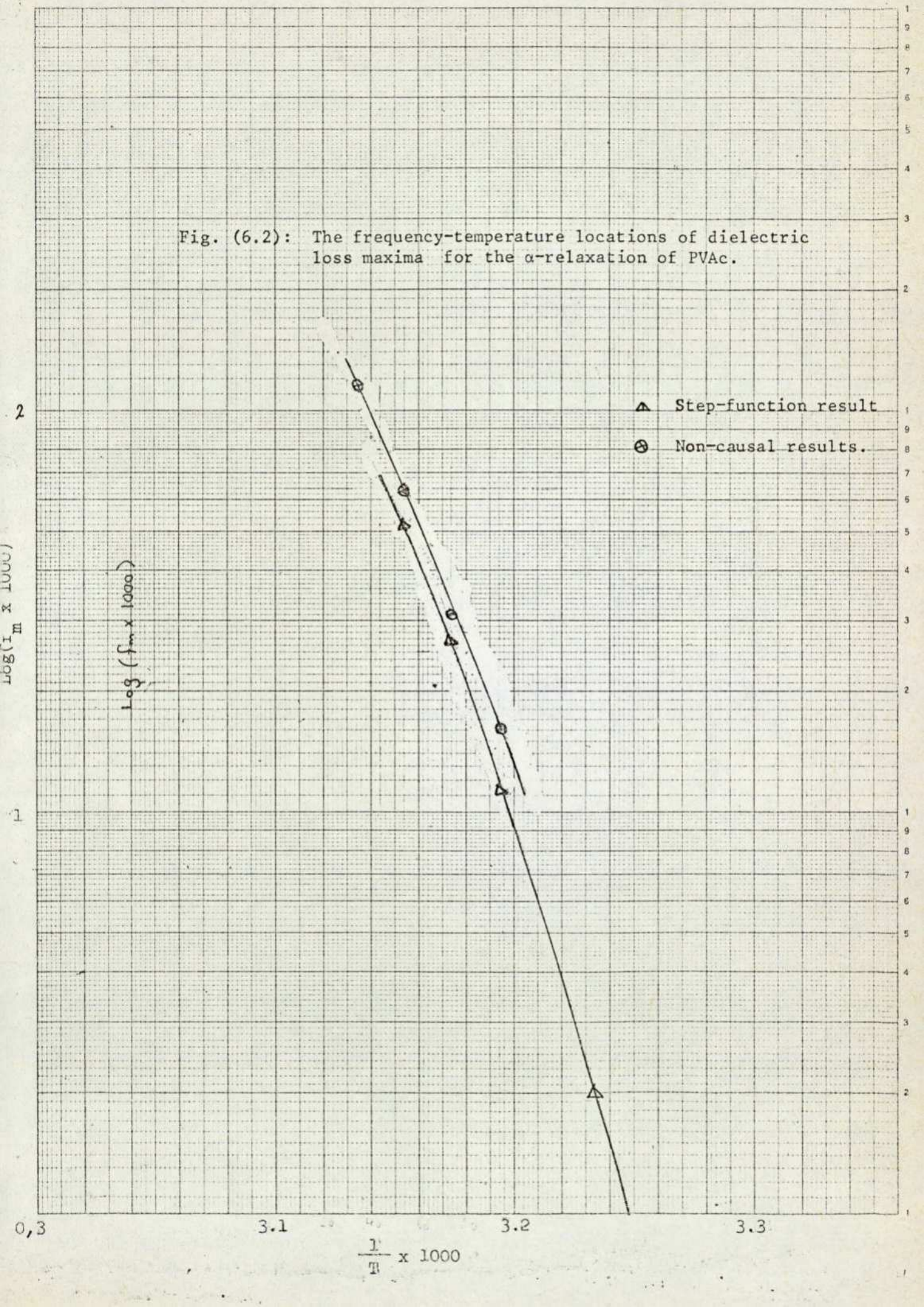

it is required to plot $(T - T_g)/\log (\tau/\tau_g)$ against $T - T_g$ (William's 1955). If the temperature dependence of τ is ruled by WLF equation, this plot gives straight line from which the values of C_1 and C_2 can be calculated. Unfortunately the value of τ_g is too large to determine experimentally for the polymer (PVAc), being under test in this study. Henc τ_g has to be assumed and given a value which gives the best straight line. Graphically, this means that the curve of (i.e. $\varepsilon''/\varepsilon''_m$ against $\log f/f_m$) at T can be superposed upon the curve T_g by a horizontal shift along the log t-axis equal to $\log a_T$. This method is called "reduced variable method" (r.v.m.).

However, owing to the difficulty in estimating the value of τ_g and because, in the present work, the values of τ are determined experimentaly over a fairly wide range of temperature, the r.v.m. is not required. Nevertheless, it is interesting to examine the change of distribution with temperature, because it is important to decide whether the (r.v.m.) is valid or not in case of dielectric properties. This can be done by comparing the curves obtained by plots of the normalized loss against logarithm of reduced frequency (f/f_m) at various temperatures. This is illustrated in Fig. (6.3). It should be noted that in Fig. (6.3);

a. The method of reduced variables appears to be valid since the half-widths (loss peak distribution) seem to be identical for the three results taken at different temperatures (44, 42, and 40°C). It is also, clear that the points of these different measurements lie in one curve, the solid one. This in consistent with the results, Fig. (5.16) and (5.26), where the ε'' curves were seen to shift to higher frequency as the temperature increaed but their shapes did not change.

b. The experimental curves seems slightly non-symmetrical

Fig. (6.3): Dielectric absorption curve for PVAc.

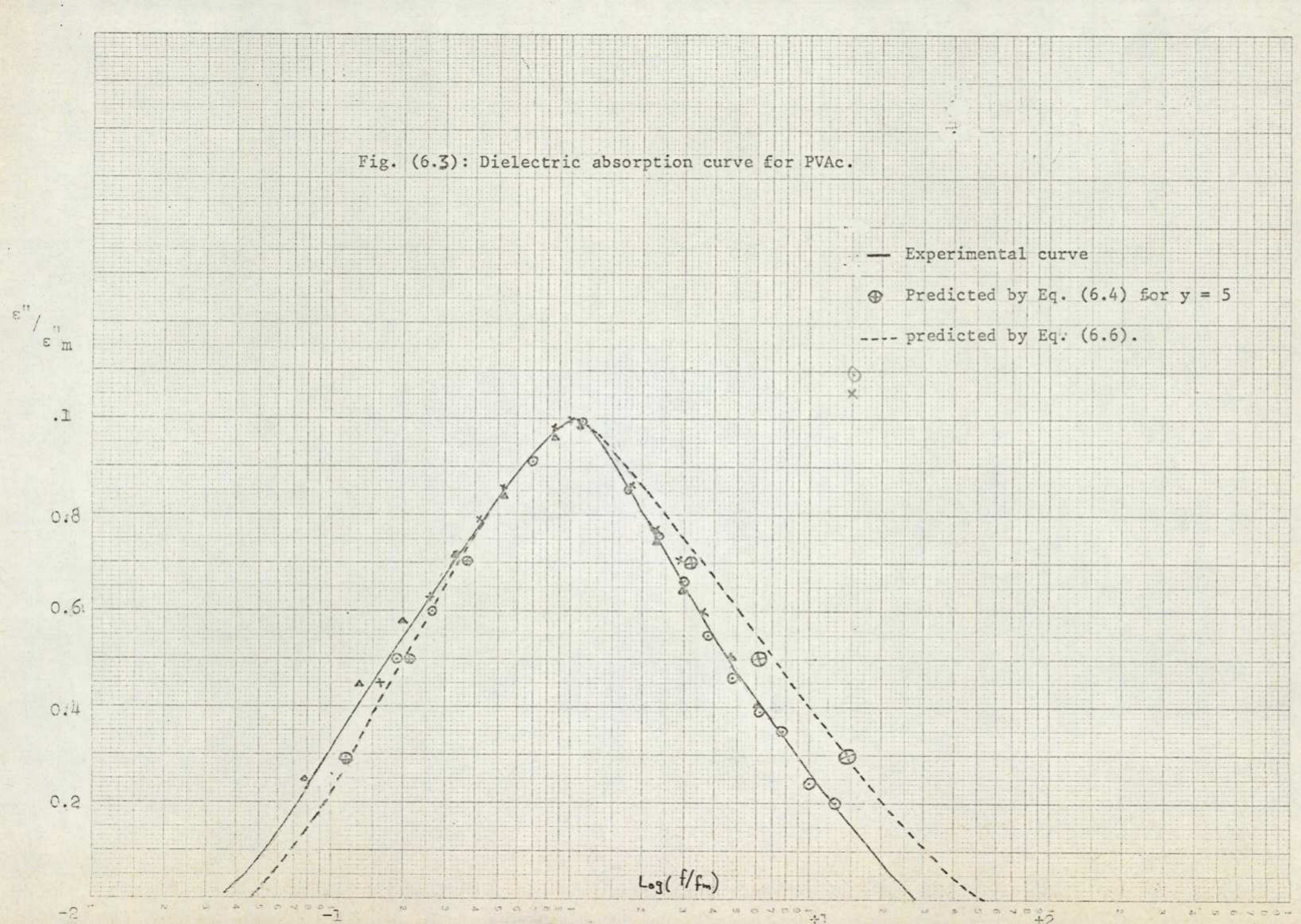

being broader on the low-frequency side. This is in agreement with Fig. (6.2) where the temperature dependence of τ is not ruled by the Arrhenius equation.

c. The experimental curve seems to be in fair agreement with the theoretical curves predicted by the theory of Yamafuji and Ishida (1962). This theory treats the dielectric α-relaxation in terms of the co-operative rotational motions of dipolar groups with the main chain.

Yamafuji and Ishida obtained an expression for ε^* of the following form;

$$\varepsilon^* = \varepsilon' - j\varepsilon'' = \left[(1 + j\omega\tau_o Y)\ (1 + j\omega\tau_o Y^{-1})\right]^{-\frac{1}{2}} \quad .... \quad (6.11)$$

where τ_o and Y terms can be found in many text books. The above equation, however, tends to Debye absorbtion curve if Y tends to unity;

$$\varepsilon^* = \frac{1}{1 + j\omega\tau_o} \quad ..... \quad (6.12)$$

In the limit $Y \to \infty$ Eq. (6.4) becomes;

$$\varepsilon^* - j\varepsilon'' = \frac{1}{\left[(1 - \omega^2\tau_o^2) + j\omega\tau_o\right]^{\frac{1}{2}}} \quad ..... \quad (6.13)$$

For the special case $\omega^2\tau_o^2 << 1$ this equation is identical with the empirical equation of Davidson and Cole (1941). Hence plots of ε'' or $\varepsilon''/\varepsilon''_m$ against log ω or log ω/ω_m should be non-symmetrical, corresponding to "skewed" Cole-Cole are (1941).

Following William's (1967) the limiting theoretical curve according to Eq. (6.13) is shown in Fig. (6.4) as well as those points (⊕) calculated from Eq. (6.11) using Y value equal to 5. The master curve seems to be identical with both curves but slightly narrower.

d. The Frohlich, Kirkwood and Coworkers theoretical curves were excluded for the following reasons;

i) both curves are symmeterical, different from the slightly non-symmetrical experimental curve.

ii) both theories result in broad half-width curves, especially the one predicated by the barrier theory of Frohlich, different from the experimental one.

iii) the Kirkwood-Fuoss theory also predicts that the "average" relaxation time should be proportional to the average degree of polymerization. This result is not observed for bulk amorphous polymers (William's 1967).

iv) Frohlich's theory is based on the assumption that; each relaxation time is given by Arrhenius equation, where Fig. (6.2) shows this is not true and ΔH is found to be a function of temperature.

e. In non-causal dielectric measurements the ratio f_s/f_c was chosen to be 32 and hence f_c was alway a small fraction. Owing to the sharp character of the filter cut-off frequency, those higher frequency compenents of ε'' were filtered and hence there are not enough points for comparison.

CHAPTER SEVEN.

CONCLUSION

Once a laboratory computer is available, the method described in Chapter (6) can be easily realised and replace the existing ones which are extremely tedious and of questionable accuracy.

It is now possible to carry out dielectric measurements, over a wide range of frequency and temperature, with a simple economical, fast and accurate method.

The automatic obeying of the sampling theorem in this method, using a high ratio of f_s/f_c, and the using of the special unit to perform the F.T. give results without distortions and remove the necessity for putting a lot of effort in programming the computer respectively.

As a result of this work an accurate, portable micro-computer instrument for the measurement of dielectric relaxation has become a practical possibility.

CHAPTER EIGHT.

Suggestion For Further Work.

There is a tremendous scope for further work in this field. Certainly more efforts could be made to perfect the method of an ideal low-pass filter such as :

1. The instrument outlined in the discussion should be built.

2. Employing a falling ideal low-pass filter response, instead of the one being used in this work (rising), to make sure that the measured energy losses are only those due to dielectric relaxation. This could be done by replacing program No. 4 by a new one to instruct the computer: a) to normalize the maximum and minimum values of the filter response to + 10 and 0 volts instead of + 5 and - 5 volts respectively, b) to output the + 10 volts first and proceeding to output the rest values.

3. Delaying the dielectric response sampling a time equal to $1/2f_s$ where f_s is the sampling frequency, after outputing each value of the filter response. This should be done to avoid sampling the high frequency part of the dielectric response resulting from the presence of the stepwise progression in the filter response. This, together with the use of low-pass filter, to filter these dielectric responses, will give less distortion in the results.

4. Increasing the ratio (f_s/f_c) value by employing small value of x in Equations (4.17) and (4.18) to calculate Si(x). This has the advantage of : a) increasing the sampling rate for each measurement and hence less distortion will be obtained, b) obtaining a smoother filter response (i.e. more steps of lower magnitude in a given interval).

Now, considering the measurements in general, once the instrument is constructed it would be a simple matter to study dielectric relaxation

in other polymers and over an increased range of temperature. This could be easily done since the value of the filter cut-off frequency is determined by the selected value of the sampling frequency and thus any range of frequency could be covered within the limitations of processing speed.

Also an investigation into the effect of plasticisers and other additives on the dielectric properties of polymers could be profitable, since there is plenty of previous work available for comparison of results.

An ultimate objective might be to use the computer on-line technique to draw:

1. Contour maps as produced by Reddish (1951), which showed dielectric permittivity as a function of frequency and temperature. A Countour map is a very efficient way of displaying these results, since dielectric behaviour over a wide range of temperature and frequency can be read at glance.

2. Cole-Cole arc (i.e. ε' versue ε'')

3. The normalized values of ε'' (i.e. $\varepsilon''/\varepsilon''_m$) versue log (f/f_m).

However, if computer can produce the above plots, it will confirm this as a most useful and powerful method of analysing dielectric properties, and the manipulation of the data enquires would represent a comparitively simple exercise in software generation.

CHAPTER NINE.

References and Bibliography

1. Anderson, J.C. (1964) "Dielectrics". Chapman and Hall Ltd. London.

2. Arthur, F.K.P. (1968) "Fundamentals Of Electricity And Magnetism" Routhedge and Kegan Pual Ltd. London.

3. Baird. M.E. (1968), Rev. Mod. Phy., Vol. 40, No. 1 p. 219.

4. Bottcher, C.J. (1952) "Theory Of Electric Polarization" Elsevier Publishing Company, Amsterdam.

5. Bouvier, B. (1970) "Dielectric Materials, Measurement and Application" I.E.E. Conf. Publ. No. 67, p. 328.

6. Boyed, R.H. (1959), J. Che. Phys., 30, p. 1276.
Brigham, E. (1974) "Fast Fourier Transform" Pentics-Hall.

7. Broens, O and Muller, F.H. (1955), Kolloid . Z., 140 p. 121; 141 p. 20; ibid, 141 p. 20.

8. Brophy, J. (1966) "Basic Electronics For Scientists" McGraw-Hill Book Company, New YOrk.

9. Cath, P. G and Peabody, A.M. (1971), Anal. Chem, 91A p. 43.

10. Churcher, B.G. and Bannott, C. (1926), World Power, Vol. 5 p. 282.

11. Cole, R.S. and Cole, R.H. (1942), J.Chem. Phy, Vol. 10 p. 98; Vol. 9 p. 341 (1941).

12. Crapnell, T.A. and Richmond, E.I. (1969),J.I.E.E., Vol. 37, No. 6.

13. Curtis, A.J. (1961), J. Res. Nat. Bur. Stand, 65A, No. 3 p. 185.

14. Daniel, V.V. (1967) "Dielectric Relaxation" Academic Press. New York.

15. Davies, M. (1969) "Dielectric Properties and Molecular Behaviour" Chapter 5, Van Nostrand Reinhold Company, London.

16. Davies, M. and Edwards, A. (1967), Trans Faraday. Soc, 63 p. 2163.

17. Deloor, G.P. (1956) "Dielectric Properties of Heterogeneous Mixtures" Thesis, Leiden.

18. Deutsch, K. Reddis, W. and Hoff, E.A. (1954), J. Polym. Sci, 13 p. 565.

19. Davidson, D.W., Auty, R.P. and Cole, R.H. (1951), Rev. Instrum, Vol. 22 p. 678.

20. Evison, J. (1975) "Analysis of Stimulated Current Transients In Dielectrics, With The Use of An On Line Computer." Ph.D Thesis, The City University.

21. Frohlich, H. (1949) "Theory Of Dielectrics" Oxford University Press, London.

22. Fuoss, R. and Kirkwood, J.G. (1941), J. Am. Chem. Soc., 63 p. 385.

23. Fouss, R. (1941), ibid, 63 p. 369 and 378.

24. Gall, W.G. and McCrum, N.G. (1961), J. Polymer Sci., 50 p. 489.

25. Glasston, S., Laidler, K.J. and Eyring, H. (1941) "The Theory of Rate Processes" McGraw Hill. New York, Chap. IX.

26. Gross, B. (1941), Phy. Rev., Vol. 59 p 748.

27. Hamon , B.V. (1952), Proc. Instn. Elect. Engrs, Vol. 99 p.115, Part IV, Monograph 27.

28. Harrop, P.J. (1972). "Dielectrics" Butterworths, London.

29. Hartshorn, L. (1954) "The Insulation of Electric Equipment" Chapman and Hall, London.

30. Havrenek, A. and Bakule, R. (1967), J. Polymer. Sci., Vol. C, No. 16 (1) p. 351.

31. Hendus, H., Schnell, G., Thurn, H. and Wolf, K. (1959), Ergebn. Exakt. Naturwiss, 31 p. 220.

32. Hill, N., Vaughan, W.E., Price, A.H. and Davies, H. (1969) "Dielectric Properties and Molecular Behaviour" Van Nostrand Reinhold Company, London.

33. Hodgman, CH. D., Weast, R.C. and Selry, S.M. (1958) "Handbook of Chemistry and Physics" Rubber Pub. Co. Cleveland.

34. Hopkinson, J. (1901) "Original Papers" Vol. 2 p. 199. Cambridge University. Press. London.

35. Hyde, P.J. (1970), Proc. IEE, Vol. 117, No. 9 p. 1891.

36. Ishida, Y. and Yamafuji, K. (1961), Kolloid. Z., 177 p. 97.

37. Ishida, Y., Yamafuji, K., Ito, H. and Takayanagi, M (1962), Kolloid. Z, UZ, Polym, 184 p 97.

38. Ishida, Y. and Matsuo, M. (1964), Kolloid. Z., 199 p. 70.

39. Jackson, W. and Forsyth, J.S.A. (1945), J.I.E.E, 92,3 p. 23.

40. Jones, H.J. (1971) "Digital Processing Of Analogue Signal (Software) Using A Ferranti FM 1600 B Computer. Special Project, City University.

41. Kabalyan, Yu. K., Bagdasaryan, R.V. and Melkonyan, R.V. (1966), Arm. Ktim. Zh., 19, 12 p. 909.

42. Keithly Instrument (1972) "Electrometer Measurements".

43. Kendal, B.R.F. and Zabielski, M.F. (1970), Elect. Lett, 6 p. 776.

44. Kolesov, S.N. (1967), Vvsokomol Soedin, A., 9, 9 p. 1860 ; Polym. Sci. USSR, 9 p. 2098 (1967).

45. Kolesov. S.N. (1967), Izvest. Akad. Nouk, Uzb, USSR, Ser Fiz. Mat. Nauk 11 (4) p. 54.

46. Kolesov, S.N., Vvendenskaya, L.A. and Kheraskov, N. (1967), Plast. Massy. 9 p. 12; Soviet Plastics, 9 p. 15 (1967).

47. Luther, H. and Weisel, G. (1957), Kolloid. Z. 154 p. 15.

48. Mason, P. (1964), Polymer, 5 p. 625.

49. Martin, J. "Programming Real - Time Computer Systems". Prentice - Hall.

50. McCrum, N.G., Reed, R.E. and Williams, G. (1967), Anelastic and Dielectric Effects In Polymeric Solid" John Wiley, New York.

51. Mikhailov,.G.P. and Edel'nant, M.P. (160), Vysokomal. Soedin, 2 p. 287.

52. Mikhailov, G.P., Labanov, A.M. and Mirkamilov, D.M. (1968), Vysokomal. Soedin, A, 10 p. 826; Polymer. Sci. USSR, 10 p. 959 (1968).

53. Mikhoslov, G.P. and Gotlib, Yu. Ya (1966), Vysokomal. Soedin, 9, A, 9 p. 1967; Polymer. Sci. USSR., 9 p. 2219 (1967).

54. Mikhailov, G.P. and Mirkamlov. D.M. (1966), ibid, 8, 8 p. 1351; Polymer. Sci. USSR, 8, 8 p. 1483 (1966).

55. Moorhouse, R. (1971) "FM 1600B Software". Special Project Report, City University.

56. Paul, M. (173) "Signals, Systems, and the Computer." Intext Educational Publishers, New York.

57. Pelzer, H. and Wingner, E. (1932), Z. Phys. Chem., B, 15 p. 445.

58. Perrin, F. (1934), J. Phys. Radium, 5, p. 497.

59. Praglin, I. and Nichols, W.A. (1960), Proc. I.R.E., 48 p. 771.

60. Preseley, S.P. (1966), Rev. Sci. Inst., 37 p. 643.

61. Provisional Fixpac Manual, Ferranti Ltd., Digital System Depart.

62. Oakes, W.G. and Robinson, D.W. (1954), J.Polym. Sci., 14 p. 505.

63. Reddish, W. (1951), Trans. Faraday. Soc., 46 p. 459; Soc. Chem. Ind, Monograph No. 5 p. 138 (1959).

64. Reddish, Bishop, Buckingham and Hyde, (1971), Proc. IEE, Vol. 118, No.1.

65. Reynolds. J.A. (1955) "The Dielectric Constants Of Mixtures" Thesis, London.

66. Roberts, S. (1966). Report No.66 - C - 333, "General Electric Research and Development Centre" Schenectady. New York.

67. Rhodes, G. M. (1971) "Laben 1024 Channel Pulse Height Analyser (Correlation)". FM1600B Computer Peripheral Equipment Guide, City University.

68. Saito, S.S. and Nakajima, T. (1957), Bull. Electroleh.Lab (Japan) 21 p. 16; Kolloid-Zeitschrift and Zeitschrift, Vol. 189 p. 116 (1963).

69. Schallamach, A. and Thirion, P. (1956), Trans. Faraday. Soc, 45 p. 887.

70. Schebier, D.J. and Mead, D.J. (1957), J. Chem. Phys., 27 p. 326.

71. Schebier, D.J. (1961), J. Res. Natn. Bur. Stand, Vol. 65C p. 23.

72. Schmieder, K. and Wolf, K. (1953), Kolloid. Z., 134 p. 149.

73. Scott, A. and Harr's, W. (1961), J. Rev. Nat. Bureau of Standard, Vol. 65C, p. 181.

74. Sillars, R.W. (1973) "Electrical Insulating Materials and Their Applications" I.E.E. Publication, London.

75. Smyth, C.P. (1955) "Dielectric Behavior and Structur" McGraw. Hill Book Company, Inc. New York.

76. Spreadbury, D. (1971) "Computer Real-Time Clock" Special Project, City University.

77. Van Beck, L.K.H. (1967), Progress in Dielectric, 7 p. 69.

78. Van Turnhout, J. (1975) "Thermally Stimulated Discharge of Polymer Electrets" Amsterdam, Elsevier.

79. Von Hippel, A.R. (1954) "Dielectric and Waves" John Wiley and Sons, London; "Dielectric Materials and Applications" Chapman and Hall, London. (1958).

80. Wada, Y and Yamomoto, K. (1956), J. Phys. Soc. Japan, 11 p. 887.

81. Weingarten, I. R. (1955), Rep. Conf. Elect. Insut, p. 53.

82. Wilding, P.J. (1974) "Computer Aided Measurement of Low Frequency Dielectric Relaxation In Polymeric Solids" B.Sc. Project, City University, London.

83. Williams, G. (1963), Polymer, Vol. 4 p. 27; Faraday. Soc. Vol. 58 p. 1041 (1962); Trans. Faraday. Soc, 60 p. 1556 (1964).

84. Wurstlin, F. (1953), Kolloid, Z., 120 p. 84; 34 p. 135 (1953 ; ibid, 113 p. 18 (1949)).

85. Yamafuji, K. (1960), J. Phys. Soc. Japan, 15 p.2295.

86. Zaky, A.A. (1970) "Dielectric Solids" Routhedge and Kegan Paul Ltd. London.

APPENDICES

Appendix A

A - 1 Fourier Transform (F.T)

Basic F.T. Analysis:-

The essence of the F.T of a waveform is to decompose or separate the waveform into a sum of sinusoids of different frequencies. If these sinsoids sum to the original waveform then we have determined the F.T of the waveform. The pictoral representation of the F.T is a diagram which displays the amplitude and frequency of each of the determined sinusoids.

The F.T identifies or distinguishes the different frequency sinusoids (and their respective amplitudes) which combine to form an arbitrary waveform. Mathematically, this relationship is stated as

$$H(j\omega) = \int_{-\infty}^{\infty} h(t)\, e^{-j\omega t}\, dt \qquad \ldots\ldots\ldots \qquad (A.1)$$

where h(t) is the waveform to be decomposed into a sum of sinusoids, $H(j\omega)$ is the F.T of h(t).

However, if the waveform h(t) is not periodic then the F.T will be a continuous function of frequency; that is, h(t) is represented by the summation of sinusoids of all frequencies. The F.T is then a frequency domain representation of a function contains exactly the same information, as that of the original function in the time domian; they differ only in the manner of presentation of the information.

The Fourier Integral :-

Consider a pair of relations called the fourier transform pair:

$$F(j\omega) = \int_{-\infty}^{\infty} f(t)\, e^{-j\omega t}\, dt \qquad \ldots\ldots\ldots \qquad (A.2)$$

$$f(t) = \frac{1}{2\pi} \int_{-\infty}^{\infty} F(j\omega)\, e^{j\omega t}\, dt \quad \ldots\ldots \quad (A.3)$$

The first of these evaluates a frequency sepctrum $F(j\omega)$ from a given function of time $f(t)$. The integrand of equation (A.3) is $F(j\omega)\{\cos \omega t + j \sin \omega t\}$. Hence, equation (A.3) represents $f(t)$ as an infinite sum of frequency component.

In general, $F(j\omega)$ is complex quantity of $j\omega$. It is a sum of real and imaginary terms:

$$F(j\omega) = R(\omega) + jX(\omega) \quad \ldots\ldots\ldots\ldots \quad (A.4)$$

where $R(\omega)$ and $X(\omega)$ are both real functions of ω. Now replace $e^{-j\omega t}$ by Eulers relation in equation (A.2). This yields

$$F(j\omega) = \int_{-\infty}^{\infty} f(t)\, (\cos \omega t - j \sin \omega t)\, d \quad \ldots\ldots \quad (A.5)$$

Thus

$$R(\omega) = \int_{\infty}^{\infty} f(t) \cos \omega t \, dt \quad \ldots\ldots\ldots\ldots \quad (A.6)$$

$$X(\omega) = \int_{\infty}^{\infty} f(t) \sin \omega t \, dt \quad \ldots\ldots\ldots\ldots \quad (A.7)$$

However, if $f(t)$ is real, then $R(\omega)$ is an even function of ω and $X(\omega)$ is an odd function of ω, such that when ω replaced by $-\omega$ in equations (A.6) & (A.7), $R(\omega)$ remains unchanged while $X(\omega)$ must be replaced by $-X(\omega)$.

A - 2. Convolution

Convolution Integral :-

Convolution of two functions is a significant physical concept in many diverse scientific fields. The convolution of the two functions $f_1(x)$ and $f_2(x)$ is written as $f_1(x) * f_2(x)$ and is

defined by the integral

$$f_1(x) * f_2(x) = \int_{-\infty}^{\infty} f_1(y)\, f_2(x-y)\, dy \quad \ldots\ldots\ldots \quad (A.8)$$

Note that the integrand consists of the product of the first function multiplied by the second which has been reversed in time (note the -y) and time shifted. Note that x is treated as a parameter (constant) in the integration.

If we let $z = x-y$, the convolution becomes

$$f_1(x) * f_2(x) = \int_{-\infty}^{\infty} f_2(z)\, f_1(x-z)\, dz \quad \ldots\ldots\ldots \quad (A.9)$$

Then

$$f_1(x) * f_2(x) = f_2(x) * f_1(x) \quad \ldots\ldots\ldots\ldots \quad (A.10)$$

Thus the order of convolution is unimportant.

Time Convolution Theorem:-

Possibly the most important and powerful tool in modern scientific analysis is the relationship between equation (A.8) and its Fourier transform. This relationship, known as the convolution theorem, allows one the complete freedom to convolve mathematically in the time domain by simple multiplication in the frequency domain. This states that if

$$f_1(t) \leftrightarrow F_1(j\omega) \quad , \quad f_2(t) \leftrightarrow F_2(j\omega)$$

$$f_1(t) * f_2(t) \leftrightarrow F_1(j\omega)\, F_2(j\omega) \quad \ldots\ldots\ldots \quad (A.11)$$

Thus, the Fourier transform of the convolution of two functions of time is the product of their individual transforms. To prove this result

we apply equation (A.2) to the convolution; this yields

$$f_1(t) * f_2(t) \leftrightarrow \int_{-\infty}^{\infty} \left[\int_{-\infty}^{\infty} f_1(x)\, f_2(t - x)\, dx \right] e^{-j\omega t}\, dt \quad \ldots (A.12)$$

Now, assume that $f_1(x)$ and $f_2(x)$ are such that the order of integration can be interchanged; thus:

$$f_1(t) * f_2(t) \leftrightarrow \int_{-\infty}^{\infty} f_1(x) \int_{-\infty}^{\infty} f_2(t - x)\, e^{-j\omega t}\, dt\, dx \ldots . \quad (A.13)$$

By substituting $\delta = t - x$ the term in the brackets becomes

$$\int_{-\infty}^{\infty} f_2(\delta)\, e^{-j\omega(\delta + x)}\, d\delta = e^{-j\omega x} \int_{-\infty}^{\infty} f_2(\delta) e^{-j\delta}\, d\delta$$

$$= F_2(j\omega)\, e^{-j\omega x} \quad \ldots\ldots\ldots \quad (A.14)$$

Equation (A.14) can then be rewritten as

$$f_1(t) * f_2(t) \leftrightarrow \int_{-\infty}^{\infty} f_1(x)\, e^{-j\omega x}\, F_2(j\omega)\, dx \quad \ldots\ldots . \quad (A.15)$$

$$f_1(t) * f_2(t) \leftrightarrow F_1(j\omega)\, F_2(j\omega) \quad \ldots\ldots\ldots\ldots\ldots \quad (A.16a)$$

The converse, such as;

$$f_1(t)\, f_2(t) \leftrightarrow \frac{1}{2\pi}\, F_1(j\omega) * F_2(j\omega) \quad \ldots\ldots\ldots\ldots \quad (A.15b)$$

can be proved similarly.

A-3 Waveform Sampling :-

If the function h(t) is continuous at t = T, then a sample of h(t) at time equal to T is expressed as

$$\hat{h}(t) = h(t)\, \delta(t - T) = h(T)\, \delta(t - T) \quad \ldots\ldots\ldots \quad (A.17)$$

Therefore, if h(t) is continuous at t = nT for n = 0, ± 1, ± 2 .... then

$$\hat{h}(t) = \sum_{n=-\infty}^{\infty} h(nT)\, \delta(t - nT) \qquad \text{.....} \qquad (A.18)$$

is termed the sampled waveform h(t) with sample interval T. Sampled h(t) is then an infinite sequence of equidistant impulses, each of whose amplitude is given by the value of h(t) corresponding to the time of occurrence of the impulse. Figure (A2) illustrates graphically the sampling concept. The sampled function A2(e) is equal to the product of the waveform shown in Fig (A2(a)) and the sequence of impulses $\Delta(t)$ illustrated in Fig (A2(b)). We call $\Delta(t)$ the sampling function; the notation implies an infinite sequence of impulses separated by T. The F.T's of h(t) and $\Delta(t)$ are shown in Fig's (A2(c) and (d)), respectively. From the frequency convolution theorem, the desired F.T is the convolution of the frequency functions illustrated in Fig's (A2(c) and (d)). The F.T of the sampled waveform is then a periodic function where one period is equal, within a constant, to the F.T of the continuous function h(t). This last statement is valid only if the sampling interval T is sufficiently small.

If T is chosen too large, the results shown in Fig (A3) are obtained. Note that as the sample interval T is increased (Fig's A2(b) and A3(b)), the equidistant impulses of $\Delta(j\omega)$ becomes more closely spaced (Fig's A2(d) and A3(d)). Because of the decreased spacing of the frequency impulses, the convolution with the frequency function $H(j\omega)$ results in the overlapping waveform shown in Fig (A3(f)). This distortion of the desired F.T of a sampled function is known as aliasing. As described, aliasing occurs because the time function was not sampled at a sufficient high rate; the sample interval T is too large. An examination of Fig's (A3(c) and (d)) points up the fact that convolution overlap will occur until

Figures removed for copyright reasons

Figure A2 Graphical frequency convolution theorem development of the Fourier transform of a sampled waveform (p. 233)

Figure A3 Aliased Fourier transform of a waveform sampled at an insufficient rate (p. 234)

Figue A4 Graphical derivation of the sampling theorem (p .236)

the separation of the impulses of $\Delta(j\omega)$ is increased to $1/T = 2f_c$, where f_c is the highest frequency component of the F.T of the continuous function h(t).

A.4 Sampling Theorem :-

The sampling theorem states that if the F.T of a function h(t) is zero for all frequencies greater than a certain frequency f_c, then the continuous function h(t) can be uniquely determined from a knowledge of its sampled values,

$$h(t) = h(nT) \sum_{n=-\infty}^{\infty} \delta(t - nT)$$

In particular, h(t) is given by

$$h(t) = T \sum_{n=-\infty}^{\infty} h(nT) \frac{\sin 2\pi f_c(t - nT)}{\pi(t - nT)} \quad \ldots\ldots\ldots \quad (A.19)$$

To construct a proof of the sampling theorem, recall from the discussion on constraints of the theorem that the F.T of the sampled function is identical, within the constant T, to the F.T of the unsampled function, in the frequency range $-f_c \leq f \leq f_c$. From Fig (A2(f)), the F.T. of the sampled time function is given by $H(j\omega) * \Delta(j\omega)$. Hence, as shown in Fig's (A4(a), (b) and (c)), the multiplication of a rectangular frequency function of amplitude T with the F.T of the sampled waveform is the F.T $H(j\omega)$

$$H(j\omega) = |H(j\omega) * \Delta(j\omega)| \, Q(j\omega) \quad \ldots\ldots\ldots\ldots \quad (A.20)$$

The inverse F.T of $H(j\omega)$ is the original waveform h(t) as shown in Fig (A4(f)). But from convolution theorem, h(t) is equal to the convolution of the inverse F.T of $H(j\omega) * \Delta(j\omega)$ and of the rectangular frequency function. Hence, h(t) is given by the convolution of

$h(t)$. $\Delta(t)$ and $q(t)$;

$$h(t) = |h(t)\ \Delta(t)| * q(t)$$

$$= \sum_{n=-\infty}^{\infty} |h(nT)\ \delta(t - nT)| * q(t)$$

$$= \sum_{n=-\infty}^{\infty} h(nT)\ q(t - nT)$$

$$= T \sum_{n=-\infty}^{\infty} h(nT)\ \frac{\sin\left[2\pi f_c(t - nT)\right]}{\pi(t - nT)} \quad \ldots\ (A.21)$$

Equation (A.21) is the desired expression for reconstructing $h(t)$ from a knowledge of only the samples of $h(t)$.

We should note carefully that it is possible to reconstruct a sampled waveform perfectly only if the waveform is band-limited. In practice, this condition rarely exists. The solution is to sample at such a rate that aliasing is negligible; It may be necessary to filter the signal prior to quantization to insure that there exists, to the extent possible, a band-limited function.

A-5 Frequency Sampling Theorem:-

Analogous to time domain sampling there exists a sampling theorem in the frequency domian. If a function $h(t)$ is time-limited, that is

$$h(t) = 0 \quad |t| > T_c$$

then its F.T $h(j\omega)$ can be uniquely determined from equidistant samples of $h(j\omega)$. In particular, $H(j\omega)$ is given by

$$H(j\omega) = \frac{1}{2T_c} \sum_{n=-\infty}^{\infty} H\left(\frac{n}{2T_c}\right) \frac{\sin\left[2\pi\ T_c(f - n/2T_c)\right]}{\pi\ (f - n/2\ T_c)} \quad \ldots\ (A.22)$$

The proof is similar to that of the time domain sampling theorem.

A-6 Discrete Fourier Transform (D.F.T) :-

In evaluating the F.T, $H(j\omega)$, of the function, $h(t)$, we have assumed so far that, the function $h(t)$ is a continuous function of time consisting of an infinite set of points in the time domian. In this section a special case of the continuous F.T which is amenable to machine computation will be developed. The approach will be to develop the D.F.T from a graphical derivation based on continuous F.T theory. To simplify the analysis, we shall calculate the area under the curve, $f(x)$ as shown in Fig (A5), using horizontal and vertical line segments. This figure illustrates

$$\int_{x_a}^{x_b} f(x)\, dx$$

where $x_a = x_o$ and $X_b = X_N$. Now, if $f(x)$ is assumed to be constant at $f(X_k)$ for $X_k \leq X \leq X_{k+1}$; that is

$$f(x) = f(X_k), \quad X_k \leq X \leq X_{k+1}$$

Hence, if the curve is divided into N equal areas

$$\Delta x = \frac{X_b - X_a}{N} = \frac{X_N - X_o}{N}$$

Then the area of the K_{th} rectangle is $f(X_k - 1)\, \Delta x$. Therefore, the approximate form of the integral is given by

$$\int_{x_a}^{x_b} f(x)\, dx = \Delta x \sum_{n=o}^{N-1} f(x_n) \qquad \ldots\ldots\ldots\ldots \qquad (A.23)$$

Applying this to F.T of equation (A.1), we have

$$F(j\omega) = \Delta t \sum_{n=-N/2}^{N/2-1} f(t_n)\, e^{-j\omega t_n} \qquad \ldots\ldots\ldots \qquad (A.24A)$$

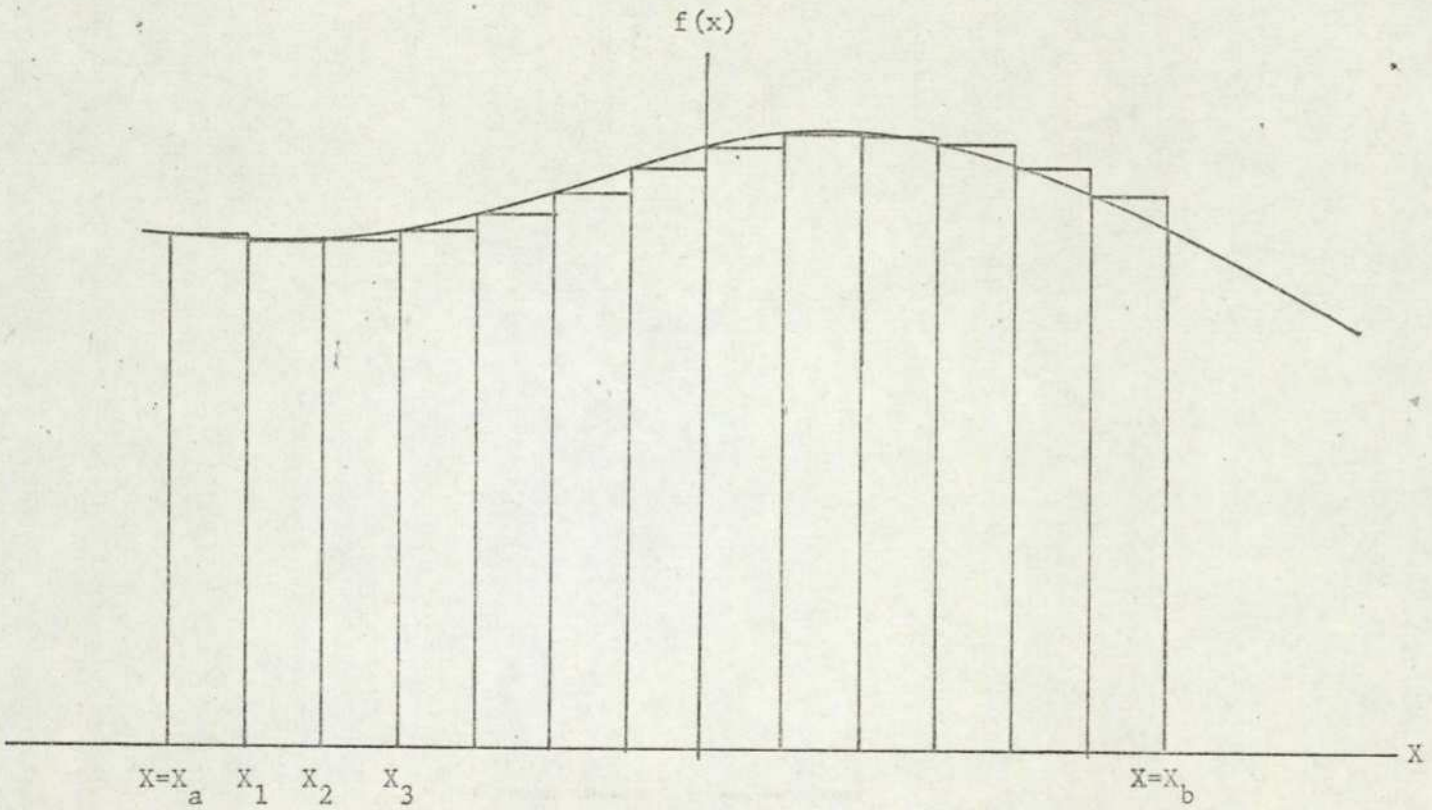

Fig(A5): Approximation to a curve using horizontal and Vertical line segments.

Note that N was chosen as an even number so that we could integrate symmetrically about t = o. For most practical cases, f(t) = o for t < 0. In such cases, we integrate from t = o to t = ∞. Thus, the approximation is of the form.

$$F(j\omega) = \Delta t \sum_{k=o}^{N-1} f(t_k)\, e^{-j\omega t_k} \qquad \ldots\ldots\ldots\ldots \quad (A.24B)$$

proceeding in a similar fashion, we can approximate the inverse F.T of (A.2) by

$$f(t) = \frac{1}{2\pi}\, \Delta\omega \sum_{n=-N/2}^{N/2-1} F(j\omega_n)\, e^{j\omega_n t} \qquad \ldots\ldots\ldots \quad (A.25)$$

where

$$\Delta\omega = \frac{2\omega N/2}{N}$$

Now let us consider a procedure for evaluating equation (A.25). First we shall relate Δt and $\Delta\omega$. Let T be the entire time integrated

$$T = t_N - t_o$$

Hence

$$\Delta t = T/N \qquad \ldots\ldots\ldots\ldots \quad (A.26)$$

We are sampling the signal every Δt seconds. Then, from section (A.4), the maximum bandwidth of the signal ω_a is given by $\pi/\omega_a = \Delta t$ or $\omega_a = \pi/\Delta t$. Since we have chosen N samples in both the time and frequency domains, $\omega_a = \frac{N\Delta\omega}{2}$. Equating these two values of ω_a, we obtain

$$\Delta\omega = \frac{2\pi}{N\Delta t} = \frac{2\pi}{T} \qquad \ldots\ldots\ldots\ldots\ldots \quad (A.27)$$

Substituting equations (A.26) and (A.27) in equations (A.24B) and (A.25), we have

$$F(j\omega_n) = \Delta t \sum_{k=o}^{N-1} f(k\Delta t)\, e^{-2j\pi kn/N}$$

$$f(t_k) = \frac{\Delta\omega}{2\pi} \sum_{n=-N/2}^{N/2-1} F(jk\Delta\omega)\, e^{j2\pi kn/N} \qquad \ldots\ldots\ldots \quad (A.29)$$

where $t_k = k\Delta t$ and $\omega_n = n\Delta\omega$

Making use of the fact that equation (A.28) is periodic in n with period N. we can replace n by n + N and write equation (A.29) as

$$f(t_k) = \frac{\Delta\omega}{2\pi} \left| \sum_{n=o}^{N/2-1} F(jn\Delta\omega)\, e^{j2\pi kn/N} + \sum_{-N/2}^{-1} F(jn\Delta\omega)\, e^{2\pi kn/N} \right|$$

and

$$F\left|j(-\frac{N}{2} + a)\,\Delta\omega\right| = F\left|j(\frac{N}{2} + a)\Delta\omega\right|$$

In addition

$$e^{j2\pi k[-(N/2)+a]/N} = (-1)^k\, e^{j2\pi ka/N} = e^{j2\pi k[(N/2)+a]/N}$$

Thus, the summation from - N/2 to - 1 can be replaced by one from N/2 to N - 1. Hence equation (2.29) can be written as

$$f(t_k) = \frac{\Delta\omega}{2\pi} \sum_{n=o}^{N-1} F(jn\Delta\omega)\, e^{j2\pi kn/N} \qquad \ldots\ldots\ldots\ldots \quad (A.30)$$

For purposes of abbreviation, we use the following notation

$$f_k = \Delta t\, f(k\Delta t), \quad F_n = F(jn\Delta\omega), \quad f'_k = f(k\Delta t) \quad \text{and} \quad F'_n = \frac{\Delta\omega}{2\pi} F_n$$

Substituting in equations (A.28) and (A.30), we obtain

$$F_n = \sum_{k=o}^{N-1} f_k\, \omega^{nk} \qquad \ldots\ldots\ldots\ldots\ldots\ldots \quad (A.31)$$

and

$$f'_k = \sum_{n=o}^{N-1} F'_n\, \omega^{-nk} \qquad \ldots\ldots\ldots\ldots\ldots\ldots \quad (A.32)$$

where $\omega = e^{-j2\pi/N}$.

In general, for all N of F_n, we can write

$$F_o = \omega^{o(o)} f_o + \omega^{o(1)} f_1 + \ldots \omega^{o(N-1)} f_{n-1}$$

$$F_1 = \omega^{1(o)} f_o + \omega^{1(1)} f_1 + \ldots \omega^{1(N-1)} f_{N-1}$$

A.7 Fast Fourier Transform (F.F.T) :-

The procedure which is called the fast fourier transform, was firstly developed by T.W. Cooley and J.W. Tukey, (1965) to reduce the amount of computation involved in evaluating the D.F.T. and thus, results in a great saving in the computation time. It is also, sometimes called the Cooley - Tukey algorithm.

To use the F.F.T., only certain discrete values of N, the total number of samples will be allowed. This is done to make the computation simpler. In general, N should be an integral power of 2.

$$N = 2^r \qquad \ldots\ldots\ldots\ldots\ldots \qquad (A.33)$$

where r is an integer. Now, consider D.F.T's for two functions. The first is for a set of N/2 samples which consist of f_k for all even values of K. The second transform is a set of N/2 samples which consist of f_k for all odd values of k. let

$$g_k = f_{2k} \qquad \ldots\ldots\ldots\ldots\ldots \qquad (A.34)$$

and

$$h_k = f_{2k+1}, \quad k = o,1 \ldots = \frac{N}{2} - 1 \ldots\ldots\ldots \qquad (A.35)$$

Then g_k corresponds to f_k for all even values of k and h_k corresponds to f_k for all odd values of f_k. The D.F.T's of g_k and h_x are given, see equation (A.31), by

$$G_n = \sum_{k=o}^{(N/2)-1} g_k \, e^{-j(4\pi/N)nk} \qquad \ldots\ldots\ldots\ldots \quad (A.36)$$

$$H_n = \sum_{k=o}^{(N/2)-1} h_k \, e^{-j(4\pi/N)nk} \qquad n = o,1 \ldots., \frac{N}{2} - 1 \ldots.. (A.37)$$

Note that $4\pi/N$ rather than $2\pi/N$ appears in the exponent since N is replaced by N/2 in each of these summations. Also note that since g_k has only half of the number of sample points G_n can only be evaluated for N/2 values. A similar statement can be made for h_k and H_n. Now, let us write F_n in terms of G_n and H_n, such that

$$F_n = \sum_{k=o}^{(N/2)-1} g_k \, e^{-j(2\pi/N)2nk} + \sum_{k=o}^{(N/2)-1} h_k \, e^{-j(2\pi/N)(2k+1)n} \ldots (A.38)$$

Comparing this with equations (A.36) and (A.37), we have

$$F_n = G_n + e^{-j(2\pi/N)n} H_n, \quad n = o,1, \ldots., \frac{N}{2} - 1 \ldots\ldots\ldots (A.39)$$

F_n is periodic, hence, G_n and H_n will themselves be periodic with period N/2, hence,

$$G_{(N/2)+n} = G_n \qquad \ldots\ldots\ldots\ldots\ldots\ldots \quad (A.40)$$

$$H_{(N/2)+n} = H_n \qquad \ldots\ldots\ldots\ldots\ldots\ldots \quad (A.41)$$

Then substituting in equation (A.38), we have

$$F_{(N/2)+n} = G_n + e^{-j(2\pi/N)[(N/2)+n]} H_n$$

or

$$F_{(N/2)+n} = G_n - e^{-j(2\pi/N)n} H_n$$

Substituting equation (A.31), we obtain

$$F_n = G_n + \omega^n H_n, \quad n = o,1, \ldots, \frac{N}{2} - 1 \quad \ldots\ldots\ldots \quad (A.42)$$

$$F_{(N/2)+n} = G_n - \omega^n H_n, \quad \frac{N}{2} + n = \frac{N}{2}, \ldots. \quad N - 1 \ldots. \quad (A.43)$$

Note that $\omega^{[r + (N/2)]} = - \omega^r$ ..... (A.44)

Thus, using equations (A.40) and (A.44), equations (A.42) and (A.43) can be written as

$$F_n = G_n + \omega^n H_n, \quad n = o,1, \ldots, n - 1 \quad \ldots\ldots\ldots \quad (A.45)$$

Equation (A.45) indicates that the D.F.T can be expressed, using N samples, in terms of two D.F.T's using N/2 samples each. The advantage of doing this is, if N samples are used, in general, on the order of N^2 arithmetic operation are required to evaluate the D.F.T. Thus, to evaluate both G_n and H_n, $2(\frac{N}{2})^2 = \frac{N^2}{2}$ operations are required therefore, both of these transforms can be evaluated using half the operation needed to evaluate F_n. In general 2N operations (multiplication and addition) are required to obtain F_n from G_n and H_n. However $\frac{N^2}{2} + 2N$ is usually much less than N^2 when N is large.

The number of operations can still be greatly reduced remembering that G_n and H_n, each of them is the D.F.T of g_n and h_n, respectively. Each of these D.F.T's can be split into a sum of two transforms corresponding to N/4 samples. Similarly each of these transforms can be split into two D.F.T.'s each corresponding to N/8 samples each. (This is why N is chosen equal to 2^r.) This operation can be repeated until the transform of a one-point function is taken. (The D.F.T of a one-point function is the function itself). This complete operation is the F.F.T. in general it can be shown that $\frac{3}{2}$ N $\log_2$ N arithmetic operations are required in F.F.T. while N^2 are required in the D.F.T. This represents a saving of (1.5 Log_2 N)/N and for large N, this can be substantial.

Appendix B

Linear Time System

A linear System is one whose output, due to a sum of (sets of) inputs, is the sum of the outputs resulting when each (set of) input(s) acts separately. Such a system is said to satisfy the principle of superposition.

B-1 Linear System Response; Relation To Transfer Function, Inpulse Response:-

Assume we are dealing with a linear system, shown in Fig (B1), which has a single input f(t) and whose response to it is g(t), such that;

$$T\{f(t)\} = g(t) \qquad \ldots\ldots\ldots\ldots \qquad (B.1)$$

Now suppose that the input signal is a very specific one; the unit impulse $\delta(t)$ and if its response to it is h(t) then

$$T\{\delta(t)\} = h(t) \qquad \ldots\ldots\ldots\ldots \qquad (B.2)$$

Assume that the F.T's of h(t), f(t) and g(t) exist and are given by

$$\begin{aligned} h(t) &\leftrightarrow H(j\omega) = 1 \\ f(t) &\leftrightarrow F(j\omega) \\ g(t) &\leftrightarrow G(j\omega) \end{aligned} \qquad \ldots\ldots\ldots\ldots \qquad (B.3)$$

Making use of $g(t) = \int_{-\infty}^{\infty} f(y)\, h(t - y)\, dy$ and using equation (A.16), we can write;

$$G(j\omega) = H(j\omega)\, F(j\omega)$$

or, equivalently,

$$H(j\omega) = G(j\omega)/F(j\omega) \qquad \ldots\ldots\ldots\ldots \qquad (B.4)$$

Thus, the F.T of the output of a system is the F.T of the impulse

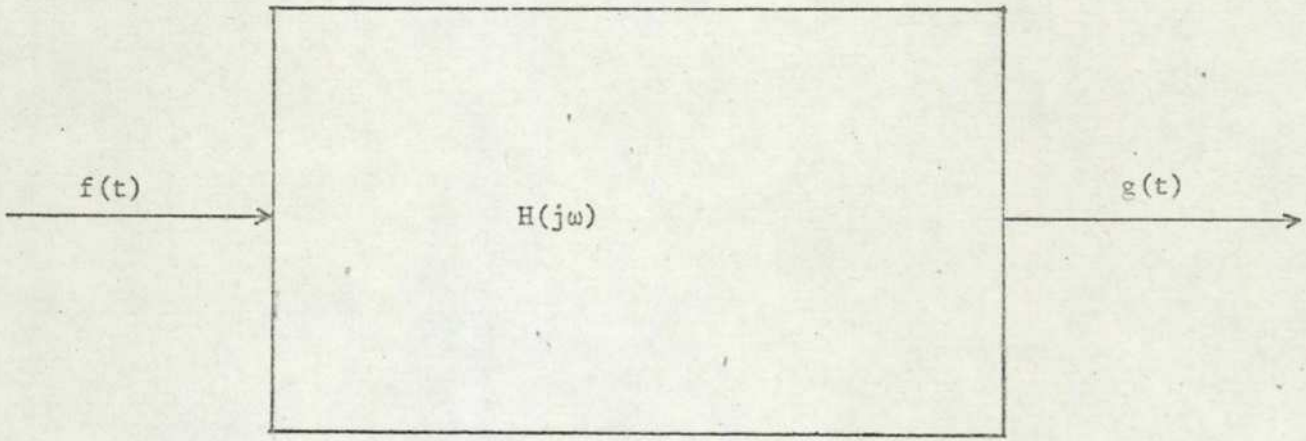

Fig. (B.1): System whose transfer function is H(jω).

response times the F.T of the input and the F.T of the response to a unit impulse is the transfer function.

B-2 Relation Between The Unit Impulse And Unit Step Responses:-

In general, for a linear, time-invariant system, if we know the unit impulse response, the unit step response, or the response to an arbitrary signal whose Fourier spectrum is not zero for any value of ω, one can find the response to any arbitrary signal. For example equation (B.4) can be used to obtain the transfer function $H(j\omega)$ if the Fourier spectrum of the input and output signals are known.

We have also expressed $g(t)$, the response of a system to an input signal $f(t)$ in terms of the impulse response $h(t)$. This relation is (see equation (A.8))

$$g(t) = \int_{-\infty}^{\infty} f(y)\, h(t - y)\, dy \quad \ldots\ldots\ldots \quad (B.5)$$

Consequently, if the response of the system to the unit step function, $U(t)$;

$$U(t) = \begin{cases} 1 & \text{for } t > 0 \\ 0 & \text{for } t > 0 \end{cases} \quad \ldots\ldots\ldots \quad (B.6)$$

is $a(t)$, then we can write from equation (B.5)

$$a(t) = \int_{-\infty}^{\infty} U(y)\, h(t - y)\, dy \quad \ldots\ldots\ldots \quad (B.7)$$

or, equivalently, see equation (A.10)

$$a(t) = \int_{-\infty}^{\infty} h(t)\, U(t - y)\, dy \quad \ldots\ldots\ldots \quad (B.8)$$

However, $U(t - y) = 0$ for $y > t$ and $U(t - y) = 1$ for $y < t$,

hence

$$a(t) = \int_0^t h(y)\ dy \qquad \ldots\ldots\ldots \qquad (B.9)$$

Thus, the unit step response is the integral of the unit impulse response.

Appendix C

Representation Of Dielectrics By Lumped Circuit Equivalents:-

The current-voltage diagram, (see Fig (3.3), measured for a Capacitor dielectric at one frequency only, allows any number of circuit interpretation. The simplest equivalent picture would be that the capacitor housing contains an ideal condenser C_i and a resistor R in series or in parallel combination Fig (C.1). How well either one of these circuits simulates the behavior of the actual dielectric can be established only by calculating the frequency response of these networks and then comparing them with the dielectric response characteristic actually observed.

In the series arrangement the applied sinusoidal voltage equals the sum of the voltage drops across the resistor and the capacitor; in the parallel arrangement the total sinusoidal current is equal to the sum of the currents passing the two circuit elements. Hence we obtain:

i. Series Arrangement

$$V = IR + \frac{\int Idt}{C_i} \quad \ldots\ldots\ldots\ldots \quad (C.1)$$

$$= I\left(R + \frac{1}{j\omega C_i}\right)$$

$$Z = \frac{V}{I} = R + \frac{1}{j\omega C_i} \quad \ldots\ldots\ldots\ldots \quad (C.2)$$

ii. Parallel Arrangement

$$I = \frac{V}{R} + C_i \frac{dv}{dt} \quad \ldots\ldots\ldots\ldots \quad (C.3)$$

$$= V\left(\frac{1}{R} + j\omega C_i\right)$$

$$Y = \frac{I}{V} = \frac{1}{R} + j\omega C_i \quad \ldots\ldots\ldots\ldots \quad (C.4)$$

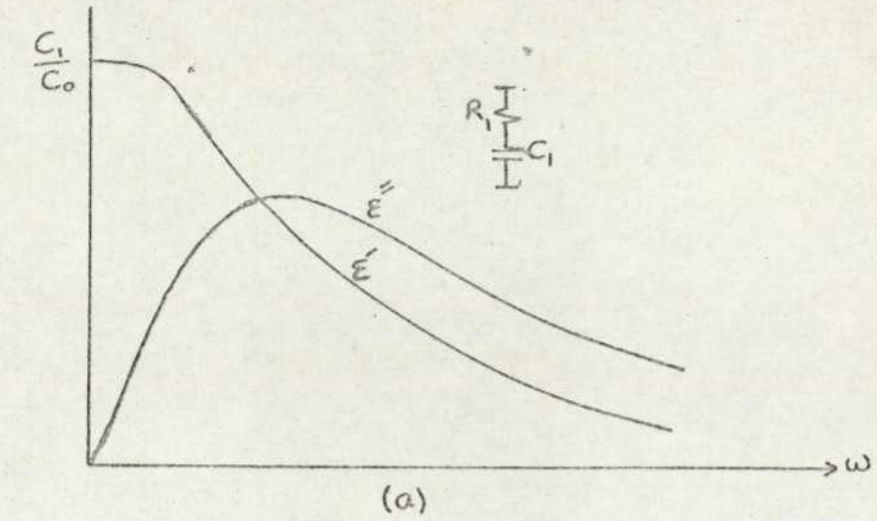

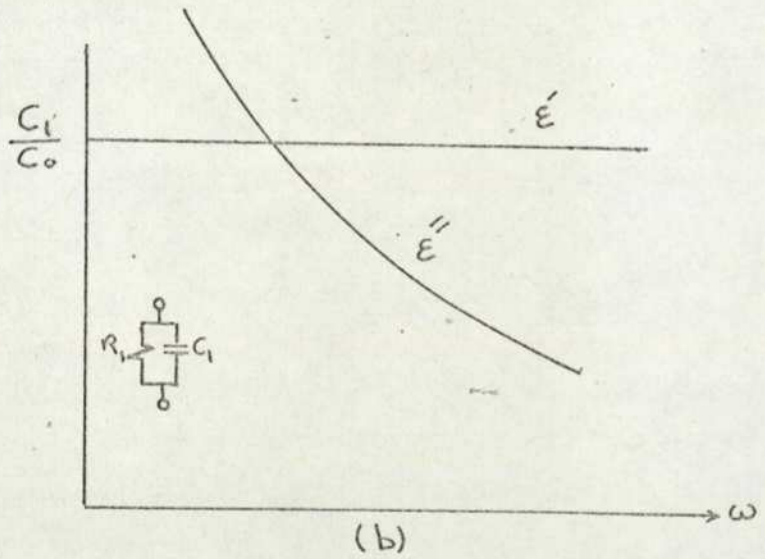

Fig. (C.1): Simplest equivalent circuits for capacitor dielectric.

In terms of the complex permittivity, a capacitor of the geometrical capacitance C_o has the admittance (Anderson, 1965)

$$Y = \frac{1}{Z} = (\varepsilon'' + j\varepsilon') \frac{\omega C_o}{\varepsilon_o} \quad \ldots\ldots\ldots \quad (C.5)$$

By equating the admittances of the two circuit arrangements to this expression, we arrive at the equivalent values for the relative dielectric constant, loss factor and loss tangent:

i. Series Arrangement

$$\varepsilon' = \frac{C_i \varepsilon_o}{C_o(1 + (\omega RC_i)^2)} \quad \ldots\ldots\ldots\ldots \quad (C.6)$$

$$\varepsilon'' = \frac{\omega R C_i^2 \varepsilon_o}{C_o(1 + (\omega RC_i)^2)} \quad \ldots\ldots\ldots\ldots \quad (C.7)$$

$$\tan \delta = \omega RC_i \quad \ldots\ldots\ldots\ldots \quad (C.8)$$

ii. Parallel Arrangement

$$\varepsilon' = \frac{\varepsilon_o C_i}{C_o} \quad \ldots\ldots\ldots\ldots\ldots \quad (C.9)$$

$$\varepsilon'' = \frac{\varepsilon_o}{RC_o} \quad \ldots\ldots\ldots\ldots\ldots \quad (C.10)$$

$$\tan \delta = \frac{1}{\omega RC_i} \quad \ldots\ldots\ldots\ldots\ldots \quad (C.11)$$

Obviously, as Fig (C.1) shows, the frequency dependence of these two elementary circuits has completely different trends.

However, dielectric spectra that can be represented by combinations of RC circuits are called relaxation spectra. A common criterion of such spectra is that, whereas the loss tangent as function of the frequency may rise and fall, the dielectric constant can only stay constant or fall, as the frequency increases.

Appendix D

Dielectric Permittivity and Its Voltage-step Response:-

Having discussed F.T. and the convolution theorem in the previous sections we have now enough tools to deal with the response of the linear system to voltage-step. It is intended to show here, the manner in which the permittivity of a dielectric is related to its step-voltage response.

Now, if the dielectric is considered as a linear system with an input x(t) and an output y(t), then the response of the dielectric (i.e. i(t)) can be expressed in terms of an applied stimulus (i.e. $\frac{dv}{dt}$ where v represents a unit step function) such that,

$$i(t) = C(t) * \frac{dv}{dt} \qquad \ldots\ldots\ldots\ldots\ldots \qquad (D.1)$$

where C(t) is the impulse response of the system (see App. (B.2)). Expressing equation (D.1) in the complex frequency domain gives;

$$I(s) = C(s) \cdot s \cdot V(s) \qquad \ldots\ldots\ldots\ldots \qquad (D.2)$$

for a step of height V and $V(s) = \frac{\hat{v}}{s}$

so

$$I(s) = \hat{v}\, C(s) \qquad \ldots\ldots\ldots\ldots \qquad (D.3)$$

If C is a parallel plane capacitor of area A and thickness d, then,

$$C(s) = \frac{\varepsilon_o A}{d}\ \varepsilon^*(s) \qquad \ldots\ldots\ldots\ldots \qquad (D.4)$$

or back in the time domain

$$i(t) = \frac{\varepsilon_o A \hat{v}}{d}\ \varepsilon^*(t) \qquad \ldots\ldots\ldots\ldots \qquad (D.5)$$

It should be noted that $\varepsilon^*(t)$ represents an impulse response in the sense that it is obtained by the inverse transformation of a frequency response. i(t) is the measured current response to a step of voltage, and in the low frequency range this is more easily measured then the response to a sinusoidal stimulus. The complex dielectric

constant for real frequencies is determined by F.T. of (D.5)

$$\varepsilon^*(\omega) = \varepsilon'(\omega) - j\varepsilon''(\omega) = (d/\varepsilon_o AV) \mathcal{F} i(t)$$

where $\mathcal{F}$ denotes F.T.

Appendix E

Interfacial Polarization:-

In considering mechanisms of polarization in chapter 2, the electronic and atomic polarization were identified as arising from displacement of electrons or atoms due to the applications of a field. This is called distortional polarization, distinguishing it from orientational polarization arising from rotation of the molecular dipoles. The mechanism here differs totally from those so far discussed. Previously, the atoms and molecules found themselves under the influence of a local-field consisting essentially of the applied field, modulated by the polarization of the surroundings. Now, large-scale field distortions enter, caused by the piling up of space charges in the volume or of surface charges at the interfaces of dielectric (Von Hippel, 1958).

The classical example of interfacial polarization is the Maxwell-Wagner two-layer condenser Fig (E1). The dielectric consists of two parallel sheets of materials (1) and (2), characterized by their dielectric constant, conductivity, and thickness $(\varepsilon_1', \delta_1, d_1)$ and $(\varepsilon_2', \delta_2, d_2)$, respectively. When a d.c. field is suddenly applied, the initial field distribution corresponds to electrostatic requirement of constant flux density

$$D_1 = D_2$$

or

$$E_1/E_2 = \frac{\varepsilon_2'}{\varepsilon_1'} \qquad \ldots\ldots\ldots\ldots \quad (E.1)$$

whereas the final distribution follows from the condition of current continuity

$$J_i = J_2$$

or

$$E_1/E_2 = \delta_2/\delta_1 \qquad \ldots\ldots\ldots\ldots \quad (E.2)$$

The transient which links the initial and final state may be derived from the equivalent circuit of Fig(E2). The applied voltage V, which is a constant, will always be given by

$$V = V_1 + V_2 \qquad \ldots\ldots\ldots\ldots \qquad (E.3)$$

The condition of current continuity, i.e. $E_1 \sigma_1 = E_2 \sigma_2$, is represented in the equivalent circuit by

$$C_1 \frac{dV_1}{dt} + \frac{V_1}{R_1} = C_2 \frac{dV_2}{dt} + \frac{V_2}{R_2} \qquad \ldots\ldots\ldots \qquad (E.4)$$

substituting from (E.3) we have

$$\left.\begin{aligned} (C_1 + C_2) \frac{dV_1}{dt} + \frac{V_1}{R} &= \frac{V}{R_1} \\ \text{and} \qquad (C_1 + C_2) \frac{dV_2}{dt} + \frac{V_2}{R} &= \frac{V}{R_2} \end{aligned}\right\} \qquad \ldots\ldots\ldots \qquad (E.5)$$

where

$$R = \frac{R_1 R_2}{R_1 + R_2}$$

Rearranging and integrating give

$$\frac{t}{CR} = - \text{Log} \left(\frac{V}{R_2} - \frac{V_1}{R} \right) + \text{Const} \qquad \ldots\ldots\ldots \qquad (E.6)$$

and a similar equation for V_2. The initial condition are that V is applied at t = 0, at which time the voltage will be distributed between condensers in the inverse ratio of their fractional capacitances, i.e.

$$V_1 = V \frac{C_2}{C_1 + C_2} \qquad \text{and} \qquad V_2 = V \frac{C_1}{C_1 + C_2}$$

Using this in equation (E.6) leads to

$$V_1 = V - \frac{R_1}{R_1 + R_2}\left(1 - \frac{(1 - C_2R_2)}{\tau}\, e^{-t/\tau}\right)$$

and similarly

$$V_2 = V\,\frac{R_2}{R_1 + R_2}\left(1 - \frac{(1 - C_1R_1)}{\tau}\, e^{-t/\tau}\right) \quad \ldots\ldots \text{(E.7)}$$

where $\tau = CR = (C_1 + C_2)\,\dfrac{R_1 R_2}{R_1 + R_2}$ ..... (E.8)

and is the time constant of the complete circuit. However, we may use the equivalent circuit to obtain the frequency - dependence of permittivity, as follows:

$$Y = \frac{Y_1 Y_2}{Y_1 + Y_2}$$

$$= \frac{\left(\frac{1}{R_1} + j\omega C_1\right)\left(\frac{1}{R_2} + j\omega C_2\right)}{\frac{1}{R_1} + \frac{1}{R_2} + j\omega(C_1 + C_2)} \quad \ldots\ldots\ldots\ldots \text{(E.9)}$$

$$= \frac{1}{R_1 + R_2}\left(\frac{1 - \omega^2\tau_1\tau_2 + \omega^2\tau(\tau_1 + \tau_2) - j\omega\tau(1 - \omega^2\tau_1\tau_2) + j\omega_1(\tau + \tau_2)}{1 + \omega^2\tau^2}\right) \ldots \text{(E.10)}$$

where $\tau_1 = C_1R_1$ and $\tau_2 = C_2R_2$

From definition of the admittance of an equivalent condenser;

$$Y = j\,(\varepsilon' - j\varepsilon'')\,C_o \quad \ldots\ldots\ldots\ldots\ldots \text{(E.11)}$$

where

$$C_o = \frac{A}{d_1 + d_2}$$

Thus equating (E.11) and (E.10)

$$\varepsilon' = \frac{1}{C_o(R_1 + R_2)} - \frac{\tau_1 + \tau_2 - \tau + \omega^2\,\tau\,\tau_1\,\tau_2}{1 + \omega^2\,\tau^2} \quad \ldots\ldots \text{(E.12)}$$

at $\omega = 0$

$$\varepsilon' = \varepsilon_s = \frac{\tau_1 + \tau_2 - \tau}{C_o(R_1 + R_2)} \quad \ldots\ldots\ldots\ldots \quad (E.13)$$

and at $\omega = \infty$

$$\varepsilon' = \varepsilon_\infty = \frac{\tau_1 \tau_2}{\tau} \frac{1}{C_o(R_1 + R_2)} \quad \ldots\ldots\ldots\ldots \quad (E.14)$$

Substituting in (E.12) we have

$$\varepsilon' = \varepsilon_\infty + \frac{\varepsilon_s - \varepsilon_\infty}{1 + \omega^2 \tau^2} \quad \ldots\ldots\ldots\ldots \quad (E.15)$$

Comparing Equation (E.15) with (2.23) it will be seen that the variation of ε' is precisely the same as that for the case of Debye relaxation, and τ may identified with the relaxation time. Thus by measurement of the real part of permittivity it is not possible to distinguish between the effects of interfacial and orientational polarizability.

From (E.11) and (E.10) we also have

$$\varepsilon'' = \frac{1}{\omega C_o(R_1 + R_2)} \frac{1 - \omega^2 \tau_1 \tau_2 + \omega^2 \tau(\tau_1 + \tau_2)}{1 + \omega^2 \tau^2} \quad \ldots\ldots\ldots \quad (E.16)$$

hence, using (E.13) and (E.14)

$$\varepsilon'' = \frac{1}{\omega C_o(R_1 + R_2)} + \frac{(\varepsilon_s - \varepsilon_\infty)\,\omega\tau}{1 + \omega^2 \tau^2} \quad \ldots\ldots\ldots \quad (E.17)$$

The second term of (E.17) is exactly the Debye relaxation equation (2.24), but there is an additional term inversely proportional to frequency. This means that the losses, represented by ε'', tend to infinity as ω tends to zero. Thus the case of interfacial polarizability may be distinguished from Debye relaxation frequency. In the Debye case ε'' drops towards zero as the frequency is lowered.

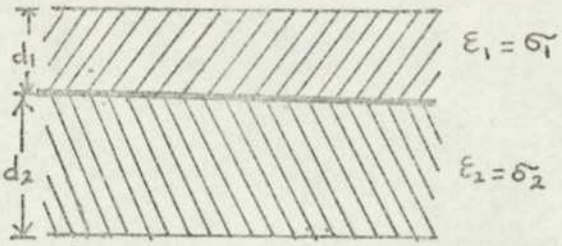

Fig. (E.1) Maxwell-Wagner two layer condenser.

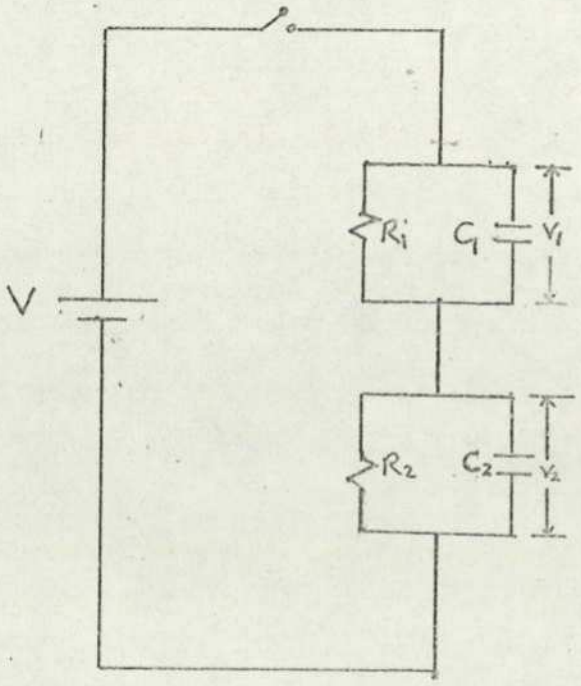

Fig. (E.2) Equivalent circuit of two layer condenser.

Appendix F

How Does The Delay Step-Function Affect The F.T. Of The Dielectric Response:-

Referring the App (A-3), the function g (t), Fig (F1), can be written as ;

$$g(t) = h(t)\, U(t) \qquad \ldots\ldots\ldots\ldots \quad (F.1)$$

where h(t) represents the system's impulse response and U(t) is a unit step-function, such that

$$U(t) = \begin{cases} 0 & t < 0 \\ 1 & t < 0 \end{cases} \qquad \ldots\ldots\ldots\ldots \quad (F.2)$$

Accordingly:

$$g(t) = h(t) \quad \text{for} \quad t > 0 \qquad \ldots\ldots\ldots\ldots \quad (F.3)$$

Now, if h(t) is assumed to be an exponential (i.e. $h(t) = e^{-at}$, where a is a constant), then the usage of equation (A.2) gives;

$$G(j\omega) = \int_{-\infty}^{\infty} h(t)\, U(t)\, e^{-j\omega t}\, dt \qquad \ldots\ldots\ldots\ldots \quad (F.4)$$

$$= \int_{o}^{\infty} e^{-(a + j\omega)t}\, dt$$

or

$$G(j\omega) = \frac{1}{a + j\omega} \qquad \ldots\ldots\ldots\ldots \quad (F.5)$$

putting $G(j\omega) = R(\omega) + j\, x(\omega)$ and multyplying equation (F.5) by $\frac{a - j\omega}{a - j\omega}$, we obtain,

$$R(\omega) = \frac{a}{a^2 + \omega^2} \qquad \ldots\ldots\ldots\ldots \quad (F.6a)$$

and

$$x(\omega) = \frac{\omega}{a^2 + \omega^2} \qquad \ldots\ldots\ldots\ldots \quad (F.6b)$$

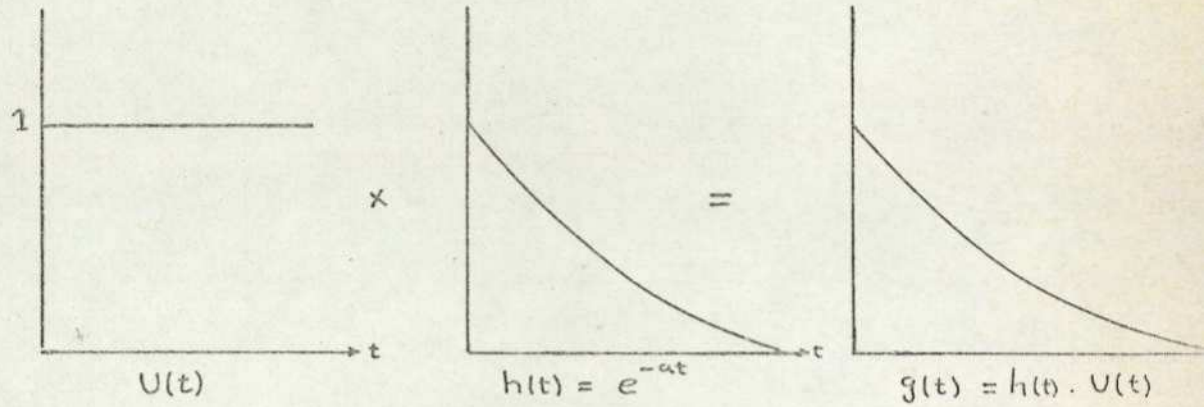

Fig. (F1) : A step function starts at t = 0.

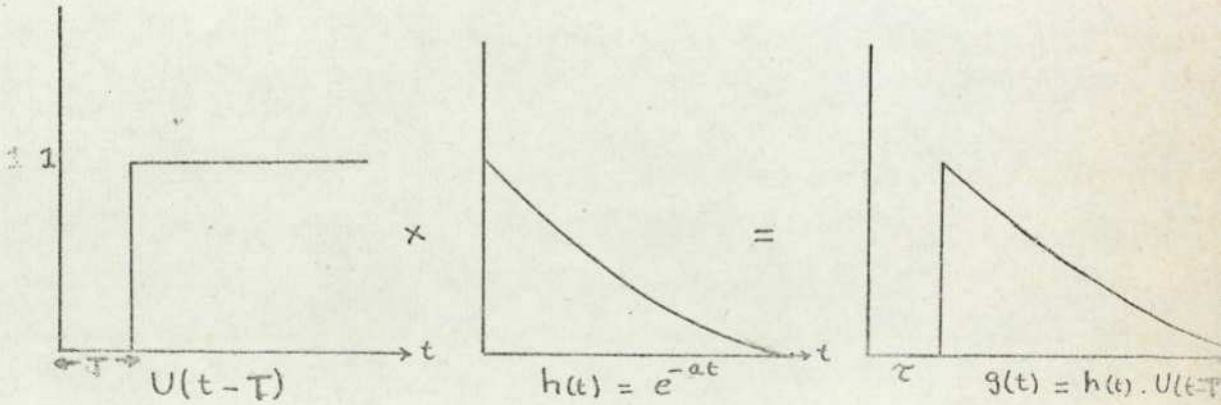

Fig. (F2) : A step function starts at t = T.

Now, if the step function U(t) is delayed by T along the t-axis such that

$$U(t) = \begin{cases} 0 & t < T \\ 1 & t > T \end{cases} \qquad \ldots\ldots\ldots\ldots \quad (F.7)$$

Then, we have

$$G(j\omega) = \int_{T}^{\infty} e^{-(a + j\omega)t} \, dt$$

Hence

$$G(j\omega) = \frac{e^{-aT}}{a + j\omega} \; e^{-j\omega T} \qquad \ldots\ldots\ldots \quad (F.8)$$

putting $e^{-j\omega T} = \cos \omega T - j \sin \omega T$ and multyplying equation (F.8) by $(a - j\omega/a - j\omega)$, we obtain

$$G(j\omega) = \frac{(a - j\omega)\, e^{-aT}}{a^2 + \omega^2} \; (\cos \omega T - j \sin \omega T) \quad \ldots\ldots \quad (F.9)$$

Seperating the real part from the imaginary, we have

$$R(\omega) = \frac{e^{-aT}}{a^2 + \omega^2} \; (a \cos \omega T - \omega \sin \omega T) \quad \ldots\ldots\ldots \quad (F.10a)$$

and

$$X(\omega) = \frac{e^{-aT}}{a^2 + \omega^2} \; (a \sin \omega T + \omega \cos \omega T) \quad \ldots\ldots\ldots \quad (F.10b)$$

Now, if T is taken to be small enough compared with the time required to sample the whole waveform, we have:

1. $e^{-aT} = 1$, provided a is small as well. In fact, Frohlich (1949) assumed that $a = 1/\tau$, where τ is, the relaxation time of the dielectric material, independent of time but may be depend on temperature. In case of polymeric solid material τ is very longe and hence a is a small fraction.

2. If ω is small, then the first and the second terms in equation (F.10a) will tend to a and zero respectively. The corresponding terms

in equation (F.10b) will tend to zero and ω respectively. Hence, equation's (F.10a) and (F.10b) may be written as;

$$R(\omega) = \frac{a}{a^2 + \omega^2} \quad \ldots\ldots\ldots\ldots \quad (F.11a)$$

$$X(\omega) = \frac{\omega}{a^2 + \omega^2} \quad \ldots\ldots\ldots\ldots \quad (F.11b)$$

Therefore, both the low frequency components of real and imaginary parts of the F.T of the system response to delayed step-function are not affected since, equations (F.6a) and F.6b) are just the same as equations (F.11a) and F.11b).

3. To show how, the high frequency components of the real and imaginary parts of the F.T of the system to delayed step-function, are affected by the latter, numerical values will be given to a, T and ω and used in equations (F.6) and (F.10).

Relaxation times for polymeric solid materials are in general, very long (i.e. 90 sec at room temperature). Let us, however, assume that τ = 50 sec hence, $a = \frac{1}{\tau}$ will equal to 0.02 sec^{-1}.

The highest sampling rate used for ε' and ε'' evaluation, in the present work, was 6 Hz. Therefore the highest frequency associated with ε' and ε'' components is 3 Hz and $\omega = 2\pi f$ will be equal to $6.\pi$. The values of $R(\omega)$ and $X(\omega)$ calculated from equations (F.6) and (F.10) for T = 3 and 5 sec are listed below.

ω rad/sec	T = 0		T = 3		T = 5 sec	
	Eq (F.6)		Eq (F.10)		Eq (F.10)	
	R(ω)	X(ω)	R(ω)	X(ω)	R(ω)	X(ω)
6π	5.63×10^{-5}	5.3×10^{-2}	5.3×10^{-5}	5.0×10^{-2}	5.1×10^{-5}	4.8×10^{-2}
2π	5.06×10^{-4}	1.6×10^{-1}	4.8×10^{-4}	1.5×10^{-1}		
π	2.03×10^{-3}	3.2×10^{-1}	1.9×10^{-3}	$.3 \times 10^{-1}$		

It is apparent from the above table that the differences between R(ω) and X(ω) calculated from equation (5-6) and those calculated from equation (5-10) are not that critical and become smaller as ω gets smaller. However, errors becomes more serious when T increased and hence, (-aT) becomes more negative. This also implses that when τ decreases at high temperature, $a = \frac{1}{\tau}$ increases and e^{-aT} becomes a small fraction. Therefore, values of ε' and ε'' associated with both high and low frequency components should be divided by the correction factor e^{-aT}.

It is still necessary to emphasise that, the above theoretical treatment is confined to the case when the decay function h(t) is assumed to be an exponential and the relaxation of the material is Debye's type.

Appendix G

The Application Of Real Time Computing

G-1 Introduction :-

The computer used for this work was a Ferranti 1600B mini computer. This is a 24 bit machine, unlike most minis which are 16 bit. This has three addresses per instruction, making it effectively twice as powerful as a one address machine.

The configuration shown in Fig (G1) includes 32k of store, a disc store, 2 teletypes, a paper tape reader and Punch, a D/A and A/D converters, a visual display unit (V.D.U) and a graph plotter. Computer operation is controlled from the teletype keyboard, and the machine is normally ready to receive an instruction unless another programme is currently being processed.

The (V.D.U) made up from aTektronix storage tube provides a fast noise free output. A graph plotting subroutines incroporating several facilities were available to ease the process of analysing the current transients and assist the preparation of graphs. The facilities of this included;

a - variable sized axes

b - preset or auto scaling of X and Y axes

c - the ability to title the axes easily .... etc.

d - the possibility or having several plots on the same axes (with different symbols)

e - plots on either the V.D.U. or plotter.

Towards the end of the duration of this research, a Breakpoint programme was developed to ease the tracing the fault in the programme being used.

The available software was programmed in "FIXPAC": an assembly

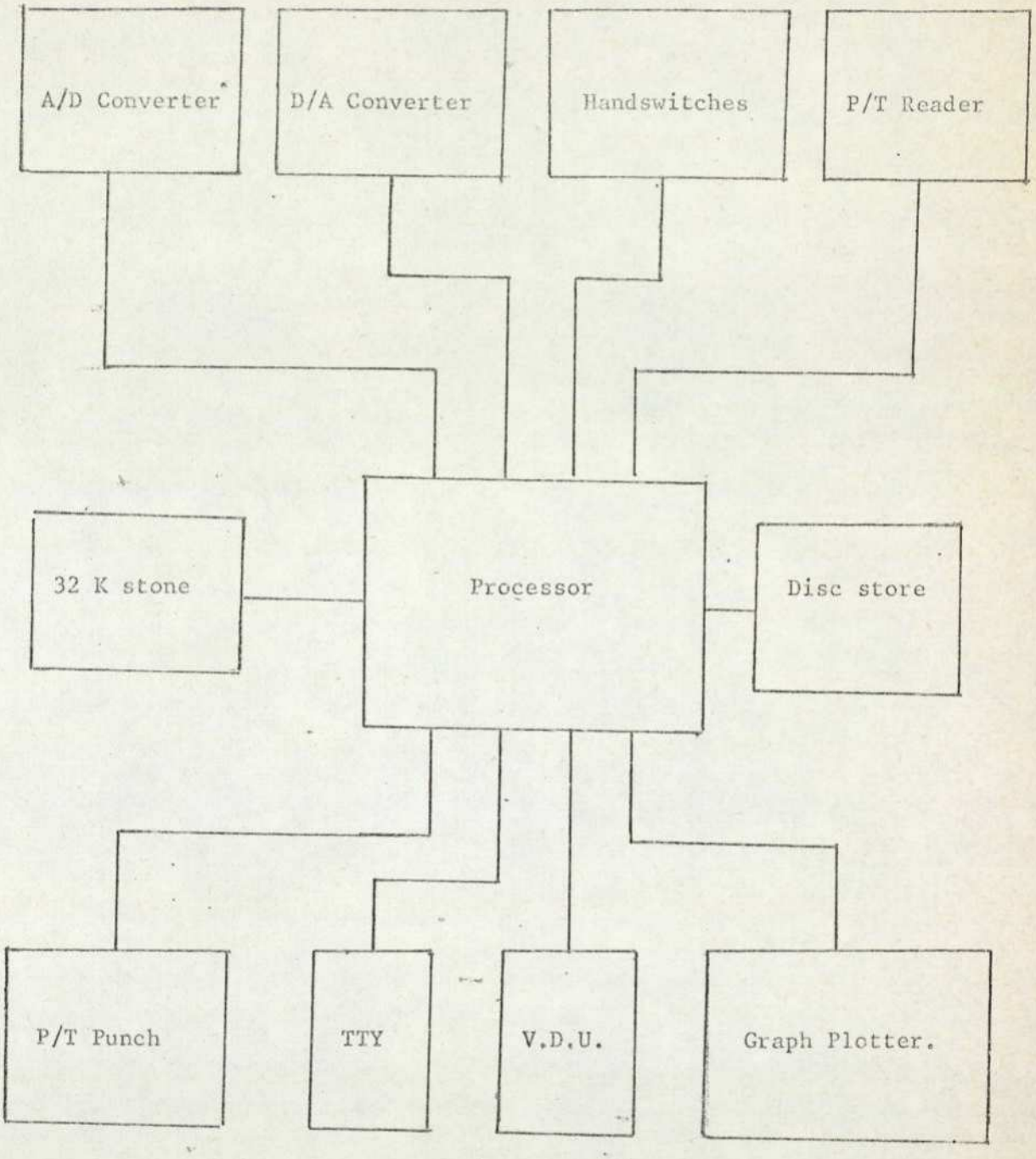

Fig. (G.1):- The Computer Configuration.

level language having almost a one to one correspondance between written instruction and the words in store. Programming in "FORTRAN" could be used, but data and programme interrupts, which enable powerful on-line operation, are programmable in "FIXPAC" language.

The important operations involved with on-line input and output work with the FM 1600B are discussed below:

G-1-1 On-Line Working:-

The terms on-line and real-time often present an unclear concept. In an attempt to clarify the situation, the definitions as given by Martin (Ref, 49) are given here.

"An on-line system may be defined as one in which the input data enter the computer directly from their point of origin and/or in which output data are transmitted directly to where they are used."

"A real-time computer system may be defined as one which controls an environment by receiving data, processing them and returning the results sufficiently quickly to affect the functioning of the enviroment at that time."

G-1-2 Interrupts :-

Interrupts occur in two forms, data interrupts, which can take place during the processing and at the end of an instruction, and programme interrupts, which can only occur at the end of an instruction.

Data interrupts cause data to be transmitted to or from the computer by a peripheral. A data interrupt when completed may initiate a program interrupt, depending on the peripheral being used.

A program interrupt causes the currently running program, often reffered to as the main program, to be held up so that a special program, the interrupt program, may be entered. This interrupt program may be utilised for processing of the new data or generating more data for dispatch.

Peripherals, however, are connected to the computer via a standard interface system, the design philosophy of which can be found in paper by Crapnell and Richmond (Ref, 12). The particular interface used by the FM 1600B is the 22 - channel Ferranti 'B' Standard Interface. Each channel has eight control lines associated with it (Table G-1) and has access to a common 24 - bit 'data highway'.

Thus, before an interrupt can occur, the QS staticiser for the channel to which the peripheral is connected must be sat so that the peripheral is put on-line.

If the interrupt is to be initiated by the program the QM staticiser must be set which subsequently sets the AQD function of the peripheral. The setting of AQD is dependant on the particular peripheral as it will either request a control word to define the operation required (Table, G-2) or will set the AQD lines for the only operation that it is capable off. The peripheral replies with a Cycle Request (by setting R) to the computer, asking for a transfer of data.

For a peripheral initiated interrupt, providing the QS staticiser is set, the peripheral starts the interrupt by sending a Cycle Requests.

The J line is then set by the computer to signify the transfer may take place. The data highway gates are subsequently opened by the peripheral setting the K line and completing the handshake sequence.

Data is consequently transmitted according to the setting of the AQD lines.

If a Control Word (CW) has been requested it is sent via the data highway, where upon it resets the AQD lines so that subsequent transfers may take place in the required mode. Further data is transmitted in sequence until the computer issues the end of the data block, normally by clearing the QM staticiser.

If the peripheral being used requires a program interrupt to occur it does so in a manner similar to a data interrupt. The AQD lines are set to 010 by handware to inform the computer that the next stage should be entered. The function unit then reads store location 25, which should have been loaded with the machine instruction 7000 0 0 which instructs the computer to store a link and load the instruction address register NO with the Interrupt Program Address (IA). The Status Word(SW) is passed from the peripheral along the data line to the computer, its structure being dependant on the peripheral.

Comments

1. Each channel has three External Q staticisers associated with it, known as the QS, QM and QF staticisers. These Q staticisers are additional to the Internal Q staticisers. The operation and the use of both types are defined in the Fixpac Manual (Ref, 61).

2. The control Word (CW) :- This word contains the information required to select the peripheral, if the (PCU) serves more than one, set up the required operating conditions of this peripheral and defins the next type of transfer i.e. it may set the next state of A,Q and A. Its address is held in the Control Word Pointer (CP). During the data interrupt the address in the (CP) is indexed by unity.

3. The address of the location where the next item of data is stored in the Data-Word Pinter (DP). During the data interrupt the address is indexed by unity.

4. The location which is loaded with the start address of an interrupt program or subroutine associated with the channel is called the Interrupt - Program Address Word (IA).

5. Status Word (SW) contains the information conncerning the success or failure of the data transfer and then pass it from the peripheral to the computer. Details of other uses of (SW) can be found in Fixpac Manual.

Signal	Name	Source	Use
S	Transfer Select	computer	To put peripheral on-line
M	Transfer Engage	computer	To start computer initiated transfers
A	Address	peripheral	To define the type of transfer required
Q	Qualifier	peripheral	
D	Direction	peripheral	
R	Cycle Request	peripheral	To request a data transfer
J	Handshake	computer	To cause data to be transferred
K	Controls	peripheral	

Table (G-1): The Control Line To a Peripheral (Ref 20).

AQD	Use
000	Data In to Computer
001	Data Out of Computer
010	Programme Interrupt
011	Control Word Out of Computer

Table (G-2): The function of the AQD lines:

G-2 The Real Time Clock :-

The Real Time Clock (R.T.C) was built by D. Spreadbury (Ref, 76) and the information given here is that concerned with the software.

G-2-1 The Mode of Operation :-

The clock work in one of the three modes.

The Request Mode, which returns to the computer a data word T, representing the time elapsed since the last such request.

The Interrupt mode, which uses a data word supplied by the computer, initiates a Program Interrupt at the time interval as specified in the data word.

The Trigger mode, which is similar to the interrupt mode except that a trigger pulse is supplied instead of a program interrupt being initiated.

Each time the peripheral performs the required operation, the clock is reset to zero and commences to count at the specified rate.

G-2-2 The Control Word :-

The Control Word is used to specify the mode of operation (m) and the range of the clock (r).

m is a 2 bit word, when the clock is reset by setting m to 00, the three modes of operation are terminated without subsequent transfers.

r is a 4 bit word which represents a positive number used to define the range or time represented by the maximum value of the data word. Thus the Elapsed Real Time (E.R.T) is given by equation (G-1). For r

set to zero, the clock counts in intervals of 0.5 μs

$$E.R.T = T \times 2^{r} \text{ seconds} \quad \ldots\ldots\ldots (G.1)$$

where T is a fraquation.

G-2- 3 The Data Word :-

The Data Word is a 24 bit word which contains the information to, or received from the peripheral (the status word transmitted by peripheral during a program interrupt is the data word T).

G-3 The General Input/Output Unit :-

The General input/output unit (GIPOP) unit performs two functions in a computer system that requires slow signal transfers between a group of peripheral devices and the computer. The primary function is to provide a common peripheral control unit (P.C.U) for the peripheral devices with the unit using a cyclic scan sequence to service each device in turn. The cyclic scan determines the order in which the devices are serived and also allows each device to request as many transfers are needed to fulfil its servicing requirements. The second function of the unit is the full conversion of the peripheral's signal group to the computer's Standard Interface word format, when data is transferred from a peripheral to the computer, or vice-versa.

Each scan is initiated either by the computer or by a single peripheral master control-signal and the first transfer in each scan is a test word to the computer. If a device requires more than one transfer to satisfy its servicing needs, it generates to halt the scan until all of its transfers have been completed, the scan is then restarted

and selects the next device to be serviced. The scan can be halted, after any number of transfers, by a program interrupt being requested. When the interrupt has finished, the scan recommences from where it was halted. At the end of each scan, a mandatory program interrupt is requested and an "Output Data Available" signal is provided.

G-3-1 The Digital to Analogue Converter :-

The converter uses a 16 bit input register and treats this as two 8 bit words to give two analogue outputs with a swing of ± 5 volts.

G-3-2 The Analogue to Digital Converter :-

This converter is of the successive approximation type, with a conversion time of less than 30 μs. The input signal, which should swing between ± 10 V, is converted to a 10 bit binary number.

G-4 Computer Programmes :-

Programme No.1

This programme basically consisted of a number of subroutines joined together to form the Master Programme. Some of these subroutines (i.e. S600 and S5535) with the Master programme are shown below. The programme used to ;

1. Set up the computer ready to receive data in two different modes

a) Auto Mode:- The computer will generate the required signals and sample them according to the number and the sampling rate specified by the programme.

b) External - Triggering Mode:- The computer starts taking sampled data from an external prepheriel (i.e. A/D converter) as soon as the latter is triggred (i.e. by a nagative going edge pulse) and the pulse generater, providing sampling frequency, is on.

2. Instruct the computer to stop taking sampled data after a certain number specified by the programme itself.

3. Fourier transform the data and output them in real and imaginary forms.

4. Plot the real and imaginary parts on either required linear or longarithmic scale.

5. Calculate the power spectrum and the Amplitude spectrum.

6. Calculations can be carried out in either single length floating point or single length fixed point depending whether the subroutine S6006 or S6007 is called during the claculations respectively. The computation time required for 1024 point transfer is 1.48 seconds for the first and 1.36 seconds for the latter.

However, the programme requires a data storage area which must be at least 3N words, where $N = 2^m$ and m is an integer.

Since no shifting of the data word is carried out, no accuracy is lost as a result. However, the overall programme accuracy is still determined by that of S421 (quoted by Ferranti as $\pm 10^{-6}$).

```
N
FFT WITH A&DC RANDOM ACCESS INPUT. MASTER PROGRAM
TRH 7/4/76. REV. 11/5/76. REV.21/7/76.REV.23/7/76;
LS1500,1500,1500

←S4710      'VDU SET-UP'
←S4580      '"/CP ."'
←11,L

[0]    V22=VNO
AS15504              '.4 WORD CN. WD. DATA AREA'

V19=4
TEXT 1P1E
?AUTO(1) OR EXT. TRIG.(0)    ?M WHERE 2**M=NO OF DATA TFS.

V19=3
V23=0
←S100
←1,V21=0     'LEAVE BIT CLEAR FOR EXT TRIGG'
V22[23]←0    'SET BIT FOR AUTO'
[1]←S100     'V21 CONTAINS M'
N1=VNO,VN1 =V21
AS 6000              'CONTAINS M'
V21←BIT VN1      'V21 CONTAINS NO OF TFS'
V20=VNO
AS15500        'DATA AREA FOR 3*(2**M) TFS'
N1=VNO,VN1=V20
AS 6000,1        'S.A. OF DATA AREA'

V18 =V20-1
N1=V18
V18=-V21
V18=V18+V18
V18=V18-V21 '-3*NO OF DATA WORDS'
[5]VN1=VN1#VN1,N1+1          'ZEROISE DATA AREA'

←5,V18=V18+1<0

V23=VNO
AS5532       'IT PG'
N1=VNO,VN1=V23
AS15504,3        'FLAG'

←S5511           'VERSION 20'

V19=4
TEXT 1P1E
AWAIT EXT TRIG
N1=VNO
AS15504,3
[2]←2,VN1#0   'RETURN AFTER INTERRUPT.FLAG CLEARED IN S5532'

N1=VNO
AS6000
V21←BIT VN1      'NO OF TFS'
V0=V0,N1+1
V20=VN1
←S5514         'VERSION 0 SHIFT/INV/CLEAR DATA'
V19=4
TEXT 1P1E
?IS PLOT OF FIXED DATA  REQUIRED. YES(1) OR NO(0).
V19=3
V23=0
```

```
←S100
←4,V21=0
←10,L

[4]←S6007    'FFT FIX PT VERSION 1'
V19=4
TEXT 1P 1E
FIX PT FFT IN 1ST.(REAL) & 2ND.(IMAG) DATA AREAS.
TEXT 1P1E
PLOT REAL PART.
←10,L
V19=4
TEXT 1P1E
PLOT IMAGINARY PART.
←10,L

←S5533    'POWER SPECTRUM IN FLT PT'
V19=4
TEXT 1P1E
FLT PT POWER SPECTRUM IN 3RD. DATA AREA.
←10,L

←S5534      'AMPL. SPECTRUM IN FLT PT.'
V19=4
TEXT 1P1E
FLT PT AMPLITUDE SPECTRUM IN 3RD. DATA AREA.
←10,L

←0          'RESTART'


[10]V19=4
TEXT 1P1E
?IS LOG-SCALE X-AXIS REQUIRED. YES(1) OR NO(0).
V19=3
V20=0
←S100
←11,V21=0
←S5535
[11]←S4580,3      'VDU/CP'
←L


END

A

SF0

V
VERSION LIST;
6007 1
84 0
6000 0
5314 1
5315 1
5 30
4710 0
1020 2
1021 2
88 0
82 1
```

```
83 1
6 0
86 0
14 1
4701 0
102 3
21 20
22 30
20 6
64 3
61 2
66 3
502 0
12 30
999 1
0
```

```
     N
     COMPLETE FAST FOURIER TRANSFORM IN FLOATING POINT
     K.J.P. 15/12/1971
     U
     STK VN3,23,23
     VN3=N1,N3-1
     VN3=N2,N3-1
[22] N1=VN0,V19=VN1
     AS6000
     V7=V19,N1+1
     V15←BIT V19
     FLTV15+0
     V16=OCT14441704
     V11=V16/V15,SLF
     V15←BIT V19
     V3=V15[1],L              ''2XNO. OF POINTS'
     ←1,N1=N1+V3>0
     [1]V3=N1
     VN1=0                 'START OF EXPO. MULTI. POWERS'
     [2]V13=0
     V19=V19-1
     V8=V19-1
     V8←BIT V8
     V6=N1+2
     V12=V6-V3
     N2=V3
     [3]←4,N1=N1+2>0
     [4]VN1=VN2+V3,N2+1              'AY'
     V13=V13+2,N2+1
     ←3,V13-V12<0
     V7=V7-1
     ←2,1-V7<0
     [5]V21=1
     V22=V15[1],R
     V13=OCT00000040
     N1=V3,VN1=V13
     V9=OCT10000002
     VN1=V9,N1+1
     N2=V3
     V12=0
     V5=V15[2],R
     [6]V6=V12,N2+1
     V16=V5+V6,N2+1
     V16=VN2-V16
     V12=VN2
     ←7,V16=0
     V16=VN2-V22
     V16=V16+V6
     ←8,V16=0
     ←9
     [7]VN1=V9,N1+1              ?4
     V10=V9
     V9=-V13,SLF
     V13=V10
     VN1=V9,N1+1              ?5
     ←10
```

```
[8]VN1=V13,N1+1
V9=-V9,SLF
VN1=V9,N1+1
←10
[9]FLTVN2+0
V17=V11÷VN2,SLF
V20=V17
←S319,0                'CALCS SINE'
V13=V20
VN1=V20,N1+1        ?6
V20=V17
←S319,1                'CALCS COSINE'
V9=V20
VN1=V20,N1+1         ?7
[10]V23=N1
V21=V21+1
←6,V21-V22<0
[30]N1=VN0,V21=VN1
AS6000
V20←BIT V21
V14=V20[1],L
V22=V20[1],R
V16=V22
V18=N1
[11]V15=0
V23=V14+V18
V23=V23+1
N1=V23,V6=VN1
V12=V18,N1+1
V7=VN1,N1+1                          'COSINE'
V23=N1
[12]V17=0
V2=V12
[13]V17=V17+1                         'COUNT'
V2=V2+1                              'REAL LOCATION'
V3=V2+V22                            '1/2 REAL LOCATION'
V4=V2+V20                            'IMAGINARY LOCATION'
V5=V4+V22                            '1/2 IMAGINARY LOCATION'
N1=V3                                '1/2 REAL LOCATION'
N2=V5                                '1/2 IMAGINARY LOCATION'
V8=V7*VN1,SLF
V9=V6*VN2,SLF
V8=V8+V9,SLF
V9=V7*VN2,SLF
V10=V6*VN1,SLF
V9=V9-V10,SLF
N1=V2,V11=VN1                              'START REAL'
N2=V4,V13=VN2                              'IMAGINARY'
VN1=V11+V8,SLF                      '1 U 0'
N1=V3
VN1=V11-V8,SLF                                    '1 X 0'
VN2=V13+V9,SLF
N2=V5
VN2=V13-V9,SLF
```

```
V15=V15+1
V19=V17-V22
←14,V19=0
←13
[14]V12=V15-V16
←15,V12=0
N1=V23,V6=VN1
V12=V3,N1+1
V7=VN1,N1+1                          'COSINE'
V23=N1
←12
[15]V22=V22[1],R
V21=V21-1
←11,V21#0
FLTV20+0
N1=V18
V2=0,N1+1
[16]VN1=VN1/V20,SLF
V2=V2+1,N1+1
←16,V2-V14<0
N1=VN0,V2=VN1
AS6000
V13←BIT V2.
V11=N1+1
V4=0
V7=0
[17]V3=V2-1
V5=0
[18]←19,V4[V5]#0                      'TEST FOR BIT SET'
V7[V3]=0                             'CLEAR BIT'
←20
[19]V7[V3]#0                         'SET BIT'
[20]←21,V3=0                            'FINISHED TEST?'
V3=V3-1
←18,V5=V5+1#0
[21]V6=V4+1
←23,V4-V7>0
V9=V11+V4              'NOW INVERT REAL DATA'
N1=V9
V10=V11+V7
N2=V10,V12=VN2
VN2=VN1
VN1=V12
V9=V9+V13                'NOW INVERT IMAG. AREA'
N1=V9
V10=V10+V13
N2=V10,V12=VN2
VN2=VN1
VN1=V12
[23]←22,V6-V13>0
←17,V4=V4+1#0
[22]N2=VN3
V0=V0,N3+1
N1=VN3
V0=V0,N3+1
```

```
LDK VN3,23,23
←L
END.
Z
S
6006 0
```

```
DISCRETE FAST FOURIER TRANSFORM IN FLOATING POINT
 BY  K.J.POCKNELL;



N
CHECK SPEED OF FIXED PT. ANGLES K.J.P.   15/07/71.
U
CM=1
Q1#0
N3=192
Q1=0
V1=0
N1=VN0
AS6000
N2=VN0
AS6000
V19=0.6667,N2+1
[2] V20=V19
←S421,0
VN1=V20
VN2=V21
V1=V1+1
←2,V1-10000<0
STOP 31
END
A
```

```
N
S5535 TO CONVERT X-AXIS TO LOG SCALE & FORM SLF X-Y PAIRS
IN S15500,3100 FOR PLOT BY VDU/CP. TRH 21/7/76;


U

VN3=V23,N3-1
STK VN3,5,4
STK VN3,21,3
VN3=N1,N3-1
VN3=N2,N3-1

V19=4
TEXT 1P1E
?Y-DATA IN FLT.PT. YES(1) OR NO(0)
TEXT 1E
?START ADDRESS OF Y-DATA
TEXT 1E
?NO. OF Y-DATA POINTS
V19=3
V23=0
←S100
V3=V21
'V3≠0 IF DATA IN FLT.'
←S100
V5=V21
'S.A. OF Y-DATA'
←S100    'V21=NO OF Y-DATA POINTS'
N2=VN0
AS15500,3100
N1=V5
V2=-V21
V4=1
FLT V4+0
V5=V4
[1]V20=V5
←S339    'SLF LOG'
VN2=V20
V0=V0,N2+1
←2,V3≠0
FLT VN1+23
[2]VN2=VN1,N1+1
V0=V0,N2+1
V5=V5+V4,SLF

←1,V2=V2+1<0
V19=4
TEXT 1P1E
DATA NOW IN S15500,3100IN SLF (LOG X)-Y PAIRS

N2=VN3
V0=V0,N3+1
N1=VN3
V0=V0,N3+1
LDK VN3,21,3
LDK VN3,5,4
V23=VN3,N3+1

←L
END

Z

S
5535
S5535 TO CONVERT X-AXIS TO LOG SCALE;
```

Programme No.2

This programme was writeen in "FORTRAN" language using the avaliable Fortran compilation facilities. It used to

a. Generate the ideal low-pass filter response to the step function $Si(\omega_c t)$, see chapter (4), using both equations state below:

$$Si(x) = x - \frac{x^3}{3.3!} + \frac{x^5}{5.5!} - \ldots\ldots \quad \text{for } x = \omega_c t \leq 12$$

and

$$Si(x) = \frac{\pi}{2} - \left(\frac{1!}{x^2} - \frac{3!}{x^4} + \frac{5!}{x^6} \ldots\right) \sin - \left(\frac{0!}{x^1} - \frac{2!}{x^3} + \frac{4!}{x^5} \ldots\right)$$

$$\cos x \text{ to } x > 12$$

b. Calculate the function $G(\omega_c t)$ (i.e. $G(\omega_c t) = \frac{1}{2} + \frac{1}{\pi}$ Si $(\omega_c t)$ by dividing Si(x) by π and adding to it the value (0.5) for each value of x.

Programm No.3

The values of the function $G(\omega_c t)$ calculated so far in programme No.2, where in floating point formate and in order to output these values through the General Input-Ouput Unit (GIPOP) via the D/A converter they have to be in Fixed point formate. It is also desirable to normalized these values (i.e. maximum = 5 volts and minimum = - 5 volts) to suit the range of the D/A converter being used. Normalization was done by dividing each value of the function $G(\omega_c t)$ by the factor (Max -- Min)/2 and then multiplying it by (127) (i.e. 127 = 1111111).

This programme was written to satisfy the above requirements.

```
*CD,TT,TT,TP,TR,TT,TT,LP
      A=100.539964
      DO  6  J=1,1[illegible]5
      B=-A
      AB=A*A
      SS=0
      IF(A-12.0) 19,19,8
       AC=AB*A
      AD=AC*A
      AE=AD*A
      AF=AE*A
      AH=AF*A
      AL=AH*A
      AM=1/AB-6/AD+120/AF-5040/AL
      AM=AM*SIN(A)
      AS=1/A-2/AC+24/AE-720/AH
      AS=AS*COS(A)
      AK=AS+AM
      SR=1.57143-AK
      GO TO 15
   19 MM=A+1
      LY=3
    7 LX=LY
      BB=LY
    8 AM=LX
      BB=BB*AM
      LX=LX-1
      IF(LX.GT.0)GO TO 8
      B=B*AB
      AR=B/BB
      SS=SS+AR
      LY=LY+2
      B=-B
      MM=MM-1
      IF(MM.GT.0)GO TO 7
      SR=SS+A
   15 SR=SR/3.141592654
      IF(J.GT.512)GO TO 16
      SR=0.5-SR
      GO TO 21
   16 SR=SR+0.5
   21 WRITE(2,30) SR
   30 FORMAT(1H ,E12.6)
      IF(J.GT.512) GO TO 9
      A=A-0.19634[illegible]5409
      GO TO 6
    9 A=A+0.19634[illegible]5409
    6  CONTINUE
      STOP
       END

Z
```

```
N
CONVERT  S.S.AL-RAWI O/P DATA TAPE C.J.B  MK11;


U


[7]V19=4
TEXT 1P 1E
INPUT  2**N=
V19=5
V23=0
←S100
V15=0
N1=VN0
AS2
V14←BITV21
[8]V19=3
←S109
V5=2
FLTV5+0
V20=V20/V5,SLF
FIXV20+23
VN1=V20
V15=V15+1,N1+1
←8,V15-V14<0
N1=VN0,V15=VN1←VN1
AS2


V16=V14          'NO. OF SAMPLES'
V4=V14           'STORE V14'


          STK VN3,16,2
          VN3=V12,N3-1
          VN3=N1,N3-1


          N1=VN3
          V15=1
          V14=VN1,N1+1                ?1   'LOAD FIRST VALUE & INC N1.
          V13=V14                          'INITIAL MAX = INITIAL MIN.
 [4]      V12=VN1,N1+1                     'COPY NEXT VALUE .'
     ←3,  V12#V13=0                        'TEST FOR EQUALITY.'
     ←1,  V12-V14<0                        'JUMP IF V12<MIN.'
     ←2,  V12-V13>0                        'JUMP IF V12>MAX.'

 [3]      V15=V15+1                        'INC COUNT.'
     ←4,  V15-V16<0                        'TEST FOR END OF DATA.'
          V12=V14
          V13=V13/2,IQ                ?7
          V14=V14/2,IQ                ?8
          +0


          V15=V13-V14                 ?2   '(MAX-MIN)/2.'
          V11=V12+V15                 ?3   '     "        + MIN.'
          V12=V15+VN0
          +.00009                          'OVERFLOW PROTECTION.'
          +0
```

```
          N1=VN3,V15=VN1≠VN1          'N1=S.A.  V15=0.'

[5]       VN1=VN1-V11          ?4     'SUBTRACT V11.'
          VN1=VN1/V12,FQ       ?5     'DIVIDE DATA BY NORMALISING
                                      'FACTOR.'
          V15=V15+1,N1+1              'INC COUNT & N1.'
     ←5,  V15-V16<0                   'TEST FOR END OF DATA.'
     ←6

[1]       V14=V12                     'UPDATE MIN VALUE.'
     ←3

[2]       V13=V12                     'UPDATE MAX VALUE'
     ←3

[6]       V13=V13*2,I                 'RESTORE MAX VALUE.'
          V14=V14*2,I                 'RESTORE MIN VALUE.'
          N1=VN3
          V0=V0,N3+1
          V12=VN3,N3+1
          LDK VN3,16,2

V14=V4

N1=VN0,V15=VN1≠VN1
AS2
[3] VN1=VN1*VN0,F
+127
V19=2
V23=38
←S1
V15=V15+1,N1+1
←9,V15-V14<0
V19=4
V22=10
←S555,6
←7



END



A
```

Programme No.4

This programme, shown below, was written to:

a. Set up the computer ready to receive the number of data, from an external peripheral (i.e. A/D converter), specified by the programme in the form $N = 2^m$ where m is an integer.

b. Access the function $G(\omega_c t)$, see chapter (4), which was originally stored in the Disc store, into the computer store and output it later through the GIPOP unit, via the (D/A) coverter, after being, fixed point, and normalized (see program No.2).

c. Set up the Real-time clock and specify the time required for this real-time clock to output the function $G(\omega_c t)$.

d. Outpout, initially, a (- 5 volts) when bit (0) of the hand-switch, (see Fig (F1)), is off.

e. Output the function $G(\omega_c t)$ as soon as the bit (0) set on and sample the dielectric output response, due to the applying of the function $G(\omega_c t)$ at the same time.

f. Cyclicly shift the recorded data so that the start of the data coincides with the centre of the edge of the input waveform. The process can be realized as follows:- The first 128 out of 1024 data will be transformed to locations 1024 to 1152. The entire waveform will be then shifted 128 places to the left so that the data which was located in 128 will take place in location 0 and so on . The process will be repeated and the cycle is completed when the second 512 data replace the location of the 1st 512 data (i.e. 0 - 511 and vice versa (i.e. 1024 - 511)).

g. Fourter transform the cycliely shifted data and plotting them either on a logarithmic or linear scale in form of real and imaginary parts.

h. Calculate the Power, Amplitude Spectrum if they are required.

```
          N
          C.J.BUFFAM, S.S.AL0-RAWI 27/4/977;


          LS 2500,2500,2500


     ←0
          Q1#0
          N3 =VN0
          +23223
          ←S4710
          ←S4580
        V20←BIT10
          V21=VN0
          +10239
          ←S2021,1
           ←S2021,6
     ←1

[0]       Q1#0
          N3=VN0
          +23223

         V20←BIT10
          V21=VN0
          +10239
          ←S2021,1
 ←S2021,6


[1]       V19=4
          ←S555,2
TEXT 1P 1E
ENTER COMMAND.
          V19=5
          ←S1020,1
          AS10020
          SJV10
 AL1                                  'ERROR'
          AL2                                 'SET UP'
          AL15                                'START'
          AL5                                 'ABORT'
          AL6                                 'END'
          AL4                                 'SET TIME'
          AL9                                 'FFT'
          AL17                                'VDUCP'
          AL7                                 'LOAD DATA'
          AL19                                'DM1'
          AL20                                'DM2'
          AL18                                'EDIT'
          AL11                                'SPECTRA'

[2]       V23=0
          V19=4
TEXT 1P
NO. OF TRANSFERS (TOTAL) 2**M =
          V19=5
          ←S100
          N1=VN0,VN1=V21&V21
          AS6000
```

```
        V20=VN0
        AS15500
        VN1=V20,N1+1

        N2=VN0,VN2=VN2#VN2              'ZERO FLAGS.'
        AS10001
        VN2=V21,N2+1                    'NO OF TRS.'
        VN2=0,N2+1                      'ZERO REL POINTER. '
        VN2=0,N2+1                      'ZERO NO. OF TRS COUNT.'

        N1=VN0,V16=VN1#VN1              'ZERO COUNT.'
        AS15500
[3]     VN1=0                           'ZERO DATA AREA.'
        V16=V16+1,N1+1
    ←3, V16-4096<0
    ←1


[4]     V19=4                           'SET TIME.'
TEXT 1P
INPUT M (V20 = 2**M) =
        V19=5
        V23=0
        ←S100
        V2←BITV21
        V19=4
TEXT 1P
INPUT FRACTIONAL MULTIPLIER.....
        V19=5
        V23=0
        ←S100
        V3=V21
    ←1


[5]     ←S2021,6                        'STOP RTC.'
    ←1

[6]     V19=4
        V22=10
        ←S555,6
    ←1


[7]     V19=4                           'LOAD DATA.'
TEXT 1P 1E
TYPE THE VALUE OF N. WHERE 2**N = NO. OF DATA TO BE READ.'
        V19=5
        V23=0
        ←S100
        V13←BIT V21
        N1=VN0
        AS10000,-1
        V19=3
        V23=0
        V13=V13-1
```

```
[8]     ←S100
        VN1=V21,N1+1
    ←8, V13=V13-1>0
    ←1


[9]     N1=VN0
        AS10001,1
        V21←BIT VN1
        N1=VN0
        AS15500
        ←S6007                          'FFT FIX PT'
        V19=4
TEXT 1P 1E
FIX PT FFT IN 1ST. (REAL) & 2ND. (IMAG) DATA AREAS.
        N1=VN0
        AS15500
TEXT 1P 1E
PLOT REAL PART
    ←13,L
        V19=4
TEXT 1P 1E
PLOT IMAGINARY PART
[10]←10,N1=N1+V21<0
    ←13,L
    ←1


[11]    N1=VN0                          'SPECTRA'
        AS10001,1
        V21←BITVN1
        N1=VN0
        AS15500
        ←S5533                          'POWER SPECTRA IN FLT POINT
        V19=4
TEXT 1P 1E
FLT PT. POWER SPECTRUM IN 3RD. DATA AREA.
[12]    V21=V21[1],L                    '*2'
    ←12,N1=N1+V21<0
        V21=V21[1],R
    ←13,L

        ←S5534
        V19=4
TEXT 1P 1E
FLT PT AMPLITUDE SPECTRUM IN 3RD. ATA AREA.
    ←13,L
    ←1


[13]    VN3=V21,N3-1                    'INT SUB.'
        V19=4
TEXT 1P 1E
IS LOG-SCALE X-AXIS REQUIRED?  YES(1) OR NO(0).
        V19=5
        V23=0
        ←S100
    ←14,V21=0
```

```
          ←S5535
[14]      V21=VN3,N3+1
          ←S4580,3
          ←L



[15]      V20=V2                              'START'
          V21=V3
          V22=VN0
          AS2015
          ←S2021,2                            'SET INT'
          ←S2021,4                            'SET M'
          N1=VN0
          AS10001
[16]←5,   Q5#0
     ←16,VN1[0]=0
          ←S2021,6                            'STOP RTC'
     ←1



[17]      N1=VN0                              'VDUCP'
          AS10001,1
          V21←BIT VN1
          N1=VN0
          AS15500
          ←S4580,3
     ←1

[18]      ←S5814                              'EDIT'
     ←1
[19]      +0                                  'DM1'
          +0
          N1=VN0
AS10001,1
V21←BITVN1
N1=VN0
AS15500
V9=N1
V14=N1+V21
N2=V14,V15=VN2#VN2
[21]VN2=VN1,N1+1
V15=V15+1,N2+1
←21,V15-128<0
N1=V9,V15=VN1#VN1
V9=V9+128
N2=V9
[22]VN1=VN2,N2+1
V15=V15+1,N1+1
←22,V15-V21<0
N1=V14,V15=VN1#VN1
[23]VN1=0
V15=V15+1,N1+1
←23,V15-256<0
          +0
          +0
          +0
```

```
      ←1

[20]      +0                                        'DM2'
          +0
          +0
          +0
          +0
      ←1

          END

A

SF0
%
```

```
S2015    C.J.B RTC IT PG.;

U

Q2=0
STK VN3,23,4
VN3=V12,N3-1
VN3=V9,N3-1
VN3=N2,N3-1
VN3=N1,N3-1
N1=VN0,V12=VN1&VN1
AS10001,2          'REAL POSITION IN OP DB'
N2=VN0
AS2001,11          'GIPOP DAC'
←1,N1=N1-2<0
V20=VN1
N1=VN0
AS10000
V9=V24
←1,V20[5]#0
←6,V9[0]#0         'LOAD OP DATA'
VN2=VN1
←S2002,0           'OUTPUT'
←3
[1]←4,V12-256<0
V12=255
[4]V12=V12+1
←4,N1=N1+V12<0
VN2=VN1
N1=VN0,VN1=V12&V12
AS10001,2
←10
[6]N1=VN0
AS10001
VN1[5]#0
←10,N1=N1+2<0
[10]V23=0
V23=VN0
AS2016
V22=VN0,N1-1
AS10001,4          'ADC 2WORDS DB'
V22[23]#0          'SET FOR AUTO'
V21←BIT VN1        'NO OF TRNS'
V20=VN0+V12
AS15500            'DATA AREA'
←5,N1=N1+2<0
←5,VN1-V21<0       'TEST TO SEE IF ADC TRS COMPLETED'
←5,N1=N1-3<0
VN1[0]#0
V20=VN0
AS15500
←S5514             'CONTRAL ADC DATA'
←3
[5]VN1=VN1+1
←S2002,0           'OUTPUT TO GIPOP'
V21=1
←5,N1=N1-3<0
VN1[2]=0
←S5511             'INPUT FROM ADC'
[9]←9,VN1[2]=0     'WAIT FOR ADC INTERR'
[3]N1=VN3
V0=V0,N3+1
```

```
N2=VN3
V0=V0,N3+1
V9=VN3,N3+1
V12=VN3,N3+1
LDK VN3,23,4
←L
END
Z
S
2015
S2015    RTC IT PG. FOR SOLID DIELECTRICS  C.J.B. ;
```